

Cellulo: Tangible Haptic Swarm Robots for Learning

THÈSE N° 8241 (2018)

PRÉSENTÉE LE 26 JANVIER 2018

À LA FACULTÉ INFORMATIQUE ET COMMUNICATIONS

LABORATOIRE D'ERGONOMIE ÉDUCATIVE

PROGRAMME DOCTORAL EN INFORMATIQUE ET COMMUNICATIONS

ÉCOLE POLYTECHNIQUE FÉDÉRALE DE LAUSANNE

POUR L'OBTENTION DU GRADE DE DOCTEUR ÈS SCIENCES

PAR

Ayberk ÖZGÜR

acceptée sur proposition du jury:

Prof. A. Ijspeert, président du jury
Prof. P. Dillenbourg, directeur de thèse
Prof. T. Belpaeme, rapporteur
Prof. G. Hoffman, rapporteur
Prof. F. Mondada, rapporteur



ÉCOLE POLYTECHNIQUE
FÉDÉRALE DE LAUSANNE

Suisse
2018

Acknowledgements

I would like to thank all of my colleagues and friends with whom I may or may not have directly shared the load of producing this work. Their encouragement and support, and the times we had together make them invaluable to me whether they contributed to this thesis or not. They are **Hamed Alavi, Romain Artru, Thibault Asselborn, André Badertscher, Maria Beltran, Stéphane Bonardi, Quentin Bonnard, Mina Shirvani Boroujeni, Quentin Bouvet, Manon Briod, Daniel Burnier, Daniela Caballero, Julien Calabro, Nicolas Casademont, Shruti Chandra, Fu-Yin Cherng, Florence Colomb, Norbert Crot, Sophie Dandache, Arnaud Delamare, Pierre Dillenbourg, Yélem Dufour, Louis Faucon, Julia Fink, Roger Fong, Alexandre Foucqueteau, Kevin Gonyop, Thanasis Hadzilacos, Deanna Hood, Lukas Hostettler, Stian Håklev, Auke Ijspeert, Alexis Jacq, Wafa Johal, Ehsan Karim, Hala Khodr, Łukasz Kidziński, Kshitij** (whose personal choice of not adopting a surname I respect), **Ihor Kuras, Séverin Lemaignan, Nan Li, Lorenzo Lucignano, Francesco Mondada, Rico Möckel, Khalil Mrini, Bikalpa Neupane, Jennifer Olsen, Arzu Güneysu Özgür, Léa Pereyre, Francisco Pinto, Luis Prieto, Mirko Raca, Cristina Riesen, Joanna Salathé, Sophia Schwar, Beat Schwendimann, Indira Sen, Himanshu Verma, Massimo Vespignani, Sergei Volodin, Elmira Yadollahi, Teresa Yeo, Konrad Żoła, Jessica Dehler Zufferey and Guillaume Zufferey.**

I would like to specifically thank my colleagues who contributed scientifically or otherwise to this thesis, without whom Cellulo would not be possible. I sincerely thank **Pierre Dillenbourg** who advised me, mentored me, listened to my sometimes over-the-top ideas, more often than not took them seriously, and finally furnished me with the means of bringing them to life. I further thank **Francesco Mondada** deeply for his support during our project, technical and otherwise. Next, I wish to thank **Séverin Lemaignan** and **Wafa Johal** for their valuable intellectual and developmental input to the project and my thesis who helped give them their current shape. On the development part, I thank **Lukas Hostettler** who contributed the most to it among all those who did. I also wish to thank **Ehsan Karim** for his intellectual input and support, **Manon Briod, Maria Beltran** and **Léa Pereyre** for their excellent work on creative design, **Julien Calabro** and **André Badertscher** who helped me mass manufacture Cellulo robots, **Daniel Burnier** and **Norbert Crot** who provided advice on electronics and mechanics, and **Florence Colomb** who helped with French translations. Finally, I am grateful to all our semester project students who helped or are still helping with developmental aspects of our project: **Joanna Salathé, Alexandre Foucqueteau, Nicolas Casademont, Roger Fong, Quentin Bouvet, Arnaud Delamare, Hala Khodr and Sergei Volodin.**

Acknowledgements

I sincerely enjoyed working with and thank **Stéphane Bonardi**, **Massimo Vespignani**, **Rico Möckel** and **Auke Ijspeert** even though the prior work we did together does not appear in this thesis. I wish to thank **Jonas Brunschwig** and all other members of the **Swissnex Boston** team for welcoming us and giving us the opportunity to participate in the Cambridge Science Festival, from which we obtained valuable observations. I am grateful to **Marie-France Labelle** and **Nicolas Baltassat** of **Ecole Internationale de Genève** and **Paul Magnuson** and **Adam Bradford** of **Leysin American School** for having us at their schools for experiments. I am particularly grateful to **Mat Mcleod** of **Leysin American School** for his interest in our project and for his generous involvement in co-designing our activities. I finally thank **each and every child participant** of our experiments for providing us with valuable data and observations; in return, I hope that our robots sparked curiosity and wonder in all of you.

I am grateful to **Patrick Jermann**, **Gilles Raimond**, **Eloge Seri** and all other members of **Center for Digital Education (CEDE)** for generously sharing their filming equipment and expertise, as well as **Dinesh Dillenbourg** and particularly **Magali Croci** for their invaluable creative input when authoring professional media for Cellulo. For aiding us with technology transfer, I wish to thank **Frédéric Pont**, **Jussi Vesterinen**, **Jan Kerschgens**, **Alberto Di Consiglio** and **Isabel Casado Harrington**. Furthermore, I wish to express my sincere gratitude to all members of the **Swiss National Centre of Competence in Research (NCCR) in Robotics** for being directly responsible for funding our research, as well as bringing together competent research groups to create synergies and valuable scientific discussions. I wish to also thank the **Gebert Rüf Foundation** for the funding that allowed us to collaborate with exceptional creative professionals. Finally, I would like to thank **Wafa Johal** and my jury members **Auke Ijspeert**, **Pierre Dillenbourg**, **Francesco Mondada**, **Tony Belpaeme** and **Guy Hoffman** for spending their valuable time and effort in assessing and improving this thesis.

I sincerely thank my parents **Ariyanna Özgür** and **Nuri Özgür**, without whom I would have neither the foundation, nor the courage to come where I have. I am grateful to all other members of my family for their support, emotional or otherwise, but particularly to my aunt **Arzu Küçükıldırım** and my grandmother **Engin Özgür** for their support when very few others were there for me. Finally, and most importantly, I thank my dear wife **Arzu Güneysu Özgür** for being there for me more than any other, with unlimited patience. She is the one who can understand all my joys and sorrows, my inseparable companion, the one and only one who ever touched my soul.

Lausanne, 28 October 2017

A. Ö.

Abstract

Robots are steadily becoming one of the significant 21st century learning technologies that aim to improve education within both formal and informal environments. Such robots, called Robots for Learning, have so far been utilized as constructionist tools or social agents that aided learning from distinct perspectives. This thesis presents a novel approach to Robots for Learning that aims to explore new added values by means of investigating uses for robots in educational scenarios beyond those that are commonly tackled: We develop a platform from scratch to be “as versatile as pen and paper”, namely as composed of easy to use objects that feel like they belong in the learning ecosystem while being seamlessly usable across many activities that help teach a variety of subjects. Following this analogy, we design our platform as many low-cost, palm-sized tangible robots that operate on printed paper sheets, controlled by readily available mobile computers such as smartphones or tablets. From the learners’ perspective, our robots are thus physical and manipulable points of hands-on interaction with learning activities where they play the role of both abstract and concrete objects that are otherwise not easily represented.

We realize our novel platform in four incremental phases, each of which consists of a development stage and multiple subsequent validation stages. First, we develop accurately positioned tangibles, characterize their localization performance and test the learners’ interaction with our tangibles in a playful activity. Second, we integrate mobility into our tangibles and make them full-blown robots, characterize their locomotion performance and test the emerging notion of moving *vs.* being moved in a learning activity. Third, we enable haptic feedback capability on our robots, measure their range of usability and test them within a complete lesson that highlights this newly developed affordance. Fourth, we develop the means of building swarms with our haptic-enabled tangible robots and test the final form of our platform in a lesson co-designed with a teacher. Our effort thus contains the participation of more than 370 child learners over the span of these phases, which leads to the initial insights into this novel Robots for Learning avenue. Besides its main contributions to education, this thesis further contributes to a range of research fields related to our technological developments, such as positioning systems, robotic mechanism design, haptic interfaces and swarm robotics.

Keywords: *Robots for Learning, Human-Robot Interaction, Mobile Robots, Swarm Robotics, Tangible Robots, Haptic Interfaces*

Résumé

Les robots deviennent progressivement un des outils pertinents des technologies modernes de formation qui tendent à améliorer l'éducation, qu'elle soit formelle ou informelle. La principale valeur ajoutée de ces robots, appelés "Robots pour l'Apprentissage", a jusqu'ici reposé sur une vision constructiviste combinée aux vertus de l'interaction sociale. Cette thèse cherche à révéler de nouveaux atouts éducatifs des robots, au-delà des scénarios utilisés dans les autres approches de robotique éducative : Nous visons à développer une plate-forme entièrement nouvelle qui est "aussi polyvalente que papier et crayon", c'est-à-dire, qui est maniable, familière, et utilisable dans des nombreux domaines de formation. A partir de ce principe, nous dessinons les contours conceptuels de notre plate-forme qui est composée des plusieurs robots tangibles contrôlés par des appareils mobiles répandus (tels que les smartphones ou les tablettes), produits à bas coût, de la taille de la main et qui évoluent sur des feuilles de papier imprimées. Ces objets physiques et manipulables permettent de représenter des objets concrets ou abstraits, que les apprenants ont autrement de la peine à visualiser, et d'interagir avec ceux-ci pendant les activités d'apprentissage.

Nous développons cette plate-forme en quatre phases itératives, chacune composée d'une étape de développement et de plusieurs étapes de validation. Premièrement, nous développons des interfaces tangibles positionnées avec précision, caractérisons la précision de cette localisation et testons l'interaction avec des apprenants lors d'une activité ludique. Deuxièmement, nous intégrons la locomotion dans les interfaces tangibles afin de les transformer en robots mobiles, caractérisons à nouveau la performance et testons la notion de déplacer le robot par rapport à suivre le mouvement du robot et/ou de le déplacer alors qu'il oppose une résistance. Troisièmement, nous ajoutons la réaction haptique à nos robots, mesurons son degré d'utilisabilité et testons les robots lors d'une leçon complète exploitant cette nouvelle fonctionnalité. Quatrièmement, nous développons la possibilité de former des essais avec nos robots et testons cette version finale de notre plate-forme dans une leçon co-conçue avec un enseignant. Nos expériences, au cours desquelles plus de 370 écoliers ont été impliqués, enrichissent nos savoirs sur l'utilisation de ces nouveaux robots pour l'apprentissage. En plus de ses contributions à l'éducation, cette thèse contribue aux systèmes de positionnement, aux mécanismes robotiques, aux interfaces haptiques et à la robotique en essaim.

Mots clefs : *Robots pour l'Apprentissage, Interaction Humain-Robot, Robots Mobiles, Robotique en Essaim, Robots Tangibles, Interfaces Haptiques*

Contents

Acknowledgements	i
Abstract	iii
Résumé	v
Contents	vii
List of figures	xi
List of tables	xiii
List of algorithms	xv
List of listings	xvii
List of abbreviations	xix
1 Introduction	1
1.1 Robots for Learning	3
1.1.1 Origins and Challenges	3
1.1.2 Nature of Robots for Learning: Tools <i>vs.</i> Agents	4
1.1.3 Synergies, Gaps & Motivations	12
1.2 Cellulo Project	14
1.2.1 Introduction – Research Goals	14
1.2.2 Conceptual Design & Key Ideas	16
1.3 Plan of this Thesis	20
2 Phase I – Localized Tangibles	23
2.1 Introduction	23
2.1.1 Background	23
2.1.2 Problem Statement	24
2.1.3 Related Work	24
2.2 Theory – Location-Coding Dense Optical Patterns	27
2.2.1 From Microdots to the Primary Difference Sequence	27
2.2.2 From the Primary Difference Sequence to Actual Coordinates	28

Contents

2.2.3	Sectors & Final Coordinate Space Size	31
2.2.4	Decoding Orientation	31
2.2.5	Error Correction	32
2.3	Localization Pipeline Design	33
2.3.1	Image Processing	33
2.3.2	Grid Estimation	34
2.3.3	Probabilistic Treatment	37
2.3.4	Decoding	39
2.4	Implementation – Cellulo Robot Version 1	40
2.4.1	Printable and Document-Compatible Dot Pattern	41
2.4.2	Hardware Design	43
2.4.3	Exposure of the Image	44
2.4.4	Focusing & Framing of the Image	45
2.4.5	Image Capture & Processing	46
2.4.6	Open-Source Software Release	46
2.5	Supervised Validation	46
2.5.1	Overview	46
2.5.2	Procedure	47
2.5.3	Results	47
2.5.4	Conclusion	50
2.6	Ecological Validation	51
2.6.1	Overview	51
2.6.2	Activity Design – Treasure Hunt	52
2.6.3	Results & Discussion	55
2.6.4	Conclusion	57
3	Phase II – Actuated Tangibles	59
3.1	Introduction	59
3.1.1	Background	59
3.1.2	Problem Statement	60
3.1.3	Related Work	60
3.2	Development – Permanent Magnet-Assisted Ball Drive	63
3.2.1	Approach and Key Principles	63
3.2.2	Magnetostatic Wheel-Magnet Interaction Analysis	65
3.2.3	Dynamics of Single Ball Drive	68
3.2.4	Towards a Complete Drive – Kinematics & Dynamics of Robot	71
3.3	Implementation – Cellulo Robot Version 2	74
3.4	Supervised Validation	77
3.4.1	Overview	77
3.4.2	Procedure	77
3.4.3	Results	79
3.4.4	Conclusion	81

3.5	Ecological Validation	82
3.5.1	Overview	82
3.5.2	Windfield Study – Design & Participants	83
3.5.3	Results & Discussion	85
3.5.4	Conclusion	86
4	Phase III – Haptics with Actuated Tangibles	87
4.1	Introduction	87
4.1.1	Background	87
4.1.2	Problem Statement	88
4.1.3	Related Work	89
4.2	Development – Haptics & Motion Controller	92
4.2.1	Overview	92
4.2.2	Haptic Interaction & Controller Considerations	93
4.2.3	Controller Design	95
4.3	Supervised Validation	100
4.3.1	Introduction	100
4.3.2	Procedure	100
4.3.3	Results	106
4.3.4	Conclusion	112
4.4	Ecological Validation	113
4.4.1	Overview	113
4.4.2	Activity Design	115
4.4.3	Lesson Design	116
4.4.4	Participants & Data Collection	120
4.4.5	Calculated Metrics	121
4.4.6	Results & Discussion	122
4.4.7	Conclusion	127
5	Phase IV - Building Tangible Swarms	129
5.1	Introduction	129
5.1.1	Background	129
5.1.2	Problem Statement	130
5.1.3	Related Work	131
5.2	Development - Tangible Swarms	134
5.2.1	Overview	134
5.2.2	Wireless Communication Considerations	134
5.2.3	Application Framework Design	137
5.2.4	Learning Activity Design - Particles in Matter	146
5.3	Quantitative Validation	149
5.3.1	Overview	149
5.3.2	Activity & Test Design	149
5.3.3	Participants & Data Collection	152

Contents

5.3.4	Swarm Interaction Metrics	153
5.3.5	Results & Discussion	154
5.3.6	Conclusion	159
5.4	Qualitative Validation	159
5.4.1	Overview	159
5.4.2	Lesson Design	160
5.4.3	Participants, Testing & Data Collection	165
5.4.4	Results & Discussion - Learners' Perspective	170
5.4.5	Results & Discussion - Teacher's Perspective	174
5.4.6	Conclusion	176
6	Conclusion	177
6.1	Overview	177
6.2	Scientific Contributions	178
6.2.1	Technological Contributions	179
6.2.2	Conceptual Contributions	180
6.3	Shortcomings & Future Work	181
6.3.1	Localization	181
6.3.2	Locomotion	182
6.3.3	Haptics	183
6.3.4	Swarm	183
6.3.5	Robots for Learning	184
6.4	Research Goals Revisited	185
6.5	Impact and New Perspectives	187
A	Anoto Number Sequences	189
B	Particles in Matter Source Code	191
	Bibliography	197
	Curriculum Vitae	217

List of Figures

1.1	Typical scenes from learning activities where robots are used as tools <i>vs.</i> as agents	5
1.2	Mechanical buildability spectrum of programmable tool robots	8
1.3	Concept Cellulo activities	17
1.4	Cellulo activity design space	20
2.1	Organization of printed microdots in the Anoto grid	27
2.2	The localization pipeline	33
2.3	Dot detection through image segmentation and two-pass binary blob detection	34
2.4	Initial estimation example for the grid, before refining	35
2.5	Possible locations of dots and how they are attributed probabilities	37
2.6	Best decoding region selection and subgrid refinement	39
2.7	Cellulo version 1 software architecture	41
2.8	Choice of symbol glyphs in the dot pattern font	41
2.9	Exploded view of Cellulo robot version 1	42
2.10	Cellulo robot version 1	44
2.11	Cross-section of the optical system, side view	45
2.12	Accuracy of x coordinate measurements	48
2.13	Accuracy of y coordinate measurements	48
2.14	Accuracy of orientation measurements	49
2.15	Playground used in Treasure Hunt	53
2.16	Interaction schemes used in Treasure Hunt	54
2.17	Scene from Treasure Hunt	56
3.1	Overview of our permanent magnet-assisted ball wheel design	64
3.2	Magnetostatic wheel-magnet interaction analysis parameters	66
3.3	Magnetostatic wheel-magnet interaction analysis results	66
3.4	Pull forces and wheel potentials for selected magnet dimensions	67
3.5	Magnetic field lines in a single ball wheel-ring magnet assembly	68
3.6	Dynamics of single ball drive	69
3.7	Kinematics & dynamics of the Cellulo robot	71
3.8	Cellulo robot version 2	74
3.9	Exploded view of Cellulo robot version 2	75
3.10	Trajectory for locomotion performance evaluation	77

List of Figures

3.11	Ball drive <i>vs.</i> omni-wheel drive robot built as baseline	78
3.12	Typical trajectories followed by robots	79
3.13	Windfield playground	82
3.14	Scene from the Windfield study	83
3.15	Screen captures of the Windfield activity application	84
4.1	Planar haptic interfaces in the literature	89
4.2	Cellulo version 3 software architecture	93
4.3	Motion & haptics controller	96
4.4	Casual backdrive assist transfer functions	98
4.5	Printed activity sheets for the supervised haptics experiment	101
4.6	Shapes used in the Find Shape task	105
4.7	Paths used in the Re-Move task	105
4.8	Time taken to complete each level in level-based tasks	106
4.9	Sample paths performed in Re-Move	108
4.10	Average accuracies of participants in Re-Move	108
4.11	Sample paths performed in Follow Path	109
4.12	Distance to the path in Follow Path	109
4.13	Average distance to correct answers in precision tasks	110
4.14	Participant performance in Match	111
4.15	Maximum levels reached in Find Shape	112
4.16	Feel the Wind and Control the Wind screenshots	114
4.17	Windfield post-test questions	119
4.18	Sample scene from Windfield	120
4.19	Time to find the first pressure point(s) in <i>Feel the Wind</i>	123
4.20	‘Approach’ patterns towards high pressure points	124
4.21	Maximum score obtained by each group in Control the Wind	125
4.22	Post-test results in Windfield	127
5.1	Cellulo version 4 software architecture	136
5.2	Particles in Matter - Solid, liquid and gas states	146
5.3	Particles in Matter - “Shake” interaction	148
5.4	Particles in Matter - “Launch” interaction and heat transfer	148
5.5	Pre/post-test animations for the quantitative Particles in Matter study	151
5.6	Scene from the quantitative Particles in Matter study	153
5.7	Learning gain/loss in the quantitative Particles in Matter study	155
5.8	Learning across groups in the quantitative Particles in Matter study	156
5.9	Net learning across all participants in the quantitative Particles in Matter study	157
5.10	Relationship between learning and swarm interaction in the quantitative Particles in Matter study	158
5.11	Scenes from the qualitative Particles in Matter studies	164

List of Tables

2.1	Prominent absolute indoor localization methods in the literature	25
2.2	List of Cellulo robot version 1 components and costs	43
2.3	Overall localization performance	49
2.4	Treasure Hunt task completion times	56
3.1	List of Cellulo robot version 2 components and costs	76
3.2	Comparative performances of proposed and baseline drives	80
4.1	Windfield lesson plan and didactic sequence	116
5.1	Pre & post-test questions for the quantitative Particles in Matter study	150
5.2	Particles in Matter lesson plan and didactic sequence	160
5.3	Pre, mid & post-test questions for the qualitative Particles in Matter studies	166
5.4	Units of knowledge discovered in Particles in Matter qualitative experiments	167
5.5	Results from the Particles in Matter qualitative experiment 1	168
5.6	Results from the Particles in Matter qualitative experiment 2	169



List of Algorithms

2.1	Constrained k -means algorithm to find grid directions	36
2.2	Algorithm to construct quasi-probability matrices	38
5.1	Physicomimetic swarm control algorithm	143



List of Listings

5.1	Declarative “Hello World” program	139
5.2	Example declarative physicomimetic swarm program	145
B.1	Particles in Matter source code	191

List of abbreviations

2D 2 Dimensions 27, 31, 34, 51, 121, 130
3D 3 Dimensions 8, 51, 66, 90, 130, 133
AISI American Iron and Steel Institute 76
API Application Programming Interface 95, 97, 99, 135, 137, 138, 144, 178
BCI Brain-Computer Interface 132
CCTV Closed-Circuit Television 45
CI Confidence Interval 109, 157, 158, 173, 174
CNC Computerized Numerical Control 47, 94
CSCL Computer Supported Collaborative Learning 1
DC Direct Current 72, 74
DMA Direct Memory Access 46
DOF Degree(s) of Freedom 24, 27, 33, 51, 60–62, 64, 65, 67, 71, 88–92, 98–100, 112, 182
DPI Dots per Inch 41, 50
FEA Finite Element Analysis 65, 83, 115
FFF Fused Filament Fabrication 43, 76, 79
FOV Field of View 45
FPU Floating-Point Unit 46
GPS Global Positioning System 23
GUI Graphical User Interface 116, 120, 132, 137, 139, 144, 191
HCI Human-Computer Interaction 89, 112, 179
HRI Human-Robot Interaction 5, 10, 13
HSI Human-Swarm Interaction 131, 134, 153, 154
IMU Inertial Measurement Unit 80
IoT Internet of Things 180
IR Infrared 24
LED Light Emitting Diode 41, 43, 44, 52, 93, 136, 141, 184

List of abbreviations

LIDAR Light Imaging, Detection and Ranging25
μC Microcontroller	41, 93, 136
MHI Mobile Haptic Interface89, 90
MJM Multi-Jet Modeling79
MOSFET Metal-Oxide-Semiconductor Field-Effect Transistor43
MOOCs Massive Open Online Courses	1
MRS Multi-Robot Systems	129, 130, 133, 138
NBR Nitrile Butadiene Rubber70, 76
NFC Near-Field Communication	184
NIR Near Infrared44
PCB Printed Circuit Board43
PDF Portable Document Format41, 46
PID Proportional-Integral-Derivative77
PLA Polylactic Acid43, 70, 76
PTFE Polytetrafluoroethylene70, 76
PWM Pulse-Width Modulation95
QML Qt Modeling Language	137–140, 144
R4L Robots for Learning	3–6, 9, 12, 14–16, 20–22, 177, 178, 180, 181, 184–187
RFID Radio-Frequency Identification25
RGB Red, Green, Blue43
SLAM Simultaneous Localization and Mapping50
SPP Serial Port Profile41, 93, 130, 136
SRAM Static Random-Access Memory46
STEM Science, Technology, Engineering and Mathematics10, 12–16
SVG Scalable Vector Graphics99
USB Universal Serial Bus	135–137
UWB Ultra Wideband24, 25
WYSIWYG What-You-See-Is-What-You-Get	132, 140

1 Introduction

At least since Ancient Greece, an effective scheme was used for formal education: A group of learners being instructed by a teacher in a classroom. Over the course of humankind's history, not only its repertoire of knowledge vastly expanded and its civilization greatly developed, but many reforms and improvements were also made to the environment, methodology and philosophy of education: Learning was secularized, institutionalized, governmentalized and standardized. Despite these improvements, the teacher/classroom/learner scheme was sufficient in transferring this body of knowledge to the new generation and it remained, for the most part, the same until the end of the 20th century.

Now, the coming of the Information Age is profoundly transforming the learning needs of the newest generations, to the point where the “factory model” classrooms are beginning to fall short in equipping new learners with the 21st century skill set. We are finding out through advances in cognitive development and neuroscience that the old, rigid classroom paradigms that “produced” information learning as if on an “assembly line” can no longer be relied on to build skills that are increasingly necessary on today's interconnected and digital world where learning occurs at all times: The learners must now think creatively, be able to work as parts of diverse teams, and show digital information literacy. Thus, the teaching/classroom/learning paradigms must also update to accommodate these needs.

New trends in learning technologies offer answers to these needs and reflect the anticipated paradigm shifts. Arguably as successors to the analog overhead projectors, computers made their impact on learning and classrooms through digitally interactive displays of content. Through the networking allowed by the widespread diffusion of the internet, this approach gave birth to Computer Supported Collaborative Learning (CSCL) which emphasized shared learning and development. Nowadays, platforms that serve such purposes are becoming increasingly lightweight and portable with laptops, tablets and smartphones. One step further, classrooms themselves may become digital as a result of Massive Open Online Courses (MOOCs) researched and developed in the last decade where the learners and the teachers may no longer need to convene in time and space, in theory allowing a never before seen degree of learning diffusion through free access to content and software.

Chapter 1. Introduction

Parallel to all these media-oriented developments, robots began entering learning environments as a means of introducing more hardware-oriented materials to learners. The first educational robot ever was the Logo Turtle by Papert ([1]) that let learners program a mobile tabletop robot with a pen that can leave a visible trace of the robot's motion. The vision in making this robot available to learners as a programmable tool relied on Piaget's *constructivist* view of cognitive development ([2]), stating that learners should be proactive builders of their own knowledge instead of receivers of inert and absolute information disseminated by outside sources. Since this construction is theorized to be relative to the learner and the environment, proper "materials" are required to be embedded in the surrounding environment. The Logo Turtle was proposed as this very material, a "computational object to think with", that is environmentally present, open to personal identification and programmable. Indeed, this first robot was tightly interconnected with the then-emerging "computer culture" and thus created a central theme of "letting learners program a simple robot" which sparked the programmable learning robot movement that persists today.

The central belief to this archetypical robot was that through programming it, that is in itself an act of creation, not only the learning of those skills that are directly in focus while programming (such as problem solving and mathematics) would be facilitated, but the learning of a wide range of other skills would also potentially be improved. Papert did not believe in traditional classrooms, organized education or curricula in general. His robot was an enabler as learners built their own knowledge inside environments that were envisioned to look radically different than what schools looked like at that time. Whether organized education or curricula have no future is still a matter of open debate, one that this thesis is not written to address.

Instead, this thesis proposes a novel robotic approach to technology-enhanced learning that revisits the roots of educational robots to learn from them, such as the Logo Turtle and those that came later and were inspired by it, in the modern landscape of robots for learning. Ours will be a practical endeavor in addressing the immediate and genuine challenges encountered in introducing such technologies to education; unlike Papert, we will focus on the shorter term gains instead of working towards longer term metamorphoses. Throughout our thesis, design and verification phases of our technologies and methods will resonate with this focus on immediate applicability, adaptability and cooperation with current learning environments and their professionals in order to grow and enhance the way these environments function instead of subverting them altogether.

The ultimate goal of the work in this thesis will be to open new perspectives in how learning technologies, in particular robotic ones, can be used in a versatile manner and in educational scenarios previously unimagined. Due to this highly exploratory nature of our effort, instead of working with established technologies to improve their current uses or create new uses for them in educational settings, we will focus on building whatever is necessary, from scratch. In other words, we will seek to expand rather than to extend. We will thus provide in the rest of this chapter the literary background for our endeavor, list the goals that drive our research and summarize the procedures that will let us address them.

1.1 Robots for Learning

We begin by providing the brief history, trends and state of the art in the use of robots by learners and teachers for a variety of educational purposes. To describe this field where we imagine no boundaries to subject matter or disciplines nor to the purpose or nature of the robots as long as they serve some form of learning, we use the term Robots for Learning (R4L), also known as Robots for Education.

1.1.1 Origins and Challenges

R4L arguably came into existence, as mentioned earlier, by virtue of the Logo Turtle created by Papert around 1980's. The vision around this robot was to provide learners programmable objects to think with to transform the way mathematics, geometry and possibly other disciplines are learned, in order for it to resemble the way first languages are learned effortlessly and naturally by young learners. This vision further entailed the transformation of educational institutions and organizations, disrupting the notions of curriculum and instruction. What this meant was that these notions were to be adapted entirely to this new constructionist paradigm where the learners learn by exploring, building and designing instead of being instructed. Moreover, the education professionals were to adapt as well, necessitating a deep, societal transformation.

How, or even why, these transformations should take place was not entirely clear at the time. For this and other reasons, such as robots and computers still being expensive and not entirely reliable, interest in educational practitioners failed to grow and R4L laid dormant for about two decades and significant advances in the field were not seen. What [3] called *teacher availability deadlock* almost certainly played a role here: As long as informatics is not in the curriculum, there is little incentive to educate teachers and as long as there are no trained teachers, there is little incentive to introduce the subject. Thus, since no party sought these progressive technologies associated with these subjects, they did not transfer to widespread use. Considering that the roots of R4L originated around the science of informatics, the focus of such endeavors was naturally to introduce informatics (or more colloquially called "programming" around many circles) into learning. Nevertheless, it is reasonable to anticipate the same teacher availability deadlock in any given innovative and disruptive technology that is not trivial to use effectively (both from teachers' and learners' perspectives) for learning. Therefore, it is clear that for any transformation in learning to occur, more work must be done first, including cooperation with the world of education.

This cooperation that will lead to the acceptance of and support for R4L within educational spheres certainly presents a number of challenges. [4, 5, 6, 7, 8, 9, 10] and other works investigate the present view and challenges on R4L: Education professionals are positive but also critical towards bringing robots in the classroom; primary perceived problems are potential expensiveness, high demand of resources (labor, time and space) and likely creation of unwanted disruption. They further express that they want the technology to adapt to their

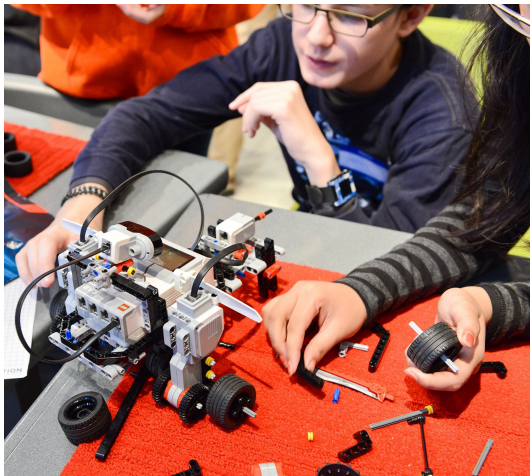
practice and not the opposite; they need to be assured that the robots are there to aid them in their profession and not to “replace” them. But what is perhaps more important is that actual long-term contributions to learning upon the introduction of robots in classrooms or in informal learning environments are not yet clearly shown through empirical evidence in many areas. From a practical point of view, but still parallel to the empirical evidence issue, the lack of educational content that feature the effective use of robots in these areas is another distinct issue that prevents the adoption of robots. As a consequence, unfortunately, R4L is still sometimes perceived as a “trend” or as part of extra-curricular activities and not as a potentially integral part of formal learning.

A clear exception where considerable empirical evidence and educational content exists is unsurprisingly R4L applied to programming, robotics, engineering and other closely related subjects. This is the case perhaps due to R4L’s historical origins, or perhaps due to the relatively more straightforward approach of applying them for the learning of such matter. Regardless, these are the disciplines where some amount of awareness in formal education exists as of today; other applications, discussed in the forthcoming sections, are still in their infancy and in considerable need of empirical evidence of their contribution to formal learning, along with collaborative verification (with education professionals) within ecologically valid settings. Given that each discipline presents its distinct and unique characteristics, methods and bodies of knowledge (of which informatics is only one), this is a substantial undertaking where global methods in proving such a statement as “robots are useful for learning in general” are not likely to be found. Instead, the meticulous exploration of the intricacies of using R4L in each domain is likely to be more successful to discover the specific added values of robots to that domain (if they exist to begin with), just as it was and is still being done for informatics. However, this is clearly a long term endeavor and thus more of a direction that the scientific R4L community as a whole is required to take. As these exploratory steps are taken and more is discovered, it is our belief that a global consciousness (that education professionals are part of) who understands the added values of R4L in each learning territory will gradually be built.

The work presented in this thesis does not claim to show that R4L is definitively useful in a given learning domain. Instead, it presents a new direction towards which the aforementioned steps of discovery may be taken. We do this by reimagining the role and added value of robots in a way that aims to address the aforementioned challenges, and in doing so, we obtain a novel robotic concept that necessarily borrows strong ideas found in the prevalent movements in the state of the art. Therefore, we now present these prevalent movements in R4L and position ourselves among them in order to later describe the thought process and ideas that lead to the generation of our concept.

1.1.2 Nature of Robots for Learning: Tools *vs.* Agents

When we consider the aforementioned origins of R4L and more recent trends, we see that most research done in the area belongs to one of two movements. Following Papert’s ideas of



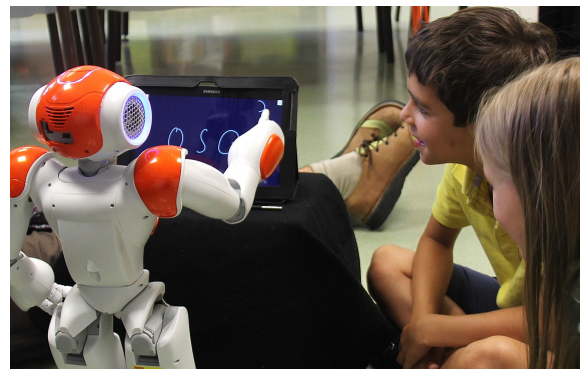
(a) Lego Mindstorms robot as educational *tool*, being built before being programmed by learners. Picture taken from www.architecture.org.



(b) Thymio robot as educational *tool*, being programmed by learners who observe its behaviors. Picture taken from www.techykids.com.



(c) Pepper robot as teaching *agent*, conducting an interactive storytelling session. Picture taken from www.roboticstrends.com.



(d) Nao robot as learning *agent*, pretending to be a peer with poor handwriting so that learners can teach it to better their own handwriting skills.

Figure 1.1 – Typical scenes from learning activities where robots are used as *tools* vs. as *agents*.

building “computational objects for thinking”, the first and older movement takes robots as *tools* where they appear natural and suitable given the application they are intended for and where the learners are in control of the robots (*i.e.* they are “above” the robots). The second and younger movement emerged with the advances in the Social Human-Robot Interaction (HRI) field where robots play the completely different role of socially capable peers or tutors, which we call the role of artificial *agents* within the learning environment, where learners are not in direct control of the robots but instead interact with them in a pseudo-social way (*i.e.* they are “at the same level” as the robots). In Figure 1.1, typical scenes from educational activities that belong to both movements are given for added clarity. Below, we explain these two distinct movements, their advantages and how they contribute to the field of R4L.

Robots as Tools

The *robots as tools* movement encompasses the idea of providing learners real robots which they can “build”, meaning constructing its hardware through kits consisting of easily connectible parts, constructing its software through programming, or both. Throughout this movement, we find a variety of educational principles that play key roles:

Learning with robots: Was initially imagined by Papert within the scope of *constructionism* for mathematics and problem solving through embedding elements found in these subjects into the creative programming process. By building the intended knowledge on one’s own (where robots are facilitators) instead of being instructed, better and easier learning is targeted. This easily extrapolates to learning programming itself and other engineering-related subjects where robots aid the learning process by their appeal, especially to younger learners to whom correctly designed robots may appear as “intelligent toys” that they are willing to play with. This affinity could translate to increased enthusiasm which in turn could lead to more science and technology interest ([11]) not exclusively in younger learners but also in older ones throughout K12 (kindergarten to 12th grade, [12]) and could inspire motivation in even older, undergraduate learners.

Learning with hands-on interaction: By having the learners build and test physical robots, aims to provide real-world grounding to and improve the learning of otherwise abstract knowledge ([13, 14]). Closely related to robotics, programming, engineering and other “technology” subjects, this physically experiential methodology intends to exploit the additional benefits of embodied learning by tangible and implicit haptic manipulation (for which robots are exceptionally suitable tools); this cannot otherwise be easily done using simulators, virtual environments or only theoretical exercises on paper.

Learning by individual parts: Lets learners understand how complex systems composed of many interconnected parts work by letting them program the individual parts and build the system using these parts ([15]). This is achieved by building individual robots through common robotic parts (*i.e.* simple sensors and actuators such as bumpers and motors) and understanding how the individual robots work, as well as by building populations of possibly heterogeneous robots and understanding how higher, population-level behaviors emerge from individual behaviors¹.

Learning with evolutionary dynamics: Lets learners build “artificial organisms” ([15, 16]) with sensors, actuators and a “mind” (*i.e.* their program) that mimic the components of biological organisms and that behave in certain ways and/or solve target problems. By understanding and improving these components and the organism that is born from their association through techniques that resemble evolutionary processes such as selective reproduction and mutation, learners can acquire progressively more desirable

¹The idea of understanding how complex systems work through programming individual components is currently being explored within the domain of *computational thinking*; these philosophies existing in the R4L literature hint at the potential efficacy of robots as tangible, physical tools in computational thinking.

behaviors or better solutions from their robots. Using this methodology, understanding how these solutions and behaviors are achieved would be clearer since learners themselves would have constructed the way that leads to these improvements.

Over the years, a multitude of robotic platforms were used as tools for learning purposes which were built around one or more principles listed above; [17] gives a comprehensive review of these. All such robots, without exception to the best of our knowledge, feature some form of programmability: Robots intended for older learners, such as undergraduate or graduate studies, tend to support real-world programming languages such as C, C++, and Python, whereas robots intended for younger learners tend to support visual programming languages with drag-and-drop blocks and connections, such as LabVIEW for Lego Mindstorms, Thymio Visual Programming Language and Scratch. Where robots intended for younger learners are actually used for older learners (such as at undergraduate level) for their cost effectiveness, which is especially the case for Lego Mindstorms, we find custom third party firmwares and operating systems that allow the programming of built robots with large a variety of real-world programming languages, which expands the platform's potential in facilitating programming education. Indeed, it is clear that a large portion of scientific work involving the tool robot idea feature the very popular Lego Mindstorms kits (see [18]), hinting at the power of this versatility provided by both flexible programmability and buildability.

A broader look at the mechanical buildability of these programmable platforms, meaning the level to which learners are able to create the hardware as well, reveals a spectrum that is summarized in Figure 1.2. Common robots range from completely buildable to completely pre-built, where buildable robots are often sold as kits in order to open prospects to building a large variety of robots that serve a multitude of purposes, including letting the learners imagine and creatively build unforeseen robots on their own; see Figure 1.1a for a typical scene in an activity using such a robot. With the same kit, *e.g.* a wheeled robot with a grabber that transports objects, as well as a legged robot that walks can be built and programmed. As these kits are explicitly marketed to younger learners, they are almost always in the low to mid price range; they are however, as mentioned before, also appealing to older learners and are used in up to undergraduate learning by virtue of this price range, as well as their buildability to suit a broad range of curriculum items, especially in the teaching of robotics. From another perspective, the emerging “maker movement” offers even more flexibility on robots that can be built through affordable rapid prototyping platforms and exceptionally lightweight computers that are becoming commercially available. The design and fabrication of these robots typically rely on open source hardware and software, as well as on maker communities built around fabrication platforms and methods. Moreover, compared to other approaches on this buildability spectrum, the design and fabrication of robots within this movement are closer to the realistic methods and processes (or at least to the preceding prototyping phases) used to design and manufacture mass produced devices for the end user. Thus, they provide not only potentially more benefit for university-level robotics curricula with manufacturing focus, but also a more realistic view of robotics for younger learners.

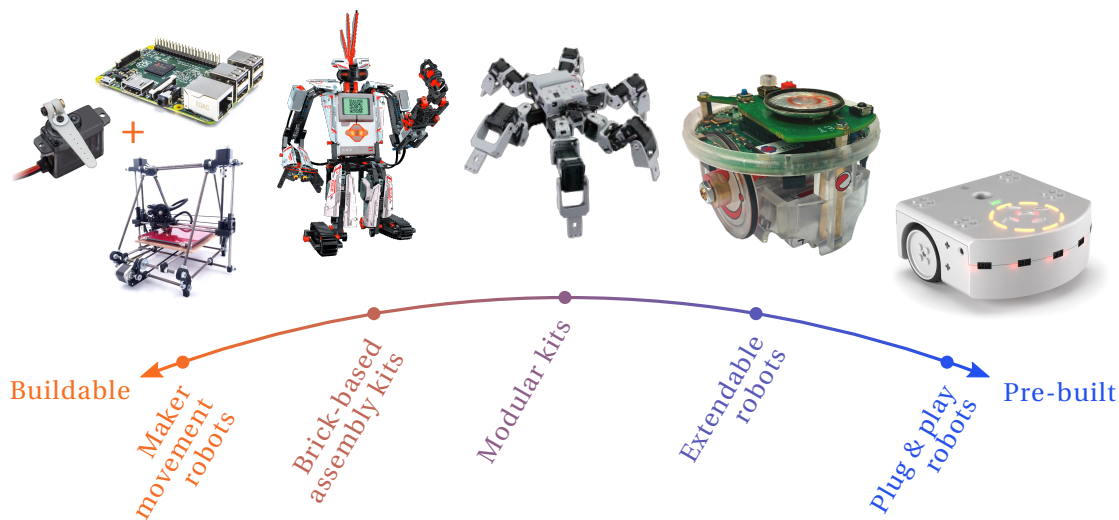


Figure 1.2 – Mechanical buildability spectrum of programmable tool robots. On the fully buildable end of the spectrum, the robots belonging to the **maker movement** are found where emerging affordable rapid prototyping platforms, or more colloquially called 3D printers (RepRap Prusa Mendel given as example above, see [19]), low-cost mini computers (Raspberry Pi given above as example, see [20]) and other off-the-shelf components (a hobby servomotor given above as example of a commonly used component, picture taken from www.dubro.com) are exploited for exceptional robot building flexibility without concern for standard robots or kits that contain all necessary components to build robots. For this reason, examples of common building blocks within this movement are provided above instead of specific robots built with them. Towards more readily usable robots, we find **brick-based assembly kits** (Lego Mindstorms EV3 given as example above, see [21]; see [22] for other similar kits such as VEX and Fischertechnik) where using the same standard kit, it is possible to build a large variety of robots such as mobile or humanoid robots with readily usable sensors, actuators and lower level mechanisms (*e.g.* gear trains, pistons, linkages), as long as the required time is invested into building these robots. Towards less buildable, we find **modular kits** (Robotis Bioloid given as example above, see [23]; see [24, 25] for other such kits) where still a considerable variety of robots can be built using monolithic actuators and sensors but easy access to lower level mechanisms is removed. Next step towards pre-built, **extendable robots** (e-puck given as example above, see [26]; see [27] for other similar robots such as iRobot Create and Khepera III) feature standard, non-modifiable, but readily usable base robots that can be extended with extra modules (such as more complex sensors or actuators) as needed; it is not uncommon to find open source robots here that allow the design, manufacturing and use of custom extension modules by a community built around the robot. On the fully pre-built end of the spectrum, we find **plug & play robots** (Thymio II given as example above², see [28]; see [29] for another such robot that is very low cost) that feature non-modifiable standard robots with predefined sets of sensors and actuators for easier and faster startup, and designs that tend to be friendlier if intended for younger learners.

²Actually covers a larger area on the spectrum as it is extendable using extra Lego bricks and programmable mini computers such as Raspberry Pi.

Pre-built robots, on the other hand, satisfy a different need that is the readiness of access to the robotic platform itself as a user-friendliness aspect; see Figure 1.1b for a typical scene in an activity using such a robot. They are typically programmable and runnable via software that is easily installed on common computers, without investing any effort beforehand in mechanical building. This plug-and-play quality is explicitly used as an asset to lower barriers of entry into programming and robotics, especially for younger learners where it is crucial to capture and maintain their attention early on. Moreover, plug-and-play robots that are intended for older users are also found in applications that do not require mechanical building. Undergraduate level programming and engineering instruction are examples of this type of application where the readiness of access saves time that is better spent learning the subject itself (*e.g.* the specific programming language or the operation of a specific type of sensor) rather than building the robots themselves for constructionist learning purposes. There exist such robots that serve higher-end purposes where learning of real-world level robotics and engineering (as opposed to robotics and engineering associated with “toy” situations and hardware) is desirable. For this reason, the pre-built end of the buildability spectrum consists of a much wider price range, starting from robots that cost two-digit prices intended to provide exceptionally easy robotics access to young learners, especially in underdeveloped countries, up to robots that cost four-digit prices intended to provide a rich set of precise sensors and actuators to undergraduate learners as well as researchers.

Up to now, these educational robots were used in the learning of a variety of disciplines. The most prevalent of these is undoubtedly programming, equally labeled with umbrella terms such as computer science or informatics in many R4L circles, examined over the years both within formal education and in informal learning scenarios such as workshops, competitions and at-home learning. An abundance of such works with promising results (that are both anecdotal and statistically validated) exists, many of which use the Lego Mindstorms series kits as mentioned before. These works, that commonly include the parallel learning of robotics and engineering concepts, as well as related skills such as problem solving and computational thinking, collectively target an impressively wide range of ages beginning from pre-kindergarten ([30, 31]), continuing into kindergarten ([30, 32, 33, 34, 35]), elementary school ([36, 32, 37, 38, 39, 33, 40, 41, 42]), middle school ([36, 43, 44, 45, 33, 40]), high school ([36, 44, 33, 46]) and up to undergraduate level in universities ([47, 48, 49, 50, 51, 52, 53, 54, 55]), where many other works exist at each level of education besides the ones cited here.

Starting from the undergraduate level, concepts from other computer science and engineering subjects are also seen to be explicitly taught through robots in addition to programming such as embedded systems, signal processing and control ([26, 54, 56]), concurrent and distributed systems ([26, 50]), operating systems ([50]) and artificial intelligence ([49, 57]). Still related to computer science, we find perhaps the most straightforward use of robots within education, that is to give undergraduate and graduate level robotics education where often virtual robot simulators are used as well ([58, 59, 60, 61]). These practices extend down to secondary and primary education, where robotics concepts are often simplified according to the learners’ level and intermixed with other engineering concepts not necessarily exclusive to robotics

Chapter 1. Introduction

where learning occurs particularly with hands-on, experiential interaction; works representing this scope of application throughout basic education are cited above.

Besides programming, robotics and engineering, topics from other disciplines were covered by programmable robots as well. Two of the most popular such disciplines are mathematics (including geometry) and physics: [62] investigates the effect of building Lego robots on curricular mathematics performance of learners, measured by standard tests. [63] presents a more data acquisition-oriented study where rounding, relationship between circles and their diameters, as well as very basic statistics are learned with built mobile robots and the data gathered from their sensors. [64] presents the hands-on learning of ratios using gears and pulleys within mobile Lego robots built by learners. [65] touches the simpler yet concept of addition and subtraction with the motions of a tangible, mobile robot built again with Lego. [66] presents a mini-curriculum that includes some geometry concepts such as distances and angles; [67] presents a much more comprehensive curriculum covering many mathematics and geometry topics. Among more broad studies, [12] covers mathematical concepts such as decimal numbers, graphing, multiplication as well as physics concepts such as forces and heat transfer (and even some chemistry concepts such as acids and bases). Newtonian motion and kinematics unsurprisingly seems to be a popular topic within physics, exemplified by [12, 68, 69, 70]. Besides these representative studies, teachers' opinions on robot usability in learning evidence the inclination towards mathematics and sciences: [71] gives such opinions on a variety of subjects (teachable with a particular robot in this instance) that clearly lean towards mathematics and sciences, where mathematics is more explicitly stated, along with physics, to be potentially teachable with the help of the robot.

To the best of our knowledge, learning of other subjects outside of mathematics and physics through tool robots are found in few, emerging instances of both published and unpublished work³. See [72] where basics of evolution, a topic in biology, is taught with a literal implementation of the aforementioned *learning with evolutionary dynamics* strategy, and [73] where learners build and program robotic models of some biological mechanisms and structures, such as plants and organs, in order to invoke hands-on learning. Finally, see [74] that provides a tangible demonstration for learning molecular reactions and bonding, a topic in chemistry, without involving programming. These, along with the aforementioned body of research strongly targeting programming, robotics, engineering and sciences, show the level of accomplishment and suitability of tool robots for the Science, Technology, Engineering and Mathematics (STEM) curriculum, as well as for raising interest for these disciplines.

Robots as Agents

The *robots as agents* approach emerged from the field of Social HRI that is a distinct branch of HRI concerned with building robots that are capable in social, emotive and cognitive aspects of

³For instance, see <https://www.thymio.org/fr:thoolproject> (in French) for educational content on the five senses, a topic from Biology.

proximal interaction with humans ([75]). Practically all such robots display anthropomorphic qualities to some degree and are more often than not humanoids; see [76, 77] for a more minimalist approach that challenges these norms through a robot concept co-designed with children. The use of social robots for education is a very recent approach whose first instances date back to about a decade earlier, when uses for other closely-related purposes already existed such as aiding people with special needs (for example the elderly as in [78] or children with autism as in [79, 80]) where promising results were obtained that justified the use of robots in such scenarios. As their potential capabilities were being shown, it did not take long before social robots were introduced to broad education for general needs, as opposed to serving special education or other special needs.

This introduction naturally required the clarification of the actual role of these socially capable robots within educational scenarios. A clear answer at that time was that robots could be effective *tutors*, where the central belief is that the process of keeping learners in emotive and cognitive states that promote learning can be automated through robots that teach in manners similar to human educators. This approach is explained by *e.g.* [81] and exemplified by many works cited throughout this section; a typical scene in an activity using the robot in such a way can be seen in Figure 1.1c.

A second approach that emerged later is the use of social robots as *peers* to learners, where robots do not directly teach but instead more indirect methods are preferred. Studies following this approach are undoubtedly more rare, and a common methodology in the robots-as-peers paradigm is to “disguise” the robot as a peer who is in need of the learners’ help. The rationale behind this methodology is that such social robots were observed to arouse a strong, persistent caring desire in young children ([82]), and appropriately designed robots may utilize this caring desire to influence the learners to teach the robot itself who plays the role of the learner; this method was previously labeled *protégé effect* ([83]). This effectively induces learning-by-teaching, a learning method where the learner takes a more active role to improve the overall efficacy of learning. This method is exemplified by works such as [84, 85, 86]; a typical scene in an activity using the robot in such a way can be seen in Figure 1.1d.

Within both of these views, the socially capable and programmable learning and teaching agents present many opportunities potentially not easily or inexpensively accessible with human tutors and peers (those marked with ► not exclusive to robots but also achievable with non-robotic computational agents or devices to some degree):

- Increased learner engagement due to robots simply being present
- Automation of bodily interaction, implementing techniques such as total physical response (use of whole-body actions in language learning)
 - One-on-one tutoring or aiding, application of personalized learning strategies
 - Modeling of and catering to the affect-related states experienced by learners
 - Automated monitoring of and adaptation to the abilities and progress of individual learners, as well as planning the future accordingly

From the learners' perspective, [87] shows that young children tend to perceive animism (life-likeness) in a robot with social competencies, namely, they ascribe cognitive and affective qualities to the robot itself. This implies both a capacity and a challenge for social robots designed to interact with children: These "life-like" robots may more easily garner children's engagement by virtue of human-like expectations from them, while their design and implementation must match these expectations to avoid negative reactions when these expectations are not matched. This is indeed an ambitious technical goal, and many studies to date using social robots unfortunately fall back to Wizard of Oz techniques to be able to conduct experiments due to the sheer difficulty of building software and hardware that achieves this. [88] presents some foundational developments that target matching these expectations in realistic settings. These developments belong to an extensive list of modules which includes speech recognition and synthesis, natural language understanding and generation, cognitive architectures with memory, human user modeling and generation of bodily expression. Despite these key developments, it is clear that there is still much room for future improvement.

When we consider the target learning domains touched by social robots up to now, we encounter a significantly different and arguably more diverse spectrum of subjects compared to tool robots, where STEM teaching is prevalent. The learning of secondary languages seems to be a recurring theme throughout the history of social R4L where an abundance of scientific effort exists, effectively going back to its earliest days; [89, 90, 91, 92, 84, 93, 85, 94, 95] are some notable works. There is certainly a strong research interest (that continues today) in using agent robots to teach language as opposed to tool robots, perhaps due to natural text/speech recognition and synthesis capabilities of agent robots that are essential to a task such as teaching language. Other subjects that were previously studied and are closely related to language are handwriting ([86]) and sign language ([96]). We further find mathematics as another popular subject, exemplified by [97, 98, 99]. Finally, the instruction of some non-curricular subjects are also encountered, including health literacy for unhealthy children ([100]), nutrition ([101]), storytelling ([102]) and dancing ([103]). Regardless of the subject, exploiting some social aspect related to the learning content (*e.g.* verbal interaction in languages, nonverbal interaction in dancing, creativity in storytelling) is unsurprisingly a common theme.

1.1.3 Synergies, Gaps & Motivations

The history of R4L, briefly given above within distinct branches of research, reveals certain synergetic themes, as well as divergent ones, among the bodies of previous work. For one, using robots for learning seems to be an attractive prospect for researchers as well as educators, regardless of the nature of the robot being used, for sourcing extra enthusiasm, "charm" and thus engagement from learners by the virtue of robots being physically active and responsive machines; they are exciting and are not yet ubiquitous in daily life. From another perspective, intelligent and programmable objects (whether they are programmed by the researchers, educators or the learners) is certainly a powerful asset in the learning environment that enables the automation and reproducibility of tasks as well as recording and processing data

related to the learning and teaching processes, which does not only apply to robots but to other “networked” computational devices as well.

On the other hand, current research on tool robots and agent robots seem to diverge in the philosophy of how learning works with robots and what the added value is of the robot within the learning environment: The tool robot approach is considerably closer to the original constructionist philosophy of learning where robots were first imagined as tools that facilitate thinking about the target concept to be constructed by the learners. The immediate next step in development brought such robots into the realm of the truly buildable, letting learners construct the robot both on the hardware and software levels in a hands-on manner, as a means of constructing knowledge. On the other hand, the younger field of social robots for learning approaches robots from a more “humane” perspective by virtue of the more recent developments in social HRI that permit the technical realization of human-like behaviors. From this perspective, the social dynamics between the learners (humans and robots) and the teachers (again, humans and robots) are more interesting to explore than how knowledge can be constructed with robots as physically manipulatable facilitators. Instead of providing this physical window to the learning content, many social agent studies prefer setups where a social robot and learner(s) interact with the help of a conventional touchscreen that provides as much content as provided by regular social interaction methods, in order to overcome the technically limited input-output capabilities of the robot such as speech recognition. However, this perspective may more easily fit to the classical understanding of teaching where learners are taught formally within classrooms by teachers. By this, it may be argued that it is easier to imagine and create the added value of social robots to learning compared to tool robots.

From the learning subject perspective, a clear distinction can be seen between the two profiles belonging to the two branches of research where both approaches seek where they fit more naturally. State-of-the-art tool robots certainly fit STEM subjects better since these subjects are more likely to highlight inherent qualities of such robots, such as the ability to bring programmed code into the physical world, access to engineering materials (mechanisms, electronics and related signals *etc.*) and repeatable and measurable sensing and actuation. There are many insights on how these qualities map to (especially constructionist) learning of specific concepts and skills within STEM, as shown by the many works cited throughout this chapter. On the other hand, the distinct approach of social agent robots does not attempt to map the inherent, “robotic” qualities of robots onto the learning practices and matter, but instead aims to enrich teaching and learning from other perspectives, such as social and affective. For this reason, it is often found that the focus and practices of works utilizing such robots is less on specific learning subjects or curricula, and more on enriching the learning process. Compared to tool robots, this particular disassociation from specific bodies of disciplines (such as STEM), has arguably led to a more diverse set of target teaching subjects in a manner less focused on providing immediately applicable curricular content.

The essence of this argument is that these distinct approaches have strengths and added educational values inherent to them, and we believe that there may be other, unexplored

approaches beyond them. In other words, we feel that there is a “gap” between these already explored approaches, and this gap resonates with the relationship between the learning content and the physicality (*i.e.* hands-on nature) of interaction: The exploitation of physicality has so far attracted learning through building and STEM applications, whereas the exploitation of social interaction, one of whose strengths is to open perspectives to a different and wider range of learning domains, has arguably overlooked physicality. The central question that positions this thesis among the state-of-the-art is thus the following: *Can we explore this gap with a novel approach of our own which not only borrows key ideas that help create the strengths of the existing approaches, but also benefits from other ideas that aim to create new robotic roles and added values in R4L?*

It may be argued that it is thus advantageous to combine the existing two approaches into one in order to obtain a sort of low-cost tool robot with social capabilities that will embody the strengths of both, which can then be augmented with other capabilities to further pursue novel added values and roles. However, we find the straightforward combination of these two approaches overly simplified and not fruitful in terms of scientific contribution. From another perspective, we do not believe that this gap is one that must be bridged in order to, perhaps, reconcile the existing two approaches. Instead, we believe that it marks another area in the vast design space that is R4L, and that it deserves in-depth exploration. Therefore, the proposed approach in this thesis will aim to offer a new perspective on the use of robots that features some of the ideas that drive the existing approaches, while investigating others that we believe are potentially profitable in terms of contribution to learning. The forthcoming sections describe this new perspective, explored within the *Cellulo* project.

1.2 Cellulo Project

1.2.1 Introduction – Research Goals

This thesis reports on the ideas, methodologies and outcomes of the *Cellulo Project*⁴ from its inception until the present day. The robots along with the related software and hardware materials created within this period of research is thus called the *Cellulo Robots* and the *Cellulo Platform* (which includes the Cellulo Robots) respectively. The goal of the Cellulo Project, as mentioned before, is to explore the aforementioned gap in R4L where we investigate new roles and added values to robots within education. To do this, we begin by envisioning ways in which we can differentiate ourselves from the existing approaches with meaningful rationales. We form these into goals that drive our research:

Build and effectively use robots for learning that are perceived as everyday objects rather than robots by both learners and teachers. – State-of-the-art robots, regardless of being tool-like or agent-like, are built to be perceived as robots by learners and teachers alike. This brings certain advantages in the design and execution processes of learning, and was

⁴See <https://chili.epfl.ch/cellulo>.

effectively used up to now. We aim to explore a different case where our robots are built in a manner that does not evoke the “robotic feeling” nor robotic capabilities; we hypothesize that this may ease the acceptance of robots within formal learning environments, as well as allow us to load non-robotic and non-agent roles onto our robots that were previously impractical.

Build simple robots for learning, perceived as tools, that promote other uses than building or programming.

– Tool robots realized up to now feature some form of mechanical buildability and/or programmability with very few exceptions; this allowed constructionist learning with notable ease. We aim to explore cases and ways where tool-like, low cost robots can be used without enforcing programmability or buildability. We hypothesize that such ways can trigger uses for robots that were not envisioned before, including the teaching of previously unexplored curricular subjects through robots.

Build robots for learning enriched with previously unpopular affordances and materials.

– R4L have explored certain well-defined robotic affordances and materials up to now: Tool robots feature *e.g.* mechanical building of robots through easily combinable parts and programmability through easily usable actuators and sensors, whereas social agents feature *e.g.* natural communication through speech, as well as the integration of portable computers shared among learners and robots. We believe there are other materials and affordances whose uses with robots are not yet well explored; prospective examples are tangible interaction that helps provide a physical connection to phenomena, and paper that is a low-cost, readily modifiable and easily redistributable medium. We believe that by introducing the possibility of working with a more diverse set of affordances and materials that likely provide original added values to learning, we will allow our robots to be incorporated into a larger variety of learning activities.

Build robots that are part of social interactions among learners and teachers without necessarily being social agents.

– Social robots up to now have been envisioned as capable agents that are an integral part in defining the social structure within the learning environment. Tool robots on the other hand, require more care when their social role is determined within the learning process when multiple humans are involved. We hypothesize that we can build tool-like robots whose social role is more easily imagined and can support multiple human learners, in the presence of the human teachers, in a more straightforward manner.

Build tool-like robots whose added value to curricular learning is easier to imagine by teachers.

– Tool robots were used in STEM learning effectively up to now where instances of scenarios imagined by the collaboration of teachers were encountered. Social robots saw less educator collaboration yet, but feature arguably wider potential curricular support (in a “subject-agnostic” manner) through social capabilities. We hypothesize that we can build tool-like robots, without explicit social competences, in order for teachers to more easily imagine the added value for curricular subjects, both within

STEM in ways previously unconsidered, and beyond STEM.

Use existing classroom materials and practices to improve the integration of our robots into formal education. – Robots and use cases were built within R4L up to now without particular regard to what already exists within the classroom, both equipment and practice-wise; this caused the robots, regardless of whether they are tool-like or agent-like, to be perceived as externally added technologies. We hypothesize that we can build robots from the ground-up with consideration of classroom practices, as well as previous work that shows what works and what does not work particularly well, in order for them to become a natural part of the classroom.

In the below sections, we present our robotic learning platform concept designed with the intention of realizing these research goals.

1.2.2 Conceptual Design & Key Ideas

We now proceed to conceptually design our robotic platform within the frame set by the above research goals. From the topmost perspective, we decide that our platform shall be composed of simple, low-cost robots to boost (mainly economic) acceptance. These shall be palm-sized mobile robots to ease the physical interaction with them, and shall further be identical and interchangeable to let teachers more easily imagine the conception of scalable learning activities with these robots that don't contain complex parts. Our robots shall operate on printed sheets of paper that feature graphics, with which we aim to garner additional acceptance for our robots and ease their conceptual management through their close association with this well known and versatile material. Finally, we decide to leverage the computational power and interaction opportunities given by mobile consumer computers (as done in social R4L) that are likely to be present within learning environments, through *e.g.* the possession of tablets by schools or smartphones by individuals, which will let us offload the computational power to these devices and design our robots with simpler and lower cost components.

We envision that the primary role that our robots play is the representation of objects both abstract and concrete where the traditional representations are either limited in some way, improvable with previously unused affordances, or simply impractical. These objects may be point-like, with certain sizes paralleling the size of the robots, or exist in shapes collectively represented by multiple robots. Through this kind of representation, multiple diverse properties of the represented objects are opened to the learner; some of which are its physical, tangible presence, its kinematic motion including the velocities and accelerations, the forces that act upon it and its behaviors in collective groups. Moreover, a secondary role is envisioned where robots exist as points of tangible interaction with the learning activity where a closer, co-located interaction is enabled with the represented objects (*i.e.* robots playing the first role). At this point, to clarify our envisioned platform and the learning environment surrounding it, we provide two conceptual activities in Figure 1.3. Following this, we provide the key ideas that shape this concept and how the real platform will be built throughout this thesis.



(a) *Solar System*: Robots simulate planets orbiting the sun. Learners can tangibly move the planets to alter their orbits or even attempt to remove the sun to see what happens when the major source of gravity disappears.



(b) *Molecules*: Robots simulate atoms with Brownian motion. Learners can tangibly interact with atoms to experiment with conditions under which molecules form and break down. We acknowledge that the design of the above scene was done by Dr. Séverin Lemaignan.

Figure 1.3 – Concept Cellulo activities that highlight various design ideas, focusing on two dissimilar subjects that feature particularly microscopic and particularly macroscopic objects.

Ubiquity

The ubiquity principle refers to our effort of blending our robotic platform into the daily learning routines of classrooms. To enable this, we follow the analogy of “pen and paper”: Our robots (the “pens”) should be a set of pervasive yet unremarkable tools that might as well have been part of the classroom without our intervention. While they should not evoke the feeling of robotics when looked at or interacted with, they should still appear to be robust and easy to use at first glance, even though they may conceal deeper affordances depending on the activity. Following the pen analogy, our robots should be found at a low price point in order to redirect the attention of educators from the number of robots that can be placed within classrooms and their cost-effectiveness, towards the use and added value of activities enabled by these robots. To achieve this, our robots should feature readiness of connectivity with mobile consumer computers (such as tablets, smartphones and laptops) that are becoming ubiquitous within classrooms and daily life in general, where computational power needs will be offloaded. Moreover, to enable straightforward replaceability of our robots similar to pens, they should be designed in such a way that does not elicit affective bonding to singular learners, contrasting the “ownership of built robots” principle of constructionist tool robot learning invoked by many previous works (some instances are [31, 36, 64, 72]). By these design choices that let our robots become “a drawerful of Cellulos” as if they were “a cupful of pens”, we aim for easier integration of our robots into the classroom ecosystem.

Practicality

The practicality principle refers to our effort of building our robotic platform in a manner suitable for classroom use within realistic lessons. To enable uninterrupted use within such scenarios, our robots must be flexible yet reliable and must not feature complex and fragile hardware and software typically found in robots. Furthermore, in order to prevent additional workload for teachers, the platform and the activities should be of a “plug-and-play” nature where time consuming initialization and calibration typical for robotics should not be found. Moreover, the use of our platform and activities should not require calibrated hardware installations that typically consume space and time to operate, and rely solely on materials that are trivial to deploy and put away. Following the analogy of “pen and paper” and in addition to tablets and smartphones, we choose paper to support our robots and host our activities, for the reason that sheets of paper are easy to reproduce and simple to integrate into the teaching methods in a way that minimizes orchestration load (see [104] for these ideas involving paper). In short, simple and robust user experience for both learners and educators should be considered with top priority when designing our platform in order to boost its practical acceptance into real-world classrooms.

Versatility

Versatility describes our effort at building a learning platform applicable to a broad range of learning scenarios and disciplines, as opposed to a tool bound to the teaching of a particular subject, such as robotics. As much as possible, our robots and the platform in general should provide a rich but simple set of affordances that are easy and natural to map to a range of topics, objects and phenomena found in an as large as possible spectrum of disciplines. We envision the learning of a distinct topic within a discipline to take part within a well-defined *activity* that is accompanied by its distinct paper sheet(s) and a software application, to ease the transition between highly dissimilar topics that use the same robots by reducing this transition to simply closing an application and launching another one on demand. In general, to better enable this versatility through the growth of our platform's activity portfolio, we should focus on collaborating with educators as teams of engineers and designers instead of relying on providing a programming language to educators and letting them create learning activities on their own.

Tangibility

The tangibility principle is inspired by the hands-on learning principles of the constructionist tool robot literature and describes our effort in building our platform as a tangible “window” to phenomena that are typically intangible. As such, the end result of our platform design should feature objects (both robots and sheets of paper) that learners are supposed to touch when interacting with them. This is not necessarily only an issue of building compliant and robust robotic mechanisms, but rather inherent to the design of the robots and activities that should be ergonomic and should exploit the fact that the robots are meant to be touched and manipulated, through physically experiential design of the learning process. Each of our robots thus brings together the functionalities of an input device, an output device and an autonomous mobile robot, where these interaction modalities should be straightforward to modulate depending on the activity and the particular role of the given robot.

Multiplicity

The multiplicity principle refers to both the multiplicity of our platform's elements and the multiplicity of learners catered to within activities. We envision that our platform's elements, namely the robots, mobile devices and paper sheets, should be easy and straightforward to duplicate to enable multiple activities running in parallel, as needed. This is enabled by the affordability of our robots, ubiquity of mobile devices that are likely to be present in large numbers, and the low cost and effort of replicating paper sheets. Moreover, as a design principle, the activities should as much as possible feature the possibility to scale up and down as needed, utilizing more or fewer number of robots, to support the desired number of learners within the same activity in order to thus support the desired level of collaborative learning through the social dynamics of teams working with the same set of robots in the

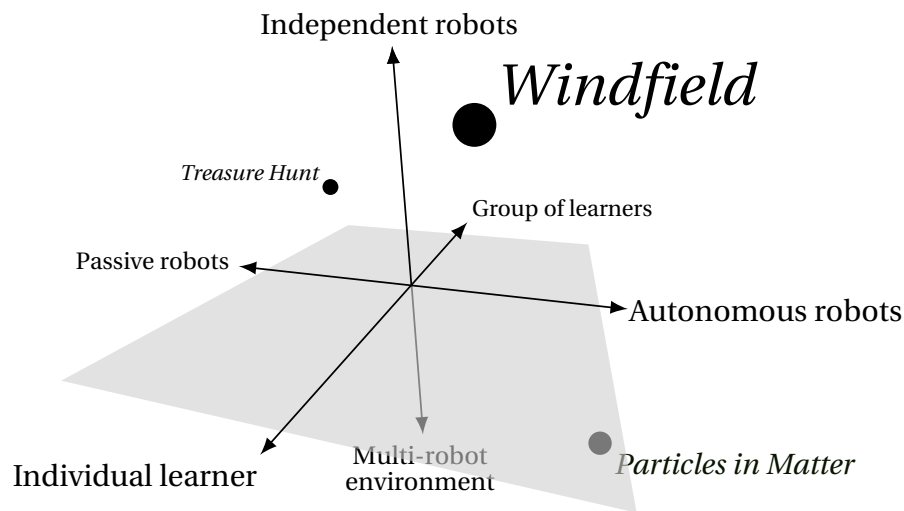


Figure 1.4 – Three dimensions of Cellulo activity design envisioned so far. Passive *vs.* autonomous robots axis denotes the spectrum along which robots are manipulated more or less by learners while moving less or more themselves. Independent robots *vs.* multi-robot environment axis denotes the spectrum of the importance of collective robot behaviors in providing meaning to the activity. Finally, individual learners *vs.* groups of learners axis denotes the spectrum along which support for larger or smaller groups of learners interacting with the same activity is provided. Naturally, an activity may occupy a volume within this space as opposed to a point. The three marked activities refer to the three activities presented throughout this thesis, namely *Treasure Hunt* presented in Section 2.6, *Windfield* presented in sections 3.5 and 4.4 and *Particles in Matter* presented in Section 5.2.4. We acknowledge that other dimensions beyond these preliminary ones can be imagined as well, such as robots being shared *vs.* assigned resources (to individual learners), heterogeneity *vs.* homogeneity of robot roles, and the activity workspace being shared *vs.* split.

same activity. Regardless of the number of learners and the number of parallel activities running within the same classroom, the same overall “pool” of identical robots is used. This allows the implementation of one-robot-to-one-learner, many-robots-to-one-learner and many-robots-to-many-learners scenarios. Based on the multiplicity of these two aspects, as well as the aforementioned spectrum of interaction modalities, we define an initial activity design space allowed by our platform, given in Figure 1.4.

1.3 Plan of this Thesis

Throughout this chapter, we provided the background perspectives and then our own perspective for R4L, which depends on the building of an entirely novel robotic platform from scratch. However, due to the large volume of design and development that will be necessary to reach our end goals, which includes the conception of software as well as electronic and mechanical hardware, we will approach this building process iteratively where we design, implement and validate incremental units of technology in a cyclic manner that bring more and more of our

envisioned platform into existence at each step. This will allow us to revisit and revise our design, pursue emergent properties of our platform and adapt our development accordingly.

While describing these iterations, which we call *Phases*, we will focus on disseminating our scientific contributions where appropriate in a broad manner instead of as specific technological enablers of our platform, in order to benefit various scientific communities and not necessarily only R4L. Where possible, we will explicitly cite our own scientific publications that present these contributions. When the entirety of the work in this thesis is considered (both previously published and not yet published), the contributions of other researchers and professionals than the author of this thesis will explicitly be noted within the introductory sections of the respective chapters. The work that is not noted to involve such contributions are to be taken as the exclusive work of the author of this thesis.

Each Phase will feature its own framing within the literary background (that expand well beyond R4L into disciplines associated with the technology being developed) and well-defined problem statements. Following these, we will detail our design and development processes, as well as the implementation of our prototypes. Finally, each Phase will feature an extensive validation step, divided into two sub-steps: First, we will validate our developments within supervised (*i.e.* “laboratory”) conditions to obtain precise and absolute performance measures, which will be beneficial in defining the isolated limits of usability of our developed technologies regardless of whether they are used in our platform or not. Second, we will validate the related developments within ecological (*i.e.* “real-world”) conditions with real users (learners, and later on, teachers), in the presence of expected noise, within the context of genuine activities featuring our platform. An exception will be the final Phase where we will focus entirely on ecological validation, as we believe that it is needed at that point for better scientific contribution to R4L. Regardless of their nature, these validation rounds will allow us to confirm and reflect on the way that distinct components of our platform work.

The entirety of our effort will be composed of four such Phases:

Phase I – Localized Tangibles (presented in Chapter 2): We will first build *accurately localized tangibles*, meaning that we will be able to know where our tangibles are on our activity sheets with high accuracy. Doing this will let us introduce a localization technique not well known into the robotics community, and carry out its supervised performance validation previously absent from the literature. We will then introduce our tangibles to children in order to measure the real-world performance of our platform and the legibility of its initial set of interaction paradigms for the first time.

Phase II – Actuated Tangibles (presented in Chapter 3): We will then integrate *locomotion* into our tangibles to make them fully functional mobile robots, through a novel mechanism design. After carrying out its supervised performance validation, similar to the previous Phase, we will once more test the interaction with our actuated tangibles with real learners, through an “in-the-wild” experiment that targets learning gains.

Chapter 1. Introduction

Phase III – Haptics with Actuated Tangibles (presented in Chapter 4): We will integrate *haptic feedback capabilities* into our mobile robots in order to explore the novel concept of low-fidelity, multi-point planar haptic interaction that emerges as an affordance opportunity from the design of our platform. Following the supervised validation step where we measure the ranges of usability of our robots by humans, we will design a full lesson with our platform's current capabilities which we will use to show quantitative learning gains with real learners.

Phase IV – Building Tangible Swarms (presented in Chapter 5): As a final step, we will enable *collective behaviors* with a large number of our robots through a software framework, to which we will contribute new extensions, in order to explore the novel concept of tangible robot swarms. We choose however not to validate this emergent property of our platform in laboratory conditions, as we do not find enough scientific contributions in doing so. Instead, we will do a more detailed ecological validation study through a lesson co-designed with a teacher and carried out with real classrooms of learners.

Within each Phase, specifically in the validation steps, the results of statistical tests will be given with conventional notations, using well-known and widely used symbols. Where used, the symbol \pm will denote a mean M and a standard deviation SD in the form of $M \pm SD$. Following these Phases, in Chapter 6, we will revisit our initial research goals and how the development and contributions presented throughout the thesis address these. We will then conclude with immediate future work, impact to the scientific R4L community, as well as more broad perspectives we believe we opened by building and validating the Cellulo platform.

2 Phase I – Localized Tangibles

2.1 Introduction

2.1.1 Background

This chapter describes the first phase of the development of the Cellulo platform, namely the development and validation of localized tabletop tangibles, with the purpose of working towards fully mobile robots. The keyword here is “localized”, or more generally “localization”, that describes the problem of recovering the pose of an object (the tangibles in our case) with respect to the environment. A fundamental problem in robotics and other domains, localization was offered solutions that take on widely varying forms depending on the constraints and requirements. These include:

- Deployment requirements (*e.g.* beacons, cameras, tags) and their end-user friendliness (*e.g.* may need to blend into the environment or be “invisible”) if they are to be deployed for a long term in human environments
- Robustness against sources of occlusion and noise that are fundamentally present in the application (*e.g.* humans)
- Power usage if battery powered devices are present and take part in the localization
- Monetary cost of devices and deployment
- Accuracy and precision requirements
- Computational efficiency of algorithms involved, possibly to achieve real-time operation
- Scalability with respect to the number of objects that are localized

At the topmost level, localization separates into indoor and outdoor localization that impose distinct requirements when the above categories are considered. Our focus, indoor localization, usually requires higher accuracy within more controlled environments, but suffers from the lack of a ubiquitous technology such as the Global Positioning System (GPS) that is very commonly used in outdoor applications. Therefore, the methods used for indoor localization of objects tend to depend on the specific application scenarios.

2.1.2 Problem Statement

Following these lines, our application scenario is framed within the context of an indoor environment (*i.e.* the classroom) where potentially many tangibles are to be localized on a tabletop in 3 Degree(s) of Freedom (DOF), namely in planar translational (x, y) and rotational around the vertical axis (θ). Humans (*i.e.* teachers and learners) are expected to closely interact with the tangibles, including moving them around and possibly kidnapping them (thus defeating localization techniques relying only on dead-reckoning) while potentially covering the objects completely with their grasp. Namely, the proposed solution must:

- Require minimal deployment effort (with little to no calibration and easy undeployment) to fit the classroom dynamic where the platform is an on-demand tool that may be called upon or removed at any given time
- Be totally robust against occlusions due to user manipulation that is a natural and essential part of the platform's operation
- Be robust against kidnapping; ensure absolute localization
- Consume as little power as possible from the battery of tangibles to ensure the autonomy lasts for at least the entire duration of the lessons
- Cost as little as possible to not induce economic stress to schools, especially as the number of tangibles increases, even if it implies sacrificing other qualities
- Provide acceptable accuracy for a human interface device that is further enhanced by locomotion and haptic feedback (discussed in the following chapters), as localization may potentially be used as the main source of positioning/encoding for all of these modules
- Recover the pose in a short enough time to allow real-time framerates (and possibly more) required by the above three aspects of the tangibles
- Allow the localization of potentially tens of tangibles in a single workspace, *i.e.* not saturate when number of tangibles increases, in order to allow swarm applications (discussed in the following chapters)

Given these requirements, we present in the following section the state-of-the-art of available localization methods and technologies that are capable of 3DOF planar localization.

2.1.3 Related Work

[105] gives a comprehensive survey of absolute indoor localization methods; Table 2.1 summarizes the characteristics of the main ones, in regard to the application context introduced above. At a glance, several methods appear attractive due to key advantages, such as Infrared (IR) light beacons, being simple and affordable; or Ultra Wideband (UWB), being non-intrusive. However, IR beacon sensing is not robust against occlusions due to clear line-of-sight requirement; and UWB is only recently becoming commercially available and affordable.

When tangibles and tabletop robots in the literature are considered, a very popular method is

Method	Cost per device	Accuracy	Deployment requirements	Occlusion robustness	Scalability	Processing load on device
Infrared light beacons	Low	Sub-mm	Beacons	None	Low	Very low
Structured light (<i>e.g.</i> Kinect)	Mid	Few cm	None	Moderate	Very low	High
Laser scanner (LIDAR)	High	Few μm	None	Moderate	Low	High
RF (Wi-Fi, Bluetooth, RFID <i>etc.</i>)	Low	Sub-m	Beacons	Moderate	Moderate	Very low
Ultra Wideband (UWB)	Potentially low	Few cm	Beacons/scanners	High	Moderate	Very low
Fiducial tag on device Motion capture	Very low	Sub-mm ([109])	Camera(s)	Moderate/ Full	High	None
Deployed fiducial tags, camera on device	Low	Sub-mm	Optical tags, possibly on paper	Moderate	High	High
Deployed capacitive patterns, sensor array on device([110])	Low	Few mm	Capacitive board	Full	High	None
Deployed optical patterns, camera on device([111, 112, 113])	Low	Few cm/ Sub-mm	Optical patterns, possibly on paper	High/Full	High	High/ Low

Table 2.1 – Prominent absolute indoor localization methods in the literature ([105] unless cited otherwise). Where used, *device* describes the tangible whose pose is recovered. Notably attractive qualities and crucial shortcomings of methods marked in green and red respectively.

Chapter 2. Phase I – Localized Tangibles

to place fiducial markers on each tangible/robot and track them with a (set of) deployed and calibrated camera(s), such as [106, 107, 108]. While this method offers high accuracy and is suitable for both tangibles (*i.e.* camera deployed on the bottom and *not on top* of the table to allow grasping) and non-manipulated robots (*i.e.* camera deployed either on top or bottom); it is not practical to deploy and calibrate the camera setup every time the platform is to be used. Instead, the setup would require that it remains untouched in the classroom at all times, potentially reducing its chances of acceptance due to the undesirable intrusive nature of this requirement.

This deployment issue naturally encourages the idea of swapping the camera(s) and the fiducial marker(s); namely equipping the tangibles with cameras that perceive the deployed fiducial markers, many examples of which are found in [105, Section 4.3]. With this approach, while accuracy remains high, occlusions may again become a problem since the camera image must contain at least one marker in theory to successfully localize. Furthermore, the (typically costly) image processing must now run on the tangible, or the image must be wirelessly streamed to a powerful server, both of which are not practical.

From here, we approach the idea of replacing singular fiducial markers with dense optical patterns, such as the ones found in [111, 112], that are fundamentally more robust against occlusions. These extend fiducial markers into patterns that encode the global absolute position, allowing localization when any visible part of this pattern is decoded. The accuracy of these methods tend to decrease (as do the accuracy of fiducial markers) with increasing distance between the camera and the patterns. Therefore, ideally, the camera should be as close as possible to the patterns while still capturing the minimum number of required pattern elements. However, the typical high processing load on the mobile device remains a problem.

The final step in our exploration is to consider miniaturizing these patterns and bringing them closer to the tangibles, which leads us to microdot patterns such as the Anoto pattern found in [113] and other related patents. By this, camera image size can be greatly reduced, decreasing the processing power needs, so much so that image processing can now run on low-end, low-power processors hosted on the tangibles. Furthermore, the microdot patterns can still be printed by consumer printers, allowing a practical deployment medium that can host graphics and be produced as large as posters. Placing these paper sheets directly beneath the tangibles completely eliminates the final shortcoming that is robustness against occlusions from user manipulation, by virtue of the closed optical system that is out of reach of the user. Subsequently, the optimal accuracy can easily be recovered by minimizing the camera-pattern distance during development.

In the following sections, we detail the theoretical working principles of the Anoto pattern (that is not our contribution but was previously presented in the aforementioned patent and others) and our development process where we design and implement the software and hardware running the image processing pipeline that decodes the pattern. Our pipeline extends and concretizes the one provided solely as an example in the patents; by this, we provide a level of

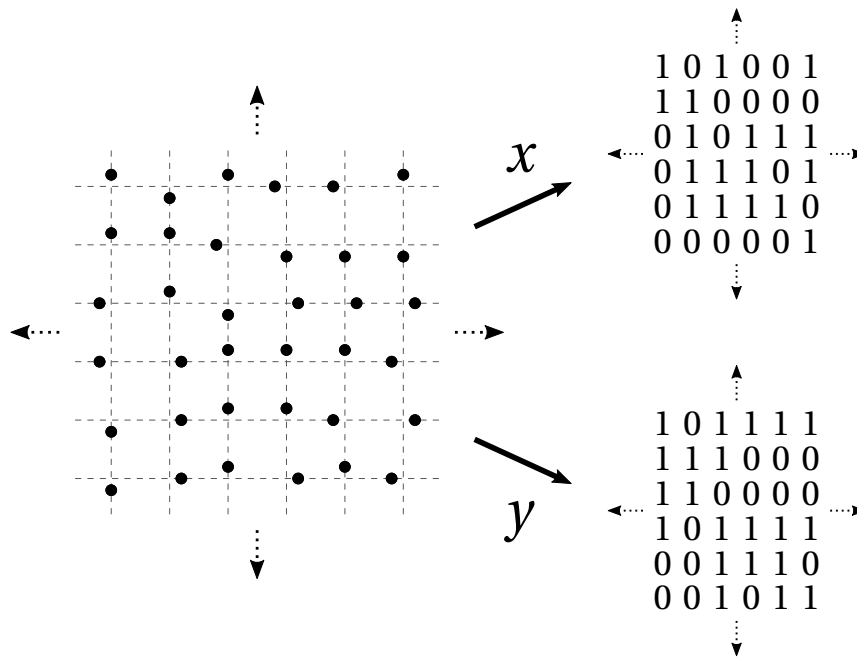


Figure 2.1 – Organization of printed microdots in the Anoto grid, continuous both horizontally and vertically. Dashed lines do not physically exist. Each dot may be in one of 4 offset positions with respect to the grid intersections (up, down, left, right), encoding two bits of information. This way, the pattern carries two independent binary matrices for x and y that are both continuous over 2D space.

detail and clarity required for scientific impact, that we find is missing from the patents and the rest of the literature. Furthermore, we release our pipeline as open-source software, which we use to rigorously characterize the 3DOF localization performance. We had previously published this pipeline and performance characterization in [114]; since then, we significantly improved the dynamic robustness (*i.e.* during motion) and framerate, and we report the most recent performances in this thesis. Moreover, we acknowledge that the theoretical study and the software implementation was done by Lukas Hostettler, and was previously presented in his Master’s thesis found in [115].

2.2 Theory – Location-Coding Dense Optical Patterns

2.2.1 From Microdots to the Primary Difference Sequence

The Anoto pattern is composed of microdots arranged in the manner seen in Figure 2.1 that uniquely identify absolute positions when a small portion is decoded, while also remaining practically imperceptible when viewed from a distance by a human. The pattern is made of four symbols (*up*, *down*, *left* and *right*) corresponding to the relative position of each of the dots to the closest grid intersection. Each of the four symbols encodes two bits, one for x and one for y . Therefore, the dots must first be perceived and the symbols they are corresponding

to must be identified. This way, the bits encoding the x position and the bits encoding the y position can be obtained.

At the core of the encoding lie quasi De Bruijn sequences. Given an alphabet (in our case, $\{0, 1\}$), such a sequence of order n contains every possible string of length n from this alphabet at most once¹. Given this, we first consider the encoding ensured by the x bits, organized in columns. In every column, the same quasi De Bruijn sequence of order 6 and length 63 (called the **main number sequence**, contains every string of length 6 in one and only one index, except 111111) is found in a cyclic manner; the only difference is that in every column, the sequence is placed with different predetermined offsets. If any consecutive 6 bits from a column are read, the index of these 6 bits within the sequence can be uniquely determined thanks to the De Bruijn property. Therefore, given 6 dots in 6 adjacent columns (*i.e.* any 6×6 matrix of the pattern), the offset differences of each consecutive column pair can be uniquely determined, resulting in a unique string of length 5, whose alphabet is $\{0, \dots, 62\}$ (see [116, Figure 4] for a visual representation of this mechanism). This string is the same for the same 6 columns regardless of the specific starting row index of the 6×6 matrix, and this ensures that these columns encode the unique x position with the unique string of length 5. This is the true power of the Anoto pattern.

With the above organization, any given set of columns $i, i + 1, i + 2, i + 3, i + 4, i + 5$ encodes the string $d_i d_{i+1} d_{i+2} d_{i+3} d_{i+4}$ where d_k is the unique offset difference between column k and column $k + 1$. Therefore, every 6 consecutive columns can theoretically encode an arbitrary symbol among $63^5 = 992,436,543$ unique symbols, depending on how the offsets, and therefore offset differences, are chosen. However, these symbols must correspond to the x coordinate, therefore they must be continuous along the column indices. In other words, if columns $i, i + 1, i + 2, i + 3, i + 4, i + 5$ encode the coordinate x through $d_i d_{i+1} d_{i+2} d_{i+3} d_{i+4}$; columns $i + 1, i + 2, i + 3, i + 4, i + 5, i + 6$ must encode the coordinate $x + 1$ through $d_{i+1} d_{i+2} d_{i+3} d_{i+4} d_{i+5}$. The sequence of these offset differences d_j is called the **primary difference sequence** and is encoded in the columns, as explained above.

2.2.2 From the Primary Difference Sequence to Actual Coordinates

The first step to ensure the aforementioned continuity is to artificially restrict the symbols in the primary difference sequence to the alphabet $\{5, \dots, 58\}$. This way, each symbol d can be decomposed into its four “unique digits”:

$$d = 5 + \alpha + 3 \cdot \beta + 3^2 \cdot \gamma + 2 \cdot 3^2 \cdot \delta \quad \text{where} \quad \begin{aligned} \alpha &\in \{0, 1, 2\} \\ \beta &\in \{0, 1, 2\} \\ \gamma &\in \{0, 1\} \\ \delta &\in \{0, 1, 2\} \end{aligned} \quad (2.1)$$

¹It can be easily proven that a quasi De Bruijn sequence of order n and with alphabet size k cannot be longer than k^n .

2.2. Theory – Location-Coding Dense Optical Patterns

With this, the sequence of d_j can be expressed as four sequences of $\alpha_j, \beta_j, \gamma_j, \delta_j$ composed of a much smaller set of symbols. This also ensures that there is a unique mapping between the d_j and $\alpha_j, \beta_j, \gamma_j, \delta_j$.

The offset differences between columns are chosen such that the sequences of $\alpha_j, \beta_j, \gamma_j, \delta_j$ form further quasi De Bruijn sequences of order 5 and lengths 236, 233, 31 and 241 respectively, called the **secondary number sequences** that are placed again in a cyclic manner. This ensures that a given string of 5 consecutive differences $d_i d_{i+1} d_{i+2} d_{i+3} d_{i+4}$ maps to 4 strings of 5 consecutive symbols ($\alpha_i \alpha_{i+1} \alpha_{i+2} \alpha_{i+3} \alpha_{i+4}, \beta_i \beta_{i+1} \beta_{i+2} \beta_{i+3} \beta_{i+4}, \gamma_i \gamma_{i+1} \gamma_{i+2} \gamma_{i+3} \gamma_{i+4}, \delta_i \delta_{i+1} \delta_{i+2} \delta_{i+3} \delta_{i+4}$); which in turn map to a unique 4-tuple of indices $(\hat{\alpha}, \hat{\beta}, \hat{\gamma}, \hat{\delta})$ in the aforementioned secondary number sequences thanks to the De Bruijn property. The lengths of these sequences are chosen relatively prime on purpose so that these indices only line up after $236 \cdot 233 \cdot 31 \cdot 241 = 410,815,348$ steps. In other words, there is a unique $x < 410,815,348$ for a given $(\hat{\alpha}, \hat{\beta}, \hat{\gamma}, \hat{\delta})$, and vice versa, with the following relations (known as the Chinese Remainder Theorem):

$$x \equiv \hat{\alpha} \pmod{236} \tag{2.2}$$

$$x \equiv \hat{\beta} \pmod{233} \tag{2.3}$$

$$x \equiv \hat{\gamma} \pmod{31} \tag{2.4}$$

$$x \equiv \hat{\delta} \pmod{241} \tag{2.5}$$

It trivially follows that:

$$x + 1 \equiv \hat{\alpha} + 1 \pmod{236} \tag{2.6}$$

$$x + 1 \equiv \hat{\beta} + 1 \pmod{233} \tag{2.7}$$

$$x + 1 \equiv \hat{\gamma} + 1 \pmod{31} \tag{2.8}$$

$$x + 1 \equiv \hat{\delta} + 1 \pmod{241} \tag{2.9}$$

This implies that the next x coordinate maps to the next indices in each of the secondary number sequences (jumping to the next respective cycles when the ends of the sequences are reached), and vice versa. Starting from the next index in the secondary number sequences will lead to the next 5-long strings: $(\alpha_{i+1} \alpha_{i+2} \alpha_{i+3} \alpha_{i+4} \alpha_{i+5}, \beta_{i+1} \beta_{i+2} \beta_{i+3} \beta_{i+4} \beta_{i+5}, \gamma_{i+1} \gamma_{i+2} \gamma_{i+3} \gamma_{i+4} \gamma_{i+5}, \delta_{i+1} \delta_{i+2} \delta_{i+3} \delta_{i+4} \delta_{i+5})$. Applying Equation 2.1 to each 4-tuple will again uniquely yield $d_{i+1} d_{i+2} d_{i+3} d_{i+4} d_{i+5}$, which is obtained by starting to read the dots (*i.e.* the offset main number sequences) from the next column. This ensures the continuity of the coordinate system.

In summary, the unique mappings (*i.e.* bijections) between various steps are:

$$x \in \{0, \dots, 410, 815, 347\} \leftrightarrow (\hat{\alpha}, \hat{\beta}, \hat{\gamma}, \hat{\delta}) \quad \text{where} \quad \begin{array}{l} \hat{\alpha} \in \{0, \dots, 235\} \\ \hat{\beta} \in \{0, \dots, 232\} \\ \hat{\gamma} \in \{0, \dots, 30\} \\ \hat{\delta} \in \{0, \dots, 240\} \end{array} \quad (2.10)$$

$$(\hat{\alpha}, \hat{\beta}, \hat{\gamma}, \hat{\delta}) \leftrightarrow \begin{array}{l} (\alpha_i \alpha_{i+1} \alpha_{i+2} \alpha_{i+3} \alpha_{i+4}, \\ \beta_i \beta_{i+1} \beta_{i+2} \beta_{i+3} \beta_{i+4}, \\ \gamma_i \gamma_{i+1} \gamma_{i+2} \gamma_{i+3} \gamma_{i+4}, \\ \delta_i \delta_{i+1} \delta_{i+2} \delta_{i+3} \delta_{i+4}) \end{array} \quad \text{where} \quad \begin{array}{l} \alpha_j \in \{0, 1, 2\} \\ \beta_j \in \{0, 1, 2\} \\ \gamma_j \in \{0, 1\} \\ \delta_j \in \{0, 1, 2\} \end{array} \quad (2.11)$$

$$\begin{array}{l} (\alpha_i \alpha_{i+1} \alpha_{i+2} \alpha_{i+3} \alpha_{i+4}, \\ \beta_i \beta_{i+1} \beta_{i+2} \beta_{i+3} \beta_{i+4}, \\ \gamma_i \gamma_{i+1} \gamma_{i+2} \gamma_{i+3} \gamma_{i+4}, \\ \delta_i \delta_{i+1} \delta_{i+2} \delta_{i+3} \delta_{i+4}) \end{array} \leftrightarrow (d_i, d_{i+1}, d_{i+2}, d_{i+3}, d_{i+4}) \quad \text{where} \quad d_j \in \{5, \dots, 58\} \quad (2.12)$$

When building the symbols in the column corresponding to the desired coordinate in the dot pattern (in order to *e.g.* print it on paper), one first calculates the secondary number sequence indices using the Equations 2.2 to 2.5 (*i.e.* Bijection 2.10). Then, the symbols in the secondary number sequences at these indices are looked up (*i.e.* Bijection 2.11). Then, the symbols are used to calculate the difference between this column and the next using Equation 2.1 (*i.e.* Bijection 2.12). Finally, the main number sequence is laid out onto the next column in a repeating manner with the calculated offset with respect to the last column. This way, the x symbols for the dot pattern for any desired coordinate window can be built, even without first calculating the symbols in the previous columns.

When decoding, assuming that 6×6 symbols are correctly perceived, the 5 offset differences between the 6 columns are first calculated by looking up the indices of each 6-long string in the main number sequence. Then, the consecutive offset differences of these indices are used to calculate the 5-long strings (belonging to the secondary number sequences) using Equation 2.1 (*i.e.* Bijection 2.12). Then, these strings are looked up in the secondary number sequences in order to obtain their unique indices (*i.e.* Bijection 2.11). Finally, the coordinate that satisfies Equations 2.2 to 2.5 is calculated using the Chinese Remainder Theorem in $O(1)$ (*i.e.* Bijection 2.10).

In both procedures above, namely producing and decoding the dot pattern, these five number sequences must be known beforehand (which can be hardcoded on both the decoding device and the pattern generator as they do not change), which are sufficient to recreate the entire pattern and decode any part of it. For completeness, the sequences used in our algorithms are given in Appendix A. Moreover, the encoding for y works independently in an identical

way in the other dimension; in other words, decoding the rows of the bit matrix belonging to y instead of columns of the bit matrix belonging to x , yields the y coordinate of the initial 6×6 matrix. This way, $410,815,348^2$ unique coordinates can be encoded in 2 Dimensions (2D).

2.2.3 Sectors & Final Coordinate Space Size

The unique number of coordinates can further be improved by vertically offsetting the entire bit matrix of x by up to 62 steps (offsetting by 63 is equivalent to not offsetting at all due to the cyclic nature of the main number sequence). This will not disturb the consecutive column offset differences (thus the x coordinates calculated up to now will remain the same) but will be undetectable unless the y coordinate is also correctly decoded. The same is valid for y , and works by offsetting the entire bit matrix of y horizontally by up to 62 steps. With this, 63^2 unique variants of the coordinate space (that has $410,815,348^2$ unique coordinates) can be generated; these variants are called the **sectors** of the coordinate space. The only limitation in extending the space in this way is that if two sectors are juxtaposed and the 6×6 matrix contains the boundary, a corrupted coordinate will be decoded since the row/column offset difference will have lost its original meaning on the boundary. In total, $(410,815,348 \cdot 63)^2 \approx 6.7 \cdot 10^{20}$ unique 2D positions can be therefore encoded. With the dot density used in our algorithms (0.508 mm on average between two dots, shown in the following sections), this allows absolute localization over an area approximately equivalent to 1/3 of the surface area of the Earth.

2.2.4 Decoding Orientation

Up to now, it was assumed that the dot pattern was perceived without any rotation by the perceiving device. However, it is not practical to assume that this is always the case, especially since our devices are tangibles. In a realistic setting, even if the grid lines are fitted correctly to the dots, the 6×6 matrix can be rotated by any one of 0° , 90° , 180° or 270° and the dots would still imply apparently correct symbols. Therefore, a choice must be made among these four before proceeding with actual decoding.

There are 3 wrong choices to make, and each one will result in reading at least one of the axes in the reverse direction (note that at this stage, the perceived axes cannot be attributed to x or y). Reading the dots in the reverse direction is equivalent to bit flipping and reversing the symbol strings encoded in the dots. Therefore, a mechanism that detects this operation is required. This is ensured by the choice of the main number sequence, which does not contain any of its 8-long substrings (note that these do *not* cover all possible 8-long strings, of which there are $2^8 = 256$) when they are bit flipped and reversed. Therefore, detecting the correct orientation requires that at least 8×8 dots are perceived; if 8-long strings in some rows or columns are not found in the main number sequence, then the direction containing the rows or columns must have been read in the wrong direction. When both directions are corrected, they can be attributed to x and y since the coordinate system is right-handed.

2.2.5 Error Correction

The methodology up to now will work, in theory, if the symbols are perfectly perceived. However, in reality, imperfect perception of the optical system, image processing and physical wearing of the dot pattern will inevitably lead to symbols being bit flipped. A final property of the main number sequence choice provides some robustness against this issue: Any 8-long substring of the main sequence is no longer found in the sequence if any *one* of its bits is flipped. Therefore, instead of attempting to directly find these strings in the sequence, it is useful to find the index that is most correlated with the string. Even if it is totally unknown which bit is flipped, this index will still be correct about 36 % of the time on average, considering all possible bit flips of all 8-bit substrings of the main number sequence (calculated by brute force). These chances can be improved if any assumption can be made on which symbol is bit flipped. In the end, our algorithms require at least an 8×8 matrix of dots to be perceived in order to perform orientation correction and 1-bit error detection (and possibly correction). The actual decoding can then proceed with potentially any 6×6 part of this matrix.

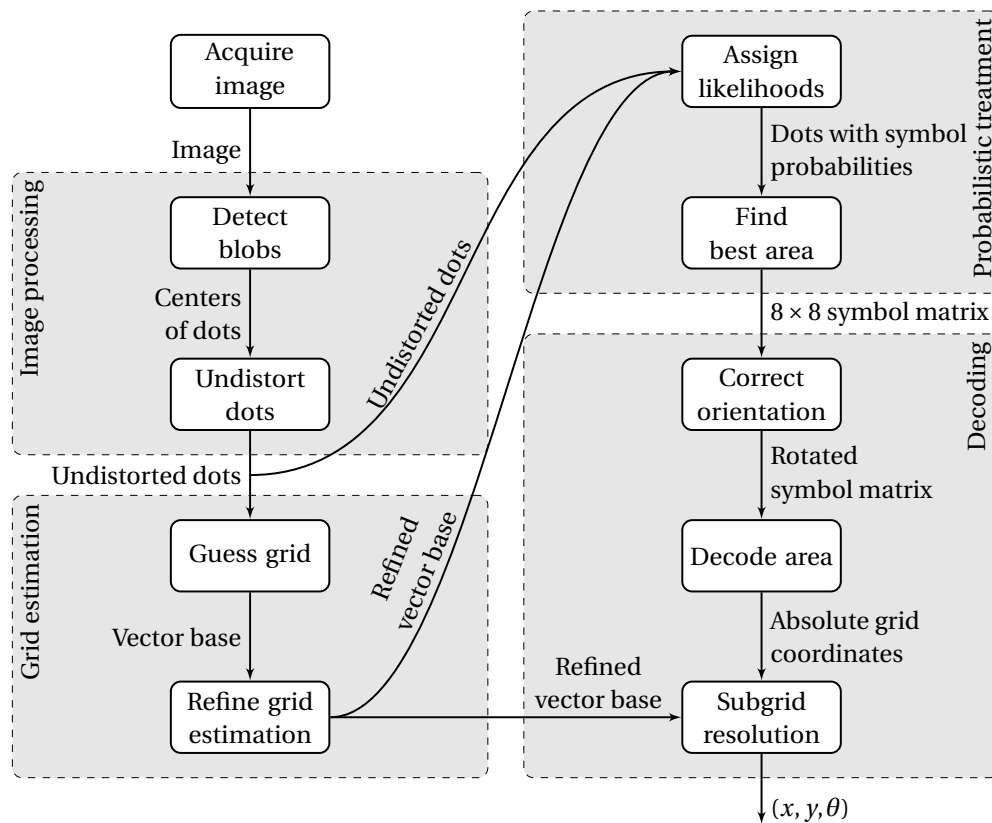


Figure 2.2 – The localization pipeline. Input camera image frames are processed to obtain the dots, which are decoded to obtain the 3DOF pose of the device that captured the image frame.

2.3 Localization Pipeline Design

Having explained the theory, we now provide the concrete algorithms that make use of the theory in order to process a camera image and decode the dot pattern, obtaining the 3DOF pose of the device that obtained the image. They are organized into the pipeline seen in Figure 2.2. This pipeline is intended to run entirely on the mobile tangible device, and is designed for simplicity. Below, the steps to our pipeline are explained.

2.3.1 Image Processing

After obtaining the camera image frame, the positions of the dots are found through a global thresholding and a standard two-pass binary blob detection algorithm (Figure 2.3) where the centers of mass of detected blobs correspond to dot positions. Only blobs with sufficiently many pixels (whose threshold is manually calibrated) are retained in order to overcome salt and pepper noise.

We assume that in practice, an optical system in close-up focus is likely to utilize a wide-angle lens in order to decrease the optical system height while imaging a sufficiently large area.

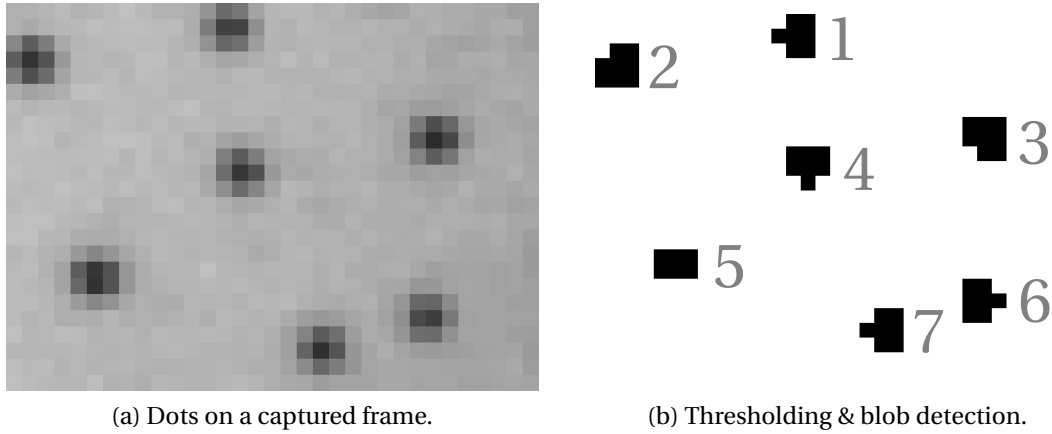


Figure 2.3 – Dot detection through image segmentation and two-pass binary blob detection. Image is scanned from left to right, then from top to bottom, and each pixel is labeled with the same segment as its top or left neighbor if they are of the same kind with the current pixel (both black or both white). If the two neighbors are the same kind but have different labels, the pixel is labeled with the smaller of these and an equivalence is recorded between these labels. In the second pass, these equivalences are resolved with the smaller label in each. With dots, this results in the type of ordering seen on the right.

These lenses typically suffer from barrel distortion, which can lead to significant positioning errors on the dots away from the center. To prevent this, we use the Brown-Conrady model (only radial distortion, 2nd degree) to correct the dot positions at each frame:

$$\vec{p}_u = \vec{m} + \vec{r}_d / (1 + k \|\vec{r}_d\|^2) \quad \text{where} \quad \vec{r}_d = \vec{p}_d - \vec{m} \quad (2.13)$$

where \vec{m} is the image center, \vec{p}_d is a given dot's position in the original image and \vec{p}_u is the same dot's undistorted position. The radial distortion parameter k is calculated offline from calibration images and is static during runtime.

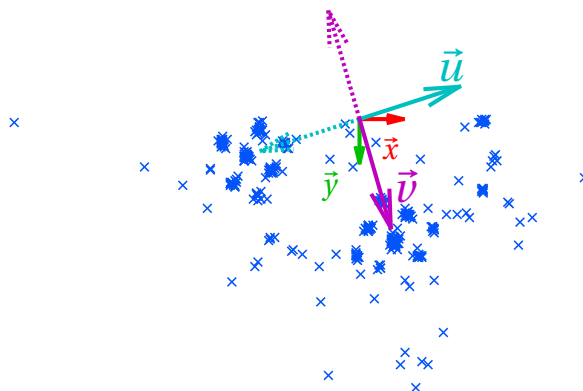
2.3.2 Grid Estimation

After finding the dot positions, the dots must be attributed to a 2D index in the virtual grid, *i.e.* index of the grid intersection from which the dot is offset, in order to be attributed their symbols (*i.e.* *up*, *down*, *left* or *right*). This grid is modeled as a vector space spanned by $\{\vec{u}, \vec{v}\}$ at an origin \vec{o} . The vectors $\{\vec{u}, \vec{v}\}$ are aligned to the grid directions and their lengths are defined to be the average physical grid spacing along their respective axes.

Since the grid is not physically visible in the image, it must be estimated using the dots, each of which lies on the grid lines but not on the intersections. Moreover, even though the dot offsets are deterministic, in a given image with enough dots, they appear as if randomly distributed. This implies that on average, there are equally many *up* dots as *down* dots, as well as equally



(a) Dot connections detected by the 4-nearest neighbor search. Blue lines mark symmetric connections (both dots agree to be neighbors) used in estimating the grid. Red circle marks the intact neighborhood center used as the grid origin. Black text that interferes with the pattern is retained to display behavior against such artifacts.



(b) Symmetric edges from the left, plotted at the same origin as the image coordinates $\{\bar{x}, \bar{y}\}$. Due to blob detection's ordering on dots, all edges point downwards. The constrained k -means algorithm assumes 4 clusters which are grouped into two pairs. After each step, each pair is forced to be symmetric around the origin. Final obtained pairs are represented with one dotted and one solid vector each.

Figure 2.4 – Initial estimation example for the grid, before refining.

many *left* dots as *right* dots. Therefore, if the original neighborhood of the dots was known, the edge vectors between the dots could be averaged to obtain the grid axis directions and the magnitudes of the mean inter-dot distances in both axes.

In order to estimate the neighborhood, the four nearest neighbors of each dot are first determined and the edges between the neighbors are recorded, of which the non-symmetric edges (where one of the two dots does not agree to be neighbors) are discarded, *e.g.* as in Figure 2.4a. Then, the symmetric edges are clustered through Algorithm 2.1 in order to find a first estimate of $\{\vec{u}, \vec{v}\}$, *e.g.* as in Figure 2.4b. The origin of the new coordinate system is found by searching for an *intact* neighborhood of 3×3 dots close to the center of the image in order to minimize cumulative errors due to the estimated length of the base vectors $\{\vec{u}, \vec{v}\}$. There are two conditions to be an *intact* neighborhood: (i) All of the four neighbors of a starting dot, namely *side dots*, must be symmetrically connected to the starting dot, and (ii) There must be exactly four other dots, namely *corner dots*, in the 3×3 dot grid that are connected to two distinct side dots. If such a neighborhood is found, a weighted average of the starting dot's and the side dots' positions is used as the origin. If not, the search continues with the next closest candidate. An example of such a neighborhood is in Figure 2.4a.

We denote the dot positions in the new coordinate system with \vec{c} ; these positions are in units of $\|\vec{u}\|, \|\vec{v}\|$. By rounding them to the nearest integer, we obtain the coordinates \vec{g} , hereafter called *grid coordinates*. Using these, the dots' offsets with respect to the grid coordinates

Input: List of symmetric edges E

Output: Main grid directions $\{\vec{u}, \vec{v}\}$

```

1: procedure CONSTRAINED  $k$ -MEANS
2:   Initialize cluster means  $\vec{m}_1, \vec{m}_2, \vec{m}_3, \vec{m}_4$ 
3:   repeat
4:     Number of dots belonging to clusters:  $n_1, n_2, n_3, n_4 \leftarrow 0$ 
5:     Accumulators:  $\vec{a}_1, \vec{a}_2, \vec{a}_3, \vec{a}_4 \leftarrow \vec{0}$ 
6:     for all edges  $\vec{e} \in E$  do
7:        $k \leftarrow$  index of smallest distance  $\|\vec{m}_k - \vec{e}\|$ 
8:        $\vec{a}_k \leftarrow \vec{a}_k + \vec{e}$ 
9:        $n_k \leftarrow n_k + 1$ 
10:    end for
11:     $\vec{m}_1 \leftarrow \frac{\vec{a}_1 - \vec{a}_3}{n_1 + n_3}$ 
12:     $\vec{m}_2 \leftarrow \frac{\vec{a}_2 - \vec{a}_4}{n_2 + n_4}$ 
13:     $\vec{m}_3 \leftarrow \frac{\vec{a}_3 - \vec{a}_1}{n_1 + n_3}$ 
14:     $\vec{m}_4 \leftarrow \frac{\vec{a}_4 - \vec{a}_2}{n_2 + n_4}$ 
15:  until  $\vec{m}_1, \vec{m}_2, \vec{m}_3, \vec{m}_4$  did not change or iterations  $> 10$ 
16:  Dots belonging to clusters:  $p_1, p_2 \leftarrow \emptyset$ 
17:  for all edges  $\vec{e} \in E$  do
18:     $k \leftarrow$  index of smallest distance  $\|\vec{m}_k - \vec{e}\|$ 
19:    if  $k = 1$  or  $k = 2$  then
20:       $p_k \leftarrow p_k \cup \{\vec{e}\}$ 
21:    else
22:       $p_{k-2} \leftarrow p_{k-2} \cup \{-\vec{e}\}$ 
23:    end if
24:  end for
25:   $\vec{u} \leftarrow$  median( $p_1$ )
26:   $\vec{v} \leftarrow$  median( $p_2$ )
27: end procedure

```

Algorithm 2.1 – Constrained k -means algorithm to find grid directions. Medians are calculated separately in x and y to reduce complexity instead of using the geometric median.

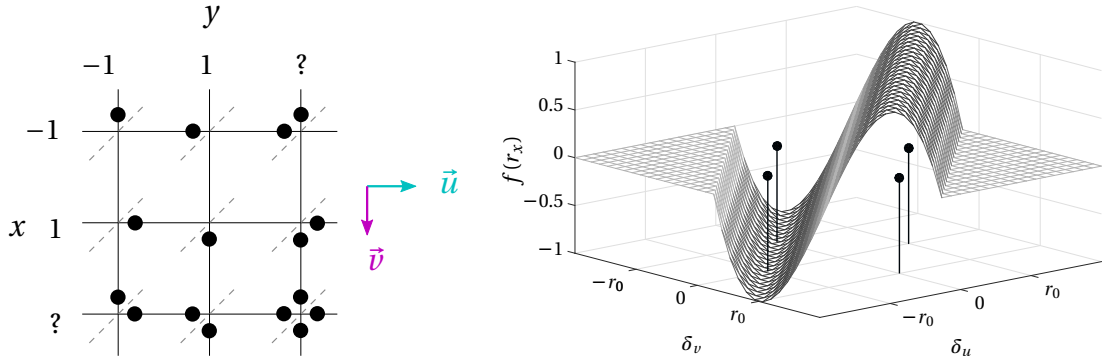
(called $\vec{\delta}$) are calculated. Namely, for a given dot position \vec{p} :

$$\vec{c} = \begin{bmatrix} \vec{u} \cdot (\vec{p} - \vec{\delta}) / \|\vec{u}\|^2 \\ \vec{v} \cdot (\vec{p} - \vec{\delta}) / \|\vec{v}\|^2 \end{bmatrix} \quad (2.14)$$

$$\vec{g} = \lfloor \vec{c} \rfloor \quad (2.15)$$

$$\vec{\delta} = \vec{c} - \vec{g} \quad (2.16)$$

The grid coordinates reveal the true neighborhood of dots: A pair of dots are now considered neighbors only if their grid coordinates are adjacent in either the \vec{u} or the \vec{v} axis. Using the true neighborhoods, the lengths of \vec{u} and \vec{v} are refined by setting them to the medians of distances between all neighbor dots in their respective axes. The grid origin is also refined using the



(a) Possible locations of dots, including ambiguous cases, and how they correspond to x, y bits (for convenience in future calculations, the 0 bit value is replaced by -1). For example, in order to find out whether the x bit is 1 or -1 , it is sufficient to know on which side of one diagonal the dot lies; for this reason, we project the dot onto the diagonal by $\delta_v + \delta_u$. The same is done for y with the other diagonal, *i.e.* by $\delta_v - \delta_u$.

(b) The quasi-probability distribution for a dot's x bit, $f(r_x) = f(\delta_v + \delta_u)$ approximates a Gaussian mixture distribution with the nominal offset positions r_0 as means. The four possible ideal dot positions are shown at these offsets. The signed quasi-probability distribution accommodates both $[0, 1]$ and $[0, -1]$ in a single equation while $|f(r_x)|$ would stand for the likelihood of a symbol carrying a correct x coordinate without discriminating the binary value. $f(r_y)$ is similar but is symmetric with respect to the other diagonal.

Figure 2.5 – Possible locations of dots and how they are attributed probabilities of carrying x and y values.

median value of the offsets, calculated separately in each of the two axes:

$$\vec{\delta} \leftarrow \vec{\delta} - \text{median}(\vec{\delta}) \quad (2.17)$$

The offsets to the grid positions $\vec{\delta}$ are finally recomputed based on the better grid estimation.

2.3.3 Probabilistic Treatment

Now that the dot offsets $\vec{\delta}$ are known, each dot must be assigned its respective symbol (*up, down, left, right*). However, the offsets will almost certainly always be significantly imperfect in realistic cases due to various factors, including printing and optical errors. Therefore, instead of directly assigning symbols to dots, we consider calculating likelihoods for each dot to be one of the symbols, thus obtaining the likelihoods for each dot to carry the specific binary values (*i.e.* 1 or -1) for both x and y .

As Figure 2.5a shows, the binary value for each of the two directions (x and y) depends on which side of the diagonals the dot lies. To attribute likelihoods for the two directions, we first project the dot offsets onto the two diagonals as follows in order to obtain the x and y offsets:

$$r_x = \delta_v + \delta_u \quad (2.18)$$

$$r_y = \delta_v - \delta_u \quad (2.19)$$

Input: Grid coordinates of all detected dots (\vec{g}_i), offsets of all detected dots ($\vec{\delta}_i$)

Output: Quasi-probability matrices $\mathbf{P}^{(x)}$, $\mathbf{P}^{(y)}$

```

1: procedure CONSTRUCT  $\mathbf{P}^{(x)}$ ,  $\mathbf{P}^{(y)}$ 
2:   Create  $\mathbf{P}^{(x)}$  and  $\mathbf{P}^{(y)}$  with size  $(\max_i g_i^u - \min_i g_i^u, \max_i g_i^v - \min_i g_i^v)$ 
3:   Initialize  $\mathbf{P}^{(x)}$  and  $\mathbf{P}^{(y)}$  with zeros
4:   for all detected dots  $i$  do
5:      $p_x \leftarrow f(\delta_i^v + \delta_i^u)$ 
6:      $p_y \leftarrow f(\delta_i^v - \delta_i^u)$ 
7:     if  $|p_x p_y| > \left| \mathbf{P}_{g_i^u, g_i^v}^{(x)} \mathbf{P}_{g_i^u, g_i^v}^{(y)} \right|$  then
8:        $\mathbf{P}_{g_i^u, g_i^v}^{(x)} \leftarrow p_x$ 
9:        $\mathbf{P}_{g_i^u, g_i^v}^{(y)} \leftarrow p_y$ 
10:    end if
11:  end for
12: end procedure

```

Algorithm 2.2 – Algorithm to construct quasi-probability matrices (one for x bits and one for y bits) that cover all detected dots. Dots associated with incorrect grid coordinates (due to incorrect detection in image processing) are overwritten by the correct dots with higher associated likelihoods.

We assume that these offsets follow a Gaussian mixture distribution, centered around nominal offsets r_0 and $-r_0$ (*i.e.* the offsets of perfectly detected dots). We extend this to a quasi-probability distribution whose range is $[-1, 1]$, where the sign corresponds to the binary value but the magnitude corresponds to actual probability as usual. We approximate this distribution with a custom polynomial function, whose shape is seen in Figure 2.5b:

$$f(r) = \begin{cases} \frac{3r}{2r_0} - \frac{r^3}{2r_0^3} & \text{if } r^2 < 3r_0^2 \\ 0 & \text{otherwise} \end{cases} \quad (2.20)$$

This distribution is used to create two quasi-probability matrices $\mathbf{P}^{(x)}$ and $\mathbf{P}^{(y)}$ that cover all detected dots, constructed according to Algorithm 2.2. A positive entry in $\mathbf{P}^{(x)}$ denotes that the associated dot's x bit is likely a 1 while how much likely is given by the entry's magnitude, between 0 and 1. A negative entry denotes the same for -1 . $\mathbf{P}^{(y)}$ works similarly for the y bit. For a given dot, the magnitude of the product of its entries in these matrices, *i.e.* $\mathbf{P}_{i,j} = \left| \mathbf{P}_{i,j}^{(x)} \mathbf{P}_{i,j}^{(y)} \right|$, represents the likelihood of that dot to represent any symbol accurately.

Since more visible dots are available on a given frame than required in a typical implementation, we have the opportunity to choose the best area among many possible areas that can be decoded, to improve robustness of the pipeline against noise. We define this area as the 8×8

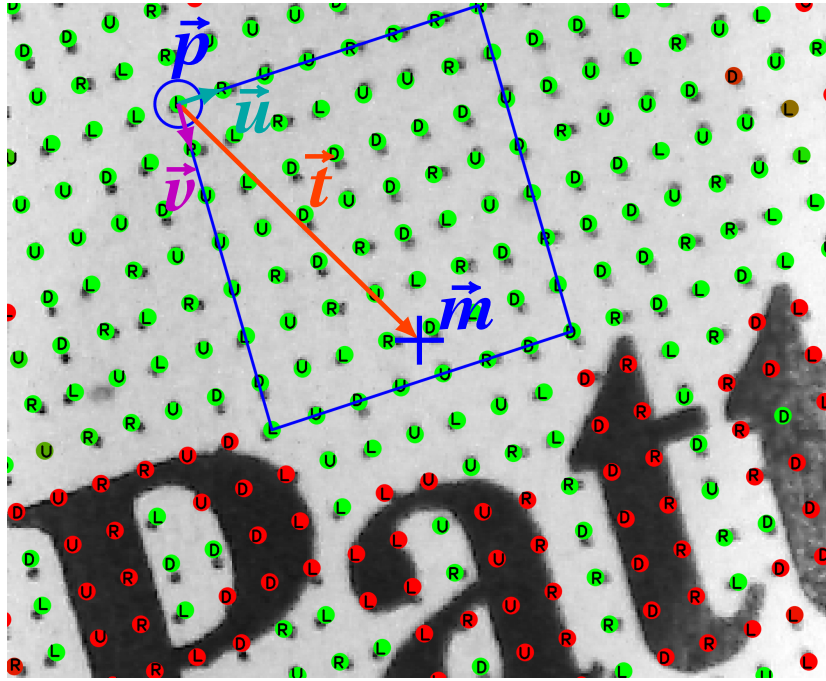


Figure 2.6 – Grid positions, marked with the colored dots (green denoting good quality; red: bad quality). The most likely symbols are marked on top of the dots (marked with R, L, D, U above). Blue square corresponds to the best area. Blue circle (\vec{p}) represents the origin of the best position to decode. Device center (\vec{m} , assumed to coincide with the image center in this particular implementation) is displaced from the decoded position as much as \vec{t} .

submatrix that has the largest sum of absolute likelihoods. Namely, we find:

$$\operatorname{argmax}_{i,j} \sum_{\substack{i \leq k \leq i+7 \\ j \leq l \leq j+7}} |\mathbf{p}_{k,l}^{(x)} \mathbf{p}_{k,l}^{(y)}| \quad (2.21)$$

Such a region in an example decoding is given in Figure 2.6).

2.3.4 Decoding

At this point, we have the 8×8 matrices of bits (independently for x and y) to be decoded, which depends on the orientation of the grid. In order to find the correct decoding orientation (among $0^\circ, 90^\circ, 180^\circ$ and 270°), we take advantage of the bit-flip-reverse robustness of the main number sequence as described in Section 2.2. Namely, we attempt to find the 8-long rows/columns both normally and after bit flipping and reversing in the main number sequence and vote on the correct direction for each axis. Then, symbols, probability matrices and $\{\vec{u}, \vec{v}\}$ are rotated by $90^\circ, 180^\circ$ or 270° accordingly, if required. The information at this point is enough to determine the device orientation θ , which is simply the orientation of the image (and, by extension, the device) in $\{\vec{u}, \vec{v}\}$ coordinates.

The decoding of x and y coordinates requires the indices of the rows and columns in the main number sequence, which is robust against one bit flip for all its 8-long substrings, as described in Section 2.2. This is exploited at this point by picking the index with highest correlation for each row/column instead of searching for them directly. With any of the 6 consecutive column indices (among 8), 5 consecutive differences are calculated and Bijections 2.12 to 2.10 are used (in that order) to calculate the x coordinate. Rows are used in an identical fashion to calculate the y coordinate.

While decoding yields the x and y coordinates in the resolution of grid coordinates, subgrid resolution (on the order of pixels, depends on the accuracy of the fitted grid) can be achieved by calculating the translation of the device with respect to the origin of the decoded submatrix:

$$\vec{t} = \vec{m} - \vec{p} \quad (2.22)$$

$$\vec{t}_{\text{proj}} = \begin{bmatrix} \vec{u} \cdot \vec{t} / \|\vec{u}\|^2 \\ \vec{v} \cdot \vec{t} / \|\vec{v}\|^2 \end{bmatrix} \quad (2.23)$$

where \vec{m} denotes the device center, \vec{p} denotes the origin of the decoded area and \vec{t}_{proj} denotes the translation of the device with respect to \vec{p} in $\{\vec{u}, \vec{v}\}$ coordinates. The final coordinates with subgrid accuracy thus become:

$$(x, y) = (x, y)_{\text{decoded}} + \vec{t}_{\text{proj}} \quad (2.24)$$

These coordinates can then be multiplied with the (nominal or estimated) physical grid distance, which depends on the implementation and is not necessarily fixed, in order to obtain the physical coordinates of the device.

2.4 Implementation – Cellulo Robot Version 1

Our robot with the proposed localization method was implemented as a standalone device. All essential hardware modules; such as localization, wireless communication, user interface and power; were included in the design except locomotion. This exclusion choice was made in order to speed up the design process and to test the localization component in a more agile manner in terms of scheduling. We call the (non-mobile) robot with this set of functionalities, the Cellulo robot version 1.

The key idea in this design process is to place all “intelligence” on a mobile device such as a tablet (or desktop computer for development purposes) and leave only the essential or high-bandwidth computational components on the robot in order to reduce production cost and power consumption. This way, our robots appear simply as peripherals to such a mobile device where the activity logic resides. By packaging lesson components involving such sets of logic into specific “mobile apps”, the platform can be made on-demand from the teacher’s point of view. This architecture is depicted in Figure 2.7.

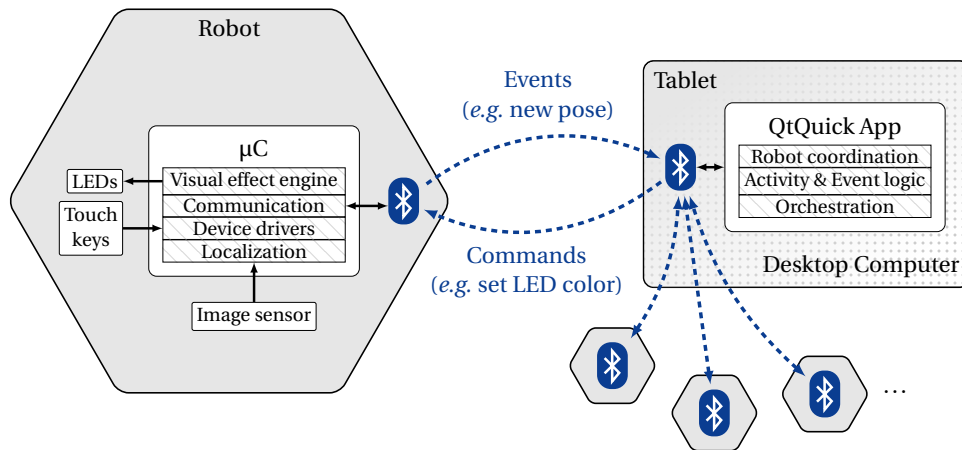


Figure 2.7 – Cellulo version 1 software architecture. Multiple robots are connected through dedicated Bluetooth 2.1 Serial Port Profile (SPP) sockets to a mobile tablet (or desktop computer for development purposes) where the activity application (written in QtQuick) resides. Diagonally lined boxes represent software components within the robot firmware or within the activity application as part of custom reusable QtQuick plug-ins where possible.

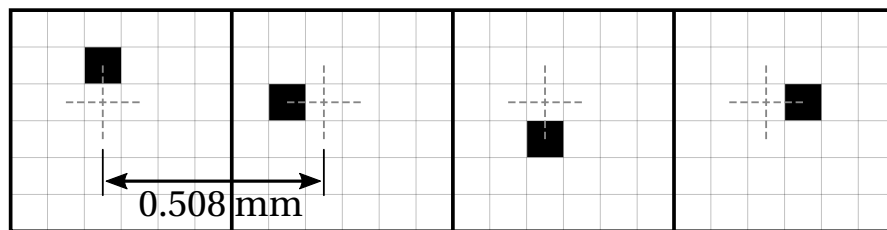


Figure 2.8 – Choice of symbol glyphs in the dot pattern font. Dots are offset from the grid centers as much as 1/6 of the grid spacing. This ensures that when the grid spacing is chosen as 0.508 mm, the dots align with the printer dots under 300 DPI density (and integer multiples such as 600 DPI or 1200 DPI commonly found in consumer printers). Dashed crosses indicate the origins of symbols, which are simply embedded in vector graphics documents as consecutive characters from this monospace font in order to produce the dot pattern.

2.4.1 Printable and Document-Compatible Dot Pattern

In order to localize, the robots require the optical dot pattern to be physically present. It is stored as a string of characters (U, D, L, R) depicting the dots, with line breaks depicting the passage to the next row of dots. This representation is then rendered using a custom font made of four glyphs representing the four possible positioned dots as shown in Figure 2.8. This way, this custom font and the string of characters can be embedded in vector graphics formats such as Portable Document Format (PDF) that can be compressed, viewed, redistributed and printed easily.

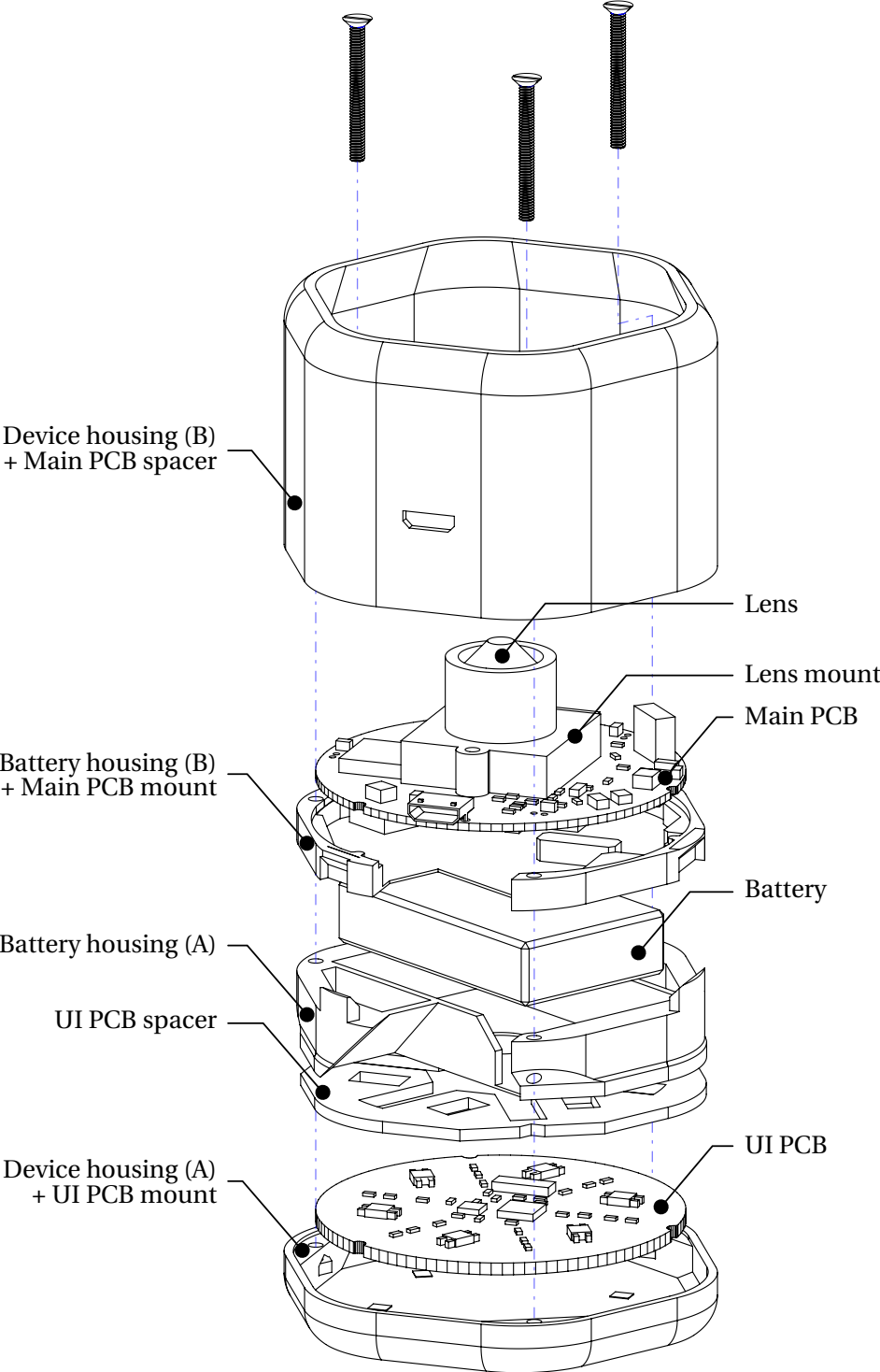


Figure 2.9 – Exploded view of Cellulo robot version 1, upside-down. Screw routes shown in dashed blue. Battery cables and PCB interconnect cable not shown.

2.4. Implementation – Cellulo Robot Version 1

Component	Part Number	Cost (€)
Microcontroller	<i>PIC32MZ1024ECG064</i>	8.51
Lens (5.5 mm focal length, S-mount)	<i>HYP0710</i>	1.90
Lens mount		0.17
Image sensor	<i>MT9V034C12STM</i>	12.86
Near Infrared LEDs for optical exposure	<i>VSMY3850-GS08</i>	3 × 0.46
Discrete MOSFET for LED switching		0.06
0.1 % precision resistors for LED voltage drop		3 × 0.29
Bluetooth communication	<i>RN42</i>	12.12
Visual LEDs	<i>ASMB-MTB0-0A3A2</i>	6 × 0.23
LED driver	<i>TLC5947</i>	4.59
Capacitive sensor driver	<i>AT42QT1070</i>	1.39
Battery (Li-Ion, 600 mAh, 902540 size)		4.66
Battery protection	<i>BQ29700</i>	0.46
	<i>CSD17527Q5A</i>	2 × 0.67
Battery charging & load sharing	<i>MCP73871</i>	1.46
Power supplies	<i>LM3671</i>	0.54
	<i>LP2980-N</i>	0.40
Other passives (terminal, capacitor, resistor <i>etc.</i>)		8.77
PCB manufacturing		11.39
Housing (28.5 g PLA) & fastening		0.85
Total		75.10

Table 2.2 – List of Cellulo robot version 1 components and their costs.

2.4.2 Hardware Design

Our robot is implemented on two double-sided Printed Circuit Board (PCB)s housing all of the relevant electronics and optics, that are entirely off-the-shelf components, in order to reduce production cost. These components provide wireless & rechargeable power, localization, a user interface with 6 Red, Green, Blue (RGB)-illuminated capacitive touch buttons, and Bluetooth communication; they and their costs at the time of implementation are given in Table 2.2. Both PCBs and the battery are enclosed in a Polylactic Acid (PLA) housing produced with Fused Filament Fabrication (FFF). The exploded view of the robot hardware can be seen in Figure 2.9 whereas the physical implementation can be seen in Figure 2.10. The device is designed to be placed directly on the printed dot pattern and moved on the horizontal plane where the downwards-facing optical system will capture the dots and the upwards-facing user interface will be open for interaction.

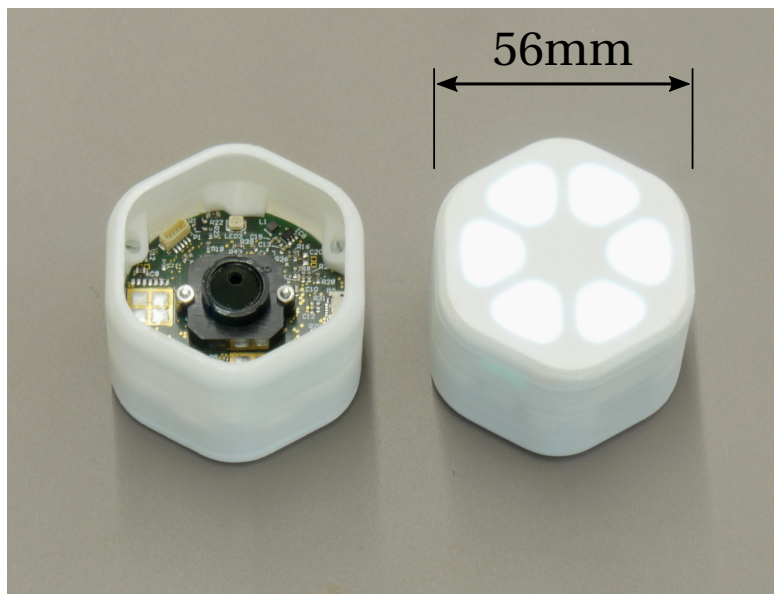


Figure 2.10 – Physical implementation of the Cellulo robot version 1: Localization, illuminated touch buttons and communication implemented. On the left: Upside down robot with exposed optical system.

2.4.3 Exposure of the Image

The scene, *i.e.* the printed dot pattern on the surface directly under the device, is exposed using three identical Near Infrared (NIR) Light Emitting Diode (LED)s evenly placed at equal distance from the optical center. Their voltage drops are constrained to be as similar as possible by precision resistors. These ensure that the scene is illuminated as uniformly as possible. To have controlled exposure, the scene is isolated from external light sources, such as ambient daylight, by the device housing itself that is 1.2 mm thick.

By choosing NIR instead of visible wavelengths, we hide the exposure light from a human user (when *e.g.* the device is picked up). However, there is a drawback: Our specific image sensor is more attuned to the visible spectrum (between 50 % and 60 % quantum efficiency) than to the infrared spectrum (with approximately 35 % quantum efficiency for the specific wavelength of our LEDs). Namely, to receive the same amount of exposure in an image, our LEDs must be lit brighter or for a longer time compared to a visible wavelength LED. An important point to note is that a human user will not be able to perceive such a short exposure time as ours (discussed below), and it is indeed possible to use visible light for exposure. The choice of NIR was nevertheless made for future experiments where dot patterns are printed with infrared ink instead of regular ink.

With our specific clock speed, the exposure time can be chosen to be as low as approximately 2.0×10^{-5} s by virtue of the image sensor's global shutter. Such a low exposure time would maximize robustness against motion but does not provide enough image brightness. For this reason, we gradually increased the exposure time to 1.3×10^{-4} s at which point the image

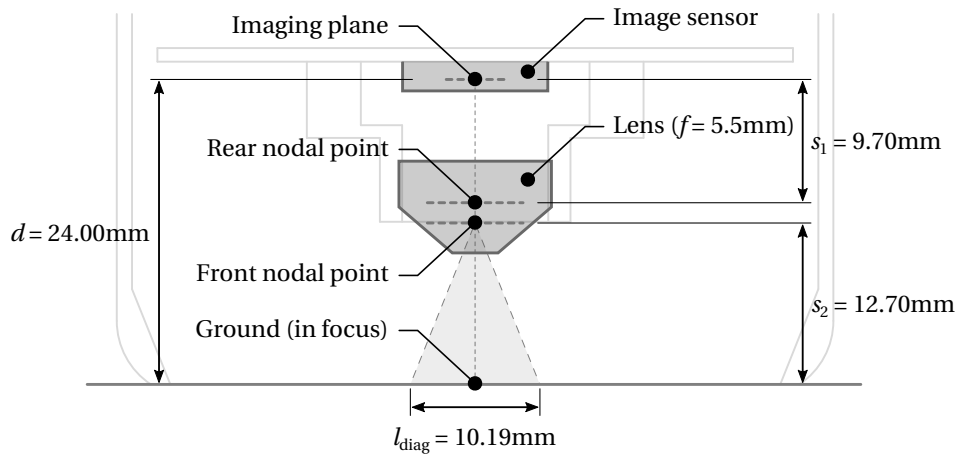


Figure 2.11 – Cross-section of the optical system, side view. d denotes the optical system height and was chosen successively by increasing the height of the housing until the lens was able to focus on the ground at some distance. l_{diag} denotes the diagonal length of the imaged area and was measured with a calibration image, which also revealed -3.2% (barrel) distortion. After focusing, s_1 was measured using the rear nodal point location given by the manufacturer’s specification. Then, s_2 was estimated by $s_1^{-1} + s_2^{-1} = f^{-1}$, which revealed the location of the front nodal point.

was sufficiently exposed so that the thresholding was satisfactory. Given the physical size of one pixel on the ground (0.046 mm) and the physical image size (furthest pixel is at 4.29 mm orthogonal distance away from the image center), it would take about 353 mm/s linear speed in the x or y axes or about 82 rad/s angular speed to cause motion blur of one pixel magnitude.

2.4.4 Focusing & Framing of the Image

In order to focus the exposed image onto the image sensor, an off-the-shelf S-mount Closed-Circuit Television (CCTV) lens is used; this lens diameter and thread pitch are standard and inexpensive products can easily be obtained. As a compromise between Field of View (FOV) and typically increased distortion, a lens with 5.5 mm nominal focal length (denoted with f) and 54° nominal diagonal FOV was chosen, which is mounted on a manual focus housing. The resulting optical system can be seen in Figure 2.11.

The suitable distance between the image plane and the point of focus on the ground (denoted with d) was found by successively increasing the device housing height in design (starting with the theoretical limit, $4f = 22$ mm) and attempting to manually focus the lens. With this, after distortion correction, the physical shape of the image becomes a 5.48×8.59 mm rectangle with a diagonal length of 10.19 mm. In this shape, an 8×8 dot matrix with 0.508 mm dot spacing must fit. Given this spacing, the nominal diagonal length of this matrix becomes $\sqrt{2} \times 0.508 \times 7$ mm.

However, in theory, the matrix may contain dots with outwards offsets at its outermost edges,

which must be perceived in the image; this adds $2 \times 1/6$ of the grid spacing to the length of the matrix. In addition, the physical diameter of one dot must also be considered, which further adds $1/6$ of the grid spacing. With these considerations, the diagonal length of the matrix becomes $\sqrt{2} \times 0.508 \times (7 + 1/6 + 1/6 + 1/6) = 5.39$ mm. This implies that in the worst case, which is when dot pattern is positioned at a 45° angle with respect to the device, at least 8×8 dots are guaranteed to fit into the image. If this was not the case, d would have to be increased or a lens with a smaller f would have to be chosen to obtain a larger area of vision.

2.4.5 Image Capture & Processing

Digital capturing of the image is done by the image sensor (global shutter, grayscale), which runs in master mode and generates all necessary timing and data signals from a clock signal. Our microcontroller (200 MHz core clock, 512 Kb Static Random-Access Memory (SRAM)), which lacks a hardware digital camera interface, uses these timing signals to capture the image data placed on a parallel bus (188×120 pixels, 8 bits per pixel) via a dedicated Direct Memory Access (DMA) channel. This ensures that the least amount of processing cycles possible are spent for this task, which runs in the background without intervention.

All of the image processing and decoding pipeline (as described in Section 2.3) runs locally on the microcontroller. In order to allow real-time operation, a number of measures are taken. Where possible, the lack of Floating-Point Unit (FPU) is compensated by manually introducing a rational number representation with fixed divisor, while taking care that no overflow occurs. Memory allocation is made statically where possible to avoid dynamic memory allocations. Lookup tables are used where feasible. Finally, the polynomial in Equation 2.20 is used instead of Gaussian distribution functions (requires exponentials) to increase performance.

2.4.6 Open-Source Software Release

Our software implementation is available under an open-source license at <http://chili.epfl.ch/libdots>. It can be built as a standalone library and has been successfully cross-compiled for low-end targets such as our microcontroller. The repository also provides a sample test application that works with a standard desktop webcam (as long as it permits to focus on close objects, so that printed dots are visible). Tools to generate dot patterns and overlay them on any PDF file are provided as well.

2.5 Supervised Validation

2.5.1 Overview

Having implemented our self-localized robots, we now focus on rigorously characterizing this localization performance. Namely, we aim to measure the accuracy (*i.e.* closeness of the measurement to the real value), precision (*i.e.* consistency of measurement) of the position

and orientation measurements, as well as the maximum framerate and power consumption of our implementation. This study is done in isolated conditions to obtain the best possible performance; this is useful to provide a reference upper bound for not only our applications but any future work that may benefit from such a localization system.

2.5.2 Procedure

Performance of individual localization coordinates (x , y , θ) were each measured separately. For x and y , the device was mounted (without modifications) on the toolhead of a Computerized Numerical Control (CNC) platform with $17\mu\text{m}$ nominal step size. For θ measurements, the device was mounted (without modifications) on a servomotor with 0.29° nominal accuracy. Commands given to this platform and servomotor were recorded as ground truth values, referred to as *nominal* values from here on.

Measurements were done on an A3 sheet carrying only the pattern and no other graphics, printed in black and white by a Xerox Workcentre 7665 laser printer. y was chosen as the paper rolling axis while x was chosen as the laser scanning axis (corresponds to head motion axis in inkjet printers). In this setup, the sources of significant systematic noise include:

- Pattern printing process inaccuracies
- Plastic device housing deformation and manufacturing tolerances
- Image sensor and lens assembly mounting inaccuracy
- Paper placement inaccuracy below the device

To measure the performance of x and y coordinates, the device was moved to 11×11 distinct positions on a 200×200 mm grid in spiral order from the center towards the periphery. 20 real-time samples were collected for each position. To measure performance of angular position, the device was rotated to 36 distinct angles over 360° . 20 real-time samples were collected for each orientation.

2.5.3 Results

The performance of positional localization can be viewed in Figures 2.12 and 2.13 for x and y respectively. 99.17% of x and 100% of y coordinates were correctly decoded. 1 out of 121 x positions was consistently measured to be in an unrelated location due to misreading of dot offsets. The performance of angular localization can be viewed in Figure 2.14. 100% of these angular positions were correctly decoded. Finally, an overview of accuracy and precision can be seen in Table 2.3.

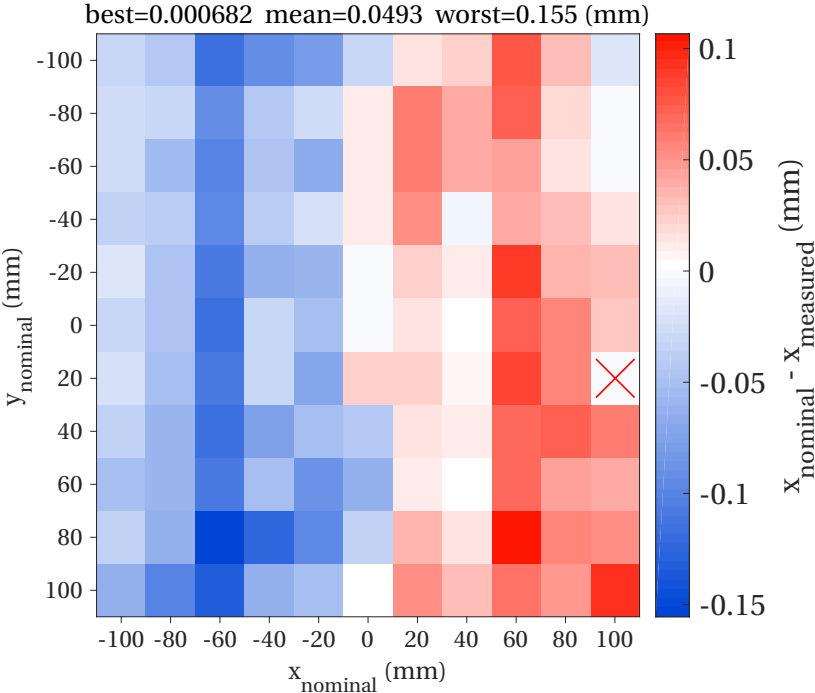


Figure 2.12 – Accuracy of x coordinate measurements when device is stationary, 20 samples each. Position marked with the cross was consistently misdecoded. Best, mean and worst accuracies are calculated with absolute values.

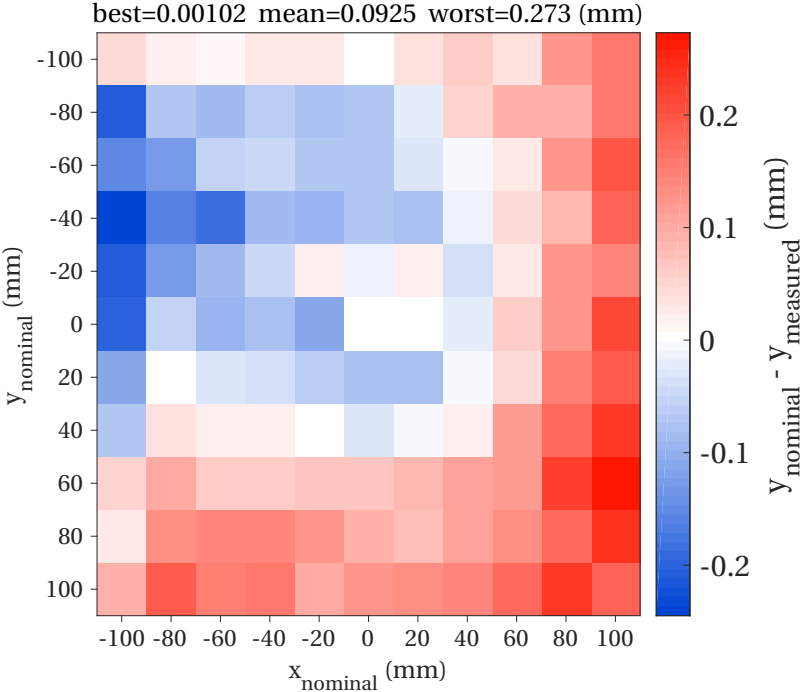


Figure 2.13 – Accuracy of y coordinate measurements when device is stationary, 20 samples each. Best, mean and worst accuracies are calculated with absolute values.

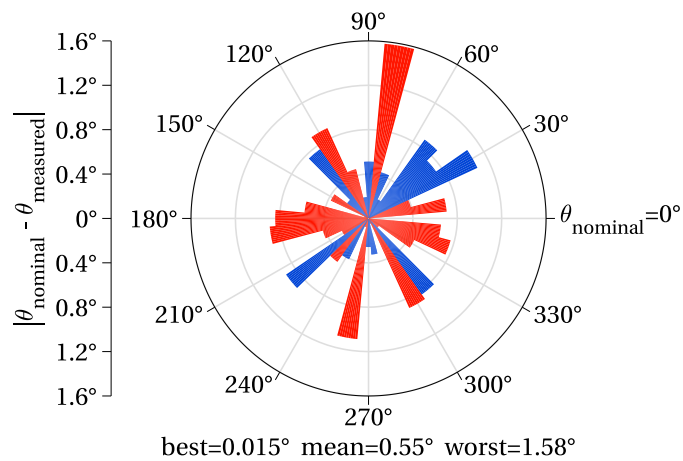


Figure 2.14 – Accuracy of orientation measurements when device is stationary, 20 samples each. Positive and negative biases are coded with red and blue respectively. Best, mean and worst accuracies are calculated over absolute values.

Coordinate	Accuracy	Precision (\pm one SD)
x	0.155 mm	± 0.010 mm
y	0.273 mm	± 0.014 mm
θ	1.581°	$\pm 0.407^\circ$

Table 2.3 – Overall localization performance when device is stationary; worst absolute values.

The average framerate of localization was initially measured to be 46.6 Hz and was further increased up to 93 Hz with improvements in software. The system was measured to consume 352mW when stationary (sleeps, wakes up every second to process one frame to decide whether moved, exits stationary mode if moved) and 873mW when moving (continuously processes frames, enters stationary mode if not moved for 5 seconds).

Figures 2.12 and 2.13 evidence that distinct regions on the paper induce biases on x and y coordinate measurements; we attribute this systematic error mainly to the pattern printing process. The y axis is seen to be significantly less accurate than the x axis (all 121×20 samples used, unpaired t-test, $p < 0.0001$). This observation leads us to consider that the uncertainties in the paper rolling process were more significant than the laser neutralizing process in our case. This may be generally true for similar axes in different printing techniques, such as the paper rolling axis *vs.* inkjet head motion axis in inkjet printers. To generalize however, tests should be done with other laser and inkjet printers.

In any case, certain x and y biases should be expected by the user of this localization method. Moreover, there is no guarantee that these accuracies are bounded across the whole localization space (unlike θ whose space and therefore accuracy is bounded). In reality, given a paper size and a specific printer, bounds for x and y accuracy can be measured; but the biases are likely to be worse across larger distances due to cumulative systematic printing errors (*e.g.*

slipping and deformation of paper).

Considering power consumption, a typical single cell 600 mAh Lithium-Ion battery, such as the one we used for our experiments, lasts for more than 2.5 hours in the worst case. In reality, it lasts longer since the device is not always moving, and will allow hours-long activity sessions.

2.5.4 Conclusion

Our measurements evidence that it is indeed possible and practical to use a low cost optical system with printed paper to achieve self-localization in many robots. The main benefits of this method can be listed as:

- Absolute localization without the need for any calibration
- Runs entirely on device; no need for a central server or external communications in the most basic scenario
- Works in real-time using off-the-shelf components with near-constant processing time per frame
- Unlimited scalability, each robot localizes itself
- Fully robust against occlusions due to user manipulation and external lighting conditions as long as the device rests on the surface and perceives about half a centimeter square of the pattern
- Designed to work while in motion, can be used *e.g.* for real-time trajectory tracking
- Simple deployment and disposal, as it only requires regular printable paper support that is to be placed on a tabletop surface and can later be removed and stored away
- Working area is only limited by printing capacity, printed patterns can be stitched together to cover larger areas if the stitching can be calibrated
- Unique “identifiers” can be attributed to copies of the same document (without the pattern) simply by assigning disjoint areas in the coordinate space to these copies and then recognizing these areas in the application; which can then be utilized in the classroom as *e.g.* per-learner activity sheets.
- Patterns are unobtrusive and can be overlaid on top of existing documents, augmenting them with localization
- Components reserved to localization sum up to about €26 per device; printable support with dot pattern can be reproduced at very low cost if damaged or if replication is needed

We also identify certain limitations to this method:

- Contrary to Simultaneous Localization and Mapping (SLAM) techniques, the environment needs to be altered by deploying the paper with the dotted pattern, however lightweight
- Printing the pattern may prove non-trivial in certain cases, especially large surfaces, as it requires exactly 1 : 1 scale and at least 300 Dots per Inch (DPI) resolution

- Accuracy and precision is dependent on the quality of the printer being used
- Provides localization in 2D space only and not in 3 Dimensions (3D); this effectively casts the activity design space onto a plane and dictates the DOF in the interaction

Within the frame of this thesis, namely building robots that operate in the classroom in large numbers, we have shown that our proposed method meets the technical requirements. There are no practical limits (from the localization standpoint) to the number of robots, and many such low-cost robots can be used in the classroom with the desired number of paper sheets that are easy to produce and store. Once the support is deployed, no calibration is required and the localization is instant as soon as the robots are placed in the activity.

From a design point of view, these developments enable the building of objects whose “places are known at all times” within the activity through accurate (to the sub-millimeter level measured in this section), global positioning. Due to relative positioning (or no positioning at all) commonly found in low-cost tabletop educational robots, typical activities feature one or few such devices carefully allocated to the learner(s) where the limited positioning of devices are either cautiously monitored or avoided altogether during the activity design stage. Transitioning from relative positioning to built-in global positioning allows the design of co-located, synchronous activities that respond immediately and unconditionally to the manipulation done to the many devices by multiple users, if desired. Moreover, this method relies on printed paper “augmented” with localization while strongly involving graphic design, where the position and motion of the robots (initiated by the users, by the robots, or by both parties at the same time; more discussion on this follows in the next chapter) can easily be planned, designed and then visualized through the printed graphics. In the following section, we describe further validations that not only probe these ideas, namely collaborative activities with a prominent graphic design aspect, but also aim to test the localization method that we developed within a real world scenario.

2.6 Ecological Validation

2.6.1 Overview

Having rigorously characterized and tested our localization system in isolated conditions, we now move on to testing it “in the wild” and exploring certain interactions that can be afforded by the current state of the platform. We aim to achieve this by designing a playful collaborative activity where no learning outcomes are yet targeted. Our main goals are to observe the performance of the localization system in the hands of children and examine the legibility and intuitiveness of the designed activity using localized tangibles. The development of this activity, published in [117], was done with the collaboration of Maria Beltran, Manon Briod (graphics and interaction design) and Dr. Séverin Lemaignan (software co-development).

2.6.2 Activity Design – Treasure Hunt

Our activity, called “Treasure Hunt”, is designed as a game where five “pirate” characters, played by robots, try to reach a “treasure chest” through a series of tasks. It is designed to be played by five children as a team where each member has one robot that they use to interact with the tasks of the activity. The robots do not move and are moved by the children as part of the tasks on a 1 m × 2.4 m activity sheet, colloquially called the *playground*, that features islands on an ocean as well as other playful graphics; it can be seen in Figure 2.15). The tablet runs the activity and displays instructions as well as playful graphics containing the characters and situations.

The tasks in the activity were designed to investigate the intuitiveness and effectiveness of a number of interaction schemes derived from the manipulative capabilities offered by our robots (exclusively non-mobile tangibles so far) that feature full-color touch keys and are movable and localized (in real-time) on a tabletop plane that contains printed graphics. These interaction schemes are given in Figure 2.16.

Before each task, the robots must be placed on specific zones on the playground marked with *A*, *B* and *C* (that are seen in Figure 2.15); interaction shown in Figure 2.16a. Each character has a specific starting zone among the 5 starting zones for each task; all of these 5 starting zones and the specific character images that these starting zones belong to are shown on the tablet before each task. However, the physical attributes of robots are identical, making it impossible to associate the robots with the characters if they are misplaced or swapped within the team. Therefore, we attempted character-robot association establishment via “character cards” that feature the image of the character and an active zone which lights the correct robot in green (as shown in Figure 2.16b) and the incorrect robots in red when placed on top.

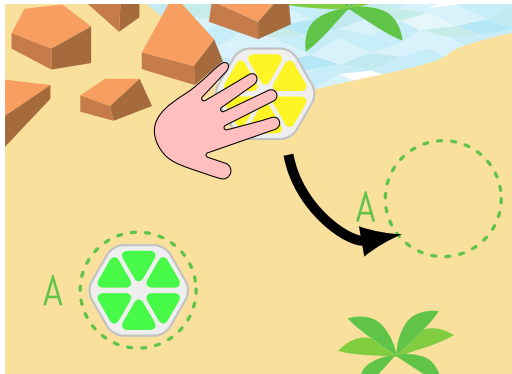
The activity on the tablet waits until the five robots are correctly placed to start the task. This establishes synchronization barriers before each task while pre-placing the robots close to the location where the task takes place. Furthermore, this design allows us to observe whether characters can be legibly attributed to robots that equally function as interface devices. The tasks within the activity are designed from a storytelling perspective, and are as follows:

Task 1: Each character must first transmit their part of the code to start the ignition on the pirate ship (starting from zones *A*). For this, each child must remember and reproduce a random sequence of 6 flashing LEDs by tapping the corresponding buttons in the given order; interaction pictured in Figure 2.16c. Team members do the task in parallel, independently or while aiding each other.

Task 2: The team must now find the key to the treasure chest that is lost in the ocean. The robots are used as “metal detectors” that are to be used to scan the ocean (starting from zones *B*) for the key while avoiding “junk” (false positives); interaction pictured in Figure 2.16d. Team members do the task in parallel and in spontaneous collaboration to explore different regions of the ocean.



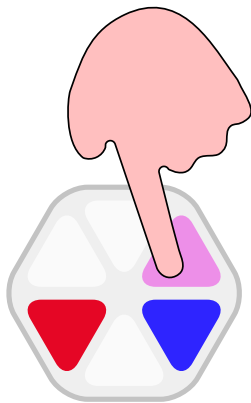
Figure 2.15 – Playground used in Treasure Hunt. Starting locations for each of the 3 tasks are visible with locations marked with A, B and C. In each task, one such location is available per team member.



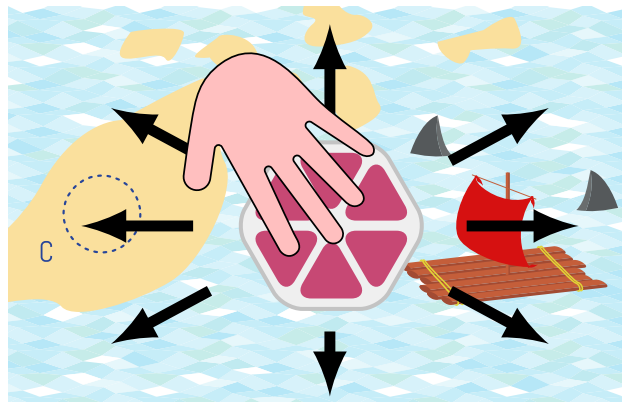
(a) *Positioning*: Placing the robots in active zones to trigger events.



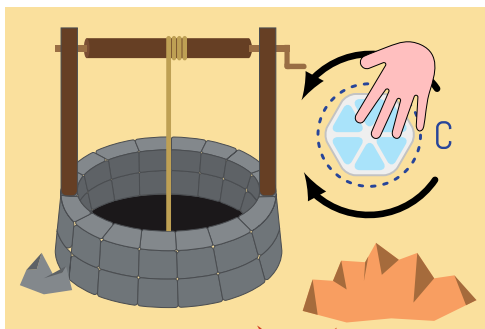
(b) *Role Assignment*: Placing the robots on character cards; correct assignment lights the robot in green.



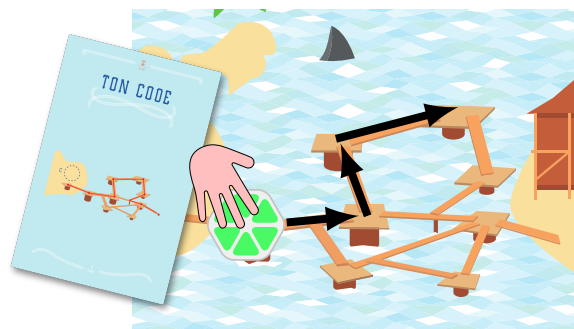
(c) *Touch*: Pressing the illuminated touch keys on the robot, e.g. in a pre-defined sequence.



(d) *Scan*: Moving the robot on the playground to find a hidden target; as the robot gets closer to the target, the color progressively changes from the “coldest” to the “warmest”.



(e) *Spin*: Turning the robot in place to change a continuous value; an animation on the tablet tied to this value accompanies the interaction.



(f) *Follow the path*: Moving the robot through the path illustrated on an auxiliary sheet without leaving the path.

Figure 2.16 – Interaction schemes used in Treasure Hunt, derived from the manipulative capabilities of our robots that feature full-color touch keys and are movable and localized on a tabletop plane with printed graphics.

Task 3.a: Now that the key is found (indicated by green color on LEDs and the tablet animations), the treasure chest must be retrieved from the bottom of a well. The robot belonging to the team member closest to the well (top right start zone C) is to be rotated as a handle to pull up the rope tied to the chest; interaction pictured in Figure 2.16e. On the tablet, a real-time animation of the chest rising from the well accompanies the interaction.

Task 3.b: The treasure chest that is retrieved must now be carried back to the ship by the remaining 4 members of the team (starting zones C). Each member must follow the path given to them on the back of their character cards in order to not step on loose rocks or planks; interaction pictured in Figure 2.16f.

2.6.3 Results & Discussion

The activity was run with a total of 85 children (11 to 14 years old) with no prior experience with Cellulo within the context of a collective school excursion, called *Journée des Classes* (English: Classes Day), where classrooms from local primary and middle schools visit our university for scientific demonstrations from a variety of research groups. The children were split into 14 groups of 5 (each child has one robot and the tablet is shared), 6 (5 children have one robot each and one child operates the tablet and reads the instructions) or 7 (5 children have one robot each and the tablet is shared among the remaining 2 children). After a brief introduction, the children were instructed to follow the indications on the tablet and no further instructions were given by the experimenters. The game lasted around 12 minutes ($M = 11:47$, $SD = 1:47$, $\min = 9:19$, $\max = 15:32$), and the children were invited to replay it if they wished (replay data not included in discussion). A sample scene from the activity is shown in Figure 2.17.

The localization system was observed to have mostly satisfactory performance in terms of accuracy and responsiveness. No performance decrease could be observed after slight progressive wear on the playground print during one day of intensive use. Three activities were run in parallel in the same room, with 3 groups on 3 tablets and 15 robots in total; none of the Bluetooth connections dropped at any time but slight delays were observed, which may have been caused by wireless interference from other Bluetooth devices or from the many Wi-Fi routers present on the experiment site.

The children interacting for the first time with the robot (even though some were at first reluctant to interact with the unknown technology) were observed to quickly understand that the robots “knew where they are” and the proposed interactions were easily picked up. Importantly, the constantly changing role of the robot; from a pirate character, to a pad to enter a code (Figure 2.16c), to a metal detector (Figure 2.16d), to a well handle (Figure 2.16e); was well accepted by the children, the tasks were all completed by all groups without any assistance: Table 2.4 provides the completion times for each of the tasks. This suggests that our goal of designing a versatile device was successfully attained in this scenario.



Figure 2.17 – Scene from Treasure Hunt during the start placement before *Task 1*.

Task	Description	$M \pm SD$	min	max
<i>Task 1</i>	Reproduce touch sequence	131.1 \pm 35.4	85	199
<i>Task 2</i>	Scan sea for key	125.2 \pm 51.6	47	222
<i>Task 3.a</i>	Rotate well handle	13.6 \pm 4.3	5	21
<i>Task 3.b</i>	Follow path	162.9 \pm 37.4	114	224

Table 2.4 – Treasure Hunt task completion times, $N = 14$ groups, all values in seconds.

Our observations specific to tasks and individual interaction elements are as follows:

- Character assignment via the character cards was generally confusing and not well received, suggesting that this method may be unsuitable for such an attribution.
- During the *Reproduce Touch Sequence* task (which is essentially a memory task), children who completed their sequence were generally observed to aid those who were still struggling with theirs, resulting in a cooperative aspect that naturally emerged. Likewise, the *Scan Sea* task naturally fostered collaboration amongst the children to effectively scan the various disjoint parts of the large playground. These indicate that in such scenarios the conceptual design of our platform (robots and paper) allowed collaborative aspects to be integrated successfully into the activity.
- The *Rotate Well Handle* task was explained only by a depiction of the robot with two

circular arrows (similar to Figure 2.16e) on the back of the character card. The interaction mechanism was picked up surprisingly fast (14 seconds on average to complete the task, as fast as 5 seconds for one group), presumably thanks to the responsive tablet animation whose continuous value was calculated using the robot's orientation in real-time. This indicates that graphical display of a tangible attribute may be a particularly strong and natural method of conveying information regarding the task.

- The *Follow the Path* task was completed by each child in about 40 seconds on average, and the completion was observed to be delayed by both children's mistakes caused by misperceiving the paths on the character cards and by occasional localization errors due to excessive contrast on some playground graphics. These locations were observed and recorded as references of unsuitable amounts of contrast for the graphics design process of future activities.

At a higher level, we have seen that children easily engage with tangible activities with printed graphics on paper. Moreover, we succeeded in ascribing a variety of roles to small robots with an unremarkable, anonymous design and observed that children easily accept and engage in such role assignment.

2.6.4 Conclusion

As a first step towards building an effective learning environment for the Cellulo project, we designed, implemented and tested a complete playful activity with users that demonstrates the combination of the Cellulo robots with augmented paper that allows self-localization. In this context, the Cellulo robots are envisioned as ubiquitous tools that could embody several different roles. These include representing specific objects or concepts related to the topic at hand, or acting as field-reconfigurable user interfaces to interact with the activity. We tested the idea that the paper is the "foundation" which the robots inhabit: The activity, created with a graphics design origin, incorporates active zones identified and interpreted by the robots as triggers for specific behaviors. Multiple pieces of paper, any desired size or shape, can be used in union to build rich activity scenarios.

Moreover, we carried out our tests within an ecological, realistic environment; with a classroom-sized group and minimal supervision. We have shown that such an activity that adheres to the teachers' constraints (including ease of use and reliability) can be implemented with our platform that offers a limited but powerful set of affordances. Up to now, our observations suggest that our platform will be suitable for practical daily classroom use.

Having concluded the first chapter of the Cellulo platform's design, namely building and testing *localized tangibles*, we now move on to the next chapter where we describe the addition of the *locomotion* module into our tangibles in order to transform them into fully mobile tangible robots. The chapter will detail the locomotion system design and, once again, include both highly controlled and ecological tests.

3 Phase II – Actuated Tangibles

3.1 Introduction

3.1.1 Background

After the development and validation cycle in Phase I (described in the previous chapter), the Cellulo platform possesses a more concrete structure, in the form of self-localized tabletop tangibles that operate on printed paper sheets. With this set of functionalities at hand, we proceed to develop, implement and validate a locomotion system for the Cellulo robots, the process of which will be detailed in this chapter. Upon adding mobility to the set of functionalities offered by our robots, we aim to move towards more ergonomic, handheld tangibles that possess haptic feedback capabilities.

The “locomotion” problem in robotics is concerned with designing powered mechanisms that allow robots to move themselves within their environments. Our focus in this thesis is terrestrial locomotion, which is concerned with moving on land upon rigid structures (such as the tops of classroom desks and tables) and is distinct from aerial, aquatic or other types of locomotion. From another perspective, locomotion separates (similar to localization) into indoors and outdoors, which usually impose distinct requirements on the locomotion system that is built. These include:

- Robustness against obstacles in the environment, or the inherent structure of the environment such as natural rough terrain
- Robustness against external disturbances
- Mechanical durability and complexity
- Safety, especially against humans
- Monetary cost, affordability
- Power consumption, efficiency
- Precision requirements
- Physical compactness, size and shape requirements
- Kinematic constraints, *e.g.* holonomic *vs.* non-holonomic

Considering these requirements, the locomotion literature converged to two distinct types of systems, that are legged and wheeled systems¹. Legged systems generally offer high robustness against rough environments at the cost of higher number of DOF, more complexity and more cost. Therefore, they address mainly, though not exclusively, outdoors scenarios. On the other hand, wheeled systems generally offer less robustness against rough environments (or are not concerned at all with such environments) but are much simpler and more efficient. As a result, they are often preferred, though again not exclusively, when dealing with indoors scenarios.

3.1.2 Problem Statement

Our work is framed within the classroom (an indoor environment) where the robots are to move on a tabletop (a plane), implying that the same three DOF as before, namely translational (x, y) and rotational around the vertical axis (θ), are to be covered. As previously mentioned, humans (learners and teachers) are expected to intensively manipulate the palm-sized robots. Our constraints are therefore listed as:

- Holonomic motion, in order to allow motion and/or haptic feedback instantaneously in any direction (in x, y and/or θ) when robot is grasped
- Mechanical robustness against being externally driven, especially since tangible and haptic interactions are essential to the platform and are expected to be employed intensively by child users
- Design composed of simple, few and preferably off-the-shelf components in order to minimize custom manufacturing steps to thereby ease the transition from a prototype design to a consumer device design
- As low cost as possible to not induce economic stress to schools, especially as we plan to employ a large number of robots within singular activities, even if this implies sacrificing other qualities such as precision of motion
- Compact enough geometry allowing the system to physically fit in a handheld volume (next to the existing systems such as localization and power), graspable by a child's hand

Given these constraints, a clear design choice is to exclude legged systems from our considerations and focus only on wheeled systems. Hence, in the next section, we give the state-of-the-art in wheeled designs that allow 3DOF holonomic motion on a horizontal plane.

3.1.3 Related Work

Holonomic Wheeled Drives

It is trivially true that for holonomic motion (requiring instantaneous motion capability towards an arbitrary direction in any configuration), wheels with at least two DOF are required. Here, a large design space exists for the individual and collective kinematics of these wheels;

¹More exotic types of systems such as crawling (whole-body) and hybrid (combining wheels and legs) systems exist but are not considered here.

[118, Section 2.3.1] gives a brief overview of this space and individual wheel designs. The first prominent example is actively steered wheels that feature two orthogonal DOF that are both driven. These are simple to build and operate, but require that some time is spent to turn the wheels into the direction of motion if the desired direction changes discontinuously, thus are not “instantaneously” omnidirectional. If the wheel is made a caster, it is actually possible to make omnidirectionality instantaneous. However, some driving elements must still remain on the link that houses the wheel itself in order to ensure that the wheel is driven; this increases complexity and decreases mechanical robustness since this link must itself also rotate to ensure control over the other DOF.

The second prominent example is Swedish wheels, also known as Mecanum wheels, omnidirectional wheels or omni-wheels, that feature two orthogonal or 45° oriented DOF, one of which is driven while the other is free to ensure low-friction backdrivability. These can move instantaneously towards any direction but are relatively less simple to build, typically less robust against obstacles and suffer from undesirable vibrations due to discontinuous contact points with the ground.

Ball wheels are the final prominent example that feature two (or three) non-collinear DOF, at least one of which is driven and the rest is/are free. Since the spherical wheel appears to have the exact same surface no matter what its orientation is, ball wheels can be made truly isotropic, ensuring the smoothest possible motion. However, they are typically difficult to build and design in such a way that ensures efficient locomotion.

Besides these principal designs, there exist more exotic ones that typically feature hybrid design elements. [119, 120, 121] propose omni-wheels with semi-spherical elements that operate in the same principle as conventional omni-wheels but retain some qualities of true ball wheels, such as isotropy and obstacle robustness, to some degree. [122, 123] propose omnidirectional tread designs that allow actuated sideways motion as well as motion parallel to the robot body, in order to exploit the high load capacity and terrain robustness of treads. [124] proposes a link-driven truncated ball wheel and an algorithm to avoid its singularities. [125] is another interesting design that utilizes a low cost flexible shape-changing wheel design.

For our application, actively steered wheels are not desirable due to the instantaneous holonomicity requirement and complexity issues. Ball drives and omni-wheels (and variants) are considerably more common and simpler than more exotic approaches, such as treads and link-driven wheels, that offer little advantage for a lightweight robot design such as the one we are aiming for. Among these two, omni-wheels are much more common, simpler to build and easier to control. However, ball drives offer significantly better vibration robustness and easier miniaturizability when components of similar sizes are considered; these are important features for our palm-sized robots that should be free of unintentional vibrations that would disturb the haptic feedback. For this reason, we decide at this point on pursuing a ball drive design. Since ball drives are difficult to realize, we will attempt to simplify its design and improve its typical bill of materials in terms of number and manufacturability of components.

Ball Drives – State of the Art

[126] describes the first two examples of ball drives where the wheel rests against rollers mounted around a tilted ring; the first design features a drive roller mounted on the horizontal plane while the second design has the ring itself actuated. [127, 128, 129] describe schemes where the wheel is driven by an omni-wheel in one axis and is free to rotate in the remaining axes. In [130] and [118, Tribolo robot], the wheel is driven by a roller located on its horizontal great circle, allowing it to rotate freely around the horizontal axis orthogonal to the driven axis. These designs all feature ball wheels with one driven and one free DOF; it is well known that ideally, by using at least 3 of any such ball wheel, a holonomic vehicle can be built.

[131] proposes a redundant scheme where each wheel is driven by two orthogonal actuated rollers in a 3-wheel configuration. Each roller's contact forces are actively regulated by pneumatic pistons to reduce wheel coating wear and increase obstacle robustness. [132] also features two drive rollers but with two sensor rollers opposite the drive rollers that encode wheel rotation and help detect drive roller-wheel slip.

[133, 134, 135] describe dynamically stable robots on a single ball wheel driven by (at least two) omni-wheels, colloquially called “ballbots”. [136] proposes a similar design where the single ball wheel is driven by two rollers, but the robot is enclosed in a spherical shell where the center of mass is located lower than the geometric center, ensuring that no dynamic balancing is needed to stay upright.

All above studies use rotating contact elements to drive the wheel, but there are alternative methods. [137] proposes a spherical induction motor scheme where a copper-over-iron spherical shell (acting as rotor) is omnidirectionally driven by multiple curved stators. [138] proposes driving a spherical wheel with an ultrasonic motor; this method has the potential for exceptional compactness and low cost.

Among the design features considered in ball drives, the nature and number of driving elements appear to be the major ones. Although inductive and ultrasonic drivers are very attractive in terms of compactness, they are difficult to implement due to extensive custom component manufacturing needs. Considering conventional rollers as drivers, all known single ball wheel designs utilize omni-wheels and derivatives in order to ensure the control over the 3rd DOF that is θ , which defeats the purpose of choosing ball wheels over omni-wheels in the presence of strict simplicity and affordability requirements. [139] contributes to these essential requirements by replacing omni-wheels by partially sliding rollers. This method, however, does not offer unlimited motion in certain combinations of x , y and θ , which may be required in our case as opposed to ballbot navigation. Therefore, it is clear that our application requires multiple ball wheels.

When the number of rollers on each wheel is considered, our scenario does not unconditionally require encoders (thanks to global absolute localization already present on each robot) or other requirements (such as precision) that call for a second (or further) actuated or sensing roller(s).

3.2. Development – Permanent Magnet-Assisted Ball Drive

Therefore, we converge on three ball wheels each driven by a single, conventional roller. However, the contact force between the drive roller and the ball wheel remains a problem, that is conventionally solved by external spring-loaded elements, which adds complexity. In the next section, we detail our design (previously published in [140]) where we “embed” the contact force mechanism into the ball wheel-drive roller system which eliminates the need for an external element that ensures this force. We then continue towards analyzing our design parameters, implementing our design and performing its supervised and ecological validation.

3.2 Development – Permanent Magnet-Assisted Ball Drive

3.2.1 Approach and Key Principles

We begin our approach by considering ferromagnetism as the source of the contact forces between the ball wheels and the driving elements, due to its simplicity and ubiquity as design element; such systems commonly consists of electromagnets, permanent magnets and ferromagnetic materials that are not permanently magnetized. Utilizing ferromagnetism to ensure the contact conditions eliminates the need for external elements that would normally ensure these conditions such as spring loaded passive rollers. In other words, the contact force mechanism will be naturally embedded in the wheel and the drive roller.

We first consider placing (a) permanent magnet(s) inside the ball wheel to pull it towards the drive roller. This is problematic however, due to the natural dipole anisotropy of magnets; placing an array of many smaller magnets along the surface can be envisioned to make the wheel magnetically near-isotropic, but would be especially complex and costly at our scales. On the other hand, dropping the magnetic isotropy constraint enables the consideration of actuating the ball wheel through external electromagnets rather than using ferromagnetism to provide the contact force. However, in such a scenario, singularities quickly arise which must be solved by multiple driving elements and sensing of the ball wheel’s state, since it is no longer isotropic. Therefore, we direct our focus to placing the permanent magnet outside of the ball wheel and leaving only ferromagnetic materials inside that are not permanently magnetized, letting it remain isotropic.

Placing (a) permanent magnet(s) in the drive roller is particularly promising, since the drive roller only needs to be isotropic around its own axis of rotation as opposed to the ball wheel that must be isotropic around all axes. The geometry of the roller thus evolves towards a cylinder with the magnetic poles placed appropriately in order to achieve magnetic isotropy during rotation. A clear opportunity at this point is to make the entire drive wheel out of a permanent magnet since cylindrical shapes are common and readily available. Furthermore, the roller magnet can be made into a ring, another readily available geometry for magnets, that will allow it to be mounted directly onto the motor shaft for extra compactness.

A final consideration is the placement of the magnetic poles; for a single dipole magnet, these

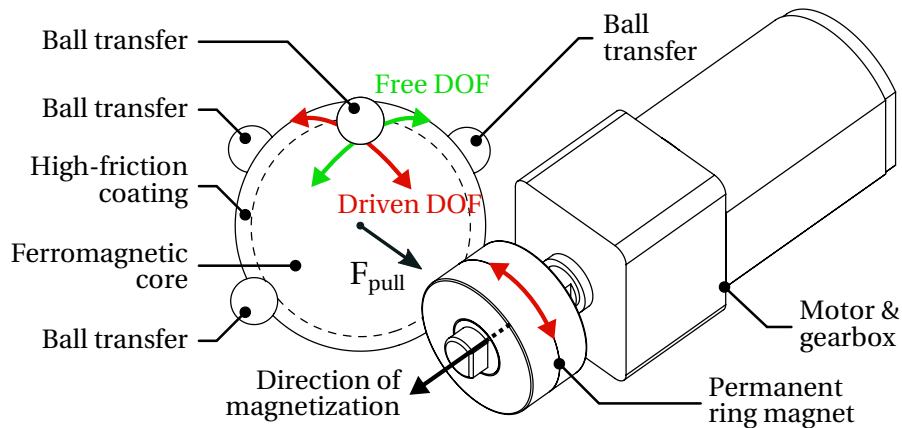


Figure 3.1 – Overview of our permanent magnet-assisted ball wheel design. The ball wheel with ferromagnetic core is driven by a permanent ring magnet that acts as the drive roller. The magnet temporarily magnetizes the wheel, exerting a pull force and generating the necessary normal force, which in turn generates the friction force that drives the wheel. The wheel thus acquires one driven and one free DOF.

can be on the top and bottom, called “axial magnetization”, or on the inside and outside, called “radial magnetization”². When compared to axial magnetization, radial magnetization would evidently provide more gain on the magnetic field strength around the position where the ball wheel would reside, since one of its poles would be significantly closer to that position. However, radially magnetized monolithic permanent magnets are difficult to manufacture and therefore expensive; for this reason, they are often manufactured in multiple segments that are magnetized separately and then glued together. Instead, axial magnetization is more desirable if the necessary magnetic field strength can be generated and the ball wheel can rest against the height of the magnet (*i.e.* is not unconditionally pulled all the way towards the poles) using conventional magnets of appropriate sizes; these two conditions were verified to be satisfiable with preliminary empirical experiments that are not detailed here.

Our ball drive design that results from this trajectory in our design space is seen in Figure 3.1. With the normal force generated by the magnetostatic interaction (*i.e.* pull) between the magnet and the wheel, the magnet can ideally drive the wheel around its axis of rotation thanks to the static contact friction while the wheel remains free to rotate around the orthogonal axis on the horizontal plane. This placement ensures that the magnetostatic interaction stays isotropic regardless of the wheel’s or magnet’s orientations, assuming that the wheel’s core is magnetically isotropic in all directions and the magnet is magnetically isotropic around its rotation axis, which may not be entirely the case due to manufacturing tolerances. In any case, given a wheel diameter and a motionless wheel, the normal force magnitude can be controlled in design by choosing the magnet size (whose analysis is given in the next section) and magnetization strength.

²Diametrical magnetization is also readily available but is not useful to our application.

3.2. Development – Permanent Magnet-Assisted Ball Drive

During motion however, the magnetic after-effect and induced eddy currents in the wheel will result in parasitic forces that impede the motion around the free DOF. This problem will be mitigated by the empirical choice of ferromagnetic wheel core material (among readily available ones offered by manufacturers) that minimizes these effects since the proper analysis of this phenomenon is beyond the scope of this thesis. Moreover, the rubber coating around the ferromagnetic wheel core (required for traction on the ground) will result in further parasitic forces due to the roller-wheel contact point having nonzero area caused by rubber deformation. This problem will be mitigated by preferring higher hardnesses when selecting the rubber coating. Apart from these, the wheels will be assumed to rotate slowly enough that these effects are negligible.

The ball wheel is loosely enclosed in a space defined by the drive roller and 4 ball transfer units: Above the wheel (bears the weight of the robot), opposite the drive roller and finally on the left and right of the wheel. As a design choice, the motor is not fixed on the frame and is left free to move along the plane perpendicular to the driven axis. The drive roller and the wheel are also free to move along this plane but are constrained by the frame and the ball transfers respectively: They are only allowed to move a very small amount such that the disturbance on the system's geometry is minimal. The magnetic pull force ensures that the wheel-drive roller contact remains unbroken during these motions. This design choice ensures that the shear loads due to external user manipulation are redirected to the robot frame and/or ball transfers instead of the motor shafts, prolonging the life of the motors and the gearboxes; this mechanism is detailed in Section 3.2.3.

Finally, the encoding of wheel rotation must be considered for odometry, which is not trivial for a design such as ours. Two low-cost solutions in the literature are optical mouse sensors on wheels (such as the one in [137]) and rotary encoders on the motor shaft. Instead of these, we rely on our absolute global localization method described in the previous chapter by estimating the wheel velocities using the robot velocity (v_x, v_y, ω) with trivial inverse kinematics, the collective geometry of the wheels being known beforehand.

3.2.2 Magnetostatic Wheel-Magnet Interaction Analysis

The magnetostatic interaction between the ball wheel and the magnet depends on the physical dimensions of both objects and is not trivial to predict. Nevertheless, it is desirable to know under which design dimensions the ball will rest along the height of the magnet (and will not be pulled entirely towards the poles), where it rests and how much force will be exerted on it. In order to determine these, initially, the ball wheel dimensions were fixed according to readily available and practical manufacturing dimensions that conform to our envisioned robot size: The ferromagnetic wheel core diameter was thus chosen to be 14 mm with a rubber coating that is 1 mm-thick (thinnest available). The pull and shear forces on the wheel were then simulated using *COMSOL Multiphysics 5.2* (Finite Element Analysis (FEA) software) for parametric magnet dimensions and position, as seen in Figure 3.2.

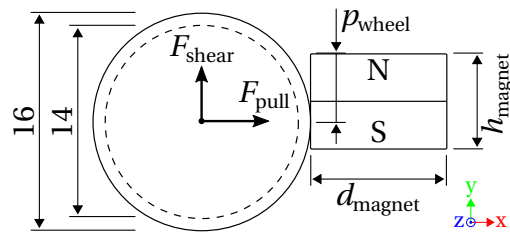
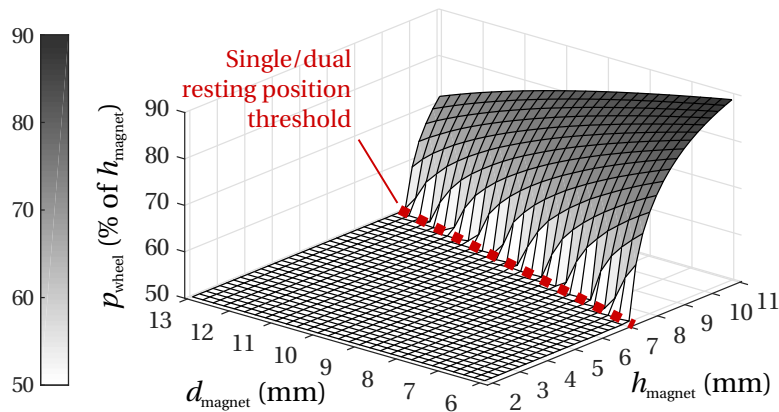
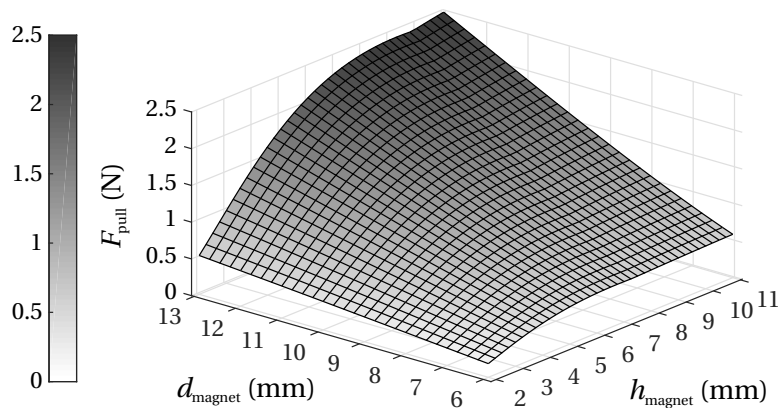


Figure 3.2 – Magnetostatic wheel-magnet interaction analysis parameters and calculated quantities, top-down view, dimensions in mm. The ferromagnetic wheel core diameter was chosen as 14 mm with a 1 mm-thick rubber coating. With these, the shear and pull forces (F_{shear} and F_{pull}) exerted on the wheel are simulated for a range of magnet diameter (d_{magnet}), height (h_{magnet}) and wheel position (p_{wheel}) values. Ring magnet hole diameter was set to 40 % of d_{magnet} . This constitutes a 3D parameter space.



(a) Wheel resting position(s). For every $p_{wheel} \neq 50\%$ (above threshold), there is trivially a second resting position at $100\% - p_{wheel}$ (not shown above) due to the magnet's dipole symmetry.



(b) Pull forces exerted on the wheel at resting position(s).

Figure 3.3 – Magnetostatic wheel-magnet interaction analysis results, calculated by *COMSOL Multiphysics 5.2*. Wheel core permeability assumed to be $\mu_r = 500$, magnet magnetization assumed to be $M = 9.75 \times 10^6 \text{ Am}^{-1}$ (calibrated by measuring force on a real magnet).

3.2. Development – Permanent Magnet-Assisted Ball Drive

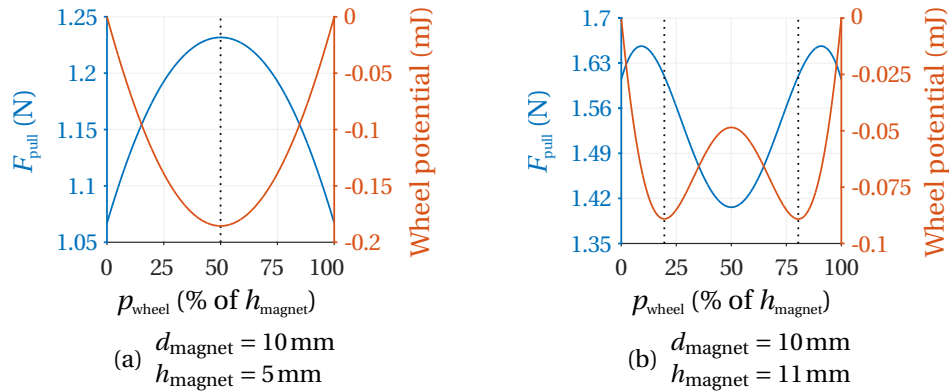


Figure 3.4 – Pull forces and wheel potentials for selected magnet dimensions, showing single and dual natural resting positions; these are marked with dotted lines.

The obtained shear forces were then used to calculate the potential of the wheel in order to determine its resting position. Throughout the section, the wheel resting position (*i.e.* d_{wheel}) is given in percentages of the magnet height (*i.e.* d_{magnet}) to remain invariant to the magnet height parametrization: 0% corresponds to the upper edge, 50% corresponds to midway between two edges *etc.* In the end, knowing how the system behaves in the design space will let us choose appropriate dimensions for our components.

The results of the analysis, namely resting positions and pull forces, are given in Figures 3.3a and 3.3b respectively. Considering the resting positions in the parameter space, it can be seen that there exists a threshold below which the wheel rests at the center of the magnet (example in Figure 3.4a), requiring small enough d_{magnet} and large enough d_{magnet} . For all such pairs of magnet dimensions, F_{pull} is observed to be symmetric around the resting position. Beyond this threshold, the wheel rests at two symmetric positions which quickly move away from the center towards the edges with larger d_{magnet} and smaller d_{magnet} (example in Figure 3.4b), but the wheel rests at some position along the magnet height and is not pulled entirely towards the poles (at least not within the tested parameter space). However, for all such pairs of magnet dimensions, F_{pull} is observed to not be symmetric around the resting positions. Finally, it is observed that F_{pull} at resting position(s) increases almost linearly with increasing d_{magnet} , but tends to increase and saturate with increasing d_{magnet} . Therefore, after a point, there is little or no F_{pull} gain with increased d_{magnet} .

Given the analysis results, we chose to remain within the single resting position region; it is desirable to have symmetric behavior around the resting position, since the wheel will inevitably move a small amount along the magnet height due to inaccuracies during motions involving its free DOF in a multi-wheel configuration. In this region, the smallest geometrically feasible pair of off-the-shelf dimensions that would ensure enough F_{pull} was chosen, which corresponds to $d_{\text{magnet}} = 10 \text{ mm}$ and $d_{\text{magnet}} = 5 \text{ mm}$. The magnetic field resulting from these magnet dimensions in the presence of the ferromagnetic wheel core can be observed in Figure 3.5.

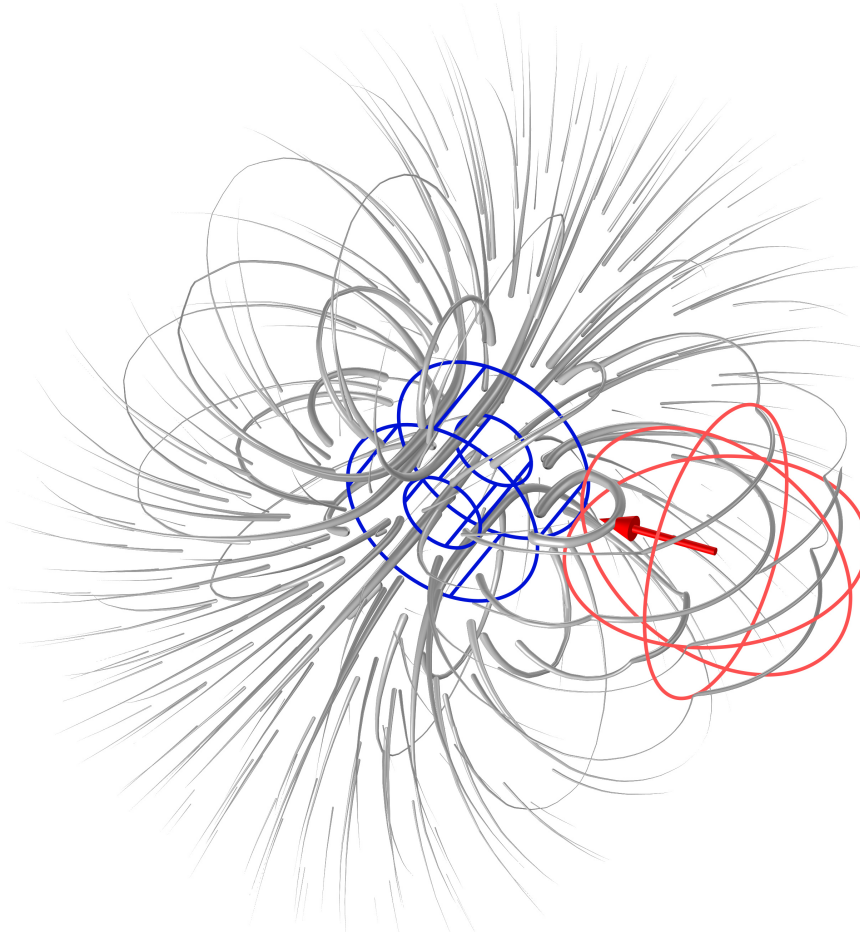


Figure 3.5 – Magnetic field lines in a single ball wheel-ring magnet assembly where $d_{\text{magnet}} = 10\text{mm}$ and $h_{\text{magnet}} = 5\text{mm}$, drawn with *COMSOL Multiphysics 5.2*, showing the expected coupling of the ferromagnetic wheel core with the magnetic field. The outlines of the magnet and wheel core are drawn with blue and red respectively. Rubber coating on the ball wheel is not shown (but was taken into account during calculations). The force applied on the wheel is shown with the red arrow, predicted to be 1.232 N.

3.2.3 Dynamics of Single Ball Drive

Now that we know the magnitudes and behaviors of forces resulting from the magnetostatic interaction between the wheel and the magnet, we focus our interest on the entirety of forces and torques acting on the elements of our system and their relations to our motor output torques during motion. First, we draw attention to the two distinct modes of operation resulting from the design choice where the magnet-motor assembly is left unmounted from the robot frame; these are seen in Figure 3.6a and Figure 3.6b and are considered separately.

By virtue of this design choice, when the robot is externally manipulated, either the wheel will rest against the opposite ball transfer (*forward mode*, $N_{bs,w} > 0$) or the magnet will rest against the frame (*backward mode*, $N_{fs,m} > 0$), depending on the actuation and manipulation

3.2. Development – Permanent Magnet-Assisted Ball Drive

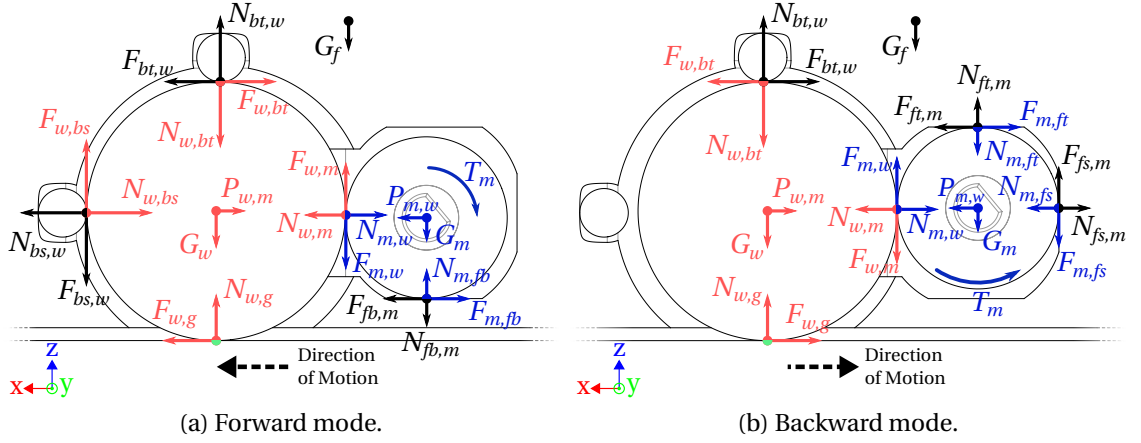


Figure 3.6 – Dynamics of single ball drive, side view. Normal, friction, gravity and magnetostatic pull forces denoted with N , F , G and P respectively. Torque denoted with T . Ball wheel, magnet, robot frame and ground (rigid bodies) denoted with w , m , f and g respectively. Different contact points on the frame denoted with bs , bt (ball transfers), ft , fs and fb (surfaces acting as plain bearings). Forces acting on wheel, magnet and frame colored in red, blue and black respectively.

forces: This redirects all external manipulation loads to ball transfers and/or the frame and prevents them from resulting in shear loads on the motor shaft. Although this method results in reduced precision, increased friction and backlash at the wheel level, it adds robustness against human interaction and potentially increases motor and gearbox lifetime using no extra parts.

From a broader point of view, knowing the effect of the motor output torque (a quantity that we can indirectly control) to the forces applied to the ground from the wheels is desirable since these are the forces that ultimately move the robot. For our considerations, we take the robot frame, the ball wheel and the motor-magnet assembly as rigid bodies. To derive the relationship between the motor output torques and the forces applied to the ground, we assume that there is no vertical acceleration, a third of the robot frame is supported by each wheel and all rigid bodies accelerate identically on the plane:

$$a_{\text{robot}} = a_{\text{magnet}} = a_{\text{wheel}} = a_{\text{frame}} \quad (3.1)$$

We further assume that the wheel does not slip against the ground or the magnet:

$$\alpha_{\text{magnet}} r_{\text{magnet}} = \alpha_{\text{wheel}} r_{\text{wheel}} = a_{\text{robot}} \quad (3.2)$$

$$F_{w,m} \leq \mu_s^{\text{wheel-magnet}} N_{w,m} \quad (3.3)$$

$$F_{w,g} \leq \mu_s^{\text{wheel-ground}} N_{w,g} \quad (3.4)$$

The magnet-robot frame frictions are always kinetic while the wheel-ball transfer frictions

Chapter 3. Phase II – Actuated Tangibles

were taken to be kinetic against the wheel surface to accommodate the worst case scenario where the ball transfer gets blocked:

$$F_{m,fs} = \mu_k^{\text{magnet - frame}} N_{m,fs} \quad (3.5)$$

$$F_{m,ft} = \mu_k^{\text{magnet - frame}} N_{m,ft} \quad (3.6)$$

$$F_{m,fb} = \mu_k^{\text{magnet - frame}} N_{m,fb} \quad (3.7)$$

$$F_{w,bt} = \mu_k^{\text{wheel - ball transfer}} N_{w,bt} \quad (3.8)$$

$$F_{w,bs} = \mu_k^{\text{wheel - ball transfer}} N_{w,bs} \quad (3.9)$$

Given the practical materials used in the implementation (detailed in Section 3.3), the following coefficients of friction were used:

$$\mu_s^{\text{wheel - magnet}} = \mu_s^{\text{NBR - Polished Nickel}} = 0.82 \quad (\text{measured}^3) \quad (3.10)$$

$$\mu_s^{\text{wheel - ground}} = \mu_s^{\text{NBR - ?}} = 0.8 \quad (\text{taken as a maximum}) \quad (3.11)$$

$$\mu_k^{\text{magnet - frame}} = \mu_k^{\text{Polished Nickel - PLA}} = 0.37 \quad (\text{measured}^4) \quad (3.12)$$

$$\mu_k^{\text{wheel - ball transfer}} = \mu_k^{\text{NBR - PTFE}} = 0.07 \quad ([141]) \quad (3.13)$$

With the above assumptions, practical values (such as masses of rigid bodies) and relations (the ones in the form of $F = ma$ and $T = I\alpha$ are omitted), the following can be derived:

$$F_{w,g} = \begin{cases} 140.0T_m - 0.0648 \text{ N} & \text{if } \textit{forward mode} \text{ and } T_m < 0.00180 \text{ Nm} \\ 128.0T_m - 0.0441 \text{ N} & \text{if } \textit{forward mode} \text{ and } T_m > 0.00180 \text{ Nm} \\ 126.0T_m - 0.0108 \text{ N} & \text{if } \textit{backward mode} \end{cases} \quad (3.14)$$

In *forward mode*, with small enough torque (first case above), the system enters a degenerate state where the robot frame is only accelerated by the top ball transfer and magnet-frame contacts (*i.e.* by $F_{fb,m} + F_{bt,w}$ where $N_{bs,w} = 0$ and $N_{fs,m} \neq 0$). In all cases, dropping the wheel-ground no slip condition (*i.e.* $F_{w,g} \leq \mu_s^{\text{wheel - ground}} N_{w,g}$ and $\alpha_{\text{wheel}} r_{\text{wheel}} = a_{\text{robot}}$ are not necessarily true) reveals that wheel-ground slip always occurs before wheel-magnet slip thanks to the magnetic pull force:

$$T_m = \begin{cases} \left. \begin{array}{l} 0.00442 \text{ Nm} \implies \text{wheel-ground slips} \\ 0.00531 \text{ Nm} \implies \text{wheel-magnet slips} \end{array} \right\} \text{if } \textit{forward mode} \\ \left. \begin{array}{l} 0.00424 \text{ Nm} \implies \text{wheel-ground slips} \\ 0.0596 \text{ Nm} \implies \text{wheel-magnet slips} \end{array} \right\} \text{if } \textit{backward mode} \end{cases} \quad (3.15)$$

³Value was measured when components were clean; in the presence of contaminants, such as dust gathered in the system from regular indoor use, it was measured to be as low as 0.66. This implies that for best performance, the wheel and the magnet must be cleaned regularly.

⁴Worst value measured. Depending on the structure of the manufactured surface, value was measured to be as low as 0.32.

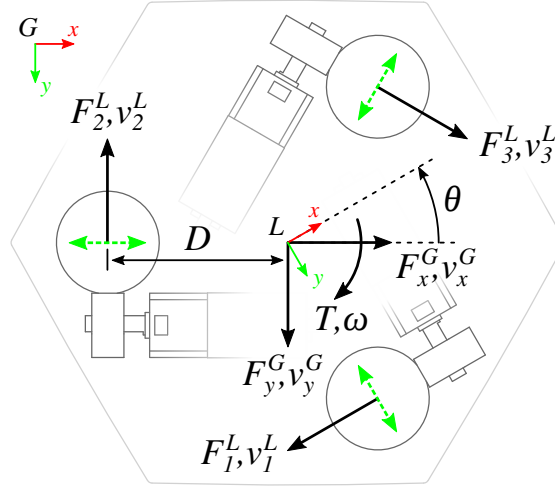


Figure 3.7 – Quantities of interest and frames of reference in the kinematics & dynamics of the Cellulo robot, top-down view. Local and global frames of reference shown with L and G respectively. Reference frames are chosen such that the z axes point downwards in order to conform to screen coordinate systems. Free DOF are marked with dashed green. Vector quantities having same direction are overlaid on same arrow. In the above state, the robot is rotated by about -30° with respect to the global frame.

This section covers the dynamics of each wheel independently under assumptions such as the existence of three wheels and equal weight distribution per wheel. However, the dynamics of a given wheel depends also on the dynamics of other wheels and the overall geometry of the system. Moreover, external manipulation by users may affect the dynamics, and may require additional sensors to detect and handle correctly. These concerns are not considered in this thesis and are left as future work.

3.2.4 Towards a Complete Drive – Kinematics & Dynamics of Robot

Now we approach the problem of building a complete locomotion system using the omnidirectional ball wheels whose individual dynamics are derived in the previous section. The derivations presented in this section were previously published in [142, Appendix] and their goal is to relate motor outputs (quantities we have direct control over) to robot velocities and output forces (quantities we wish to control). The scalar and vector quantities and the frames of reference that are referred to throughout the section are given in Figure 3.7. First, we give the inverse kinematics that is well known for the geometry of our robot (given also in *e.g.* [127, 128, 130]), from which the forward kinematics can be derived easily:

$$\begin{pmatrix} v_1^L \\ v_2^L \\ v_3^L \end{pmatrix} = K^{-1}R(-\theta) \begin{pmatrix} v_x^G \\ v_y^G \\ \omega \end{pmatrix} \quad (3.16)$$

where:

$$K^{-1} = \begin{pmatrix} -1 & 0 & D \\ 1/2 & -\sqrt{3}/2 & D \\ 1/2 & \sqrt{3}/2 & D \end{pmatrix} \quad \text{and} \quad R(\theta) = \begin{pmatrix} \cos\theta & -\sin\theta & 0 \\ \sin\theta & \cos\theta & 0 \\ 0 & 0 & 1 \end{pmatrix} \quad (3.17)$$

[143] gives the dynamics of an omni-wheeled robot; the transmission from the ground forces to robot forces and torque hold in our case as well:

$$\begin{pmatrix} F_1^L \\ F_2^L \\ F_3^L \end{pmatrix} = C^{-1}R(-\theta) \begin{pmatrix} F_x^G \\ F_y^G \\ T \end{pmatrix} = C^{-1}R(-\theta) \begin{pmatrix} m a_x^G \\ m a_y^G \\ I_z \alpha \end{pmatrix} \quad (3.18)$$

where m , I_z are the mass and the moment of inertia of the robot around the z axis respectively, F_j^L correspond to $F_{w,g}$ from the previous section and:

$$C^{-1} = \begin{pmatrix} -2/3 & 0 & 1/(3D) \\ 1/3 & -\sqrt{3}/3 & 1/(3D) \\ 1/3 & \sqrt{3}/3 & 1/(3D) \end{pmatrix} \quad (3.19)$$

Considering that the robot orientation is known at all times in our case (given by onboard global localization), the above equations can be used to calculate the necessary wheel forces in order to obtain the desired force/torque output from the robot.

In order to relate motor outputs to the wheel-ground forces, we take the torque-angular velocity relation for each of our three Direct Current (DC) motors:

$$T_j = c_U U_j - c_\omega \omega_j \quad (3.20)$$

where U_j , ω_j and T_j are the output (*i.e.* voltage), angular velocity and torque (corresponds to T_m in the previous section) of the j^{th} motor respectively and c_U , c_ω are positive constants. This can also be expressed as:

$$T_j = c_U U_j - c_v v_j^L \quad (3.21)$$

assuming no slip between the drive roller-wheel and wheel-ground contacts where c_v is another positive constant. In the previous section, it was derived that the wheel-ground force can be expressed as a discontinuous piecewise linear function of the motor torque. Simplifying this function by ignoring the degenerate state (entered by a narrow torque band) allows us to express this linear dependency in only two regions that depend on the direction of the wheel's motion:

$$T_j = c_F(\text{sgn}(v_j^L))F_j^L + c(\text{sgn}(v_j^L)) \quad (3.22)$$

3.2. Development – Permanent Magnet-Assisted Ball Drive

where $c_F(s)$ and $c(s)$ are dual constants that take two different values depending on their input s (theoretical values derived in Equation 3.14 gives acceptable starting points for these constants, before further calibration). $c_F(s)$ represents the force-torque coupling and therefore is always positive while $c(s)$ represents friction and is the same sign as s , resulting in the additional torque requirement. Taking Equations 3.21 and 3.22 together yields:

$$c_U U_j - c_v v_j^L = c_F(\text{sgn}(v_j^L)) F_j^L + c(\text{sgn}(v_j^L)) \quad (3.23)$$

At this point, we make the further simplification that the robot's mass and moment of inertia are negligible so that it can accelerate/decelerate instantly from the user's point of view. It was empirically measured that the implemented robot (described in detail in the next section) can reach its maximum velocity (about 185 mm/s) in 0.23 s and maximum angular velocity (about 7.2 rad/s) in 0.40 s when the motors are driven with full output, justifying this simplification. Then Equation 3.18 is approximately equal to the zero vector, making the wheel-ground forces approximately zero:

$$c_U U_j \approx c_v v_j^L + c(\text{sgn}(v_j^L)) \quad (3.24)$$

Plugging in Equation 3.16 and dividing by c_U :

$$\begin{pmatrix} U_1 \\ U_2 \\ U_3 \end{pmatrix} \approx \hat{c}_v K^{-1} R(-\theta) \begin{pmatrix} v_x^G \\ v_y^G \\ \omega \end{pmatrix} + \begin{pmatrix} \hat{c}(\text{sgn}(v_1^L)) \\ \hat{c}(\text{sgn}(v_2^L)) \\ \hat{c}(\text{sgn}(v_3^L)) \end{pmatrix} \quad (3.25)$$

Here, $\hat{c}_v = c_v/c_U$ and $\hat{c}(s) = c(s)/c_U$ where c_v and c_U are to be calibrated. This allows calculating the motor outputs for the desired isolated robot motion.

In the presence of user interaction however, the robot is likely to be blocked in place. In this case, the magnet-wheel contact will be broken with enough motor torque. Assuming unlimited static wheel-ground friction and ignoring internal dynamic frictions, a theoretical $F_{j,\max}^L = 1.01$ N can be transmitted to the ground, limited by the magnet-wheel contact. These correspond to $F_{x,y,\max}^G = 1.75$ N and $T_{\max} = 0.0848$ Nm, again theoretical⁵. Until the contact is broken, the motors are stalled and their torques are transmitted directly to the ground after some portion is lost to internal friction. Equations 3.21 and 3.22 thus become:

$$T_j = c_U U_j \quad \text{and} \quad T_j = c'_F F_j^L + c'(\text{sgn}(F_j^L)) \quad (3.26)$$

where c'_F and $c'(s)$ now depend on the exact configuration that the robot is grasped in (*i.e.* whether the wheels are in *forward* mode, *backward* mode or in intermediate positions); detecting this configuration properly would require additional hardware, such as internal tactile or force sensors at the wheel and magnet level. $c'(s)$ again represents the additional

⁵ $F_{x,y,\max}^G$ was empirically observed to be 0.78 ± 0.10 N (measured from all 6 sides) when the robot is not grasped and to be up to 1.99 ± 0.21 N with a 500 g weight on top of the robot simulating a strong grasp.

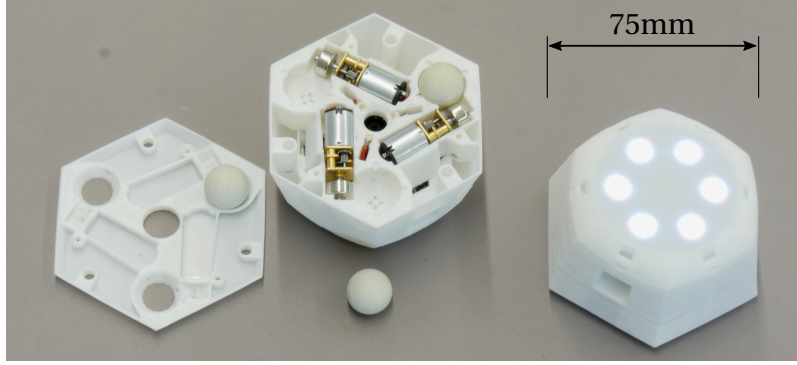


Figure 3.8 – Physical implementation of the Cellulo robot version 2: Locomotion implemented, ergonomics and appearance refined. On the left: Upside down robot with open housing exposing locomotion components and optical system in the center. Two ball wheels out of sockets for visibility.

torque lost to friction (now static) and is the same sign as T_j which is the same direction as F_j^L . Associating the above two equations and plugging them into Equation 3.18:

$$\begin{pmatrix} U_1 \\ U_2 \\ U_3 \end{pmatrix} = \hat{c}_F' C^{-1} R(-\theta) \begin{pmatrix} F_x^G \\ F_y^G \\ T \end{pmatrix} + \begin{pmatrix} \hat{c}'(\text{sgn}(F_1^L)) \\ \hat{c}'(\text{sgn}(F_2^L)) \\ \hat{c}'(\text{sgn}(F_3^L)) \end{pmatrix} \quad (3.27)$$

Here, $\hat{c}_F' = c_F'/c_U$ and $\hat{c}'(s) = c'(s)/c_U$ where c_U is the same as before and c_F' and $c'(s)$ are to be calibrated with average values, providing an approximate solution to the lack of the aforementioned sensors, whose addition is not desirable with our strict cost and simplicity constraints. After $F_{j,\max}^L$ (*i.e.* when the magnet-wheel contact is broken), the magnet will apply a kinetic friction force to the wheel that will be transmitted to the ground, resulting in the clamping of the force applied to the robot at the wheel level. Considering the nominal stall torque of our practical motors (0.0348 Nm at 3.7 V, given in the next section), this maximum force corresponds to only 14 % of the drive's (theoretical, per wheel) capacity. Therefore, the force output can only be controlled in this narrow band when the robot is blocked and the outside dead band is reserved for motion.

3.3 Implementation – Cellulo Robot Version 2

We implemented our proposed drive and integrated it into our existing robots, whose electronic design was previously made to accommodate 3 DC motors through 3 motor drivers that were left unpopulated. In addition to these, the housing was redesigned to accommodate the locomotion components as well as to have better ergonomics when grasped; we acknowledge that the “look and feel” of this housing was achieved by Léa Pereyre. We call this new mobile robot hardware, seen in Figure 3.8, the Cellulo robot version 2.

3.3. Implementation – Cellulo Robot Version 2

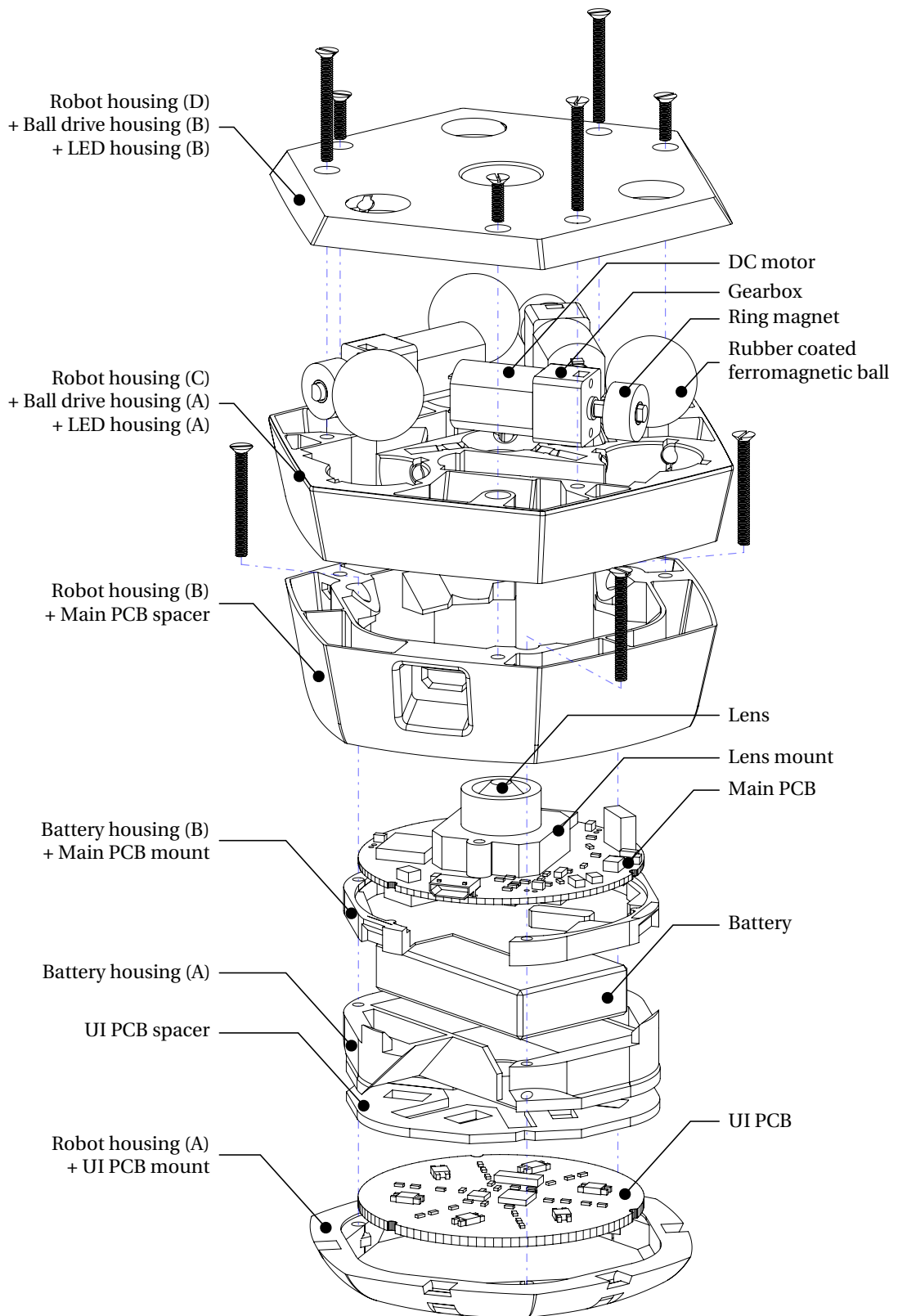


Figure 3.9 – Exploded view of Cellulo robot version 2, upside-down. Screw routes shown in dashed blue. Battery cables, motor cables and PCB interconnect cable not shown.

Component	Part Number	Cost (€)
Components in version 1 (Table 2.2) except housing and fastening		74.25
Ball wheels		1.30 × 3
Ball transfer units		0.06 × 18
Magnets		0.44 × 3
Motors (with integrated gearbox)	<i>Pololu 2364</i>	13.18 × 3
Motor drivers	<i>BD6210HFP</i>	1.31 × 3
Housing (53.3 g PLA) & fastening		1.91
Total		125.93

Table 3.1 – List of Cellulo robot version 2 components and their costs.

Similar to the first version, the frame (including ball transfer enclosures embedded within it) and motor shaft adapters for the magnets were manufactured using FFF with PLA. As before, the frame has a hexagonal form (about 75 mm width, 80 mm end-to-end) enclosing all components and isolating them from the exterior except three 11 mm-diameter holes on the bottom where the wheels are exposed. The ground clearance is 0.8 mm and the entire locomotion subsystem fits inside a height of 19 mm, measured from the ground. The entire assembled robot weighs 167.8 g. The exploded view displaying the locomotion components and their relation to the rest of the robot (mostly unchanged) can be seen in Figure 3.9.

Apart from the above, all components are off-the-shelf. This includes the ball transfer units which are simple Polytetrafluoroethylene (PTFE) balls enclosed in the frame. This low performance method of producing ball transfers was preferred since at our scales, it is very difficult to obtain off-the-shelf, low-cost and high-performance ball transfer units. Two more ball transfers were added to the bottom of each wheel to keep them from contacting the frame when the robot is picked up; they are not active during normal motion. The ball wheel core (14 mm diameter) material was chosen to be American Iron and Steel Institute (AISI) 1010 low carbon steel that was empirically tested to have better performance compared to higher carbon or stainless steel balls in terms of parasitic forces due to eddy currents and magnetic after-effect. A pure iron core would have better expected ferromagnetic performance but was not preferred due to steel ball bearings being more readily available.

A 1 mm-thick coating completes the wheel diameter to 16 mm, as previously envisioned. Empirical testing among Silicone, Neoprene and Nitrile Butadiene Rubber (NBR) (common materials that typically have desirable qualities such as high friction) revealed that NBR has the best friction performance and wear resistance, which was then selected as our coating material in Shore A 90 hardness, the hardest available at the manufacturer. A nickel-plated Neodymium magnet of N42 magnetization (material and strength that was previously used in the analysis presented in Section 3.2.2) was chosen in the previously envisioned dimensions. These and

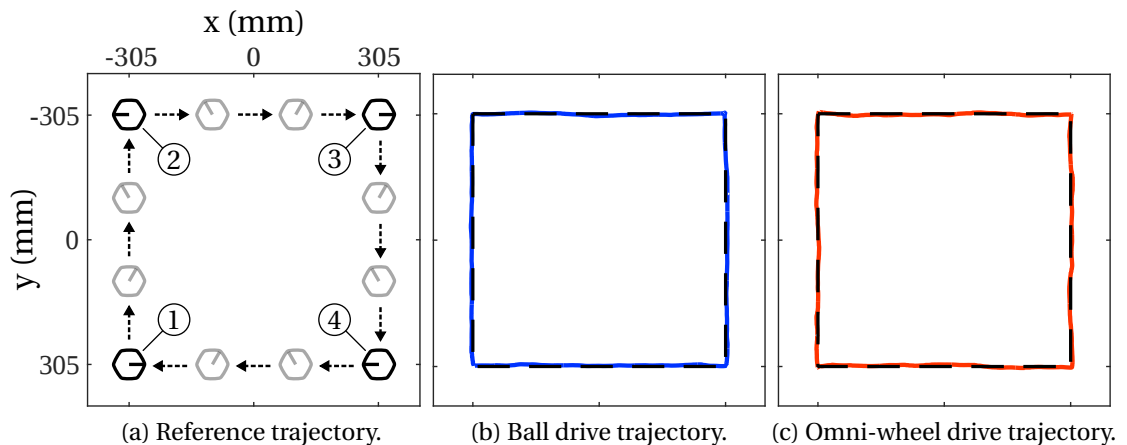


Figure 3.10 – Reference trajectory for locomotion performance evaluation, designed to fit on an A0 sheet; robots were simply commanded to move to the next goal pose with given maximum velocities at poses ①, ②, ③ and ④. Typical x, y trajectories executed by both robots are also given as an overview of the performances.

other components are listed in Table 3.1 with their cost at the time of our implementation.

The motors are driven with a motion controller that tracks a command pose by determining the required robot velocity (v_x, v_y, ω) in a closed loop fashion with a Proportional-Integral-Derivative (PID) controller. Motor outputs (U_1, U_2, U_3) are then calculated from the required robot velocity using Equation 3.25. This simple controller was observed to be adequate for the evaluation made in the following section; improvements to it will be presented in the next chapter, along with haptics controllers that produce force outputs from the robot.

3.4 Supervised Validation

3.4.1 Overview

Having implemented mobile robots, we now focus on rigorously characterizing the locomotion performance, similar to how we characterized the localization performance in the previous chapter. Now, rather than the accuracy of the reported absolute pose, we aim to measure the fidelity of our robot in following trajectories composed of these poses as a pure measure of locomotion performance. As before, this study is done in laboratory conditions in order to obtain the best possible performance; this is useful to provide a reference upper bound for not only our applications but any future work that may benefit from such a locomotion system.

3.4.2 Procedure

In order to measure the trajectory following fidelity, the square trajectory seen in Figure 3.10a that involves simultaneous linear and angular motions was selected and printed on an A0 sheet

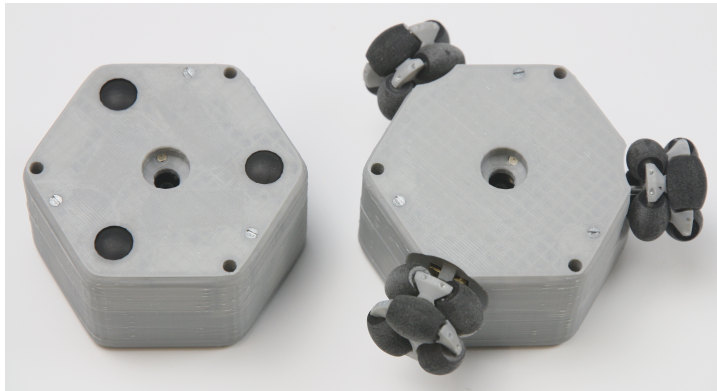


Figure 3.11 – Our ball drive robot with a temporary development frame built for this study (on the left), otherwise identical to our final implementation, in comparison to the omni-wheel drive robot built as a baseline (on the right). Both robots rest bottom-side-up.

for the robot to follow with 150 mm/s maximum linear velocity and $\pi/4.067$ rad/s maximum angular velocity. Commands to track the next pose were given on the corners of the trajectory when they are reached, *i.e.* a total of 4 times. The particular use of global localization in the motion controller ensures that the goals are eventually reached, but it does not ensure tracking of real velocities and therefore fidelity to the ideal trajectory in a closed loop.

This calibrated open loop method was preferred for the measurement of the lower bound of performance in a scenario where the wireless communication is limited with the master device (*e.g.* tablet) that stores the arbitrary trajectory to be tracked. In more involved scenarios, the communication channel may have high enough bandwidth and low enough latency that allows the closed loop control of the robot velocities by the master device that stores and processes the trajectory, or the robot may support the prior transmission of the previously known trajectory to be tracked⁶. In these scenarios, we hypothesize that higher trajectory tracking fidelities can be achieved since the deviation from the trajectory can be corrected in real time, which is not attempted in this study.

Furthermore, an alternative version of our robot was built with omni-wheels, seen in Figure 3.11, to be compared with our ball drive design. As previously mentioned in Section 3.1.3, omni-wheels are arguably the most common choice in building holonomic drives and are well studied; as such, it is useful to have an omni-wheel drive as a baseline. This drive was built to have the same geometry and kinematics except the wheel offset from center: 46.9 mm *vs.* 28 mm in the ball drive. The same manufacturing methods and components were used except 50 : 1 gear reduction motors instead of 30 : 1 due to the different size of wheels. Care was taken during frame manufacturing that both robots have roughly the same weight; the ball drive robot weighs 178.9 g (reduced further in the final implementation to achieve the weight reported in Section 3.3) whereas the omni-wheel drive robot weighs 178.1 g.

⁶In the next chapter, we describe the addition of such an option, namely the tracking of composite cubic Bézier curves that are transmissible over the communication channel, to the motion trackers available on our robots.

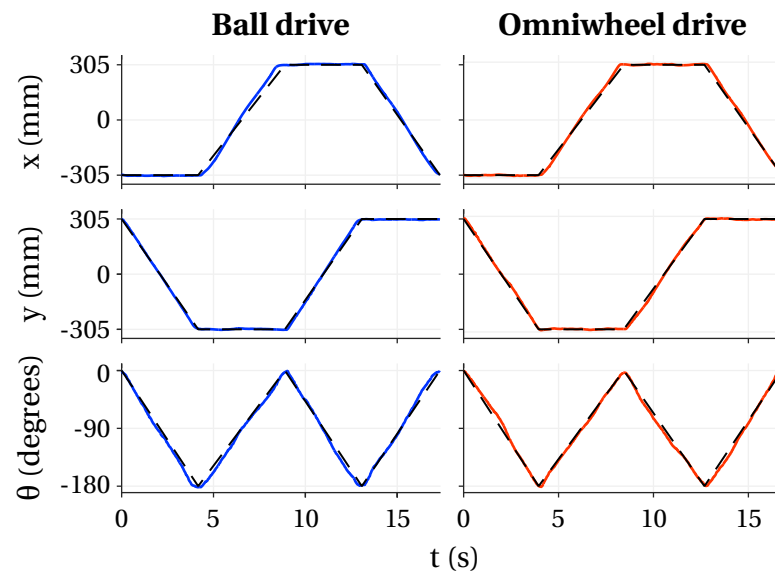


Figure 3.12 – Typical trajectories followed by robots. Dashed lines indicate values of ideal trajectory.

The 30 mm-diameter omni-wheels were custom manufactured due to the lack of such a small size off-the-shelf. The rims were manufactured with FFF while the rollers (hard plastic core, 1 mm-thick Shore A 85 hardness rubber-like exterior) were manufactured with Multi-Jet Modeling (MJM) for €2.18 per roller. The same motion controller was used with appropriately calibrated coefficients in both robots for fair comparison.

10 runs were done for each robot where pose data were collected from the robots' own global localization systems at about 46.6 Hz (subsequent to this study, this framerate was improved to the one reported in Section 2.5.3). These measurements were taken as ground truth since the accuracy and precision of either of the locomotion systems are expected to be much lower than the localization system that is entirely solid state. In this setup, the sources of significant systematic error are identified as:

- FFF and MJM tolerances, notably for magnet-shaft adapters, ball transfer housings and omni-wheel rollers
- Ball wheel fabrication tolerances: Off-center core results in anisotropic moment of inertia and magnetostatic interaction forces
- Off-the-shelf motor variances, causing some wheels to consistently rotate more than others with the same input

3.4.3 Results

The typical trajectories followed by the ball drive and omni-wheel drive robot can be seen in Figures 3.10b and 3.10c (only x , y components) respectively as an overview of the performances of both drives. A more detailed look at typical performances of all pose components

Mode	Measured quantity	Omni-wheel drive	Ball drive
Mean	$ x_{\text{sampled}} - x_{\text{ideal}} $	7.53 ± 8.26 mm	11.1 ± 11.3 mm
	$ y_{\text{sampled}} - y_{\text{ideal}} $	6.66 ± 7.80 mm	6.52 ± 7.07 mm
	$ \theta_{\text{sampled}} - \theta_{\text{ideal}} $	$4.40 \pm 3.14^\circ$	$5.40 \pm 3.80^\circ$
Worst	$\max x_{\text{sampled}} - x_{\text{ideal}} $	33.3 ± 6.3 mm	44.6 ± 4.5 mm
	$\max y_{\text{sampled}} - y_{\text{ideal}} $	34.0 ± 4.8 mm	30.8 ± 7.4 mm
	$\max \theta_{\text{sampled}} - \theta_{\text{ideal}} $	$12.9 \pm 1.9^\circ$	$14.9 \pm 2.0^\circ$

Table 3.2 – Comparative performances of proposed ball drive and baseline omni-wheel drives, values given with \pm one standard deviation. In **Mean**, all samples from all 10 runs were taken ($N_{\text{ball drive}} = 8183$, $N_{\text{omni-wheel drive}} = 7705$) while in **Worst**, maximum deviation of each run was taken ($N_{\text{ball drive}} = N_{\text{omni-wheel drive}} = 10$).

is given in Figure 3.12, showing the slightly worse performance of the ball drive *vs.* the more accurate omni-wheel drive.

To quantitatively compare the performances of the two robots, deviations from the ideal trajectory (defined as the accelerationless constant-velocity trajectory from one command pose to the next) were calculated for each sample, separately for x , y and θ . The worst deviations for each run, as well as the overall average deviations are compared in Table 3.2. These deviations are expected to be similar for trajectories that are tracked with similar velocities, regardless of trajectory length, as long as the localization accuracies (used as ground truth) can be ensured to not be significantly worse.

The results indicate that the omni-wheel drive performed better in x and θ while the difference in y was not statistically discernible (due to the alignment with the orientations in the trajectory). This clear performance gap can be explained by our design choice to leave the wheel-magnet-motor assembly free to increase robustness against external user manipulation, as well as low performance components with poor manufacturing tolerances (particularly wheels and ball transfers) affecting the dynamics of overall the system more compared to the omni-wheel drive.

From another perspective, the omni-wheel drive was haptically observed to vibrate significantly more compared to the ball drive due to discontinuous contact points with the ground, as expected. This difference can be quantified with Inertial Measurement Unit (IMU)s attached to the robots that measure the vertical acceleration during the runs, which is left as future work. Furthermore, even though we produced the smallest sized omni-wheels that we were able to with similar manufacturing methods and costs, we were not able to achieve the volumetric compactness that was permitted by the ball drive. If the performance differences provided above (and other shortcomings discussed in the next section) can be tolerated in a given application, the ball drive design can be preferred over the traditional omni-wheels for these added benefits (and others, again discussed in the next section).

3.4.4 Conclusion

This section presented the validation of our permanent magnet-assisted ball drive design where we quantitatively characterized the performance and compared it against a baseline built with popular and common omni-wheels. From a qualitative perspective, the key benefits of our design are:

- Almost fully made of low cost off-the-shelf components
- Naturally compact geometry
- Less vibration and smoother motion compared to more popular omni-wheels
- Mechanical components that must be exposed to the outside world (rubber sphere segments) exceptionally small and simple, potentially reducing distractions and cognitive load in (mainly younger) learners
- Equivalent control on drive roller-wheel contact force with simpler elements compared to traditional passive mechanisms in other ball drive designs (*e.g.* spring-loaded passive roller, drive roller deformation)
- Robustness against physical user interaction by virtue of leaving the wheel-magnet-motor assembly unmounted, permitted by the magnetic force preservation

However, certain drawbacks must be taken into account:

- Not suitable for high-precision applications due to leaving the wheel-magnet-motor assembly unmounted from the frame and due to extensive use of contact dynamics
- Robot should be lightweight enough due to low load bearing capabilities of simple ball transfer units
- Robot should be small enough in size; larger robots would require potentially too large and dangerous magnets and too heavy ball wheels
- Ground surface should be flat enough (*e.g.* tabletop) due to low ground clearance
- Encoding ball wheels is not trivial if a localization system such as ours is not present
- Has less simple dynamics compared to more common elements such as omni-wheels
- Due to the frame bearing the magnet, produces considerable audible noise
- Extra maintenance may be required in the long-term due to extensive use of contact dynamics and potentially due to the accumulation of contaminants in the bearings

Considering the target application presented in this thesis, namely building learning activities for the classroom featuring many palm-sized robots that are capable of haptic feedback and are open to physical interaction, we believe the above features are essential: Omnidirectionality and the absence of vibration are necessary for the flexibility and quality of motion and haptic feedback; compact geometry is required for the handheld size of robots; affordability is important to ensure enough number of robots can be placed in a classroom; and robustness against manipulation is desirable to allow unlimited physical interaction by child learners. In the following section, we present an ecological validation phase where we not only observe the mechanical operation of our mobile robots in the hands of children but begin testing activities that focus on learning.



Figure 3.13 – Windfield playground, playable area $1.7\text{ m} \times 0.66\text{ m}$, microdot pattern omitted. Start and finish lines seen on the leftmost and rightmost edges, as well as obtainable points associated with cities are designed as part of another phase of the activity that is presented in the next chapter.

3.5 Ecological Validation

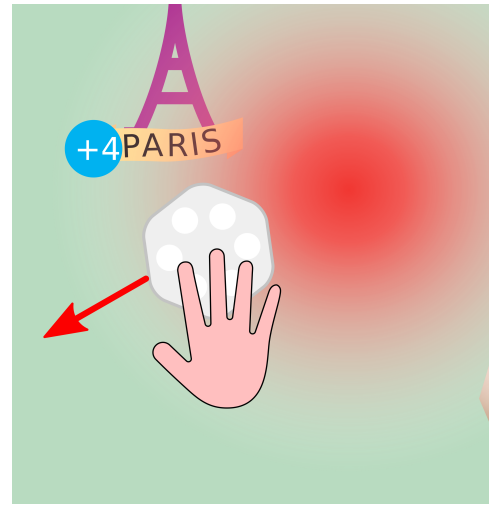
3.5.1 Overview

At this point, our robots feature validated mobility and mechanical robustness against intense external user manipulation for the goal of simultaneously *moving* and *being moved*. From the perspective of users (namely the learners) that are interacting with a small mobile robot, it may not be entirely clear that our robot is intended to be a tangible haptic interface as well as an autonomous robot. Unlike traditional autonomous robots that are often dangerous to interact with (for the user and/or for the robot) or do not actively utilize physical interaction, our robot is able to *intentionally promote* physical interaction thanks to its conceptual and mechanical design.

Therefore, similar to the one presented in the previous chapter, we now choose to perform an ecological validation cycle for our tangible robots where we aim to build and test an activity whose meaning is established around the concept of moving *vs.* being moved. Moreover, we will build our activity with a curricular learning theme in order to move towards the actual application area of our platform. By proposing this activity to child learners and observing their use of our platform, we will test the adequacy of our hardware and software design, as well as gain insight on the perception of the movability of our robots and its added value to learning. On a more practical note, we acknowledge that the development of the activity we are about to present (previously published in [117]) was accomplished with the collaboration of Maria Beltran, Manon Briod (graphics and interaction design) and Dr. Wafa Johal (software co-development and experiment co-design).



(a) Child probing the wind at the south of Paris.



(b) Robot's force output, representing the wind caused by the (invisible) pressure points.

Figure 3.14 – Scene from the *Windfield* study, displaying the haptic interaction that embodies the force of the wind created by atmospheric pressure points. Here, a high pressure point (red area on the right) causes outward winds, pushing the grasped robot (on the left) according to the calculated direction and strength of the wind (red arrow on the right) at that location.

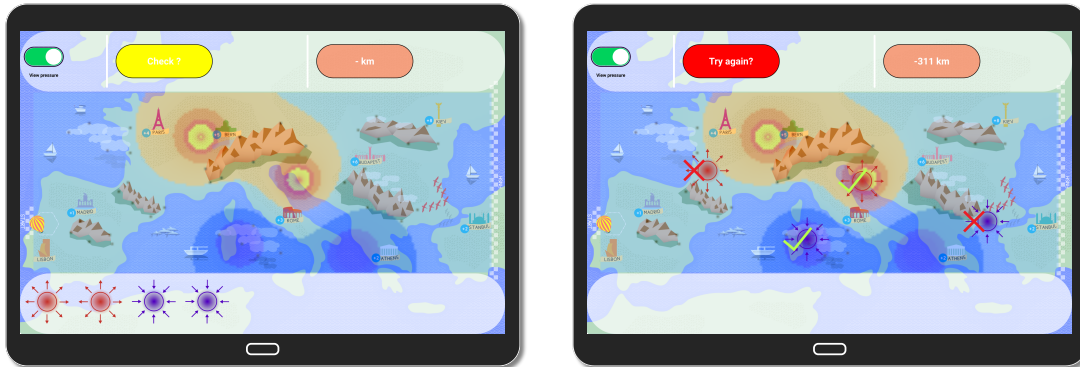
3.5.2 Windfield Study – Design & Participants

Our activity, called *Windfield*, is designed as a learning game that aims to teach the creation mechanism of winds through atmospheric pressure differences. It takes place on the geographical map of Europe (playground seen in Figure 3.13) where the individual robots are introduced as “hot air balloons” that can be placed anywhere on the map by the learners. Through haptic feedback, the localized force of the winds affecting the hot air balloons are conveyed to the learners as long as the robots are grasped, detected by the capacitive touch sensors on the top surface⁷; this interaction is summarized in Figure 3.14.

Multiple atmospheric pressure points that are high or low are placed on the map prior to the learners' interaction. Following their real physical counterparts, these points affect the pressure over the entire playground and their effects diminish with distance. Given all pressure points and their positions, atmospheric pressure values are calculated over a grid spanning the entire playground (resulting in a simplified FEA-like method). These values are then used to calculate the pressure gradient on a given position, which dictates the intensity and direction of the wind on that position; additional factors that affect the wind such as the Coriolis effect or the geographical landscape features are not considered.

Given these points that are not directly visible, the activity pushes the learners to explore the

⁷In principle, force/torque sensors on the grasped surface are required to control the force feedback in a closed loop that are not present on our robots due to cost and scheduling issues.



(a) Atmospheric pressure (hidden to the participant). (b) Participant's guesses for the pressure points.

Figure 3.15 – Screen captures of the Windfield activity application running on the tablet. Position of the hot air balloon is synchronized with the position of the robot on the real playground (seen close to the bottom left corner). Low and high pressure areas are represented in blue and red respectively.

map, “feel” the winds and discover the locations and directions (*i.e.* high or low) of the pressure points creating these winds. After discovering, they indicate their guesses by dragging and dropping the corresponding icons on the tablet (where the playground and the locations of the hot air balloons are displayed), as seen in Figure 3.15. After playing the game, the learners are expected to gain the knowledge that:

1. The wind blows from high to low pressure areas
2. The strength of the wind diminishes with increasing distance from pressure points

We ran the study during two open-door events on two consecutive days for more than 6 hours in total; these were the *Cambridge Science Festival 2016* and a prior event advertised and realized at *Swissnex Boston* tied to the festival. The two events attracted about 15,000 attendees, most of which were children accompanied by their parents; the festival alone was estimated to contain 75,000 face-to-face interactions with such attendees and demonstrators like us. The child attendees came to our tables at their discretion and stayed as much as they wanted, during which they became participants of our study if they interacted with our activity non-trivially (*i.e.* excluding children who were just looking and were manipulating the robots/tablets aimlessly and leaving). Given this particular context, our study is not targeted to verify well-controlled experimental conditions but is envisioned as a “stress test” of the reliability of our hardware and software, and as a situation where we aim to observe a large number of participants interact with and learn from our actuated tangibles.

Prior to the activity, the participants were told what the activity is about and what the robots are standing for. The atmospheric pressure points and how they “blow wind outwards” and “suck winds inwards” were also introduced. After the activity, the ages of the participants were asked. Under these circumstances, with 3 activities running in parallel on 3 separate

playgrounds and tablets, we estimate that about 150 children ranging from 5 to 14 years old participated in our study and attempted to find the hidden pressure points for durations ranging from 2 minutes to 15 minutes.

3.5.3 Results & Discussion

We observed that children engaged easily with the activity in general and did not show reluctance to manipulate the robots. From the opposite perspective, we were asked multiple questions such as “*Where can we buy these [robots]?*”, “*Are you giving these [robots] away?*”, “*Can we take this [playground sheet] with us?*” that suggest that the platform was approachable and attractive. In a few instances, the parents did not let their children approach the activity due to the presence of a tablet; these children were presumably being raised in a “mobile device-free” manner until a certain age. This indicates that tablet-free modes of operation are a factor in the acceptance of Cellulo and their development may be necessary in the future.

Due to the use of capacitive touch sensors to detect the presence of the grasp, the participants were required to grasp the robot from the top. This caused side grasps (observed to be the most prominent instinctive grasp towards our robots without any priming) and top grasps where the palm did not touch the robot surface to remain undetected. Despite this, the haptic modality of conveying a planar force was generally well-received, most children were able to backdrive the robot easily and tell in which direction the robot was pushing their hand when asked. However, the difficulties that were encountered in sensing the presence and properties of the grasp effectively indicate that better sensors that cover more of the grasped surface area must be integrated into the robots in the future.

The effectiveness of the interaction was observed to depend on the directionality of the force: Low pressure points were almost always found before high pressure points since “following the wind” naturally led the robot to one of the low pressure points, acting as sinkholes. On the contrary, high pressure points were more difficult to find as they push the robots away and require the exploration of the surrounding area to be uncovered, which was performed by a fewer number of participants.

From the learning perspective, the age group of the participants had a clear impact on their performance. Children under 11-12 years old (the majority of our participants) often could not find the high pressure points. The ones that did find them were still not able to give satisfactory answers to questions like “What do you think the wind is doing?” or “How do you think wind is connected to the pressure points?”. Youngest participants (5-6 years old) were observed to have difficulties reaching over the far side of the playground and grasping the robot; this prevented them from properly interacting with the activity and underlines that the interactions with the robots and physical size of the playground must be adjusted to the target age group.

Participants over 11-12 years old were generally able to understand that pressure points acted

in all directions by scanning around the points and finding them. Some children exhaustively searched and found all pressure points by spending an abundant time in the activity. Some were able to provide answers to the aforementioned questions such as “It seems to blow from these high points to these low points.”, often pointing at the pressure points on the playground itself. This indicates that children were able to transfer their findings from the tablet to the physical playground, and suggest – at least for older children – that the combination paper, robot, tablet can be perceived as a single, multi-modal, educational tool to help teach these phenomena. We did not find clear evidence, however, on the understanding of decreasing wind intensity with distance to pressure points within any age group, implying that such complex phenomena cannot easily be discovered on one’s own and hints at the importance of a pedagogical scenario that must be designed along with the activity.

3.5.4 Conclusion

In this section, we presented the design and testing of the very first Cellulo activity with a learning theme that demonstrates the use of our robots that can move (in this case in the form of haptic force feedback) and be moved (in this case in the form of the ability to be backdriven and placed anywhere). Through this capability, we enabled the learners to physically experience and understand a complex and invisible phenomenon found in the formal curriculum, that is the interplay of the atmospheric pressures, in a natural manner.

Our hardware, designed with the constraints of real and unsupervised use in classrooms, proved approachable, intuitive and effective in this particular instance. We deployed and collected 3 copies of our activity hardware, namely mobile robots, paper playground sheets and tablets, to and from the experiment sites with considerable ease without the need for any calibration; this mirrors the practicality that we expect in using our platform in real teaching scenarios in classrooms. We acknowledge that this validation had a rather informal nature where we aimed to observe which aspect performed well in general and which aspect did not; in the following chapters, more formal studies that shed clearer light on learning will follow.

Having concluded this chapter where we focused on building *actuated tangibles*, we acknowledge that the study presented in this section relied heavily on haptics as an interaction modality, despite the lack of a formally designed haptics module. It is certainly interesting to advance this aspect of our robots in order to build towards a more comprehensive, well-designed and validated set of haptic outputs, as opposed to the preliminary approach used in this activity. For this reason, in the following chapter, we focus on designing a complete *haptics* module that lets us characterize and validate the haptic performance of our robots. Subsequent to the determination of this performance, we present a study that incorporates an improved version of Windfield where we aim our attention at measuring clear learning gains and observing effects of Cellulo on individual exploration patterns and collaboration in multi-learner teams.

4 Phase III – Haptics with Actuated Tangibles

4.1 Introduction

4.1.1 Background

At this point, following the two design, prototyping and testing iterations that were described in the previous two chapters, we possess robots that are *accurately localized* within the activity and that can *holonomically move and be moved*. More broadly, our robots are a tangible interface to many point-like objects (abstract or concrete) residing in planar workspaces where they represent the spatial presence and motion of these objects. Moreover, by the virtue of their tangibility, they have the emergent potential to convey virtual forces that act on these objects. Depending on the needs of the activity, these may be a due to *e.g.* a virtual force field acting on the object, the tactile characteristics of a virtual surface (such as roughness) or simply an event taking place within the activity resulting in informative feedback.

Then, with this vision, we begin approaching a two-layered problem. First, we must design and test a subsystem for our robots that is capable of generating the aforementioned forces, *i.e.* a “haptics” subsystem. Second, we must start focusing on integrating our platform to learning environments, as education is the conceived application which shaped and will continue to shape the design of the platform. Our robots, that are to become *haptic-enabled handheld robots* by the end of this chapter, are envisioned in the long term as part of large, collaborative, paper-based workspaces shaped by the requirements of the classroom ecosystem, the teacher and the curriculum.

“Haptics” refers to the sensory perception (by humans) and recreation (by devices) of mechanical forces, *i.e.* the sense of touch. It is a distinct field from, yet tightly interconnected with, robotics. It is typically approached from two distinct perspectives, namely *tactile* and *kinesthetic* ([144]). Tactile haptics is concerned with the sense of the nature of contact with objects, often attempting to model and reproduce surface characteristics such as friction. Kinesthetic haptics, on the other hand, is concerned with the sense of position and motion of objects and associated forces, such as weight. Again, haptic systems have characteristic

constraints that affect the designed devices:

- DOF that are to be covered and kinematic constraints
- Size of the workspace, as well as physical size and shape of the device
- Mass (lower is better) of the device
- Available stiffness (higher is better) offered by the device
- Programmability
- Precision requirements
- Monetary cost, affordability

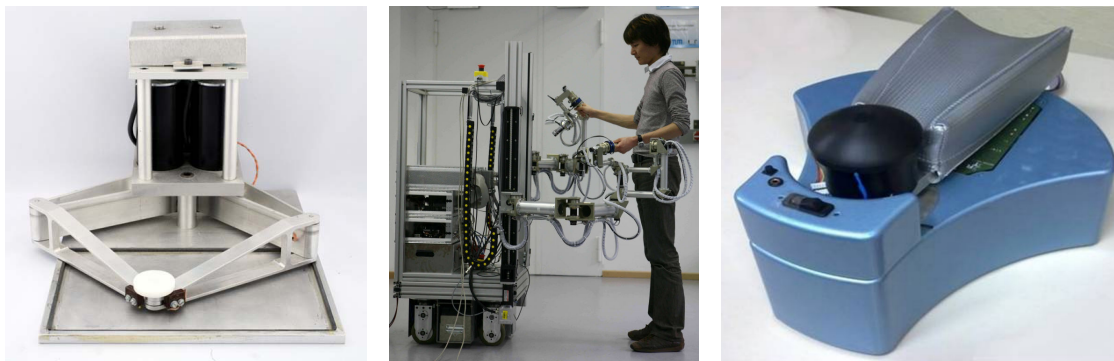
Note here that, unlike the locomotion problem, power consumption, energy efficiency and mechanical complexity are not among the typical constraints, since state-of-the-art haptic devices are almost exclusively grounded desktop mechanisms (powered by mains electricity) with specific professional target markets where the usage of the device can be accurately characterized so that robustness against intensive usage is not usually required. Moreover, by virtue of these professional target markets, affordability can often be sacrificed to obtain the commonly high degrees precision and DOF required by the professional setting, such as robot-assisted surgery or industrial teleoperation.

4.1.2 Problem Statement

As stated in the previous chapters, our work is framed within the classroom environment, in large, collaborative workspaces. Some constraints that were already defined (with haptics in mind, besides other operation modalities), such as mobile operation on a plane and low cost, as well as scheduling issues encourage us to finalize the hardware design within the scope of this thesis and not improve it further, and to focus only on software to enable haptics on our already existing robots.

Our target is the ability to give haptic feedback (both kinesthetic and tactile) along the same DOF, namely translational (x, y) and rotational around the vertical axis (θ), through a software motion/haptics controller. An improved pose/trajectory tracker must be designed so that our devices may fully operate as mobile robots (to enhance *moving*). Since the design of our locomotion system incurs considerable frictional impedance, a “backdrivability assistance” module must also be designed in our controller (to enhance *being moved*). When this design is obtained, our aim will be to characterize the precision with which our robots are able to generate haptic feedback and its perception “quality” by humans, since our devices have particularly low precision due to non-groundedness (*i.e.* removability from the operation surface which interrupts the actuation) and very low cost.

Moreover, we will re-explore the concept of moving *vs.* being moved within a learning setting with focus on haptics, which was not attempted with a tangible handheld multi-robot interface such as ours before to the best of our knowledge. Here, having an array of devices that are both autonomous robots, as well as tangible haptic interfaces, holds interesting opportunities



(a) “Pantograph” – A grounded high precision haptic interface that accommodates one fingertip in a small workspace ([145]). Picture taken from www.microsoft.com.

(b) A Mobile Haptic Interface (MHI) that accommodates two hands in a practically unlimited workspace, while also allowing vertical motion outside the plane ([146]).

(c) A desktop Mobile Haptic Interface (MHI) with arm rehabilitation focus that accommodates the hand and the forearm in a large workspace ([147]). Picture taken from www.eruffaldi.com.

Figure 4.1 – Prominent instances of (largely) planar haptic interfaces in the literature.

for collaboration among learners that we will aim to exploit.

In the following section, we will provide the state-of-the-art of haptic device designs comparable to ours, as well as the state-of-the-art of a developing field still mostly separate from haptics, called Active Tangible Interfaces, that touches the idea of moving *vs.* being moved and provides useful insights from the Human-Computer Interaction (HCI) perspective. A brief but up-to-date overview of haptics in education will follow.

4.1.3 Related Work

Haptic Device Design

2DOF (x, y) or 3DOF (x, y, θ) planar haptic devices, comparable to our envisioned device, can be used as interfaces to point-like objects residing on a plane; see Figure 4.1 for a brief overview of such devices in the literature. [148] gives one of the first examples in the literature of what can be called a “haptic mouse”. It operates on a conductive surface and can resist the user’s motion by means of the force generated by controlled eddy currents (same method as described in [149]) for kinesthetic feedback and can pulse the left mouse button for tactile feedback. It is shown in this study that users’ response times in a traditional window-based desktop environment can be improved with the addition of the aforementioned haptic component to the mouse cursor. Despite the practically unlimited workspace offered by such a design, the ability to create spontaneous motion to give haptic feedback in any direction rather than only opposing the present motion of the device remained a challenge.

The literature on devices with practically unlimited workspace was thus primarily reserved

to simple tactile feedback (found mainly in patents and numerous commercial products released in the past two decades that typically utilize low cost vibration motors) while the focus on kinesthetic and high resolution tactile feedback remained exclusive to more elaborate grounded desktop mechanisms with limited workspace and higher fidelity. Such mechanisms include a 2DOF cartesian robot ([150]), a 3DOF wire-driven mechanism ([151]), a 2DOF 5-bar linkage ([145], see Figure 4.1a), a dual 2DOF 5-bar linkage that redundantly extends [145] into a 3DOF planar mechanism ([152]) and finally a 6DOF parallel redundant mechanism that results in a 3DOF planar interface ([153]).

A potential solution to the limited workspace problem is offered by Mobile Haptic Interface (MHI)s ([154, 155], see Figure 4.1b). These human-sized interfaces combine a mobile base with a limited-workspace haptic device and follow the locomotion of the operator (thus extending the workspace to the entire walkable floor) in industrial teleoperation and virtual space exploration scenarios. Later studies involving similar devices designed for similar purposes include [156, 157, 146]. More recently, [147, 158] proposed relatively smaller (forearm-sized), link-free desktop MHIs with a strong application focus on upper arm rehabilitation (see Figure 4.1c). While these devices certainly mark an improvement towards our goal of building collaborative workspaces composed of many handheld tangible haptic devices, they do not aim to address miniaturizability and inexpensiveness concerns that are absolutely essential for such a platform as ours. Moreover, they are evaluated from a rehabilitation perspective in very specific use cases where corrective performance of the device in path following tasks is measured. For our purposes, evaluation from a more didactic perspective is required where we measure the comprehension of the haptic information that the user is receiving and the sensitivity of this perception, which is among the aims of this chapter.

However, most of the device design and control literature focuses on mechanisms that allow to operate within a (limited) 3D space for greater workspace versatility; these mechanisms are typically either (i) Variants of the Delta robot design ([159] *i.e.* 3 parallel arms connected to a base where the end effector or the user handle is located), (ii) In the form of serial link chains, or (iii) Hybrids of parallel and serial mechanisms. Two of the most popular low cost commercial devices are Novint Falcon ([160]) and PHANTOM Omni ([161]). Apart from these, there exists a substantial body of research that is devoted to designing high-end haptic input/output devices for bilateral control of high-end surgical manipulators, as well as haptic-enabled rehabilitation. Compared to the state-of-the-art, the novelty of our design is providing many points of haptic interaction within (possibly many) large workspaces in the form of a tangible user interface, while remaining very low cost but sacrificing precision and being confined to tabletops.

Active Tangible Interfaces

Active Tangible Interfaces, namely interfaces that use actuation on its tangible items, also constitute an interesting research area. Studies concerning this modality are mostly of an exploratory nature, suggesting potential applications and differing mainly by their system design. [162, 163] are the first examples in the literature of active tangible interfaces, in the

form of 2DOF electromagnetically actuated tokens on a tabletop; [164] later extended this to 3DOF and discussed some haptic interaction possibilities.

[165, 166, 167] propose a more conventional approach that is small-size differential drive robots on a graphically active tabletop. [168] showed a programming environment implemented with such an interface. [169] further extended this approach to include tactile feedback. Other less conventional approaches to actuation are ultrasonic proposed by [170] and vibration drive used by [171, 172]. These studies approach the vision of many points of interaction within large workspaces, but do not fully exploit (or are not concerned with) the haptic interaction potential of such interfaces. They are typically concerned with novel applications to the presented user interfaces.

Haptics in Education

[173] gives a useful review of haptics in education where a number of studies indicate that haptics improves motivation and attention, whereas it is not clear whether it actually improves learning. Other studies mentioned in the review report the potential of haptic devices in kinesthetic and embodied learning, as well as in learning of “invisible phenomena”. The review also suggests the limitation of the commonly used single point-probe exploration method, the potential benefits of the existence of multiple haptic probes (albeit imagined as fingertip probes) and the typically high cost of such devices. Our motivations naturally include this increase in enthusiasm and the exploration of kinesthetic/embodied learning, and our proposed design will address the multiplicity and high cost problems among others.

From a conceptual point of view, the idea of exploring the educative opportunities of low precision affordable haptic devices dates back to early 2000's; [174] first proposed the usage of an off-the-shelf haptic mouse (grounded with very limited workspace) for accessible science education. [175] later proposed Lego Mindstorms for as a reconfigurable haptic platform to teach undergraduate mechanics, robotics and programming. Another popular low-cost design to teach STEM subjects is the haptic paddle found in [176, 177] and others.

Apart from these, higher-end devices were also used in teaching diverse focused matter across various levels of education. These include middle-school cell biology ([178]), middle/high-school virus biology ([179]), handwriting ([180]), levers in middle-school physics ([181]), Pascal's principle and friction in high-school physics ([182]), accessible geometry ([183]), Coriolis effect in middle-school physics ([184]), graduate molecular life science ([185]) and buoyancy in undergraduate physics ([186]).

Of the above concrete studies, only one reported definitively worse scores when haptic feedback was added. A small portion of the rest only claimed the potential of said haptic interfaces (due to the lack of evaluation in a real context) while the majority was able to confirm effective learning of the subject matter. About half of the latter studies were able to show that the addition of haptic feedback improved learning in some way over using other modalities alone.

We believe this background shows potential and is motivating to pursue haptic feedback capabilities on our learning platform.

4.2 Development – Haptics & Motion Controller

4.2.1 Overview

In the previous chapter, we designed the locomotion system to enable our robot's motion with respect to the requirements of our envisioned classroom learning setting, such as robustness against user manipulation, low complexity and cost. We opted for a holonomic locomotion system to enable instantaneous motion and force output towards any direction, even when the robot is possibly blocked by the user's grasp. Holonomicity is missing from almost all state-of-the-art consumer robotic platforms comparable to ours, *i.e.* well-localized palm-sized tabletop robots, which typically favor wheeled differential drives, or more recently vibration drives, for the reason that they are exceedingly simple and inexpensive to manufacture, compact and well understood.

However, we believe it is a profitable endeavor to enable holonomicity in our robots to approach a more versatile tangible interaction experience where both the input (from the user, *i.e.* being moved) and output (towards the user, *i.e.* moving) motions are unrestricted as long as within the tabletop workspace. The output motions, where haptic feedback is categorically found, are particularly sensitive to this requirement as simply removing all friction between the tangibles and the workspace along the blocked DOF to enable unrestricted motion originating from the user (found in traditional tangibles) is certainly not sufficient to enable unrestricted motion originating from the tangible. For this particular reason, holonomic motion is necessary where all DOF are controllable and have ideally maximum traction over the workspace.

With all such DOF controlled, as shown in Section 3.2.4, it is possible to obtain a view of our robots as point-like objects with poses, velocities and output forces and torques within the global workspace frame rather than the local robot frames, as enabled by the accurate global localization system. These global poses and velocities are known onboard the robots at all times, and can be broadcast wirelessly to the central controller. In addition, capacitive touch keys are used to detect whether the robot is grasped, in order to modulate haptic output. With these resources, the aim of this section is to develop the firmware module onboard the robots that will drive the motors according to the motion and haptic feedback needs. The envisioned result of this development is denoted as Cellulo version 3 (previously published in [142]), and Figure 4.2 shows an updated view of the software architecture composed of the aforementioned components.

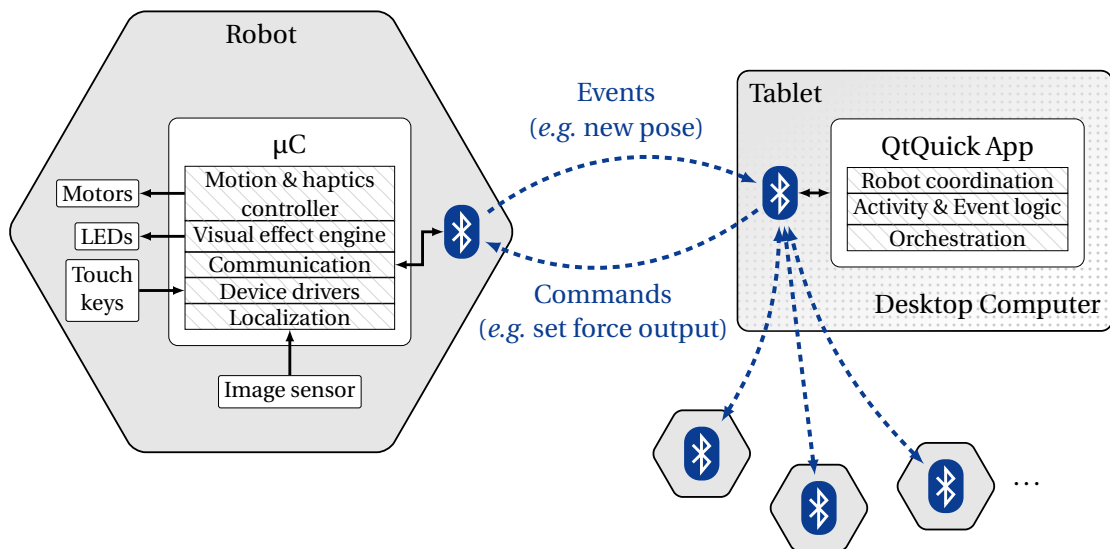


Figure 4.2 – Cellulo version 3 software architecture. As before, diagonally lined boxes represent software components within the robot firmware or within the activity application as part of custom reusable QtQuick plug-ins where possible. Motion & haptics controller integrated into the robot firmware.

4.2.2 Haptic Interaction & Controller Considerations

As described above, and developed in the previous chapters, each of our robots can obtain their global pose and command their own locomotion system to provide a velocity or force output. This allows for local motion and haptics control loops whose frequencies are bounded by the slowest element in the system, *i.e.* localization, running at about 93 Hz. While ensuring the lowest latency available with our robots (about 11 ms), these control loops would not be highly flexible nor configurable on-the-fly due to the (both volatile and non-volatile) memory limitations as well as communication bandwidth limitations. For example, using these local loops, it would not be practical to implement a dynamic force field (changing *e.g.* with time, upon user interaction with the activity or even due to the changing poses of other robots) acting on the robots since it would require recalculating and recommunicating the entire force field to each robot as soon as it changes.

For this level of flexibility, larger control loops passing over the activity application (residing on a tablet or desktop computer and acting as the central controller) through the wireless Bluetooth SPP channel can be defined. These larger control loops would receive the robot pose (with the robot's local timestamp attached to the pose in order to provide robustness against non-systematic wireless latencies) and command a goal velocity or force/torque depending on the activity. This way, for example, the aforementioned force field can be implemented without communicating any high bandwidth information related to the force field; an activity with such an implementation is presented in Section 4.4. Therefore, the overall motion and haptics controller design strategy should be to implement basic, low bandwidth and

unchanging controllers on the robot while delegating the implementation of more complex, higher bandwidth and activity-dependent controllers to the application developer.

However, running remote control loops over Bluetooth serial channels introduces a possibly slower element than localization to the system, namely wireless communication, whose latency and bandwidth performance depends highly on practical conditions. In the presence of a single robot within our typical conditions (indoor human environment with 2.4 GHz Wi-Fi networks also present, central controller within 1 m of the robot), we verified that a 93 Hz wireless control loop can indeed be practically implemented, with occasional high latencies due to packets arriving with excessive delay, after which the regular loop frequency is quickly recovered. However, when more robots are introduced, the wireless Bluetooth channels are observed to saturate which necessitates the artificial reduction of the control loop frequency, done by a configuration command sent to each robot once in the beginning of the activity. For example, with 16 robots being continuously controlled from a single central controller¹, the loop frequencies were required to be decreased to about 10 Hz to prevent saturation. This results in around 100 ms of practical minimum latency, marking an about 9-fold decrease from the optimal performance.

Given the acknowledged frequency limitations above, and other limitations given in the previous chapters, it is desirable to know the adequacy of our device to the requirements of haptic interaction in general. [187, Section 2.4] gives distinct frequency, resolution and signal-to-noise ratio requirements for both kinesthetic and tactile interaction, compiled from surveys. In summary, mainly kinesthetic interaction requires up to 100 Hz frequency; here, weight and shape impressions of objects (for which tangential force plays an important role) can be recreated with up to 10 Hz frequency. Within the 10 Hz to 100 Hz range, slippage and only some of the grating (implemented with pulses) and texture (implemented with continuous signals) impressions can be recreated. When mainly tactile interaction is considered, beyond 100 Hz and up to 1 KHz frequency is required to render an important portion of gratings, textures, stiffnesses and contact properties. Therefore, our robots, as they are now, are not capable of recreating this area where humans are most sensitive to high-quality surface characteristics. In our optimal case (93 Hz), it is possible to recreate kinesthetic information while it is also possible to recreate low-quality tactile information. When many robots are considered (10 Hz with as many as 16, and possibly lower with even more), recreating kinesthetic information is still essentially feasible while recreating most of the tactile information is not.

Moreover, resolution plays an important role in haptic interaction quality where a force feedback resolution down to 0.1 N and spatial resolution down to 0.7 mm are ideally required. In Chapter 2, we characterized the accuracy and precision of localization, from which a static understanding of spatial resolution can be obtained. Using a similar methodology (*i.e.* attachment of device to a CNC toolhead which provides the ground truth) but with

¹Observation done during the activity presented in the next chapter, which actually requires multiple Bluetooth adapters on the central controller in order to overcome the maximum allowed number of 7 connected devices through a single Bluetooth adapter. This effectively results in a hierarchical star network.

nonzero velocity, a more dynamic understanding of spatial resolution can be obtained. Given the resolution of our Pulse-Width Modulation (PWM) signals (13-bits including the sign bit) controlling the motor drivers, an understanding of force output resolution can also be obtained. However, the asymmetric and backlash-ful design of the locomotion system and the simple fact that it is an ungrounded mechanism are expected to incur considerable noise during haptic interaction, *e.g.* when the robot is slightly lifted. This complicates the characterization of resolution during actual use, especially from the user’s perspective. For this reason, we propose to directly characterize the user sensitivity to haptic feedback during typical use via a user study, presented in Section 4.3, the results of which will provide a realistic insight into the actual resolutions of our device.

Finally, considering the dynamic range of mechanical human manipulation, our robots can only cover (in the best case) up to about 2 N of the 25 N comfortably available to humans; significantly increasing this dynamic range is not feasible without increasing the mass of our robots that are to remain mobile. Therefore, whatever their resolution is uncovered to be in the end of the aforementioned user study, our robots are to be taken as lightweight, tangible haptic devices when activities are designed with them. Users must be reminded (or learn on their own) that the motion of our robots can easily be overcome, and the interaction with them in any case will remain delicate.

4.2.3 Controller Design

As mentioned above, our strategy is to design simple and easy to configure local controllers as well as remote controllers that may be of arbitrary complexity, bandwidth or operation in general. These remote controllers may contain complex descriptions of the virtual “world” to be haptically rendered. Regardless of which class of controller, the goal of both is to close the loop from the measured pose in the global frame to the motor outputs.

Our motion & haptics controller, designed with this strategy and seen in Figure 4.3, is essentially a collection of these controllers that enable various haptic or motion functionalities. The topology of the paths responsible for haptic feedback falls under the very common *open-loop impedance controller* category, where the motions are generated by the user, who receives the force output generated by the device (not measured, hence open-loop) depending on its pose and motion. Each of the local controllers can be turned on or off (via dedicated Application Programming Interface (API) calls), has multiple modes of operation (selectable via dedicated API calls) and produces a goal set of velocities (v_x, v_y, ω) or forces/torque (F_x, F_y, T) in the global frame that are converted into motor outputs using the transformations derived in the previous chapter. In the following subsections, each submodule of the controller (most of which enable haptic or motion capabilities) will be explained in detail.

Besides the local controllers, arbitrary remote controllers may be built that take the pose of the robot and whether it is kidnapped or grasped (denoted with the orange values in the controller figure, each of which generate an API event on change) and command a goal velocity or

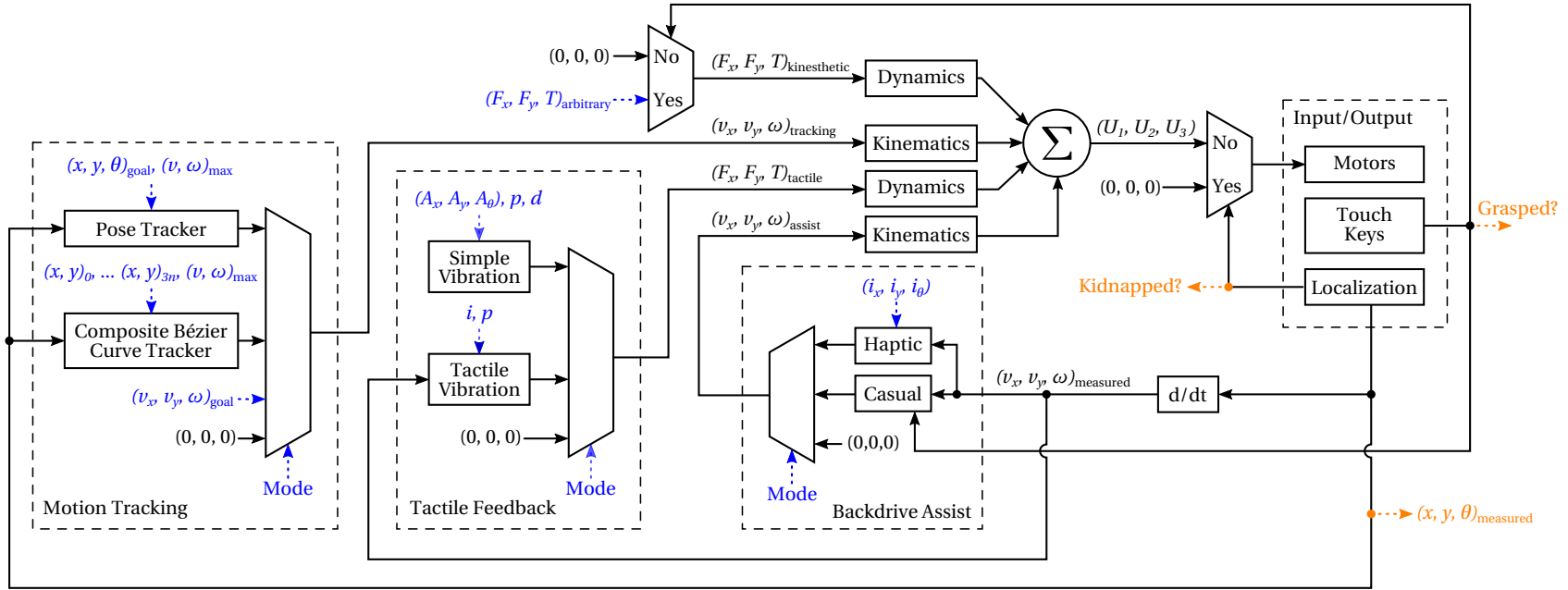


Figure 4.3 – Motion & haptics controller residing on robot. Values wirelessly sent by the central controller (residing on tablet or desktop computer) to the robot are in blue. Values wirelessly transmitted by the robot to the central controller are in orange. Using these values (taking the *pose*, as well as *kidnapped* and *grasped* states and commanding the *goal velocity* or *force/torque*), the central controller can run its own activity-dependent remote control loops that may involve suboptimal latencies due to wireless communication. Besides the central controller, local minimal latency controllers ensure *pose tracking*, *composite Bézier curve tracking*, tactile haptic feedback through *vibration* and *backdrive assistance*. U_i denote the motor outputs, as introduced in Equation 3.20. Kinematics and Dynamics blocks above correspond to the transformations given in Equations 3.25 and 3.27 respectively.

force/torque (denoted with $(v_x, v_y, \omega)_{\text{goal}}$ and $(F_x, F_y, T)_{\text{arbitrary}}$ respectively in the controller figure, both accessible via remote API calls). This essentially closes the loop from the measured pose to the motor outputs in a way that is maximally reconfigurable and flexible but is subject to the previously discussed frequency limitations of remote control loops.

Input/Output

The only sensors available to the robot are the capacitive touch sensors that sense, in this context, whether the robot is grasped, and the optical localization system that provide the global pose as well as sense whether the robot is no longer in the workspace (*i.e.* kidnapped). The grasp sensing is done in a manner similar to those found in [188, 189]; we go one step further by thresholding the sum of the raw values obtained from all touch keys². All of the sensed quantities are communicated to the central controller as API events as soon as they change. This way, the received pose change event frequency can be used to dictate the frequency of the remote control loops. Both remote and local control loops command the outputs of the sole actuator of the robot in this context, namely the motors in the locomotion system, in order to obtain motion or force/torque output from the body of the robot.

Backdrive Assist

During typical use, the user is expected to backdrive our robots linearly along the workspace as well as around their own axes. In this case, if the locomotion system is left inoperative, the user is subjected to the high frictional inertia of the robot. Previously, in Equation 3.25, the relationship between the motor outputs and robot velocity in the global frame was derived, where Equations 3.5 to 3.9 that describe the internal kinetic friction were indirectly accounted for. Here, if the perfect knowledge of the robot velocities (*i.e.* without delay or noise) was present, it would be possible to calculate the ideal motor outputs to compensate for the internal kinetic friction, under the assumption of constant velocity.

The objective of this module is to use the measured robot velocities as a replacement to the ideal robot velocities to reduce the internal frictions as much as possible, namely provide assistance in backdriving the robot. For this purpose, two distinct backdrive assist modes were designed:

Casual Mode: Is designed to be the *de facto* mode to make the robot easy and comfortable to manipulate. The goal of this mode is to reduce the frictional impedance as much as possible while ensuring the controller does not diverge, *i.e.* that the robot does not move uncontrollably due to the motion feeding back to its own input. Moreover, the robot motion should stop promptly after the user releases it in order to not give an unintentional

²This method works adequately if the user chooses a grasp that brings any part of their hand close enough to any key, but does not work for side grasps or top grasps while fingers are extended (*i.e.* the palm is far from the top surface). Other shortcomings of this method are discussed in the following chapters.

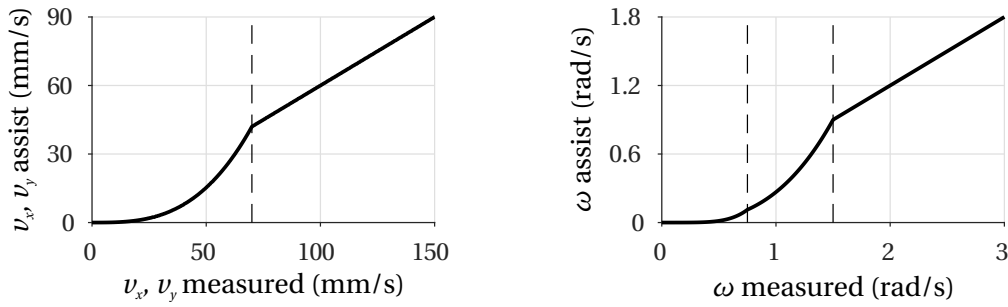


Figure 4.4 – Casual backdrive assist transfer functions, $(v_x, v_y, \omega)_{\text{assist}} = c(v_x, v_y, \omega)_{\text{measured}}$ with c tuned to be well below 1 in the linear regions to prevent the impression of autonomy. Linear velocities are decayed quadratically below a certain threshold in order to prevent jitter from feeding forward during low velocity motions; angular velocity is decayed quartically below a second threshold due to significantly higher jitter (see Table 2.3). These decay functions were chosen for their computational economy. Thresholds are shown with dashed lines.

impression of autonomy; in this mode, the robot should appear to be entirely obeying the user. To achieve this, the simple transfer functions seen in Figure 4.4 are used; these include measures to ensure the “obedience” as well as non-divergence. When a grasp is detected, instead of these transfer functions, $(v_x, v_y, \omega)_{\text{assist}} = (v_x, v_y, \omega)_{\text{measured}}$ is simply used so that the impedance is minimized; the disturbances that would normally cause the assistance to diverge can be stopped by the user with slight effort. When the detectable grasp is released, the controller goes back to the transfer functions that prevent the impression of autonomy. This way, non-detectable grasps are accommodated as well as detectable grasps. The user perceives this as easier motion when the robot is detectably grasped, *i.e.* from the top.

Haptic Mode: Is designed to simulate various surfaces that may expose the robot to less or more virtual friction. Its transfer function is $(v_x, v_y, \omega)_{\text{assist}} = (i_x, i_y, i_\theta) \circ (v_x, v_y, \omega)_{\text{measured}}$ where the coefficients i_x , i_y and i_θ are individually configurable on-the-fly in order to provide independent (possibly zero if desired) artificial viscous friction to each DOF. With this, for instance, full compliance along x axis and high friction along y can be achieved. Moreover, negative ratios can also be provided to use the motors to oppose the motion, resulting in the ability to simulate even more friction.

A minor hysteresis was introduced in both modes to enable/disable assist in order to facilitate securing the robot in place and releasing the grasp entirely; the user perceives this as slightly extra inertia when budging the robot.

Tactile Feedback

The module provides basic oscillatory force feedback and its outputs can be overlaid on the arbitrary force feedback or backdrive assist to provide tactile sensation over kinesthetic sensation, *e.g.* slight vibration over fully compliant backdrive assist to (very roughly) simulate

a rugged icy surface. Two generators are available:

Simple Vibration: Provides fixed oscillatory output with separately controllable amplitude along all DOF, period (p) and duration (d). It is possible to use it *e.g.* as an event indicator, as well as an impulse source by choosing d less than $p/2$.

Tactile Vibration: Provides continuous oscillatory output with desired period (p) whose intensities are linearly proportional (with a controllable coefficient i) to the measured robot velocities in the respective DOF. This generator is used as a very simple model of rough surfaces where more momentum will exert more force on the robot when colliding with the small bumps on the surface, assuming the collision time is constant.

More complex models can be devised that employ further inputs such as displacement, acceleration or randomly generated values. As previously discussed, these can be implemented by the application developer as part of the remote controllers running on the activity application.

Motion Tracking

The module is used to achieve the tracking of the following:

Pose: Tracks a goal pose with distinct P controllers for each DOF and with maximum linear/angular tracking velocities $(v, \omega)_{\max}$. The controllers are tuned to be high-gain so that unless the goal coordinates are near (few mm and few degrees), the velocity outputs are clamped to the commanded $(v, \omega)_{\max}$. Desired DOF can be left out to be controlled by other modules, resulting in *e.g.* fully compliant planar motion (x, y controlled by backdrive assist) while holding a specific orientation (tracking θ).

Composite Bézier Curve Trajectory: Since the conception of our playgrounds involves graphics design, vector graphics development and associated formats (such as Scalable Vector Graphics (SVG)) are key tools throughout activity design and development. Here, composite Bézier curves are widely supported, easy to use and therefore abundant. For this reason, this submodule was developed to allow the tracking of trajectories described by these curves that are comfortably manageable by graphic designers and application developers. Composite Bézier curves are an arbitrary number of cubic Bézier curves connected end-to-end, each described parametrically by:

$$B(t) = (1-t)^3(x, y)_0 + (1-t)^2 t(x, y)_1 + (1-t) t^2(x, y)_2 + t^3(x, y)_3, \quad 0 \leq t \leq 1 \quad (4.1)$$

where $(x, y)_0, (x, y)_1, (x, y)_2$ and $(x, y)_3$ are the four control points. If N individual curves are desired in a given composite curve, only $3N + 1$ control points must be communicated to describe the composite curve since each individual curve's final control point is the next one's initial control point. Similar to the pose tracker, $(v, \omega)_{\max}$ are communicated within the API call as the tracking velocities. The robot then tracks a point on the

curve ahead of its current position which advances as long as a certain distance to the tracked point is kept.

Velocity: Denotes a simple, open-loop output of robot velocities where each DOF can be individually controlled or left out. It can be used as part of the previously discussed remote controllers, as well as to provide a motion with constant velocity.

4.3 Supervised Validation

4.3.1 Introduction

Now that we have robots capable of adequate motion and haptic feedback for our envisioned classroom application, we once again advance towards validating our design within controlled conditions. In the previous chapters, we opted for instrumented measurement protocols where we measured the performance of the related submodules of our robots. However, differently from before, we now have humans as an indispensable part of the design and evaluation loop. For this reason, to measure the haptics performance of our robots, we propose a non-semantic task-based experiment to be conducted with human users where we will not only aim to directly measure users' haptic perception but also to measure their manipulation performance under realistic (but nevertheless highly controlled) use conditions. We acknowledge that this experiment was co-designed with Dr. Wafa Johal and the its design and results were previously published in [142].

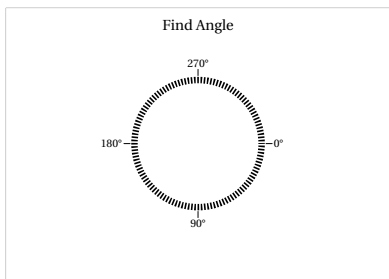
4.3.2 Procedure

Our evaluation procedure is composed of a series of 6 tasks and is designed to be done individually. Each participant does each task using a single robot, a tablet and a series of 6 distinct printed sheets of paper hosting each task; these sheets are shown in Figure 4.5. Each task presents a very specific goal, such as finding a hidden position by means of haptic feedback. The tablet only displays instructions, concise information about the current task state and the means to give answers to the tasks that require such answers. The main object of interaction (that involves only haptic feedback and motor manipulation) is the robot and not the tablet, without exception.

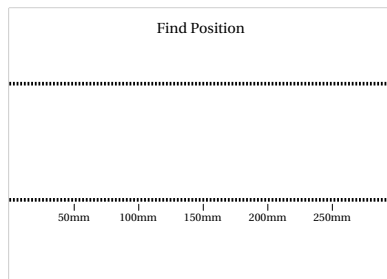
The tasks belong to one of four “features” important to the evaluation of our haptics & motion controller design that involve one or more research questions that the tasks serve to illuminate; these features and questions are as follows:

Usability:

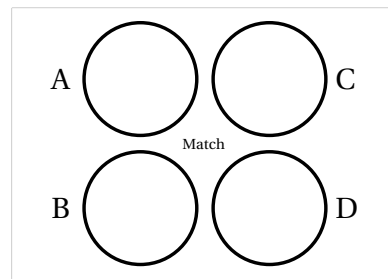
- Are our robots *usable* without training or extensive familiarization?
- Using the backdrive assistance presented earlier, can our robots easily and precisely be *backdriven* on the workspace?



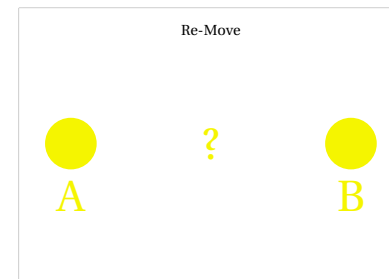
(a) Find Angle (A4)



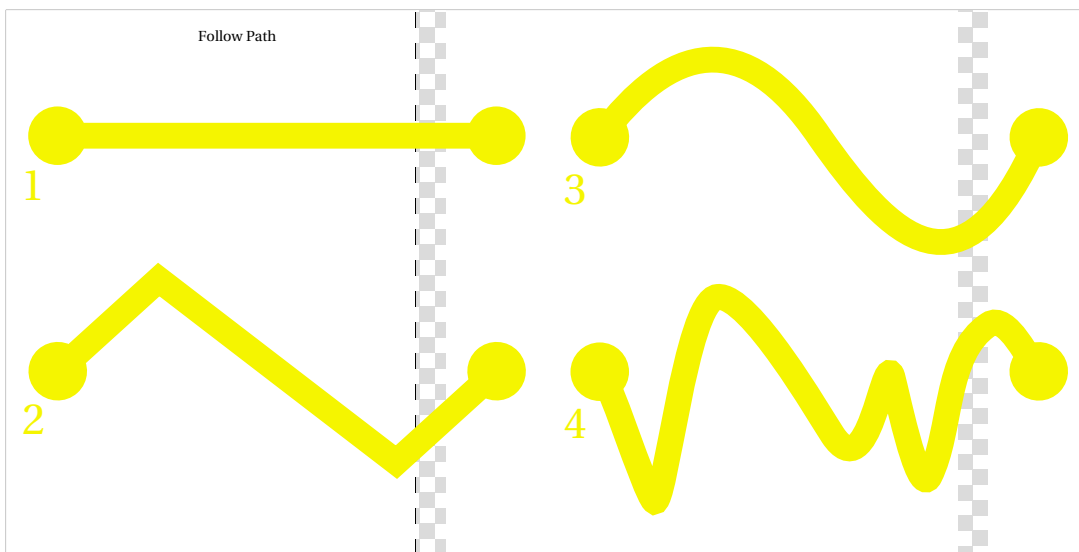
(b) Find Position (A4)



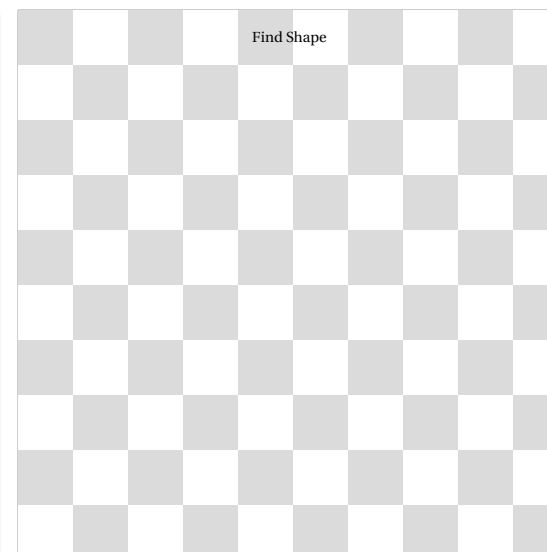
(d) Match (A4)



(f) Re-Move (A4)



(c) Follow Path (840 mm x 420 mm)



(e) Find Shape (420 mm x 420 mm)

Figure 4.5 – Printed activity sheets for the supervised haptics experiment, scale among sheets is preserved. Microdot pattern omitted. Sheet sizes noted in captions. Tasks follow the order presented in the caption labels.

Memory:

- How precisely the trajectories that are conveyed purely *kinesthetically* can be remembered?

Disturbance:

- How much *disturbative output* are our lightweight robots capable of?

Sensitivity: Using our robots, what is the useful range of haptic outputs when;

- Pinpointing a desired *angle*?
- Pinpointing a desired *one dimensional position*?
- Differentiating a *stationary planar force* from others?
- Differentiating a *closed shape* from others?

The order of the tasks were chosen to alternate between features where possible, and to increase in difficulty. Since participants were chosen so that they have not interacted with our robots before, the tasks are verbally explained in the beginning if required. Each task is of a functional and non-semantic nature, *i.e.* the participant is not supposed to perceive a virtual environment or associate the feedback with a higher-level concept. Instead, the tasks are completely self-contained and measure whether the participant can perceive and/or remember certain quantities or perform certain motor tasks correctly. Throughout the experiment, all of the measurements were done with the facilities already existing on the robot and the tablet without any external setup. In the following subsections, each task will be explained in detail.

Task 1 - Find Angle

The goal of this task is to find a randomly selected hidden orientation by means of tactile feedback while rotating the robot on the sheet seen in Figure 4.5a. Haptic backdrive assist is enabled throughout with $(i_x, i_y, i_\theta) = (-0.6, -0.6, 0.6)$, *i.e.* with high linear friction but rotational compliance. If the robot leaves the central area (indicated visually with the dashed circle), assistance is removed and it is commanded to return to the central area. This way, the robot acts as a “rotary knob” in the center of the activity sheet, conveying a discrete angle with haptic feedback.

Whenever the hidden orientation is crossed, a 30 ms torque impulse is given against the direction of crossing. The participant must give an answer that is within $\pm 5^\circ$ of the correct orientation. If correct, the participant advances to the next levels that give less and less intense feedback, calculated as:

$$|T_{\text{impulse}}| = \frac{T_{\text{max}}}{2^{\text{level}}} \quad (4.2)$$

where T_{max} denotes the maximum torque output of the robot, as measured in the previous chapter. The participant is allowed 2 wrong answers in a level except for level 0 which acts

as a tutorial with unlimited trials. The participant can also choose to give up at any time, which lets them pass to the next task. With this setup, we aim to identify the participant's sensitivity threshold, after which the impulse will start to be indistinguishable from noise and the participant will drop out. The metrics regarding the completion of this task across many participants will provide insights into the sensitivity range and usability within such an angle perception scenario.

Task 2 - Find Position

The goal of this task is to find a randomly selected hidden x coordinate on the sheet seen in Figure 4.5b and is very similar to the previous task. Haptic backdrive assist is enabled throughout with $(i_x, i_y, i_\theta) = (0.7, -0.6, 0.6)$, *i.e.* with high linear friction along the y axis but linear compliance along x axis and rotational compliance for manipulation comfort. If the robot leaves the middle band, assistance is removed and it is commanded to return within the band. This way, the robot acts as a “slider knob” conveying a discrete position. Participants are expected to answer within ± 8 mm for a correct answer. The given impulse (again for 30 ms) is:

$$|F_{x,\text{impulse}}| = \frac{F_{\max}}{1.5^{\text{level}}} \quad (4.3)$$

where F_{\max} denotes the maximum force output of the robot, as measured in the previous chapter. As before, the participant is allowed 2 wrong answers (except level 0) and the option to give up. The collected metrics and the aim in collecting these are very similar to Find Angle (namely to measure sensitivity and usability), but involves one dimensional positions instead.

Task 3 - Follow Path

The goal of this task is to move the robot along the four paths on the sheet seen in Figure 4.5c, and is similar to many path following tasks in the literature. The paths were chosen to be of varying degrees of complexity and length: The participant is tasked to follow a straight path, a piecewise straight path, a smooth but regular path and a smooth but highly irregular path in sequence. At level 0, the participant moves the robot freely along the paths with casual backdrive assist. When a path is done, the robot autonomously moves to the beginning of the next path. At levels 1-3, perturbative impulses are given orthogonal to the paths (with random time intervals in between):

$$|F_{\text{impulse}}| = (\text{level}/3)F_{\max} \quad (4.4)$$

$$d_{\text{impulse}} = \text{level} \times 100 \text{ ms} \quad (4.5)$$

where F_{\max} again denotes the maximum force output of the robot. In these levels, the participants are told to follow the path as accurately as possible. This way, each participant performs each path four times without the possibility of giving up.

The measures for this task are twofold. With level 0, we aim to gather metrics about how precisely and easily can our robots be manipulated through backdrive assist that is built to compensate for the frictional impedance of the robot. With levels 1-3, we aim to measure to what extent our lightweight, low-power and non-grounded robot can disturb the user's manipulation.

Task 4 - Match

The goal of this task is to find which 2 forces (out of 4) are identical on the sheet seen in Figure 4.5d, the robot exerts these constant forces only within the designated circles on the sheet and only in the presence of a detectable grasp. The two answers are chosen randomly at each level along with one orientation distractor that has same intensity but an orientation that differs from the answer by $\theta_{\text{distractor}}$, and one intensity distractor that has same the orientation but an intensity that differs from the answer by $F_{\text{distractor}}$. These differences are:

$$F_{\text{distractor}} = \pm \frac{0.44F_{\text{max}}}{1.2^{\text{level}}} \quad (4.6)$$

$$\theta_{\text{distractor}} = \pm \frac{180^\circ}{1.2^{\text{level}}} \quad (4.7)$$

where the sign is chosen randomly. In other words, the distractors become more and more similar to the answers as levels progress. Here, it should be noted that the dead band described in the dynamics analysis (see previous chapter) is also used extensively; the robot outputs significant amounts of audible noise when the motors are driven, whose intensity and frequency may be proportional to the motor outputs. This element was left in the experiment as it is to be expected during normal use, and may be beneficial to the task. As before, the task ends after 3 wrong answers in one level or by giving up. With this task, we aim to measure to what extent the participants can differentiate the intensity and orientation of forces conveyed by the robot, thus obtaining a general understanding of their actual force feedback resolution.

Task 5 - Find Shape

The goal of this task is to find which of the closed 2D curves (given in Figure 4.6) is hidden on the sheet seen in Figure 4.5e. The robot is used as a "scanner" (with casual backdrive assist) to probe the randomly selected shape that has a 10 mm-thick border on which the robot gives tactile vibration with intensity:

$$i_{\text{tactile}} = \frac{3.0}{1.5^{\text{level}}} \quad (4.8)$$

Due to the small number of choices, the participant is allowed only 1 wrong choice. With this task, we attempt to examine within which sensitivity range our robots are able to let the user feel (or rather discover) 2D shapes through tactile haptic feedback.

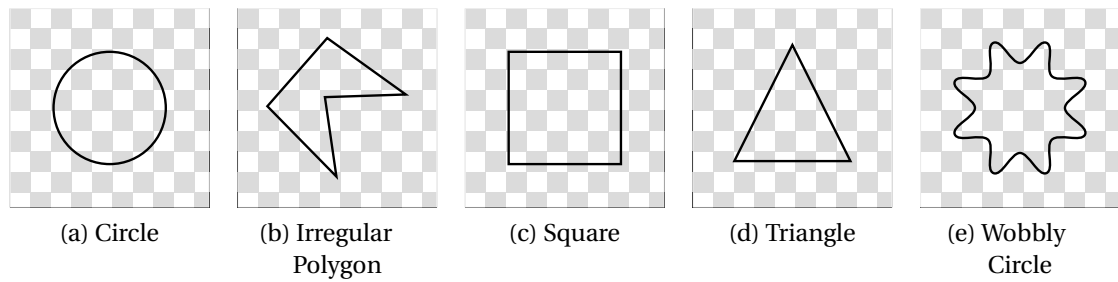


Figure 4.6 – Shapes used in the Find Shape task, also presented to the participant as choices. The 10 mm border thickness scale is preserved with respect to the sheet size in the above representations.

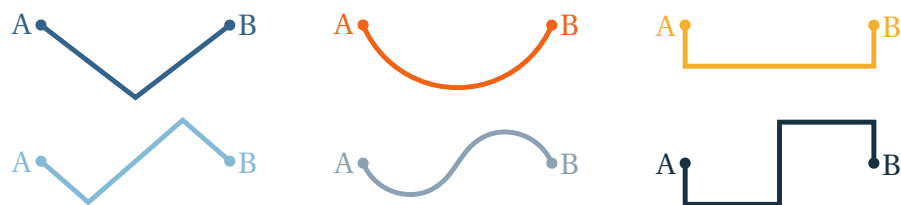


Figure 4.7 – Paths used in the Re-Move task (not presented to the participant).

Task 6 - Re-Move

The goal of this task is to kinesthetically feel the trajectory of the robot and repeat it on the sheet seen in Figure 4.5f. The participant is asked to close their eyes and grasp the robot which starts to move along one of the paths seen in Figure 4.7 and goes back to the start. The participant then moves the robot along the recalled path. Since this is a kinesthetic memory task, paths with zero or one inflexion point (and not more) were chosen. Each of the 6 paths are performed in random order once with $v_{\max} = 75 \text{ mm/s}$ (level 0), and once again with $v_{\max} = 150 \text{ mm/s}$ (level 1).

Here, we aim to measure the fidelity to the actual path with all visual components removed. With this, we simulate scenarios where the user may be obliged to look elsewhere while interacting with the robot whose motion must be kinesthetically perceived and remembered. We include two velocity levels, not to gain an understanding on sensitivity this time, but to gain an understanding of the effect of path reproduction speed and quality (that is expected to be negatively affected by increasing reproduction speed) on the participant's memory.

Participants

25 participants (10F and 15M, 31.7 ± 7.48 years old, 4% left-handed, 40% used robots in daily life before, including robotic vacuum cleaners) were recruited to perform all the tasks. None of these participants had any prior experience with our robots. Due to the repetitive nature of the tasks, the experiment was performed exclusively with adults to not introduce excessive fatigue

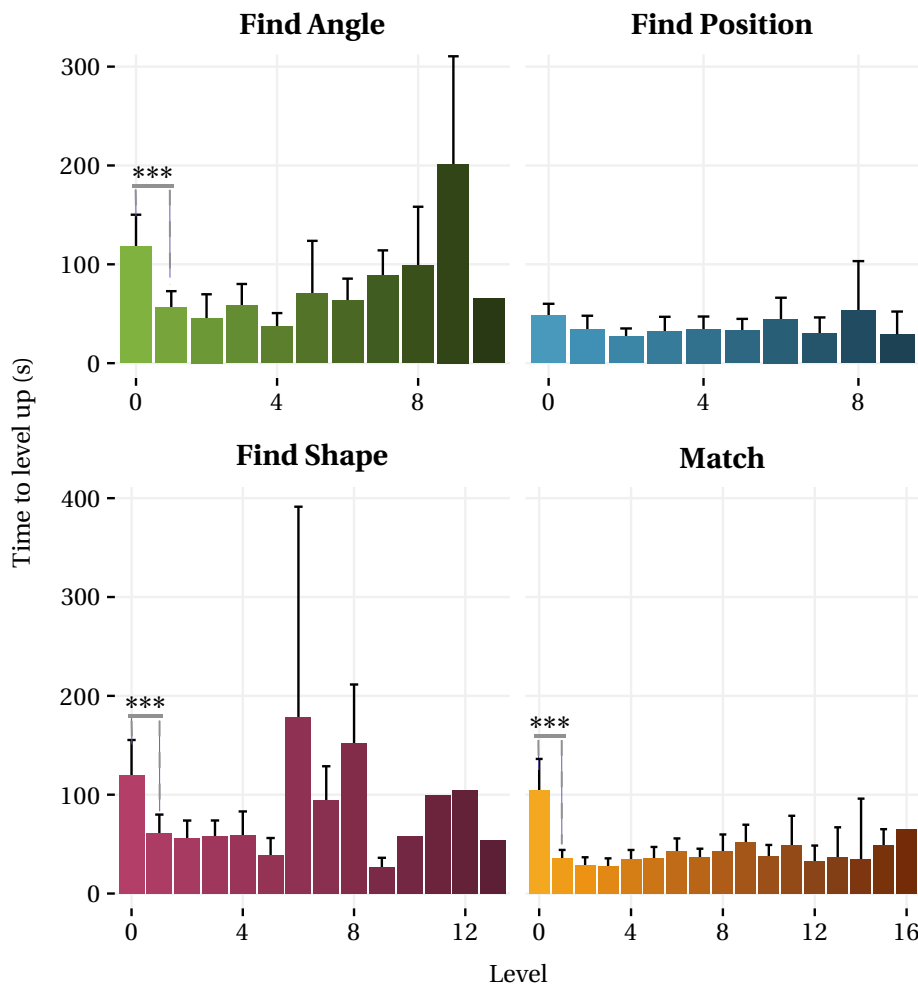


Figure 4.8 – Average time taken by participants to complete each level for Find Angle, Find Position, Find Shape and Match. Error bars denote standard deviation.

effects into our measures (the experiment took between 30 min and 50 min depending on the participant). It is known that fine motor skills, including haptic perception, are mastered by the age of 7 and only some of these, such as handwriting and drawing, continue to be refined into late childhood ([190]). This suggests that our evaluation should be repeatable with late primary school children without significant loss of accuracy on results.

4.3.3 Results

Here, we discuss our findings (through the measures from tasks described above) that shed light on the main findings associated to the aforementioned themes.

Usability

Among the tasks the participants performed, some are level-based and require a correct answer (orientation, position, shape, matching forces) to advance to the next level. Measuring the time it takes to advance to the next level in these tasks (seen in Figure 4.8) reveals the evolution pattern of the difficulty across levels: The time spent drops for all tasks after level 0, stays similar for a number of levels and then generally tends to increase as it requires more and more time due to the increasing sensitivity required to find the correct answer. Paired t-tests (within subject) between levels 0 and 1 confirm that this drop is significant except for Find Position ($p = 0.001$, $p = 0.12$, $p = 0.0001$, $p = 0.005$ for Find Angle, Find Position, Match and Find Shape respectively). This exception may be explained by the very similar nature of this task as the preceding task (Find Angle) and its already low level 0 completion time, which hints at transfer of learning.

These trends evidence that level 0 acted as a tutorial level that lasted about 2 minutes and “trained” the users (who had no prior experience with our platform) while performing the task itself without assistance from experimenters: This shows that our platform, within such tasks, is usable without formal training or extensive familiarization. It is useful to note that another exception to this finding may be in Find Shape due to the large number of participants that dropped out in very early levels (see Figure 4.15) and that made no notable progress because of the difficulty in comprehending and performing the task. A discussion regarding this task follows in the subsequent subsections and we acknowledge here that the usability in Find Shape was valid only for a subset of the participants.

Finally, we consider the Follow Path task that was designed to evaluate how the participants manipulated the robot in a task where the goal is to follow paths of various lengths and complexities as precisely as possible. At level 0 where no disturbance was given, the average distance (across all participants, all paths and all data points) to the actual path was found to be 4.04 mm (see Figure 4.12). This level of error corresponds to between 1.1 % and 0.51 % of the paths’ entire lengths and to 5.4 % of the robot’s body length, evidencing the accuracy to which the robot can be manipulated during normal use with active backdrive assist. For reference, example paths performed by two participants can be seen in Figure 4.11.

Memory

The Re-Move task had participants perceive and remember paths purely kinesthetically which they were asked to reproduce; Figure 4.9 shows examples of one of the paths performed by two participants. Two velocity levels were included to test the effect of kinesthetic motion velocity to the success of recall of these paths. The participant reproductions were used to measure the distance to the paths actually performed by the robot, similar to the Follow Path task. These measurements (seen in Figure 4.10) revealed that with increasing velocity, accuracy increased significantly for 3 out of the 4 piecewise straight paths and decreased significantly for the smooth path with one inflexion point. No significant difference was detected for the

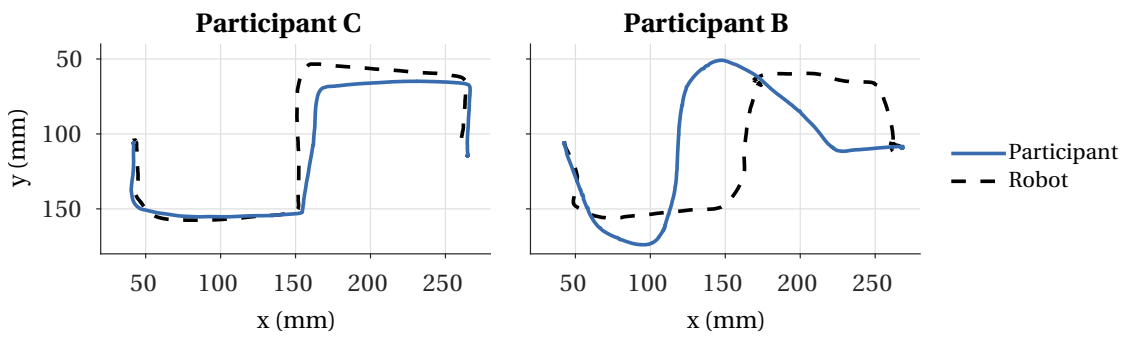


Figure 4.9 – Sample paths performed in Re-Move by one of the most successful participants (left) and one of the least successful participants (right). Since robots are grasped when performing, the reference paths (dashed) may be imperfect.

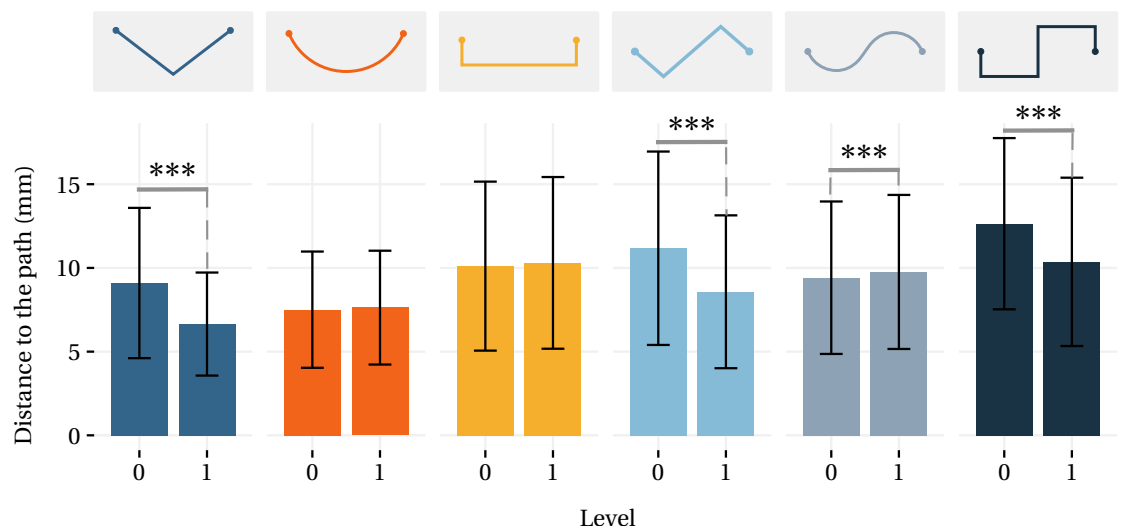


Figure 4.10 – Average accuracies of participants moving the robot along 6 different paths with 2 levels of velocity in Re-Move, error bars denote standard deviation.

remaining piecewise straight path and the smooth path with no inflexion point. This suggests that straight paths may be more difficult to recall (due to slower motion resulting in longer motion time) while smooth paths with enough inflexion points may be distorted more by faster motion, as the participants followed the actual path that was enacted by the robot that is not necessarily identical to the ideal path. When the worse of the average performances among the two levels are considered for all paths, participants were able to achieve errors of 2.76% to 3.89% of the total path lengths and 10.2% to 16.8% of the robot’s body length, evidencing the ability of the robot to convey a variety of paths with only kinesthetic feedback.

Disturbance

Additional to the level designed to test usability, the Follow Path task involved 3 additional levels designed to measure the disturbative capabilities of our robots where increasing amounts

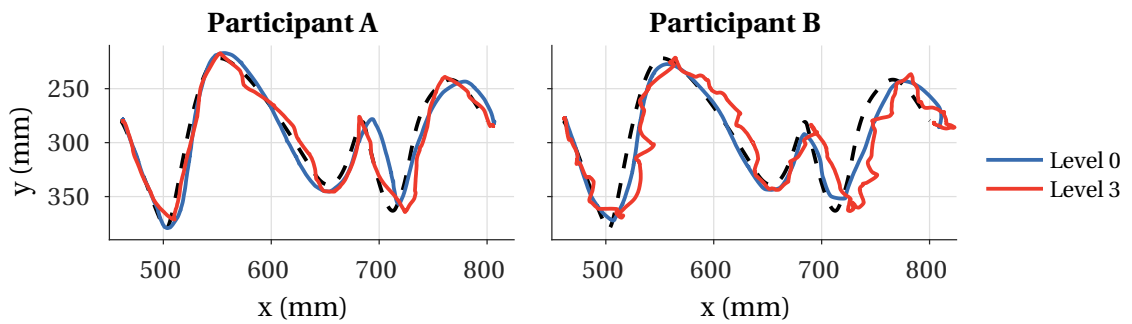


Figure 4.11 – Sample paths performed in Follow Path by one of the most effective participants (left) and one of the least effective participants (right) in counteracting disturbance.

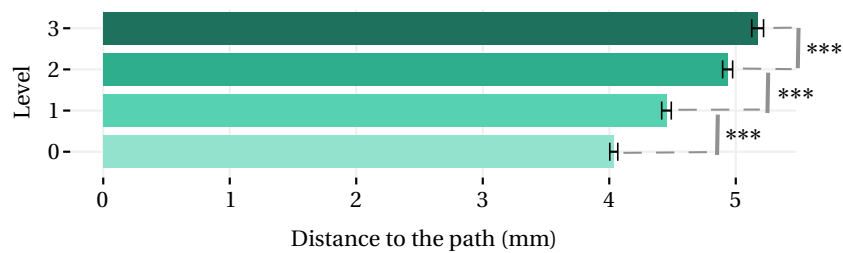


Figure 4.12 – Average distance to the path for all participants in Follow Path, with confidence interval bars at 98 %.

of disturbance was given to the participants, reaching up to the mechanical limits of our robots in the last level. Example performances by two participants in level 0 (no disturbance) and level 3 (maximum disturbance) on the most complex path is shown in Figure 4.11. Measuring the distances of participants to the ideal path (seen in Figure 4.12), we observed significant influence of increasing disturbance in all consecutive levels:

Level 0 - Level 1: $t(129540) = -21.0$, $p < 0.001$, $CI_{98\%} = [-0.46, -0.37]$ mm

Level 1 - Level 2: $t(143490) = -21.8$, $p < 0.001$, $CI_{98\%} = [-0.53, -0.43]$ mm

Level 2 - Level 3: $t(147930) = -9.53$, $p < 0.001$, $CI_{98\%} = [-0.30, -0.18]$ mm

In other words, the robot is able to add about 28% error on average (at maximum output, level 3) to the user's natural error level (at no output, level 0) which can be tuned with adjusting the output. Naturally, these outputs are limited to be informative and are not on par with the upper limits of human power output, with which there is about two orders of magnitude difference. This implies that if the user had full knowledge of the incoming disturbative output from a single robot, they would be able to counteract with ease.

Sensitivity

To measure the sensitivity to our robot's haptic outputs, we consider level-based tasks where less and less haptic feedback was given until the participant dropped out. Find Angle and Find Position tasks had participants find orientations and horizontal positions in such a

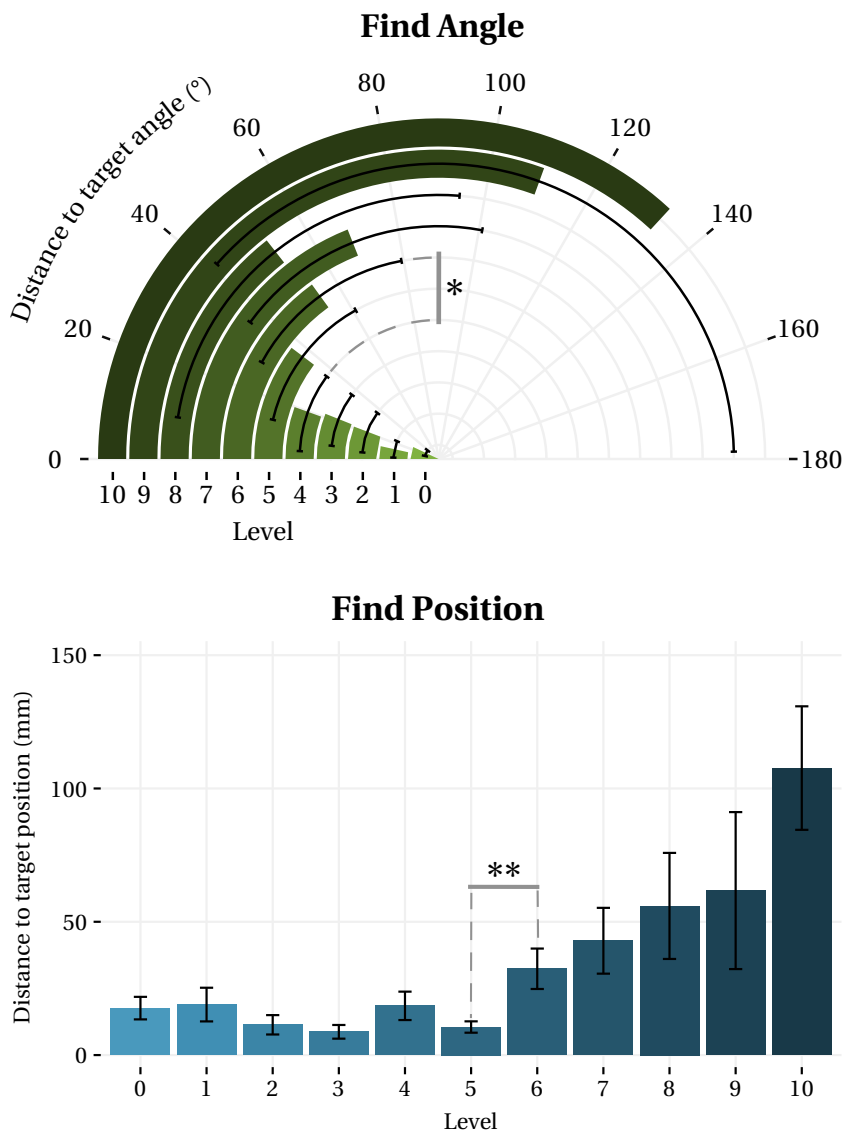


Figure 4.13 – Average distance to the correct answers in Find Angle and Find Position. All answers, including wrong ones, are considered. Error bars denote standard deviation.

way using tactile feedback. Figure 4.13 shows decreasing trends in participants’ accuracies (*i.e.* distances of given answers to the actual orientation/position where the feedback was given) as the haptic feedback becomes weaker. In both tasks, comparing these accuracies across consecutive levels reveals the locations of the hypothesized sensitivity thresholds. For angles, these sensitivities corresponds to somewhere between level 4 (where accuracy is $19.82 \pm 41.07^\circ$) and level 6 (where accuracy is $54.01 \pm 64.11^\circ$) whose difference in accuracy is significant (Welch’s $t(44.48) = -2.32, p = 0.0250$). For positions, this corresponds to somewhere between level 5 (where accuracy is $10.52 \text{ mm} \pm 12.25 \text{ mm}$) and level 6 (where accuracy is $32.36 \text{ mm} \pm 44.85 \text{ mm}$) whose difference in accuracy is significant (Welch’s $t(39.33) = -2.77, p = 0.008$). These thresholds definitively mark the points where users lose

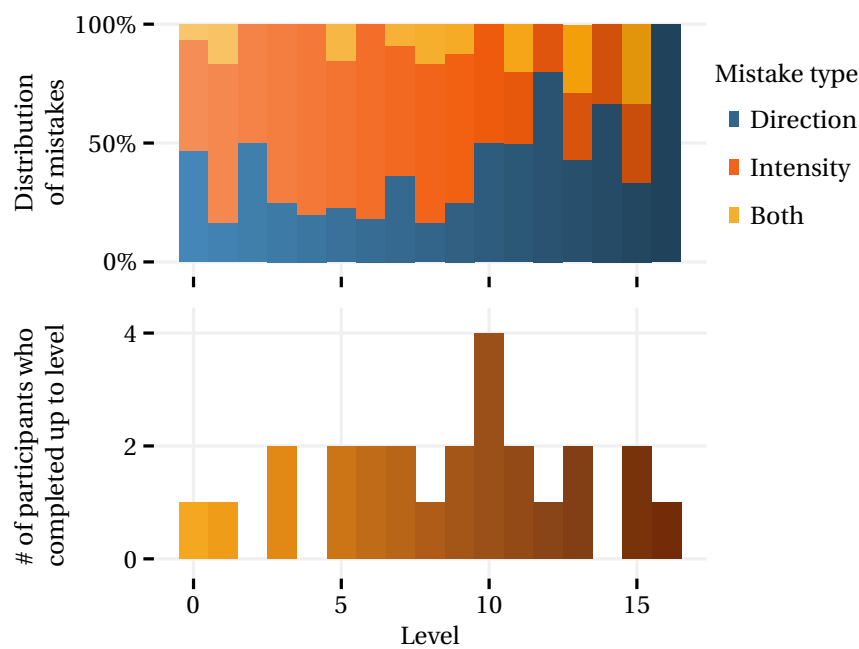


Figure 4.14 – Distribution of mistakes at each level and number of participants that completed each level as their last in Match.

precision and possibly lose comfort in perceiving the haptic feedback. More data with more sensitivity resolution may reveal more accurate threshold locations. From a success perspective, all participants except one³ reached at least level 2 in Find Angle while all participants reached at least level 4 in Find Position.

The Match task had participants differentiate forces that were more and more similar as levels progressed. Using the given answers, we separately measured how many wrong answers were given due to direction or due to intensity, shown in Figure 4.14. This shows a trend in more mistakes due to intensity compared to direction (especially in lower levels): It was observed that many participants discovered that they could use the robot’s motion inside the small operational area (10 mm diameter circle in the center of each visual area) while lightly grasping it and letting it move to observe the direction of the force, suggesting why less direction mistakes may have been made.

Moreover, as mentioned in the task description, the audible noise generated by the motors is potentially indicative of the applied force. On one hand, this modality complements the haptic feedback and may enhance the force perception. On the other hand, it may be unusable or inaccessible in the presence of many robots or a noisy environment. From a success perspective, Figure 4.14 also shows the distribution to the number of participants who reached each level, revealing a spectrum of perception resolution. All but 4 participants completed at least level 5, denoting a capability in differentiating at least 17.7% intensity (compared to

³This participant was observed to show exceptional reluctance to the device at first (as this was the first task) but then overcame this reluctance and reached level 7 in Find Position.

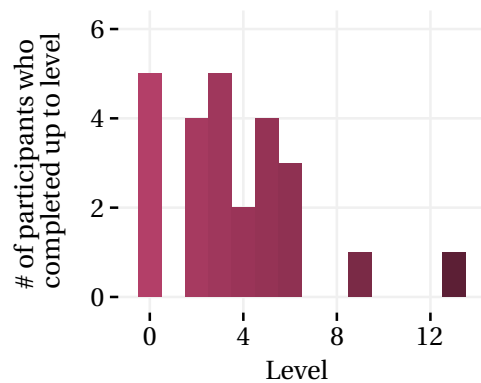


Figure 4.15 – Number of participants that completed each level as their last in Find Shape.

maximum output) and 72.3° orientation. For these few participants who did not perform as well, more training than what was available in the experiment may be necessary to improve perception performance. However, when the median of this distribution is considered, we see that the majority of the participants completed at least level 9, denoting 8.53 % intensity (compared to maximum output) and 34.9° orientation differentiation capability.

The Find Shape task had participants discover which of the five shapes was hidden on the paper sheet using tactile feedback given at the contour of the shape. We found that participants were generally not performant: Figure 4.15 shows that a significant number of participants did not progress further than level 0 where there was no limit in the number of attempts. It was observed that casually exploring the activity sheet did not reveal the shape for most participants, and that it was necessary to develop systematic scan strategies that was achieved by only few participants during the short duration they spent in the activity. This may indicate that a continuous long-distance rendering of the border (force towards/away from the border) may be a better approach to expressing 2D curves than a binary (tactile feedback on/off) border exploration method. Due to this impairment in the design of the task, we do not draw further conclusions on the contour-rendering capabilities of our robots.

4.3.4 Conclusion

In this section, we presented the self-contained evaluation of the haptics subsystem of our robots that was designed as a task-based experiment. This design was done with the Cellulo workflow in mind, where the integration of haptic interaction into activities must be easy, natural and efficient; the reasons for which include maximizing the benefit from the (essential) active participation of teachers in this design process, who do not necessarily possess technical skills. For this reason, we designed our tasks in the form of “atoms” (built around the basic DOF found in our interaction space) that can be used as on-demand building blocks. Although this may not be the optimal approach to benefit all HCI applications in general, we believe it is favorable for facilitating developer-designer-teacher communication in order to improve the co-design process of activities.

The results that were achieved in this study have several implications for this co-design process, in addition to revealing the technical capabilities of our platform within the atomic tasks that were chosen. For one, designers may choose to use the activity itself to guide first-time users of the platform into familiarizing with the interaction featured in the activity, effectively avoiding dedicated tutorials only to show the use of the device. Furthermore, in addition to utilizing printed graphics to imply and guide the motion as shown in the previous studies, we have now shown in this study that the robot's motion itself can be recognized on simple trajectories without any visual component; activities involving motion perception can now be designed with both tools in mind (visual and non-visual), using one or the other depending on need and other factors. When the motion is to be provided by the user on graphical trajectories, measurements of fidelity to the path must take the best possible accuracy performable by regular users into account, shown to be on the sub-centimeter level in this study. However, we have also shown that it is not feasible to provide the motion entirely by the robot under all circumstances (as previously predicted, mentioned briefly in Section 4.2.2); in other words, a single robot is not powerful enough to dictate the motion if the user does not allow it. If such behaviors are to be designed, the user must be informed (or ensured) to grasp the robot loosely in a manner that allows it to move on its own.

4.4 Ecological Validation

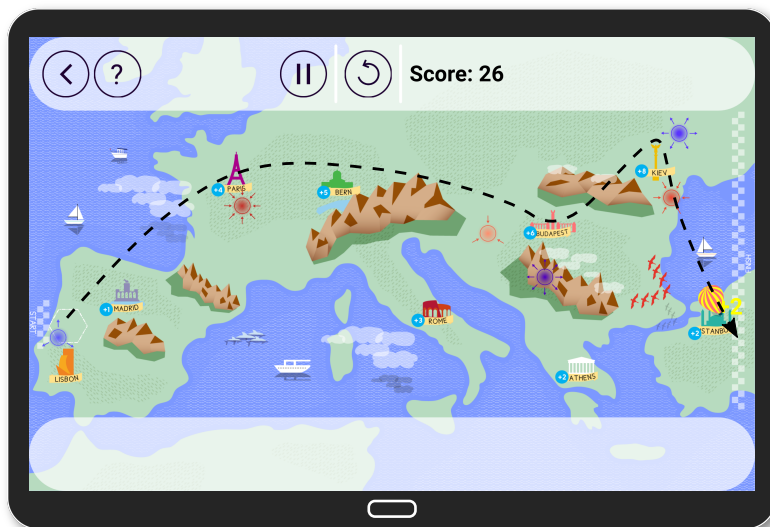
4.4.1 Overview

Following the development and supervised validation phases presented in the previous sections, we reach again the ecological validation phase of our design iteration. Now, with our robots featuring validated haptic feedback capabilities in addition to autonomous locomotion and localization, we move towards a more realistic testing scenario compared to previous chapters. In this instance, we will focus more on learning with haptic-enhanced activities rather than focusing solely on haptics that is the theme of this chapter. Our motivation is that at this point, it is not clear whether it is feasible or meaningful to integrate robots such as ours (namely tool-like tangible robots) into the curricular learning and teaching environment.

Therefore, we will now aim to build a complete lesson incorporating tangible and haptic elements where we are thoroughly inside the target application area of our platform. To achieve this, we will build upon the same Windfield activity of the previous chapter's ecological validation phase (built around the topic of atmospheric pressure and wind creation mechanism that is in the standard curriculum) to obtain a didactic sequence. With this sequence, we will build a lesson plan tailored for small groups of learners, intended to require minimal effort to setup and run during the actual lesson time in a given middle school. Instead of the "in-the-wild" approach adopted in the previous chapter where participants were free to engage in and withdraw from our activity at any time, we will now aim to have a controlled lesson through our activity that is run for the entirety of the predetermined period with all participants. Finally, at the end of this period, we will subject the participants to a brief examination in order to



(a) Screenshot from *Feel the Wind*. Among the two pressure points given, the low pressure point is found and the high pressure point is yet to be discovered. Three robots belonging to three learners are depicted with hot air balloons in their respective positions. The vector field representation of wind intensities and directions are not normally shown to the group unless they are observed to be stuck or are nearing the time limit.



(b) Screenshot from *Control the Wind*. This hypothetical solution uses all 6 available points in different intensities. The balloon follows the dashed trajectory (not shown to the learners) and collects 26 points. The locations of the cities letting learners earn points were intentionally chosen such that collecting all the available 31 points is impossible to prevent a ceiling effect.

Figure 4.16 – Screenshots from the application hosting *Feel the Wind* and *Control the Wind*.

illuminate, for the first time, whether learning is actually possible through a lesson designed with our platform. The work done by others than the author of this thesis throughout the development process that expands the previously presented Windfield activity, as well as the lesson and experiment design process, is attributed to the same persons as described in the overview of the previous chapter's ecological validation section. We further acknowledge that the development and evaluation described in this section was previously presented in [191].

4.4.2 Activity Design

We start with the same Windfield activity where learners probed the wind forces over a geographical map with their robots introduced as “hot air balloons” in order to discover how the atmospheric pressure mechanism functions, using the same playground seen in Figure 3.13. Again, high and low pressure points of various intensities create outwards and inwards winds respectively at a distance. Instead of the previously developed FEA-like method, we opted for a simpler and computationally less expensive vectorial sum of wind forces created by all pressure points that are decayed with squared distance. Other factors that affect realistic winds such as the Coriolis effect are again not considered. With these mechanics as basis, we developed two distinct phases to our activity:

Feel the Wind: The first phase of the activity is very similar to the one previously developed (see Figure 3.14) where the pressure points are hidden and the robots are used to explore desired locations on the playground with the goal of discovering the pressure points. Learners are allocated one robot each and place their guesses as a team on the tablet's graphical display where the entire playground and each robot's hot air balloon is displayed in real time; a screenshot from the application displaying this interaction can be seen in Figure 4.16a. The robots (*i.e.* tangibles) are intended to be visually mapped by the learners onto their hot air balloon counterparts on the tablet display via graphical landmarks found on the playground (*e.g.* cities, mountain ranges, clouds, boats, flock of birds, dolphins). This allows reasoning as to whether the particular forces applied to the robots are meaningful upon placing pressure point guesses on the display, since they are visible on the tablet but not on the paper playground.

Each robot in the activity self-localizes as soon as it is placed on the playground and sends its global position to the tablet application. Upon receiving a position, the tablet application calculates the virtual wind force at that position and sends back a force output command to the robot, effectively resulting in a remote control loop that depends on the configuration of the pressure points creating these winds. This output is effectuated as long as the learner's grasp is detected via the touch keys on top of the robot, resulting in a force feedback that represents the wind force. Throughout this phase, casual backdrive assist is enabled for manipulation comfort.

Control the Wind: The second phase of the activity lets learners control the positions and strengths of the pressure points to create the necessary winds to bring one hot air

Chapter 4. Phase III – Haptics with Actuated Tangibles

	Phase	Goals	Time (min)
IN.	Introduction	Introduction to platform and lesson, assessment of pre-knowledge by discussion on weather forecast video	5
F2.	<i>Feel the Wind</i> with 2 pressure points	Exploration of wind and pressure mechanism with robots	10
IV.	Informative video	Comprehension of wind mechanism and mid-term synthesis	5
F4.	<i>Feel the Wind</i> with 4 pressure points	Application of wind mechanism knowledge	15
CW.	<i>Control the Wind</i>	Transfer of knowledge into constructive use	10-20
PT.	Closing & post-test	Measurement of knowledge gain	5
			Total: 50-60

Table 4.1 – Windfield lesson plan and didactic sequence.

balloon from the start position to the finish line, stopping by as many cities as possible to collect the most points without leaving the playground. Learners place the pressure points, choose their intensities and start the simulation through the tablet; a screenshot from the application displaying this interaction can be seen in Figure 4.16b. One robot (now functioning as a mobile robot and not a haptic device) enacts the simulation with a simple pose tracking motion controller whose target is commanded by the tablet application upon receiving the poses periodically sent by the robot.

In addition to improving the previously developed activity with a proper haptics and motion controller and a better Graphical User Interface (GUI) for the tablet application to obtain *Feel the Wind*, *Control the Wind* was developed to give a didactic flow to the activity that lets the learners discover the effects of atmospheric pressure points at their discretion and then lets them transfer this knowledge and use it constructively in a game.

4.4.3 Lesson Design

A lesson taking between 50 and 60 minutes was designed with the above activity components; its plan and didactic sequence can be seen in Table 4.1. During the lesson, the experimenters act only as observers and facilitators; the learners are left to interact with the system by themselves during each phase, with the tablet providing enough information for them to be autonomous. All phases in the lesson are explained below.

IN - Introduction

The group of learners are first greeted and shown a 1 minute video clip of a television news weather broadcast where the meteorology reporter gives the current atmospheric pressure status. They are asked whether they are already familiar with the concepts used in the broadcast to verify the absence of pre-knowledge on the subject. They are then explained the subject of the lesson they are about to experience and how it is connected to this everyday occurrence whose underlying principle possibly evades their attention. They are explained that the high and low pressure points blow air outwards and absorb air inwards respectively and that they have effects at a distance that diminish when moved away. These facts are explained in the presence of brief slides that show the same icons used in the activity for high and low pressure points for easier retention.

F2 - Feel the Wind with 2 pressure points

The team of three learners are then invited over to the activity sheet and are given one robot each. They are told to put the robots on the map to feel the wind at desired locations; they are made aware of the depictions of hot air balloons that are continuously displayed on the tablet screen. They are also shown how to drag and drop the pressure points on the tablet to make guesses. At this point, the experimenters completely stop interacting with the group and let them do the activity on their own.

One high and one low pressure point (same intensity and opposite directionality) are hidden at random positions that are at least 200 mm apart from each other. The learners are not given more information unless they are observed to be stuck or are nearing the 10 minute time limit. If this occurs, they are shown the wind directions and strengths on the entire playground in the form of a vector field display. If the pressure points are found with the help of this display, the learners are invited to nevertheless feel around the newly discovered pressure points.

IV - Informative video

After the brief introduction to the activity, the learners are shown a 5 minutes informative video from a television show called *C'est pas Sorcier* (English: *It's not Magic*) aimed at explaining scientific phenomena to young children. The short clip explains how hot and cold air loses and gains density and therefore pressure with respect to its surroundings. It continues to explain how masses of air displace between these areas, resulting in winds. In the video, the same colors are used to depict high/low pressure points as in our activity.

F4 - Feel the Wind with 4 pressure points

After IV, the learners are invited to discover 2 high and 2 low pressure points (all having the same intensity) positioned randomly that are again at least 200 mm apart from each other. If

Chapter 4. Phase III – Haptics with Actuated Tangibles

they are observed to be stuck or are nearing the 15 minute time limit, they are again shown the wind vector field all over the playground on the tablet.

CW - Control the Wind

The learners are explained that in this next task, they are supposed to position 3 low and 3 high pressure points themselves in order to move one balloon across the playground and collect points by visiting cities. Points associated with cities were chosen according to how difficult they are to visit, and the cities were distributed such that it is practically possible to visit only a subset of them. They are shown how to modify the intensity of the pressure points and how to start and reset the simulation and are not aided further.

They are not given the ability to modify the directionality of the pressure points in order to encourage them to use both high and low pressure dynamics in different situations. They do this task as a team as there is a single simulation to be optimized. The progress of the group is monitored and the task is allowed to continue up to 20 minutes if room for more progress is clearly observed. Otherwise, it is finished at the 10 minute limit.

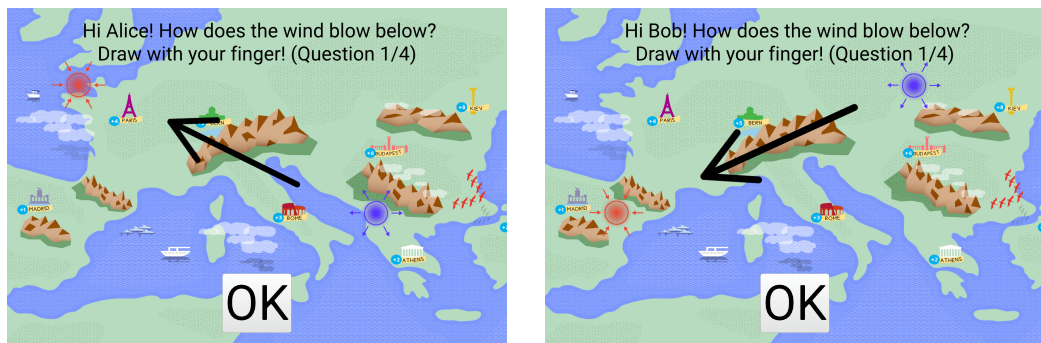
PT - Closing & Post-test

Finally, each individual member of the group is subjected to a post test composed of 4 questions (with roughly increasing difficulty) that assess different aspects of the wind formation mechanism that should have been understood as the result of the lesson. Each question displays a number of pressure points on the playground and asks the learner to draw an arrow depicting the blow of the wind in that hypothetical scenario. Screenshots depicting each question is given in 4.17; they are the following, with the aspect that must be understood to answer correctly given in quotes:

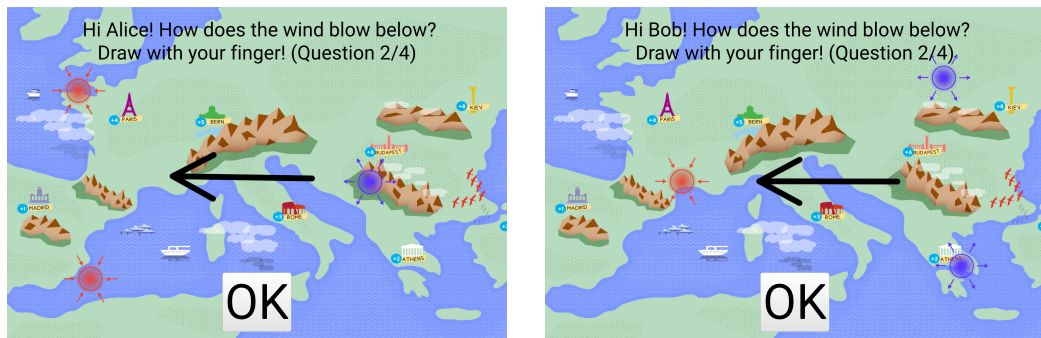
- Q1.** Two pressure points – *“Wind blows from high to low pressure”*
- Q2.** Three pressure points – *“Identical pressures have similar effect at similar distance”*
- Q3.** Two pressure points, wind in a specific area is asked – *“At similar distance, opposite pressures’ vectoral effects combine to result in winds parallel to the line that connects them, i.e. orthogonal to the weather front”*
- Q4.** Three pressure points, wind in a specific area is asked – *“At dissimilar distances, pressure that is closer has a larger vectoral effect; the resulting wind is the sum of these vectors”*

Two variants for each question were carefully and deterministically prepared, each learner is asked one of the two variants chosen randomly. During the post-test, learners are prevented from sharing any information. After the post-test, the learners are asked their general opinions about the lesson and are thanked for their participation.

4.4. Ecological Validation



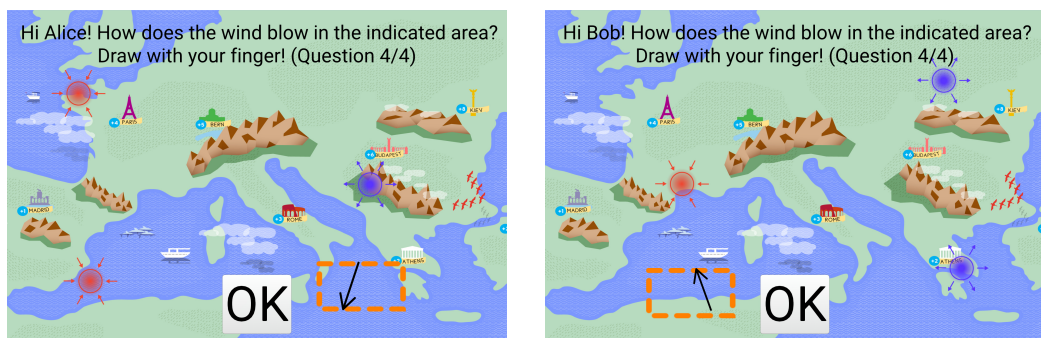
(a) **Q1:** 2 pressure points



(b) **Q2:** 3 pressure points



(c) **Q3:** 2 pressure points; draw in the box



(d) **Q4:** 3 pressure points; draw in the box

Figure 4.17 – Post-test questions, each with two variants. Each learner was asked one randomly selected variant of each question. Roughly correct answers drawn on each question.



Figure 4.18 – Sample scene from Windfield where the team of 3 learners is carrying out a Feel the Wind phase.

4.4.4 Participants & Data Collection

24 learners (12M, 12F, 11.9 ± 0.900 years-old, min. 10, max. 13) participated in the experiment in 8 groups of 3 learners during 2 days. It was verified through the age group selection (*i.e.* younger than when this subject is taught at school) and through the brief discussion in the IN phase that no formal pre-knowledge existed about the subject for any participant. The groups were formed randomly and treated separately. Each group was observed for behaviors that may explain findings later on. Poses of all robots used by all learners in all groups were recorded with maximum framerate as long as on the playground. In addition, all grasp and release events, all kidnap and return to playground events and all GUI events (such as button click, drag and drop positions *etc.*) were recorded. A sample scene from the experiment can be seen in Figure 4.18.

4.4.5 Calculated Metrics

In addition to task completion times, CW scores and accuracy of given answers to correct answers in PT, a number of other more complex metrics were calculated from the robot position sequences obtained from F4. These are given below.

Similarity of exploration across entire F4

We build the (per learner) 2D histogram of all visited positions where each bin is 20 mm × 20 mm and contains the total time spent by the robot at that location. Then, we calculate the *soft cosine similarity* ([192]) across all pairs of learners within groups, defined as:

$$S(t^a, t^b) = \frac{\sum_i^N \sum_j^N s_{ij} t_i^a t_j^b}{\sqrt{\sum_i^N \sum_j^N s_{ij} t_i^a t_j^a} \sqrt{\sum_i^N \sum_j^N s_{ij} t_i^b t_j^b}} \quad (4.9)$$

where N is the number of bins, t_i^a and t_i^b are the times spent at bin i by learner a and b respectively, and s_{ij} is the similarity index between bin i and bin j , which is calculated as:

$$s_{ij} = \begin{cases} \frac{D-d_{ij}}{D}, & \text{if } d_{ij} < D \\ 0, & \text{otherwise} \end{cases} \quad (4.10)$$

where d_{ij} is the physical distance between the centers of bins i and j . D is the maximum distance to be considered for similarity, which is chosen as the maximum size of one robot (corner to corner, 85 mm).

The similarity measure indicates the likeness of spatial coverage between two learners, and may provide insights on collaboration quality within a group. High similarity may indicate redundancy of exploration (implying low collaboration quality), but may also indicate co-exploration (and not necessarily low quality collaboration) if leader-follower effects are present. On the other hand, low similarity may indicate efficient exploration by division of labor, indicating high collaboration quality, if enough communication is present within the group.

Entropy of exploration across entire F4

With the same histograms as above, as well as with the overall histograms per group, we calculate the normalized Shannon entropy as follows:

$$H(t) = -\frac{1}{\log_2 N} \sum_i^N \hat{t}_i \log_2 \hat{t}_i \quad (4.11)$$

where N is the number of bins and \hat{t}_i is the time spent at bin i , normalized by the total time spent over all bins. Entropy measures the “disorder” of exploration; higher entropy corresponds to more equal distribution of time spent across the explored area (and *not* the

entire playground area), while low entropy corresponds to less equal time distribution, possibly due to time spent around focal points. Therefore, lower entropy may indicate “getting stuck at” or returning to certain points rather than exploring the map without revisiting previous locations.

Cross recurrence of exploration in F4

To extract temporal information, robot positions of each learner were resampled at 1 Hz (averaging all available positions closest in time) starting at the same instance to obtain synchronized positions within groups, since current robot hardware does not offer this synchronization mechanism across multiple robots. With these synchronized positions, cross recurrences between all pairs in each group were calculated with (inspired by [193] in the eye tracking literature):

$$R^{ab}(t_i, t_j) = \begin{cases} 1, & \text{if } d^{ab}(t_i, t_j) < D_{\min} \\ \frac{D_{\max} - d^{ab}(t_i, t_j)}{D_{\max} - D_{\min}}, & \text{if } D_{\min} \leq d^{ab}(t_i, t_j) \leq D_{\max} \\ 0, & \text{otherwise} \end{cases} \quad (4.12)$$

where $d^{ab}(t_i, t_j)$ is the distance between learner a 's robot position at time t_i and learner b 's robot position at time t_j , D_{\min} is the distance below which there is full recurrence (chosen as one robot width, *i.e.* 85 mm, since two robots cannot occupy the same space at the same time) and D_{\max} is the maximum allowed distance for recurrence (chosen as two robot widths, *i.e.* 170 mm). With this, we measure the normalized leader-follower index, calculated as:

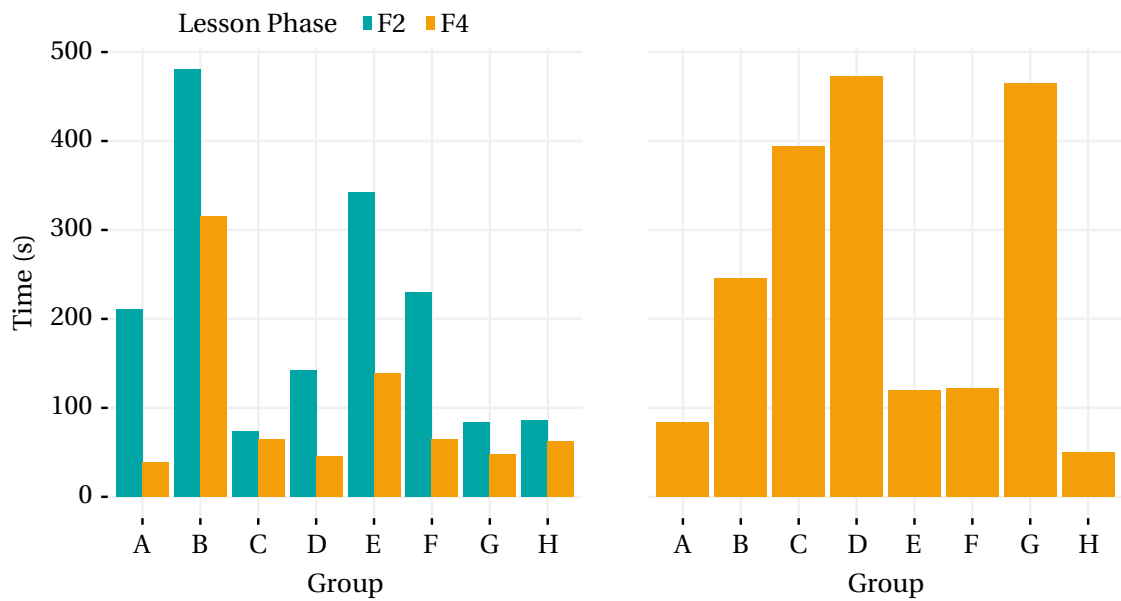
$$L^{ab} = \frac{\sum_{0 \leq t_j - t_i \leq S} R^{ab}(t_i, t_j)}{\sum_{0 \leq t_j - t_i \leq S} A^a(t_i) A^b(t_j)} \quad (4.13)$$

where S is the maximum time difference to consider (chosen as 10 seconds) and $A^a(t)$ equals 1 if learner a 's robot is on the playground and is being grasped at time t (*i.e.* active), and equals 0 otherwise; the same is valid for $A^b(t)$. By definition, L^{ab} is between 0 (no leadership) and 1 (a leads b 100 % of the time).

4.4.6 Results & Discussion

Feel the Wind

We measured the time to find the first pressure point in **F2** and **F4** (time for each group presented in Figure 4.19a) to determine the effect of midterm synthesis with the informative video. Comparison was done after artificially doubling the time in **F4** to accommodate twice the density of points on the playground. A within-group paired t-test showed significant decrease ($t(7) = 3.9773, p = 0.005$) from **F2** (205 ± 144 s) to **F4** (97 ± 93 s). This improvement hints at the effect of the informative video, but it should be noted that it may also have occurred



(a) Time to find the first pressure point in **F2** and **F4** (Feel the Wind with 2 and 4 pressure points). **F4** times are artificially doubled to accommodate twice the point density in **F4**.

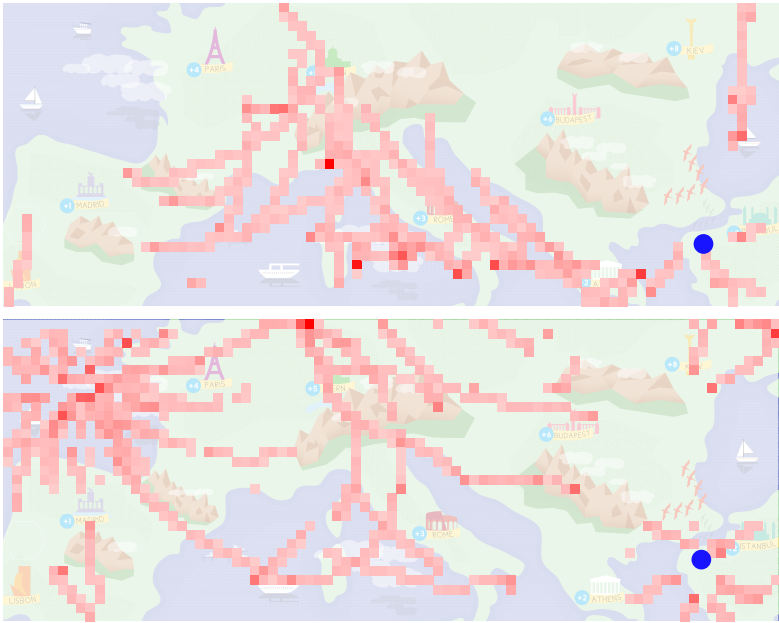
(b) Time to find the first *high* pressure point in **F4** (Feel the Wind with 4 pressure points).

Figure 4.19 – Time to find the first pressure point(s) for each group in *Feel the Wind* phases.

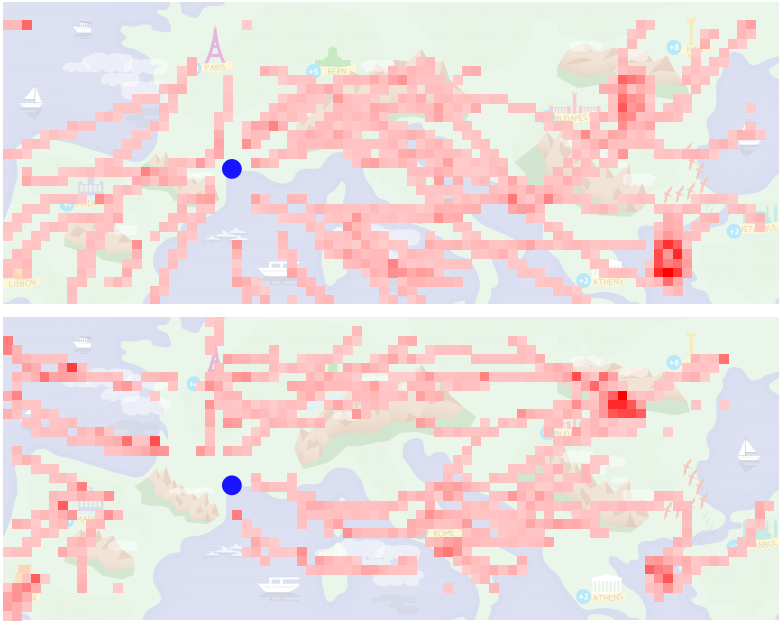
due to natural habituation to the platform, as all participants interacted with our robots for the very first time in **F2**.

During **F2** and **F4**, all groups were observed to find a low pressure point first as these points naturally act as “sinkholes” and lead the robots to themselves when they are allowed to move. This behavior may in theory damage the quality of exploration if it is allowed to emerge at all times (*i.e.* robot *moving* alone) and is not complemented by learners driving the robot where they wish to explore (*i.e.* robot *being moved*). Our observation on this is that moving did not occur at all times and was complemented to some degree by being moved: In **F4**, some groups eventually found all pressure points while the rest found at least one high pressure point (times to find the first one shown in Figure 4.19b) before being shown the visual vector field representation of winds, at which point they found the final point within a few seconds.

On the other hand, the randomized initialization of pressure points meant that groups received randomized situations and some groups were thus observed to struggle due to the circumstantial difficulty of the specific distribution of points. To mitigate this problem and to obtain better pedagogical scenarios, we believe that such situations (*e.g.* point distribution in the case of Windfield) must be designed by hand in the future to subject the learners to specific situations where their exploration will be more guided and may be more fruitful in terms of learning. Then, a catalog of such situations may be presented to the learner, who can then be guided into discovering the desired aspects of the topic one by one.



(a) Two learners in group B. Top and bottom learners approach the same point from 3 and 6 different angles respectively.



(b) Two learners in group F. Top and bottom learners approach the same high pressure point from 6 and 4 different angles respectively.

Figure 4.20 – Similar “approach” patterns towards high pressure points (marked with the blue dots) found in two different groups. Low pressure points also clearly visible in group F as the two high density areas towards the east that acted as “sinkholes”. Some focal points and traversals are visible over Mediterranean islands, boats and flocks of birds, assumed by learners to host pressure points, which was not necessarily the case.

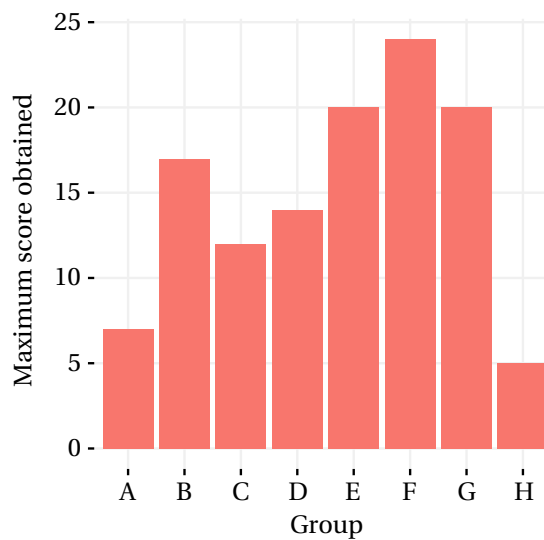


Figure 4.21 – Maximum score obtained by each group in CW. 31 points are available in total, intentionally made impossible to fully obtain.

Furthermore, positional densities of individual robots over the entire playground revealed certain patterns of interaction, seen in Figure 4.20. In certain groups, learners developed the strategy where they “approach” suspected high pressure points from different angles. In almost all groups, focal points of high density coinciding with low pressure points are observed due to the aforementioned “sinkhole” effect. More interestingly, focal points and traversals are observed over graphical items found on the playground sheet (*e.g.* boats, islands, cities) some of which can be seen in Figure 4.20. While not intentional by design, this phenomenon agrees with our observations of the dialogue within most groups; learners often thought that pressure points should be located on such graphics and conveyed this towards their groupmates. This observation, along with those made in the ecological validation phases of the previous chapters, implies that printed graphics may intentionally be designed to benefit the activity, although this was not exploited in this specific study.

Control the Wind

Figure 4.21 illustrates the maximum scores attained by groups during the entire CW. The maximum scores are observed to be widely varying across groups (14.88 ± 6.64 , min = 5, max = 24), but were not found to be correlated with the number of attempts (45 ± 36.2 , min = 17, max = 123). Furthermore, the scores were not found to be correlated with any metric from Section 4.4.5, preventing us from drawing conclusions about the transfer of knowledge. This was likely due to the trial-and-error natured approach observed from most groups allowed by the design of the activity, which is acknowledged as a shortcoming.

This approach adopted by most groups, especially towards the late stages of the activity, was observed to rely mainly on microscopic adjustments to already placed pressure points in order

to repeatedly fine-tune the trajectory of their balloons to visit more cities. We believe that the continuous nature of the workspace may be unsuitable to **CW**, and the future design of such an activity should combine a discrete space (*i.e.* a grid where pressure points can only be placed in the center of each cell) with a time interval that must be waited (such as tens of seconds) before being able to retry solutions. This approach may succeed in obliging the learners to reason about their choices instead of fine-tuning them without direction.

Post-test

The accuracy of the answers given to the post-test questions were measured by computing the angle difference between the answer and the actual wind direction, considering answers with less than 30° difference correct. This revealed three distinct categories of answers: Correct ones, incorrect ones and ones that are exactly the opposite of correct answers. We interpreted this latter type as the learner failing to recall the correct association between push/pull and the depictions of high/low pressure points, but otherwise showing correct understanding of that particular wind formation aspect. Therefore, we labeled these answers as semi-correct (again with 30° tolerance).

Figure 4.22 shows the distribution of each answer type for each group and each question. Scores for **Q1** (75 % correct and 21 % semi-correct) and **Q2** (67 % correct and 25 % semi-correct) indicate that almost all learners understood the directionality and symmetry of wind at central locations. Scores for **Q3** (50 % correct and 8 % semi-correct) and **Q4** (42 % correct) show a clear drop in performance, as these questions were more complex and required the understanding of diminishing wind intensity with distance and asymmetrical vector summation. When correctness and semi-correctness of individual scores are considered among all learners, it is seen that 33 % of them are 50 % successful, 46 % of them are 75 % successful, and the remaining 21 % are 100 % successful. This implies that all learners are at least 50 % correct or semi-correct. On the overall, 58 % of answers are correct, 14 % of the answers are semi-correct and 28 % of answers are incorrect.

Finally, the correlation between metrics described in Section 4.4.5 and post test scores were investigated. The absolute raw differences between correct answers and given answers were found to fall just short of being significantly inversely correlated with total group entropies (Pearson's $r = -0.678$, $n = 6$, $p = 0.065$); further studies with more participants may discover that learners that “do not get stuck in focal points” tend to gain more understanding of the subject phenomenon and perform better in such an activity. This is also suggested by our observations of certain groups where the “sinkhole” effect mentioned previously inadvertently pulled the robots into the (already correctly found) low pressure points and the learners visited the same location repeatedly, decreasing entropy and exploration quality. No other correlation was found between the post test scores and other measures, direct (time to find low/high pressure points, **CW** scores, number of trials in **CW**) or calculated (mean *S* and *L* within groups). This may imply that such collaboration metrics in their aggregated form may be inappropriate for predicting learning gains, or simply that there is need for more data.

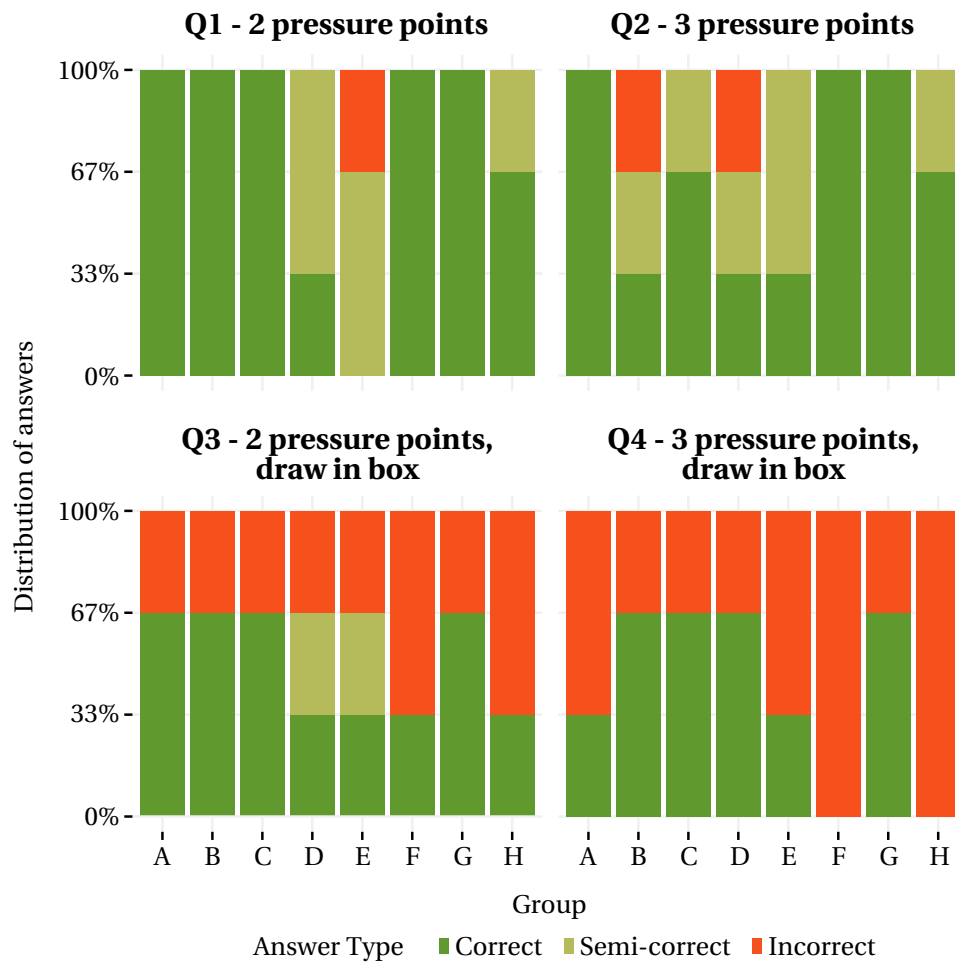


Figure 4.22 – Distribution of answers for each group and post-test question. *Correct*: answers with 30° accuracy. *Semi-correct*: answers with 30° accuracy in the complete opposite direction. *Incorrect*: any other answer.

4.4.7 Conclusion

This section introduced the first rigorously designed and studied learning activity using Cellulo, the subject of which was selected from within the actual school curriculum. We presented a lesson designed with the activity and its didactic sequence to let learners explore, apply and transfer the knowledge of simple wind meteorology using our robots. Vastly different interaction modalities that incorporate these handheld robots were used during this sequence, such as haptic and paper-based tangible interaction. These were all easily understood and effectively used: All groups found a significant portion of pressure points within time in **F2** and **F4**, most groups earned a significant portion of the total score (intentionally made impossible to fully obtain) in **CW**. Almost all learners showed learning of symmetric aspects of wind formation while about half showed learning of more complex, asymmetric vectorial aspects.

In this chapter, we designed and implemented a hybrid haptics and motion controller into our

Chapter 4. Phase III – Haptics with Actuated Tangibles

accurately localized mobile tangible robots, which we then validated under both controlled and ecological conditions, effectively obtaining *haptic-enabled handheld robots*. Moreover, we showed concrete learning gains for the very first time through an activity built around Cellulo, demonstrating that Cellulo is indeed usable as a “tool” to teach an actual curricular subject. While we clarified the interaction between a learner and a Cellulo robot, it is still not clear how the interaction between a learner (or a group of learners) and more than one robot works, where the robots do not necessarily “belong” to specific learners. Therefore, in the following chapter, we will aim to open up this final perspective where we will exploit the multiplicity of the Cellulo robots, which we believe will augment the power of our platform one last time. Using this ultimate form, we will present the co-design and real-world execution of a novel learning activity where the teacher is fully integrated in the loop.

5 Phase IV - Building Tangible Swarms

5.1 Introduction

5.1.1 Background

Following the three design, prototyping and testing iterations presented in the previous three chapters, the Cellulo platform is now composed of *well-localized, tangible handheld* robots capable of complex *motion* and *haptic feedback*. Used primarily individually up to now, our robots embody the spatial presence and motion of point-like objects and the forces externally acting on them or originating from them, as well as the user interface to each of these properties. When we consider learning within teams of learners, for whom we provided a shared and scalable workspace up to now, an evidently promising research direction is to clarify the gain from the extrapolation of the aforementioned capabilities of singular robots to teams (or possibly “swarms”) composed of multiple robots, given that they are built to be low-cost and simple. Therefore, in this chapter, we will begin the final phase of this thesis where we explore the human interaction and learning prospects of exploiting and coordinating many robots within the same activity.

Swarm Robotics is a sub-field of Multi-Robot Systems (MRS) research where typically a large number of homogeneous robots are dealt with, and historically draws inspiration from biological societies such as ants, bees and birds ([194]). Similar to their biological counterparts, swarm robots are often designed to have minimal capabilities and only local knowledge and awareness of the global world state and the state of other swarm elements in order to remain simple in their underlying hardware and software. Through distributed intelligence, emergent cooperation and the achievement of team-level tasks (that are normally not available to individual elements) are often studied where “the whole is bigger than the sum of its parts”.

Swarm robot systems are classically built and evaluated with a task-oriented approach where prominent tasks up to now have been foraging/coverage (for *e.g.* waste cleanup, search and rescue), formation control, object manipulation/transportation (for *e.g.* warehouse stocking/destocking, industrial transportation and structure assembly), multi-target observation

(for *e.g.* security, surveillance), exploration (for *e.g.* mapping unknown environments), and surprisingly, playing football. When the core field (*i.e.* MRS) is considered, distinct constraints that guide the system design and implementation are encountered, similar to those that guided the development efforts in the previous chapters:

- The nature and number of tasks or goals to be achieved, some of which are given above
- Dimensionality of the environment to be covered (*i.e.* the workspace):
 - 2D such as a tabletop or floor, covered by wheeled or legged swarm elements
 - 3D such as the entire inner volume of a building, covered by flying swarm elements
- Motion requirements of robots relative to other robots, relative to the environment and relative to external agents (*e.g.* human operators or users)
- Hardware and software complexity, directly affecting design and implementation costs
- Number of robots, scalability
- Composition of robots, *i.e.* homogeneity
- Coordination and organization, entailing communication and/or sensing requirements
- Human user/operator interaction (that leads to more novel requirements such as the ones discussed in this thesis)

5.1.2 Problem Statement

The constraints shaping our work, that is framed within the classroom environment, are already mostly determined as a result of the design iterations done in the previous chapters: Our robots work on large tabletop workspaces, are open to and actively promote tangible and/or haptic interaction and serve the purpose of human learning through carefully constructed activities. A central, non-robotic controller (*e.g.* tablet or computer) coordinates the robots (and the activity) through a star network composed of point-to-point Bluetooth SPP links.

Therefore, according to the characterization given in [195], our platform is a *cooperative, aware, strongly coordinated* and *strongly centralized* MRS and not exactly a swarm robot platform by the strictest sense, since from the hardware design point of view, ours does not exhibit a distributed nature. However, we choose to use “swarm robot platform” as an umbrella term throughout this thesis in order to emphasize the “swarm-ness” not from the developer’s point of view, who attempts to design and employ the robots to achieve a task, but from the user’s point of view who, in our case, interacts with the robots that are built and programmed for the sole purpose of making this interaction possible. Here, the collection of robots can be intentionally made to appear as if behaving like a swarm depending on the purposes of the activity employing the robots; such an activity is proposed later in this chapter where robots playing the role of “particles” (*i.e.* atomic particles as understood in Physics) are affected by forces arising from “local interactions” between other particles and elements in the system (that are in reality described globally by the central controller), leading to a collective, tangibly interactive and realistic display of “matter” composed of these particles.

While we acknowledge that in certain scenarios, distributedness may be unavoidable (due to

e.g. scalability or cost issues) and would certainly impose strong restrictions on human interaction, we will not focus on exploring human interaction in the presence of such limitations. Instead, in this chapter, the problem we will address is the viability of providing “physically distributed” human interaction using the perfect knowledge of the global world state and the collective state of the swarm robots, for the sake of maximizing the window of opportunities within the design space of user interaction with such objects as our robots. In doing so, we will attempt to shed light on the highly novel problem of human learning with tangible swarms, whose literary background, both from the perspective of human interaction with swarms and from the perspective of learning with swarms, will be given in the following section.

Following this, we will present our software framework which extends an existing swarm control approach with tangibility, and present our last learning activity that strongly benefits from this framework. Finally, using this swarm robot-enhanced activity, we will validate our learning tool with experimental studies with human learners as in the previous chapters. However, differently from the validation approach we adopted before (*i.e.* supervised “laboratory condition” validation followed by a real-world “ecological” validation), we will adopt an approach where we first validate our activity within an “in-the-wild” scenario with many learners where we will focus on reaching statistical results with quantitative data, and then within a concentrated “in-classroom” scenario where we will focus qualitatively on a smaller number of learners together with a teacher, as we find this entirely ecological approach more meaningful at this stage of design and development. In realizing these, we acknowledge the practical help by Dr. Wafa Johal, Arzu Güneysu Özgür who helped conduct the experiments and Julien Calabro who helped mass manufacture robots.

5.1.3 Related Work

Human-Swarm Interaction

Human-Swarm Interaction (HSI) is a particularly recent discipline concerned with the operation and maintenance of swarms that started gathering attention in the last few years; [196] gives the first literature review on this topic. Thus far, the research in HSI almost exclusively focused on regarding the human interacting with the swarm as an operator, possibly part of the team, commanding the robots to achieve a specific, well-defined task. Under this “operator control of swarm for task accomplishment” focus, notable examples include [197, 198, 199] that discuss methodologies, [200, 201] that propose visualization techniques, [202] that proposes performance metrics and [203, 204] that present applications.

From this operator-centric perspective, the interaction between the human and the swarm of robots is modeled with 4 key components: (i) The *operator* who controls the swarm through cognitive effort, whose complexity must be minimized similarly to computational complexity; (ii) *State estimation & visualization* that lets the operator observe the current state and predict the future state of the swarm; (iii) *Control methods* that convey the operator’s intent to the swarm through various types of inputs, that may be direct or indirect, and; (iv) The *swarm*

of robots themselves carrying out the task itself. Here, state estimation & visualization and control methods come together to form a single *interface* entity, separate from the swarm of robots. The majority of such interfaces in the literature are *remote* where the operator controls the swarm from a terminal, in a physically separate workspace. The justifications for designing such interfaces include the requirement of operation in inaccessible or dangerous areas.

The remaining state-of-the-art interfaces are *proximal* where the operator and the swarm share the same physical workspace. Here, the operator observes and commands the swarm directly through active engagement using *e.g.* speech or gestures. Therefore, the majority of research on proximal interaction is concerned with enabling this interaction via gesture recognition, face/gaze engagement detection and speech recognition; notable examples in this research direction are [205, 206, 207, 208, 209]. Apart from these, [210] proposed a Brain-Computer Interface (BCI) for relatively more implicit proximal selection of swarm elements.

Tangible Swarm Interaction

Our approach of *tangible interaction* partially falls under the category of proximal operator interaction, thus enjoying the prospect of many humans interacting with the same swarm in a significantly more straightforward manner compared to remote interfaces, but with a distinct emphasis on *user interaction* rather than *operator interaction*. Namely, our goal is that the users (in this case, a team of learners) undergo certain cognitive experiences as opposed to completing a given task using the swarm. Moreover, this physical, innate means of interaction lets us conceptually combine the interface entity and the swarm entity into one single, embodied *tangible swarm* entity. This way, the interaction from the user's perspective is potentially more natural and usable by virtue of its "What-You-See-Is-What-You-Get (WYSIWYG)" disposition; this is the reason why this type of interaction has also been called *world-embodied interaction* ([208]).

The roots of this tangible, world-embodied interaction were first described in [211] where the transition from "painted bits" in GUIs on computer screens towards "tangible bits" embedded in the physical world was envisioned. These tangible bits were conceptualized to yield better, more seamless coupling between the "cyberspace" that hosts digital media and the physical space through taking better advantage of the human senses and manual dexterity with richer affordances within the physical space that humans are accustomed to. [212] takes this vision further, into dynamic, malleable materials made up of "radical atoms" that enable bidirectional communication between the physical world and the digital, computational models. To afford the realization of such materials that change dynamically, the key capability that these building blocks must exhibit is actuation, which will let the tangibles they make up become active and kinetic where they would otherwise remain static and inert.

These building blocks are of course imaginary as the technology required to build them does not fully exist yet. The tangible swarms that started emerging in the last few years may be an advance towards attaining this fictional vision but there are indeed very few implementations

to date. Stemming from the active tabletop tangible interfaces (see **Active Tangible Interfaces** in Section 4.1.3), [213] proposes the design of a lightweight tabletop micro-robot swarm called Zooids where the design space of tangible interaction with such a large number of robots is explored, perhaps for the first time in the literature. Along many dimensions of this interaction design space, Cellulo exists at a similar point as Zooids: They both feature a possibly variable number (through *e.g.* kidnapping and returning robots from/to the workspace) of mobile and movable elements with possibly non-interchangeable identities through programmable colors or physical labels attached to the robots. However, with Cellulo we aim to have stronger representations of singular objects (“things”), particularly their physical properties and forces that act on them, with singular robots rather than aggregating robots as atoms to represent reshapable materials (“stuff”).

Finally, beyond tabletop tangibles, [214] presents a tangible micro-drone swarm where the interface is cast into 3D space. This self-levitating world-embedded programmable matter concept is certainly interesting in the long run (where it may replace tabletop interfaces with sufficient improvements), but currently presents considerable challenges to practicality and ubiquity due to various hardware constraints. The most crucial of these include rotor turbulence, resulting in flight clearance requirements and limiting some formations, and short autonomy (on the order of tens of minutes at best) due to the inefficient nature of drone flight.

Swarm Robots for Learning

The fundamental idea of swarm robotics, namely designing robots in a low-cost, simple and replaceable way in order to exploit their collective capabilities, has found its way into education over the years through a multitude of small tabletop robots designed for robotics education (and explicitly swarm robotics education later on) in the undergraduate curriculum, as well as for scientific research in general. Two of the earliest such platforms are Khepera ([215]) and Alice ([216]), developed for research and education with a strong commercialization focus. A later instance with more modern hardware is e-puck ([26]) which extended the educational potential of such robots from serving only robotics and software engineering towards being useful for a broader inventory of engineering disciplines, such as embedded systems, signal processing and computer vision.

The aforementioned robots were innovative in opening new educational perspectives with MRS and swarm robot systems, but their cost was nevertheless somewhat prohibitive. In the last few years, there has been a particular regrowth in interest to address this cost problem. [217, 218] are some notable published examples in the literature, and there have been released many others including commercially available ones; virtually all such robots feature a small body (on the order of some tens of millimeters), wireless connectivity and a differential drive, while some feature omnidirectionality through omni-wheels instead (*e.g.* [219, 220]). Another innovation towards this goal came from [171] where the robot was ultra-miniaturized and simplified through an omnidirectional vibration drive and a very limited set of sensors, decreasing one robot’s cost down to \$14 and enabling access to a truly large number of robots.

Despite these advances resulting in widely available and affordable multi-robot and swarm robot platforms, there was a distinct shortage of educational designs and applications employing these technologies. Essentially all such applications were targeted towards teaching aspects of robotics (or a wider spectrum of engineering-related subjects at best) mostly in higher education, and in some instances, in basic education. To date and the best of our knowledge, the only instance of teaching non-engineering matter using many robots with collective behaviors is proposed by [74] which uses the Droplets platform (itself unpublished at the time of writing) that improves upon [171] through more lightweight and scalable power management and more user-friendly appearance. In this very recent work, the robots are used as tangible representations of various elemental atoms (such as carbon, oxygen and hydrogen) to obtain a proof-of-concept simulation of chemical reactions but concrete learning gains were not yet shown using this simulation as part of a lesson.

For our vision of physically enhanced learning through handheld robot swarms, it is both remarkable and encouraging to witness the emergence of tangibility and world-embodiment in this very first non-engineering educational application of swarm robots outside of our own project, where bidirectional interaction is exploited for displaying how chemical reactions occur, instead of providing a classical unidirectional display. We believe that there is considerably more room for exploration in this research direction that we find exceptionally promising, and we aim to show the contributions of such interactions to learning in this chapter.

5.2 Development - Tangible Swarms

5.2.1 Overview

As mentioned before, we are interested in the prospect of treating tangible human interaction with our robots under centralized instead of distributed control to circumvent typical problems that may require solving, such as latency and synchronization among the robots, and to enable the exploration of the entire design space of tangible HSI in our scenario. Given that our robots feature a basic hardware means of recognizing grasps (*i.e.* circular array of capacitive sensors on the top surface) and wireless communication with the central controller, we proceed in this section to design a software framework that will permit the application developer to implement swarm applications in a fast, efficient and elegant manner. Following this, we will present the design of our final learning activity that readily employs the control and interaction facilities enabled by this software framework.

5.2.2 Wireless Communication Considerations

Prior to the design of our swarm application framework, we will address the local network size problem of Bluetooth that prevents a large number of robots from connecting to the same activity. Bluetooth version 2.1, that was initially selected as the main means of communication for readiness of connectivity with consumer devices that are likely to be present in the

classroom, only allows a maximum of 8 devices in one local network (also called a *piconet*) where 7 point-to-point links exist between one of the devices and each of the remaining 7. In other words, one device can only connect to 7 other devices. Technical documents detailing the means of interconnecting more devices using Bluetooth are scarce (possibly due to the lack of the need for communicating with such a number of devices in any given consumer network), and we will therefore now explore how controlling swarms using Bluetooth could be achieved under practical conditions.

A potential solution is to implement a *scatternet*, namely connecting the central controller to a number of robots, all of which are in turn connected to other robots, and so on, resulting in a tree structure (also called a *hierarchical star network*). To achieve this, the central controller must be able to control the dynamic formation of this network as well (transparently to the user), requiring connection establishment and termination calls in the robot API, as well as packet relay facilities, for example with a protocol such as the one in [221]. To circumvent the dynamic formation of this network, the non-leaf internal robot nodes in this tree can prospectively be replaced by other consumer devices that remain connected to the non-robot subnetwork (which includes the central controller) and that implement a relay application in software that is only tasked with connection establishment, termination and packet relay. A problem that arises in this scenario is that each point-to-point link within the non-robot network must carry all of the robot communication bandwidth that ultimately passes through itself. In the simplest case (7 internal nodes, each of which connect to the central controller and $7 - 1 = 6$ unique robots, resulting in $7 \times 6 = 42$ robots in the network), this amounts to the total bandwidth of 6 robots¹. Other topologies, such as a chain network, will suffer from the same problem (as well as from possibly increased latency due to higher number of hops) as long as the maximum active connection limit stands.

Our approach to mitigate this problem is to employ more than one Bluetooth connection point (also called an *adapter*) on the central controller device and to not use devices as relay nodes. This approach will replace the wireless Bluetooth links, that would normally be tasked to carry the bandwidth of more than one robot, with wired links that typically support significantly higher bandwidth and provide lossless transactions naturally more easily. This way, we can not only use additional Universal Serial Bus (USB) adapters that are abundant and obtainable with low cost (on the order of €10 per adapter) but we can still use the internal Bluetooth adapter present in virtually all consumer devices, as we did in the previous chapters in a practical manner, even in the absence of additional external adapters. Additionally, we choose to implement a separate software module than the activity applications, to which we delegate the task of managing the controller-robot Bluetooth sockets in software. This module is in the form of a long-lived daemon that communicates with the activity application through a local software socket (or with possibly any inter-process communication method) and provides it a “robot pool” API. The final software architecture that is composed of these modules is given in Figure 5.1.

¹Empirical tests resulted in the saturation, and thus constant intermission in packets, of a network with only a single internal node and 5 robots, each part of a 10 Hz motion control loop running on the central controller.

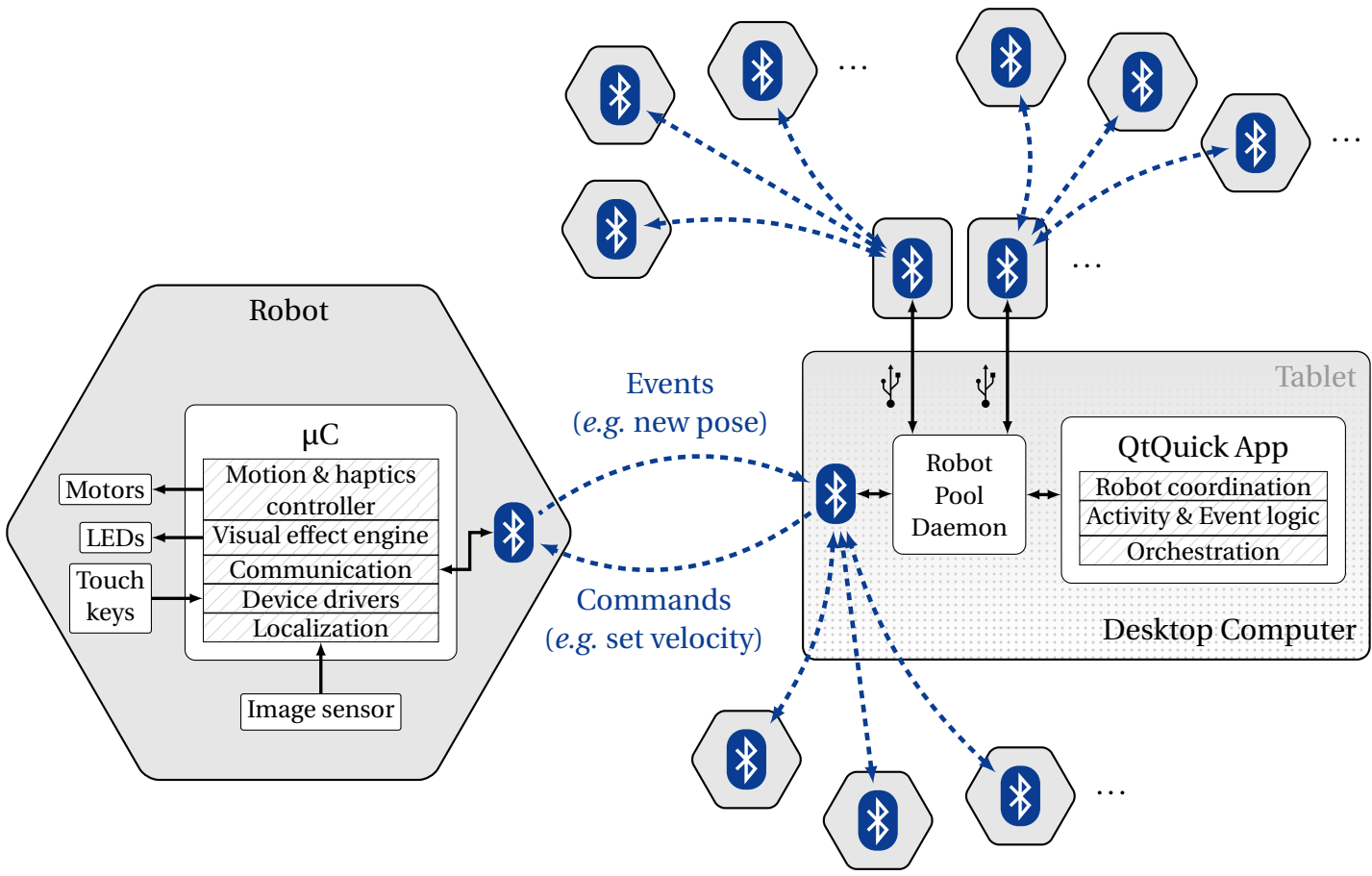


Figure 5.1 – Cellulo version 4 software architecture. As before, diagonally lined boxes represent software components within the robot firmware or within the activity application as part of custom reusable QtQuick plug-ins where possible. Direct communication with the internal Bluetooth adapter from the QtQuick application is replaced by a long-lived daemon that communicates with the internal Bluetooth adapter, as well as external adapters through USB. Bluetooth SPP software sockets are kept open within this daemon that acts as a “pool” of robots from the application’s perspective, which “requests” and “releases” robots from and to this pool.

Bluetooth 2.1 standard defines 79 non-shareable channels where communication through a single point-to-point link hops over these channels in a pseudo-random fashion up to 1600 times a second in order to reduce interference. This implies that in the best case (no collisions and external interference whatsoever), a maximum of 79 Bluetooth links may coexist. Under more realistic conditions, however, it is reasonable to expect more interference and fewer devices to effectively be able to coexist. We successfully tested 16 robots connected over 3 adapters, communicating simultaneously and continuously with the 10 Hz remote controllers running in the activity application. Connection with even more robots may be possible but must be tested. Moreover, we observed that when more than 5 robots are connected to a single adapter and are continuously communicating with 10 Hz, the entire piconet saturates; this was observed to be the case for some adapters (and not necessarily for all of them) and is likely to be a limitation of the specific adapter implementation, which implies that 5 robots connected to one adapter instead of 7 is a more realistic and practical limit to be adopted by the swarm application developer.

Finally, it must be noted that at the time of writing, most Bluetooth stacks found in consumer devices do not support or even enumerate more than one Bluetooth adapter; the operating systems featuring these stacks include Android (up to version 6.0), iOS (up to version 10), Windows (up to version 10) and OS X (up to version 10.12). The only Bluetooth stack capable of operating multiple Bluetooth adapters at the time of writing is BlueZ (version 5.43), which is commonly found in most Linux distributions. This limitation is purely conventional and not due to hardware or software limitations; in other words, the support for multiple adapters in the stack is simply not implemented due to lack of common need. For this reason, all of the experiments presented in this chapter were obligatorily conducted on a laptop running Linux and not on a tablet. This limitation may be lifted in the future through the official implementation of this support within the aforementioned operating systems, or through the introduction of a custom Bluetooth stack built for each of these systems that has this support. A relatively simpler solution would be a custom device with multiple Bluetooth adapter modules, hosting the aforementioned robot pool daemon which communicates with the activity application that resides on the consumer device through *e.g.* USB.

5.2.3 Application Framework Design

Programming Language & Paradigms

At this point, the framework to develop Cellulo applications consists of custom modules that provide the Cellulo robot API, as well as some utility functions and objects, built within the QtQuick platform ([222]) which was initially conceived for rapid GUI development. Within this framework, the developer can either: (i) Write low-level native code in C++ for components that presumably need more efficiency and optimization, performing tasks such as computational algebra or image processing; (ii) Write high-level declarative code in Qt Modeling Language (QML); (iii) Use a combination of both with QML wrappers for the native components.

QML, used for the entirety of our application development, is a primarily declarative (and secondarily procedural), object-oriented programming language with three main constructs:

Objects: These components allow the user to simply declare objects, their behaviors and the behaviors of their attributes without being concerned about their creation, destruction, allocation or concurrent operation. From a MRS perspective, this presents interesting opportunities such as being able to more easily define how robots behave individually, as well as collectively in groups; this idea was previously probed in *e.g.* [223, 224] within the functional programming domain. In our case, an example object is `CelluloBluetooth` which represents the API and connection to one Cellulo robot.

Objects are declared as part of a tree hierarchy where simply declaring an object inside another object will make the outer object the parent of the inner one; this can be used organizationally, as well as functionally for some objects. Creating a new `.qml` file will create a new reusable class of object where it extends the root object declared within the file, inheriting the properties as well. For example, `CelluloRobot` inherits from `CelluloBluetooth` (acquiring all of the regular API) and exposes the velocity of the robot (among other properties), that is not transmitted by the robot but calculated locally, as a readable property. In addition, classes written in C++ can be exported easily as such QML objects if desired.

Properties: These can be understood as variables belonging to objects, whose types range from boolean to integer, floating point, arrays, generic objects, as well as others. Differently from classical variables, these can be *bound* to other properties, formulas depending on other properties and even other declared objects (thus acting as pointers). These bindings are automatically and transparently calculated as the depending properties change; the user may work with these properties as if they were updating instantly, as if writing mathematical equations on paper. For example, `CelluloRobot`'s built-in `macAddr` property can be bound to the output choice of a drop-down box containing many robot addresses. In addition to the built-in and inherited properties, custom properties can be declared while declaring the object itself.

Signals & Slots: Signals can be understood as events belonging to objects, whereas slots can be understood as internal procedures of objects. Each signal has an associated auto-generated slot where inline procedural JavaScript code is written that is run when the event occurs (marking the procedural part of the language); through this mechanism, event-based architectures may be built similarly to [225]. In our case, for example, `CelluloRobot` has a built-in `keyTouched` signal that triggers the `onKeyTouched` slot with an argument called `index` denoting which key was touched. An example standalone slot is `setGoalPose(x, y, theta, v, w)` and similar slots exist for each robot command. Additionally, custom signals describing custom events and custom slots describing custom procedures may be declared while declaring the object itself. Moreover, given signals can be connected to given slots, ensuring that the procedures are run whenever each event occurs.


```

1  import QtQuick 2.2
2  import Cellulo 1.0
3
4  ApplicationWindow{
5      ComboBox{
6          id: macAddrSelector
7          model: ["00:11:22:33:44:55", ..., "66:77:88:99:AA:BB"]
8      }
9      CelluloRobot{
10         macAddr: macAddrSelector.currentText
11         onConnectionStatusChanged: {
12             if(connectionStatus == Cellulo.ConnectionStatusConnected)
13                 setVisualEffect(Cellulo.VisualEffectConstAll, "white");
14         }
15         onPressed: setVisualEffect(Cellulo.VisualEffectConstAll, "green")
16         onKeyReleased: {
17             if(!keys[0] && !keys[1] && !keys[2] && !keys[3] && !keys[4] && !keys[5])
18                 setVisualEffect(Cellulo.VisualEffectConstAll, "white");
19         }
20     }
21 }

```

Listing 5.1 – Declarative “Hello World” program written in QML. Here, the robot (object `CelluloRobot` that has no GUI component within the `ApplicationWindow`) is lit green (via local slot `setVisualEffect(...)`) when any key touch event occurs and is lit white when all keys (exposed via local property `keys []`) are released. The address of the robot (`macAddr`) is effectively always equal (*i.e.* bound) to the chosen address from a drop-down box (the `ComboBox` named `macAddrSelector`) where the opening and closing of the Bluetooth socket is handled transparently in the native Cellulo module as the desired address changes.

Given these language constructs, a sample “Hello World” program that may be written with Cellulo (that does not use the aforementioned robot pool daemon facility) is given in Listing 5.1. With these functionalities, it is straightforward to declaratively describe behaviors of individual robots within the activity through their properties, events and commands in an explicit manner; the Treasure Hunt activity presented in Section 2.6 and the Windfield activities presented in sections 3.5 and 4.4 were rapidly implemented using such descriptions. However, it is not entirely clear how collective behaviors or interaction could be implemented with such descriptions; in theory, using only the functionalities at hand that cater to individual robots, the relationships between all pairs of robots must be explicitly described.

The next step to obtaining rapid swarm application development is to combine these per-pair descriptions into collective interaction descriptions and encapsulate these collective descriptions inside reusable objects. This will result in a “toolbox” of behaviors (described by these reusable objects) that concern either individual robots or many (possibly all) robots collectively. The application developer can choose to reuse components from this toolbox or create custom behaviors by extending the base behavior objects. However, providing the developer a “free-to-use” behavior toolbox introduces the following problem whose solution is certainly not trivial: How should the effects of many behaviors be combined meaningfully?

Physicomimetic Swarm Control

The swarm behavior arbitration problem has an elegant solution in the literature, called *Physicomimetics*, that represents the robots as point-like particles with mass affected by external virtual forces (see [226] for an overview and [227] for a more detailed account, including its applications to classical tasks such as formation control, surveillance and chemical source localization). These virtual forces, the behavior of which is to be designed by the application developer, are not necessarily required to conform to real-world forces that govern the behavior of physical particles, and are thus more flexible. The robots enact the motions of these particles (henceforth called *elements* to emphasize the distinction with real-world particles) and the resulting system is therefore essentially a physics simulation. In other words, for all swarm elements e , the following is simply simulated in discrete time:

$$\vec{a}_e = \frac{1}{m_e} \sum \vec{F}_e, \quad \vec{v}_e = \int \vec{a}_e dt, \quad \vec{X}_e = \int \vec{v}_e dt \quad (5.1)$$

where m_e denotes the virtual mass/moment of inertia of e , \vec{F}_e denotes the virtual forces/torques acting on e , \vec{v}_e denotes the linear/angular velocities of e and \vec{X}_e denotes the pose of e . The aforementioned forces can depend on the world description, the discrete or continuous states of the element, as well as the collective states of other elements. By thinking of robots in terms of these elements and designing the simple forces that affect them, the developer aims to achieve complex, scalable control over the swarm. In the context of this approach, the combination of many dissimilar forces (that can be understood as behaviors) does not necessarily yield optimal results but is well-defined (as simply the vectorial sum of all forces) and straightforward to comprehend and consider during design.

Within the frame of Cellulo, our first contribution is to integrate physicomimetic swarm control to our declarative framework. We achieve this by designing base behavior objects where the actual, usable behaviors that extend these base behaviors may simply declare the parametric *description* of the behavior (*e.g.* the reusable mathematical formula of the virtual force) and implement the procedural *application* of the behavior (*e.g.* accumulate the reciprocal forces between each element pair, calculated by the reusable formula declared earlier, onto the private sum of forces belonging to each element within the pair)². Such behaviors may be developed according to need and redistributed as part of the aforementioned “toolbox” approach. When designing the swarm, the developer may simply declare the desired collective behaviors that affect the swarm within the prospective `Swarm` object, as well as the behaviors that affect individual elements within the relevant prospective `SwarmElement` objects. While declaring these behaviors, their parameters (exported as QML properties) may be declared such that they depend on the properties of other behaviors or other objects outside the swarm, obtaining a truly WYSIWYG description of the swarm.

Our second contribution is the extension of physicomimetic swarm control descriptions

²The graph-based declarative representation proposed in [228] is a promising alternative to this mostly procedural method of defining virtual forces. The exploration of this representation is left as future work.

towards supporting tangible swarm elements. For this, it is fundamental to consider individual elements as well as groups, as a given user will likely grab few swarm elements, possibly as few as one, as a frequent method of interaction with individual elements or with groups. Furthermore, it is essential to expand the design toolbox with other object types than virtual forces, in order to implement a versatile, tangible swarm. Two such object types that we find useful to isolate are *phenomena*, that are used to produce different consequences than virtual forces that modify the motion, and *detectors*, that are used to detect desired user interaction patterns. Using these design considerations, as well as others gathered from empirical observations, we define the set of abstract base objects that capture the various aspects of tangible swarm behavior, given below:

Force: Describes the aforementioned virtual forces that affect the velocity and pose of swarm elements over time. Has **IndividualForce** and **CollectiveForce** variants that affect one selected swarm element and the entire swarm (in a way that likely depends on inter-elemental relationships) respectively. We further define that the resulting actual forces may be *hidden* or *visible* (F^{hidden} and F^{visible}); these equally affect the physics of the elements but one is *haptically visible* when an element is grasped while the other is not, to prevent utility forces from reaching the user. Examples of forces are:

EnforceLinearVelocity (extends **IndividualForce**): Applies (visible) force towards the element traveling direction until a given velocity is reached.

RobotPositionCatchUp (extends **IndividualForce**): Applies (hidden) force towards the associated robot's pose if element falls back for longer than a time interval.

Exclusion (extends **CollectiveForce**): Applies increasingly stronger (visible) repulsive force to each pair of elements below a distance threshold.

PotentialWell (extends **CollectiveForce**): Applies a short-range (visible) repulsive or attractive force to keep each pair of elements at a distance.

Phenomenon: Describes arbitrary phenomena that affect arbitrary properties of swarm elements; it is up to the developer to ensure that these objects operate correctly on the target properties. Has **IndividualPhenomenon** and **CollectivePhenomenon** variants that work similarly to the variants of **Force**. Examples of phenomena are:

ColorOutput (extends **IndividualPhenomenon**): Lights the associated robot's LEDs with a given color and effect on a given event or state.

HeatTransfer (extends **CollectivePhenomenon**): Transfers "heat" (a custom property that must be declared by the developer at each element) between any element pair with different heats; transfer occurs faster with closer distance.

Rule: Describes limits or system laws that cannot be violated; if violation occurs, the **Rule** is tasked to bring back violating values within acceptable ranges. Has **IndividualRule** and **CollectiveRule** variants that work similarly to the variants of **Force**; collective rules can also be understood as global rules if they describe limits that do not depend on the inter-elemental interactions. Examples of rules are:

RobotPositionHardSync (extends *IndividualRule*): Resets the element's pose to the associated robot's pose if robot falls back for longer than a given time interval.

StrictContainer (extends *CollectiveRule*): Describes a zone whose borders cannot be exited with motion.

Calculator: Are utility objects where costly calculations, whose results are shared among other objects, are delegated to prevent repetition. Has *IndividualCalculator* and *CollectiveCalculator* variants that work similarly to the variants of *Force*. Examples of calculators are:

ZoneEntryCalculator (extends *IndividualCalculator*): Calculates the entry vector of an element to a zone (*i.e.* vector from the closest point on the zone border to the element); can be reused to calculate *e.g.* haptic feedback or bouncing.

KineticEnergyCalculator (extends *CollectiveCalculator*): Calculates the total kinetic energy of the swarm for *e.g.* display purposes.

Detector: Describes signal generators or property describers that depend on detected user interaction patterns. Has *IndividualDetector* and *CollectiveDetector* variants that work similarly to the variants of *Force*. Examples of detectors are:

LaunchDetector (extends *IndividualDetector*): Emits a signal when the robot is grabbed, moved and then released, with the mean velocity vector during this motion as parameter.

PinchZoomDetector (extends *CollectiveDetector*): Emits a signal when exactly two robots/elements are grasped and moved, with the two elements as parameters.

Motion: Describes “extra” motions that are overlaid on top of the physics simulation which do not affect it; they are developed as convenience objects to supply the developer with physics-transparent motions that would otherwise break the simulation. Consequently, it is not trivial to design such objects that result in collective motions, since the very mechanism that makes collectivity possible (*i.e.* physics) is neglected. For this reason, only *IndividualMotions* exist, whose examples are:

IndependentOscillation: Oscillates the element with given period and amplitude.

DeltaPoseVelocity: Adds a given pose and/or velocity to the element pose and/or velocity, for *e.g.* rotating the element transparently based on a calculator's output.

Here, the given examples of functional objects consist of those independent of the learning activity or domain (such as *RobotPositionCatchUp*), as well as those that are dependent (such as *HeatTransfer*). Given these, the application developer must either declare existing behaviors or define new ones that do not yet exist. These behaviors are then declared within the swarm declaration, with proper connections among them that ensure the desired swarm operation (as property-property connections or signal-slot connections). When these declarations are made, the swarm and element objects automatically detect these behaviors and their types in order to enumerate them in appropriate sets. Then, the swarm operation is handled transparently to the developer and the user through Algorithm 5.1.

Input: Global swarm update period ΔT , swarm S , all elements $e \in S$

```

1: procedure SWARM UPDATE
2:   repeat
3:     for all elements  $e \in S$  do
4:        $\vec{F}_e^{\text{hidden}} \leftarrow \vec{0}$ ;  $\vec{F}_e^{\text{visible}} \leftarrow \vec{0}$ ;  $\vec{X}_e^{\text{individual}} \leftarrow \vec{0}$ ;  $\vec{V}_e^{\text{individual}} \leftarrow \vec{0}$ 
5:     end for
6:     for all collective calculators  $c^{\text{collective}} \in S$  do
7:       call UPDATE of  $c^{\text{collective}}$  ▷ Does not modify any element
8:     end for
9:     for all collective phenomena  $p^{\text{collective}} \in S$  do
10:      call UPDATE of  $p^{\text{collective}}$  ▷ May modify any custom property in all elements
11:    end for
12:    for all collective forces  $f^{\text{collective}} \in S$  do
13:      call UPDATE of  $f^{\text{collective}}$  ▷ Accumulates to  $\vec{F}_e^{\text{hidden}}$  and/or  $\vec{F}_e^{\text{visible}}$  in all elements
14:    end for
15:    for all elements  $e \in S$  do
16:      for all individual calculators  $c_e^{\text{individual}} \in e$  do
17:        call UPDATE of  $c_e^{\text{individual}}$  ▷ Does not modify any property of  $e$ 
18:      end for
19:      for all individual phenomena  $p_e^{\text{individual}} \in e$  do
20:        call UPDATE of  $p_e^{\text{individual}}$  ▷ May modify any custom property in  $e$ 
21:      end for
22:      for all individual forces  $f_e^{\text{individual}} \in e$  do
23:        call UPDATE of  $f_e^{\text{individual}}$  ▷ Accumulates to  $\vec{F}_e^{\text{hidden}}$  and/or  $\vec{F}_e^{\text{visible}}$ 
24:      end for
25:      for all individual motions  $m_e^{\text{individual}} \in e$  do
26:        call UPDATE of  $m_e^{\text{individual}}$  ▷ Accumulates to  $\vec{X}_e^{\text{individual}}$  and/or  $\vec{V}_e^{\text{individual}}$ 
27:      end for
28:    end for
29:  every  $\Delta T$  milliseconds
30: end procedure

31: on event NEW ROBOT POSE AVAILABLE( $\Delta t$ ) of  $e$ 
32:   if state $_e$  is “Moving” then
33:      $\vec{V}_e \leftarrow \vec{V}_e + (\vec{F}_e^{\text{hidden}} + \vec{F}_e^{\text{visible}})\Delta t$  ▷ Mass  $m$  in  $\vec{a} = \vec{F}/m$  omitted for practicality
34:      $\vec{X}_e \leftarrow \vec{X}_e + \vec{V}_e\Delta t$ 
35:     for all collective rules  $r^{\text{collective}} \in S$  do
36:       call UNVIOLATE( $e$ ) of  $r^{\text{collective}}$  ▷ Modifies  $\vec{V}_e$  and/or  $\vec{X}_e$  if they violate the rule
37:     end for
38:     for all individual rules  $r_e^{\text{individual}} \in e$  do
39:       call UNVIOLATE of  $r_e^{\text{individual}}$  ▷ Modifies  $\vec{V}_e$  and/or  $\vec{X}_e$  if they violate the rule
40:     end for
41:     call SET GOAL POSE & VELOCITY( $\vec{X}_e + \vec{X}_e^{\text{INDIVIDUAL}}$ ,  $\vec{V}_e + \vec{V}_e^{\text{INDIVIDUAL}}$ ) of robot $_e$ 
42:   else if state $_e$  is “Moved” then
43:      $\vec{V}_e \leftarrow \vec{V}_{\text{robot}_e}$ 
44:      $\vec{X}_e \leftarrow \vec{X}_{\text{robot}_e}$ 
45:     call SET GOAL FORCE & TORQUE( $\vec{F}_e^{\text{VISIBLE}}$ ) of robot $_e$ 
46:   end if
47: end event
    
```

Algorithm 5.1 – Physicomimetic swarm control algorithm. Physics update is done per-element at every new robot pose (on NEW ROBOT POSE AVAILABLE($e, \Delta t$)) to better synchronize with the robot. Forces and phenomena that affect these swarm elements are updated regularly (in SWARM UPDATE), with preferably lower period ΔT than the per-element physics update.

In this section, we presented our software framework that lets us rapidly program tangible swarms. Our approach brings together three powerful programming techniques, namely *declarative programming*, *event-based control* and *physicomimetics*, the combination of which, in our opinion, will speed up the development and boost the legibility, succinctness and reusability of code that describe behaviors of swarms, especially novel tangible ones. In Listing 5.2, we provide such an example program that implements an orthogonal (*i.e.* square) grid that can be freely manipulated (*i.e.* moved and rotated), resized (*i.e.* inter-elemental distance changed) and restructured (*i.e.* connections of elements broken/remade and elements added/removed during runtime) through naturally manipulating one or many elements. Here, `CelluloRobotPoolClient` transparently provides access to many `CelluloRobots` that stay connected to the robot pool daemon. Another GUI tool is used briefly before the actual application to set up the connections between the daemon and actual robots.

Such interactions are by definition based on a particle physics simulation where changes to the system do not instantaneously result in motion; elements move from one place to another through acceleration and deceleration, spreading motions over time. In addition, the force-based description of behaviors may result in less efficient executions compared to near-optimal executions, achieving the requested outcomes after possibly spending more time or energy. The result is that the user must adjust to this slower, inexact but more natural interaction in order to convey desired commands to the swarm resulting in correct executions. If such executions are not acceptable in a given application, the developer may choose to leave out physicomimetics in order to develop declarative and/or event-based behaviors (through our aforementioned robot API that provides objects such as `CelluloRobot` that can explicitly control every aspect of a given Cellulo robot) that operate on strict definitions. Finally, through QML's tight integration with JavaScript, any amount of procedural code can be integrated, if desired, into the declarative framework to obtain a traditional robot control implementation. This integration can reach up to 100% through an implementation such as `ApplicationWindow{ Component.onCompleted: { /* JavaScript code */ }}` that lets the given procedural code run once at application launch where normally declarative QML objects may be dynamically created and used as JavaScript objects.

While we believe that this framework is useful for the aforementioned style of swarm development, it has a number of shortcomings. We acknowledge that the current state of the framework does not easily allow the definition of heterogeneous sub-groups within the swarm, nor does it provide a clear mechanism to dynamically create these groups, to transfer elements from one to the other and to merge or split them. This could be solved by another object called `SwarmGroup` that exists between `Swarm` and `SwarmElement` and that defines a concept of “membership” for `SwarmElements`, which is left as future work. Furthermore, it may not be straightforward for robot application developers to think in terms of physics-based behaviors instead of the usual method of listing a sequence of commands given to each robot. What is more crucial is that physicomimetics is not necessarily universal; some behaviors may require such sequences of commands given to individual robots. In this case, the developers may revert to traditional techniques, still easily within their reach using our framework.

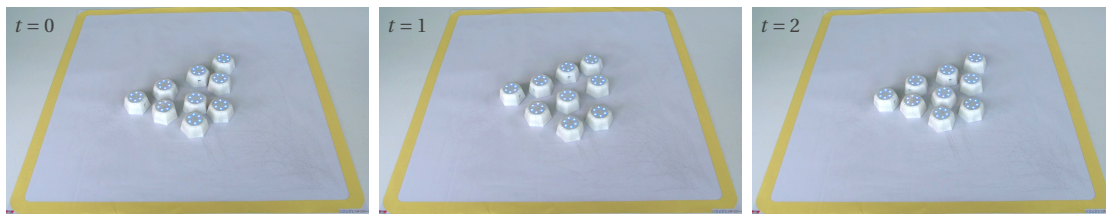
```

1  CelluloRobotPoolClient{ id: client } //Interface to the robot pool daemon in Figure 5.1
2
3  Swarm{ //Implements SWARM UPDATE from Algorithm 5.1
4      property real gridSize: 100 //Inter-elemental distance, initially 100 mm
5
6      RepeaterList{ //Extends the built-in Repeater, expects count and provides index
7          count: client.robots.length //Number of elements, as many as robots
8
9          SwarmElement{ //Implements NEW ROBOT POSE AVAILABLE(e,Δt) from Algorithm 5.1
10             id: element
11             robot: client.robots[index] //Associated robot to this element
12
13             /* Individual phenomena */
14             ConstantColorOutput{ activeState: "Moving"; color: "#808080" }
15             ConstantColorOutput{ activeState: "Moved"; color: "#80FF80" }
16
17             /* Individual detectors */
18             GrabDetector{ //Grab/release detector
19                 onGrabbed: element.setState("Moved")
20                 onReleased: element.setState("Moving")
21             }
22         }
23     }
24
25     /* Collective (possibly global) rules */
26     MaxLinearVelocity{ maxVelocity: 185 } //Hard limit in mm/s
27     MaxAngularVelocity{ maxVelocity: 7.5 } //Hard limit in rad/s
28     StrictContainer{ //Container borders, strictly uncrossable as long as on paper
29         paper: CelluloZones.loadZone(":/containerPaper.json") //Border of whole paper
30         zone: CelluloZones.loadZone(":/containerZone.json") //Actual usable zone
31     }
32
33     /* Collective detectors */
34     PinchZoomDetector{ //Detects when exactly two elements are grasped and moved around
35         onPinchZoomed: { //Has arguments element1 and element2 denoting grasped elements
36             if(priv_connectedCalculator.isConnected(element1, element2))
37                 gridSize = element1.position.minus(element2.position).length();
38         }
39     }
40
41     /* Collective calculators */
42     ConnectedCalculator{ //Whether each pair is connected, i.e. closer than maxDistance
43         id: priv_connectedCalculator
44         maxDistance: gridSize*(Math.sqrt(2) + 1)/2
45     }
46
47     /* Collective forces */
48     GlobalViscousDamping{ c: 3.0 } //Damping that prevents excessive movement
49     Exclusion{ separation: gridSize } //Repulsion keeping all elements apart
50     AttractionFirstDegree{ //Attraction pulling only connected elements together
51         separation: gridSize
52         connectedCalculator: priv_connectedCalculator
53     }
54     ExclusionSecondDegree{ //Repulsion between elements connected to the same element
55         separation: gridSize*Math.sqrt(2) //Will create square grid with enough elements
56         connectedCalculator: priv_connectedCalculator
57     }
58 }

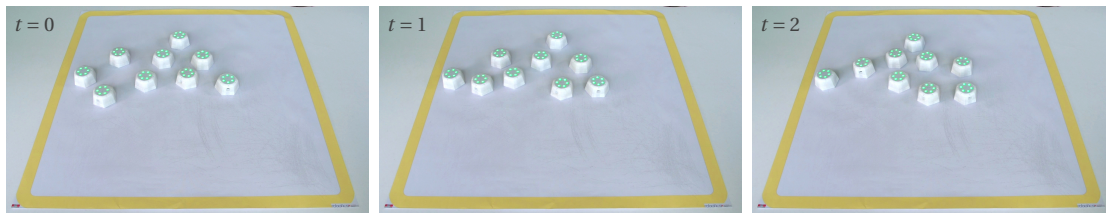
```

Listing 5.2 – Declarative physicomimetic swarm program that implements an orthogonal “grid” of robots (irrelevant code omitted). Manipulating one robot tangibly displaces the grid while manipulating two connected robots (“pinch-zoom”) rotates, displaces and resizes the grid.

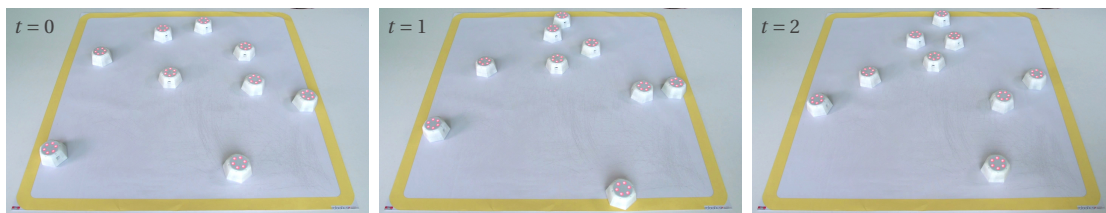
Chapter 5. Phase IV - Building Tangible Swarms



(a) *Solid* matter in high temperature, just before melting. Without user interaction, the crystal structure is preserved, but can be broken and reformed by strong enough tangible manipulation. With weak enough manipulation, particles(s) may be manipulated to move the entire crystal. Particles oscillate in their place; amplitude and frequency, as well as inter-particle distance, are higher compared to solids in lower temperatures. Forces that keep these structures together, as well as the force that oscillates the particles, can be haptically felt when grasping the robots.



(b) *Liquid* matter in high temperature, just before evaporating. Without user interaction, the overall “blob” structure is not preserved; the particles flow around each other without stopping where the speed is faster compared to lower temperature liquids. Like solids, blobs can be tangibly divided and combined. With weak enough (weaker than required for solids) manipulation, particle(s) may be manipulated to move the entire blob. Lone particles oscillate in place, similar to solids.



(c) *Gaseous* matter in high temperature. Particles “fly around” without stopping to fill the volume of the container over time; velocity is higher compared to gases in lower temperatures. Particles bounce off of each other and container borders. Even if a group of particles are tangibly brought together (where the repulsive force can be haptically felt), they do not stay together as a group when released.

Figure 5.2 – Particles in Matter - The behaviors of solid, liquid and gas states, denoted by blue, green and red colored robots respectively. Time flows from left to right.

5.2.4 Learning Activity Design - Particles in Matter

Using our declarative physicomimetic software framework, we proceed in this section to design a learning activity that benefits from swarm behaviors of our tangible robots, that also highlights the capabilities of our framework. To achieve this, strong topic candidates are ones where the behaviors and interactions of many similar elements are prevalently taught. Such topics are commonly found in physics and chemistry where the activity relies on simulating these behaviors and interactions; examples of such activities are:

- Building molecules with atoms, bonding
- Molecule polarity and behaviors of polar molecule collections
- Charged particles in electric and magnetic fields
- Basics of electronics and circuits
- Particle-like behaviors of light
- Micro-structures of solutions
- Particles in different states of matter

Among these topics, we opted to develop an activity to demonstrate the behaviors of particles in different states of matter, hereafter called *Particles in Matter*, by virtue of its richer learning content compared to other topics. Furthermore, for practical reasons (such as the age group of available participants for experiments), we limit our activity to provide an entry-level exposure to the micro-structures of three states of matter, *i.e.* solids, liquids and gases, where the various aspects of their behaviors are clearly conveyed through easily understandable (sometimes exaggerated) abstractions without regard to numerical or physical accuracy. Therefore, mathematical formulas, numerical values with units and the availability of calculation tasks based on these are not included in the design of our activity.

Given its context and philosophy, ours is a similar endeavor to [229] where macroscopic and microscopic behaviors and representations of objects in chemistry are bridged through engaging interactive computer simulations³. Similarly, the added values of our robot-enhanced learning activities include *making invisible visible*, as well as *making intangible tangible*, which is not found in computer simulations. On the other hand, simulations done solely in software are potentially more flexible, possessing the opportunity to present any number of elements represented and enhanced by any given graphic, compared to using robots with unchanging hardware, such as ours.

To design the actual content of our activity, we followed a rapid iterative design process where we collaborated with a middle-high school physics teacher to obtain an activity that can be used as part of a standard lesson. In the first iteration, we began by implementing and demonstrating a solid state simulation (a simplified version of Figure 5.2a without the dynamic reformation of the crystal structure) to the teacher as a means of communicating the abilities of our robotic platform and the design space of our activities. The following set of desired features resulted from the discussions with the teacher:

- Particles may be found in solid, liquid or gaseous state, whose behaviors reflect the high-level attributes of real materials in those states and are shown in Figure 5.2.
- Particles may transition smoothly from solid to liquid, as well as from liquid to gas, through increase in energy, and thus can be found in those intermediate states. This increase may be provided by the tangible “shake” interaction, seen in Figure 5.3.
- Particles can be moved around, even through kidnapping; contacting particles will transfer their energy (*i.e.* heat) in real time, as seen in Figure 5.4.

³Within this family of simulations, [230] presents the simulation of states of matter.

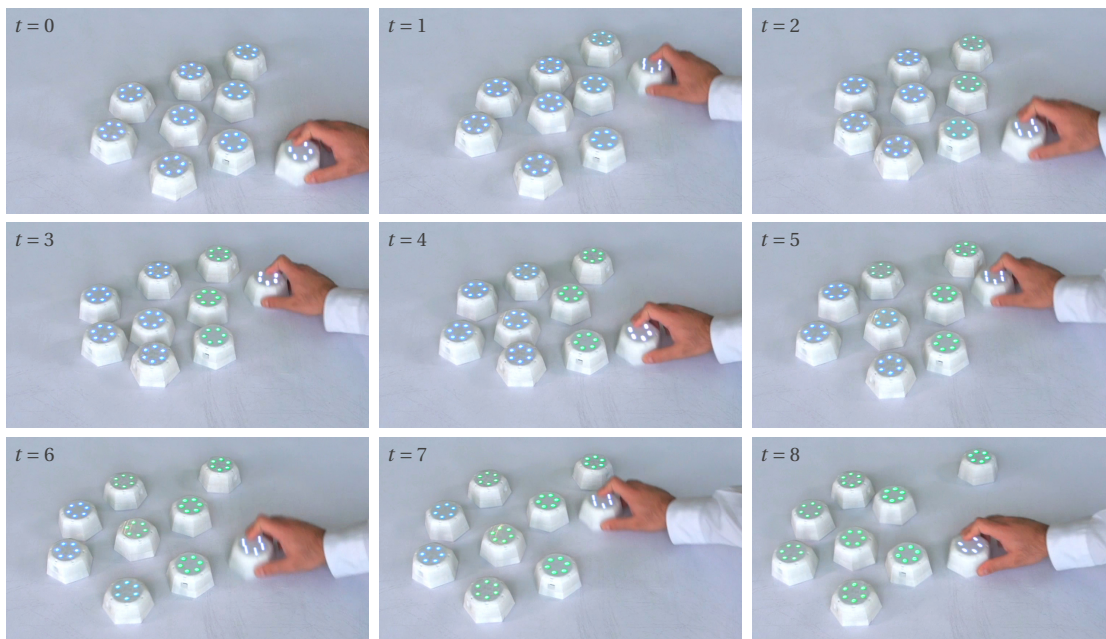


Figure 5.3 – Particles in Matter - Tangible “shake” interaction giving grasped particles oscillatory energy in the form of heat, which then dissipates throughout the solid (denoted by blue color) to raise the temperature and melt the material into a liquid (denoted by green color).

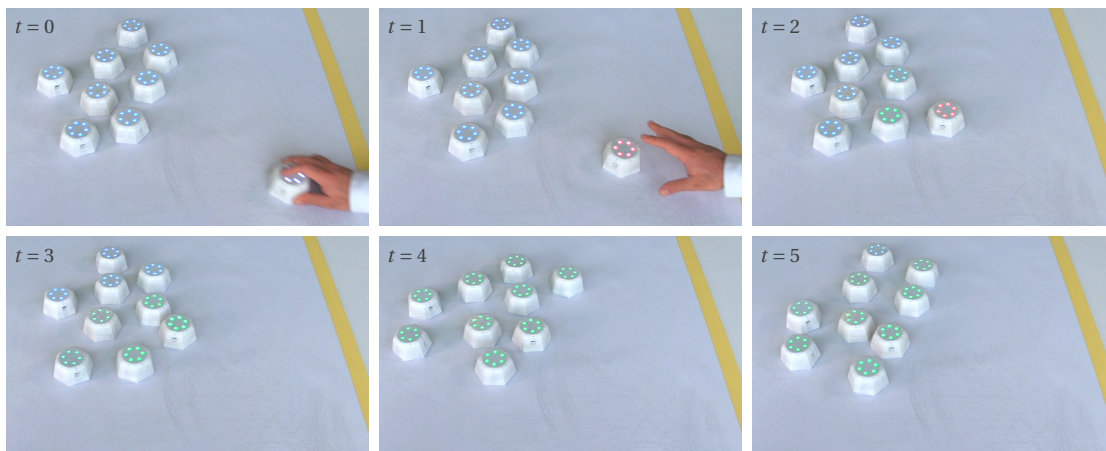


Figure 5.4 – Particles in Matter - Tangible “launch” interaction giving a grasped high-temperature gas particle (in red color) velocity. Upon contact with the high-temperature solid particles (in blue color), heat transfer occurs in real time from high heat to low heat. Finally, the solid particles melt while the single gas particle condenses to reach equilibrium in the liquid state (in green color).

With these features implemented, as the second iteration, a pilot experiment was carried out with 6 learners (in groups of 3, each group spending about 10 minutes with the activity) in order to validate the functionality of the existing features and observe what other features may be missing. For this pilot, a manual switch that enabled a global cooling effect was built

and given to the control of the teacher, since the particles tend to saturate with energy over time in the absence of any other heat loss mechanism. The group of learners were observed to quickly reach this saturation, going through solid, liquid and reaching a high-temperature gas, at which point the switch was enabled until the particles dropped down to the lowest energy state (the learners were explained that the container's cooler functionalities were enabled for the time being), in order to let the group interact with the lower energy states again.

Instead of this ad-hoc mechanism, it was decided to provide the learners an additional A4 sheet marked with "Cooler", which provides heat loss for all particles placed within. This choice was made to let learners choose which group of particles to cool at their discretion. Through this mechanism, the teacher was enabled to encourage the learners to tangibly conduct heat transfer experiments between particle groups in different states or possessing different levels of energy. Additionally, a mechanism was implemented that synchronizes the virtual element to the robot in case the robot falls behind, in the form of an individual rule and an individual force. This brought the activity closer to being entirely physical and tangible from the learner's and teacher's perspective, *i.e.* where the underlying hidden virtual simulation is indistinguishable from its robotic enactment. Finally, some colors and parameter values were tweaked for better legibility and performance.

The resulting activity was used for the experiments presented in the following sections within this chapter, whose main goal is to perform its real-world validation. These experiments, along with their discussions, are also collectively regarded as the third design iteration, whose resulting improvements to the activity are left as future work. For reference and completeness, the source code of the activity at this stage is provided in Appendix B.

5.3 Quantitative Validation

5.3.1 Overview

In this section, we present the first study conducted as an initial validation to our swarm-enhanced learning activity, in the form of an "in-the-wild" experiment. Before introducing our activity to the classroom through the teacher, we wish to obtain information on which aspects of our selected topic can be better taught by our activity, and how learning is actually affected by interacting with the tangible swarm. Our intention is to observe these effects quantitatively on a large number of learners in order to statistically confirm them, hence the examination will be more controlled even though the study is conducted in an authentic context.

5.3.2 Activity & Test Design

The learning activity to be used within this study is designed as an initial exposure to the basic states of matter where the interaction time is bounded to around 10 minutes. It was designed to accommodate a team of 2-3 learners with 6-7 robots where the learners were encouraged to

Chapter 5. Phase IV - Building Tangible Swarms

Question	Available answers	Type
Do <i>solids</i> have <i>fixed form</i> ?	(a) Yes (b) No (c) I don't know	Pick one
Do <i>liquids</i> have <i>fixed form</i> ?	(a) Yes (b) No (c) I don't know	Pick one
Do <i>gases</i> have <i>fixed form</i> ?	(a) Yes (b) No (c) I don't know	Pick one
Are <i>solids</i> <i>compressible</i> ?	(a) Yes (b) No (c) I don't know	Pick one
Are <i>liquids</i> <i>compressible</i> ?	(a) Yes (b) No (c) I don't know	Pick one
Are <i>gases</i> <i>compressible</i> ?	(a) Yes (b) No (c) I don't know	Pick one
Which state has the <i>most energy</i> ? The <i>least energy</i> ?	(a) Solid > Liquid > Gas (b) Solid > Gas > Liquid (c) Liquid > Solid > Gas (d) Liquid > Gas > Solid (e) Gas > Liquid > Solid (f) Gas > Solid > Liquid (g) I don't know	Pick one
Which state has the <i>strongest bonding</i> ? The <i>weakest bonding</i> ?	(a) Solid > Liquid > Gas (b) Solid > Gas > Liquid (c) Liquid > Solid > Gas (d) Liquid > Gas > Solid (e) Gas > Liquid > Solid (f) Gas > Solid > Liquid (g) I don't know	Pick one
Which group of particles have the <i>highest temperature</i> ?	(a) Figure 5.5b (b) Figure 5.5e (c) Figure 5.5a (d) Figure 5.5f (e) Figure 5.5c (f) Figure 5.5d (g) I don't know	Pick one
Which group of particles have the <i>lowest temperature</i> ?	(a) Figure 5.5b (b) Figure 5.5e (c) Figure 5.5a (d) Figure 5.5f (e) Figure 5.5c (f) Figure 5.5d (g) I don't know	Pick one
Which group of particles are a <i>solid</i> ?	(a) Figure 5.5f (b) Figure 5.5d (c) Figure 5.5b	Pick one or more
Which group of particles are a <i>liquid</i> ?	(a) Figure 5.5f (b) Figure 5.5d (c) Figure 5.5b	Pick one or more
Which group of particles are a <i>gas</i> ?	(a) Figure 5.5f (b) Figure 5.5d (c) Figure 5.5b	Pick one or more
Which state has the <i>most ordered</i> particles?	(a) Solid (b) Liquid (c) Gas (d) I don't know	Pick one
What can happen if the given material [Figure 5.5a] is <i>heated</i> ?	(a) Some particles can eventually evaporate and escape (b) Material can melt (c) Material can freeze (d) Material can condense (e) Particles can just accelerate without changing state (f) Particles themselves can get bigger	Pick one or more

Table 5.1 – Particles in Matter pre-test & post-test questions. A maximum of 10 minutes were allowed for each test. Correct answers (worth +1 marks), incorrect answers (worth –1 marks) and neutral answers (worth 0 marks) are denoted with green, red and gray respectively. Animations in the real tests are marked here with “Figure *”. Answers consisting of animations that are to be given to the “highest/lowest temperature” questions are in the exact order given above, *i.e.* shuffled, so that they are not ordered in terms of increasing or decreasing energy.

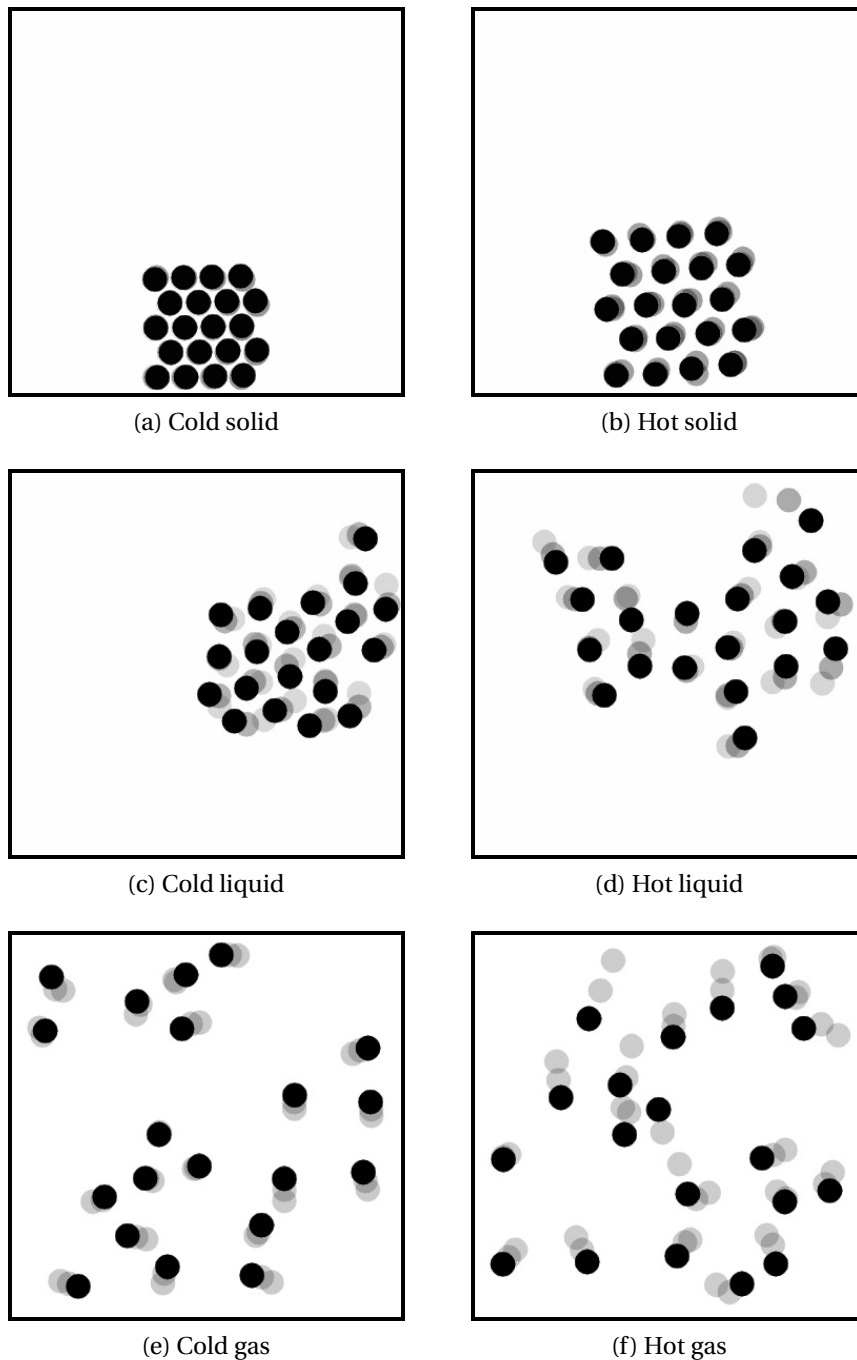


Figure 5.5 – Animations shown in the pre/post-test of the quantitative Particles in Matter study, generated using a modified version of [230]. See Table 5.1 for the questions employing these animations. Motion blur effects are provided here to give the impression of how the actual animations appear and move. Colors used on the robots to code the three states are deliberately avoided to prevent color matching instead of behavior matching. One cold and one hot version of each state is included to test energy ranking within states as well as across states. Within each state, hotter particles move faster compared to the colder ones.

discuss among themselves as to what behaviors and phenomena were being observed, as well as to argue which actions caused those results. A desktop computer (not related to the activity from the learners' perspectives) was used to host the application software.

Resulting from the discussions held with the teacher during the previous iterations, the pedagogical scenario was chosen as a semi-guided self-discovery sequence. In other words, the learners are pushed towards the path of discovering the system laws and particle behaviors through their own interactions with the swarm. For this reason, the experimenter only introduced the kinds of interactions that the learners may want to test, asked questions that are beneficial to be answered, and otherwise interacted very little with the learners. Again, resulting from the discussions held with the teacher, the association of the swarm states (color coded with blue, green and red) with the actual labeled states of matter, *i.e.* solid, liquid and gas, was not readily made; after interacting with all swarm states, the learners were encouraged to match these states to real-world solid, liquid and gas states. It was further introduced that the particles gain the energy that is given by the motion of their arms during the shake interaction. However, the facts that this energy is transferred between close particles, that the particles change state through the increase in this energy and that states are distinctly ordered in terms of increasing energy, were left to be discovered independently.

Due to the brief nature of the experiment and the time needed for tests, each learner was subjected to a short pre-test and a post-test exactly before and after interacting with the swarm. These tests consisted of the same set of multiple-choice questions given in Table 5.1, for which a maximum of 10 minutes were allowed each. To better convey questions relying on the behaviors of particles, the animations shown in Figure 5.5, which depict the behaviors of each state in low and high energy, were prepared and displayed within the questions where appropriate. To enable this moving display, the learners were subjected to the tests on tablets, which also facilitated the automated collection of results.

5.3.3 Participants & Data Collection

86 learners, 11.6 ± 0.725 years old and without formal pre-knowledge about the topic, experienced the activity within the context of another edition of *Journée des Classes* (collective school excursion explained in Section 2.6.3 where we hosted *Treasure Hunt* in a previous edition). The participants were treated in teams of 2-3 where two independent teams worked in parallel (and up to 14 robots co-existed) at a time in the same room. This way, 4-6 learners were accommodated in total at a time, which are referred to as groups. 31 such teams within 16 such groups (one group consisting of only one team) were treated where test results were gathered collectively for each group (and not for each team due to the organization of the event). The teams interacted with the swarm for 9.08 ± 1.18 minutes, during which the poses of all robots, states of the swarm, as well as all user interaction events (*e.g.* kidnaps, grasps) were recorded using only the desktop computer running the application software and the robots. As in the studies presented in the previous chapters, no other device was added to this

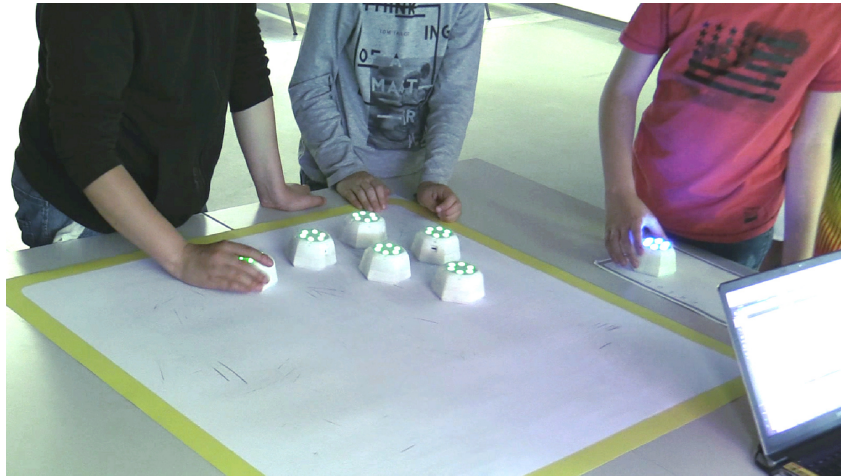


Figure 5.6 – Scene from quantitative Particles in Matter study. Team of 3 learners trying out the tangible placement interaction in order to put one particle in the cooler (A4 sheet on the right), which they will then place back in the main container next to the higher-energy particles to run a high-level heat transfer experiment.

lightweight setup such as cameras or microphones. For this reason, when swarm interaction is concerned, we extracted data on the team level (and compared with the test results gathered on the group level) and did not discern precisely which learner performed which interaction. A sample scene from the experiment can be seen in Figure 5.6.

5.3.4 Swarm Interaction Metrics

In the emerging field of HSI, interaction metrics are not yet well known. The very few efforts so far in the literature to define such metrics are mission-centric, and naturally focus on results such as task performance. Two such works are [231, 232] that both consider bio-inspired swarms and metrics. In our case, we are interested in how swarm interaction affects learning, as opposed to the performance on some task that the swarm accomplishes. For this, we focus on how much the learners tangibly interact with the swarm, and how much they are exposed to the relevant phenomena that occur within the swarm, through the following metrics (where ▼ denotes lower level metrics related to usability and ▲ denotes higher level metrics related to the specific learning context of the activity):

- ▼ *Number of grabs*: Total number of times when any particle is grabbed; a higher number of particle grabs implies that the group initiated more tangible interactions.
- ▼ *Total grab time*: Total time interval of grabbing particles; longer particle grabs implies that the group spent more time on tangible interactions.
- ▼ *Number of returns to paper*: Total number of times when any robot was returned to paper, including the times when a container change does not occur; a higher number of returns to paper implies that the group intentionally moved particles from one place to another more within the activity, potentially leading to more experimentation involving

multiple particles, such as dividing and joining collections.

- ▲ *Number of container changes*: Total number of times when any particle is placed in the cooler from the main container or vice versa; a higher number of container changes implies that the group experimented using the cooler more and was possibly exposed more to the heat transfer mechanism.
- ▲ *Number of state changes*: Total number of times when any particle changes state; a higher number of state changes implies that the group was exposed more to the state transition mechanism, without implying any tangible interaction necessary to do so.

Most of these metrics carry similar connotations to operator intervention measures within classical HSI; in other words, they measure how much the learners decided to initiate modifications on certain aspects of the swarm instead of only observing how they behave or simply not paying attention. In our case, these interventions are tangible by design and are to be made with the intentions of discovering the phenomena within states of matter, of which the learners are given leads. By exploring the effect of these metrics (with the said implications on learners' discovery) on learning, we expect to gain an insight as to whether tangible interaction with the swarm may lead to more overall learning gain within our particular application scenario.

5.3.5 Results & Discussion

Performance on Individual Aspects of the Subject

Initially, we examine which aspects of the states of matter were prevalently learned and which aspects were misunderstood, by measuring the improvement/deterioration from pre-test to post-test scores on individual questions across all learners. The results, given in Figure 5.7, show that in most aspects (14 out of 20), there were more participants who gained learning (cleared wrong knowledge or gained correct knowledge) than those who lost learning (cleared correct knowledge or gained wrong knowledge).

First aspect to be clearly misunderstood more is the recognition of solids from the behaviors of particles. Here, we observe that 76 out of 86 learners were able to correctly identify the solid state before the activity, and therefore a pre-ceiling effect was present where there was no room for improvement for most participants (*i.e.* a misconception was more likely when all participants are considered). This is not the case for liquids and gases, where liquids were confused more with gases and vice versa, before the activity.

Second notable aspect is seen in identifying whether a heated solid can perform certain state transitions. Here, it was observed that a considerable portion of the learners did not exactly know the real-world labels of these transitions (*e.g.* "evaporation" and "condensation", none of which were introduced during the activity), indicated by their questions to the experimenters during pre-test and post-test. In a similar line, the "compressibility" label was not well known (again, not introduced during the activity and was questioned during pre-test and post-test) and the corresponding questions yielded poor results.

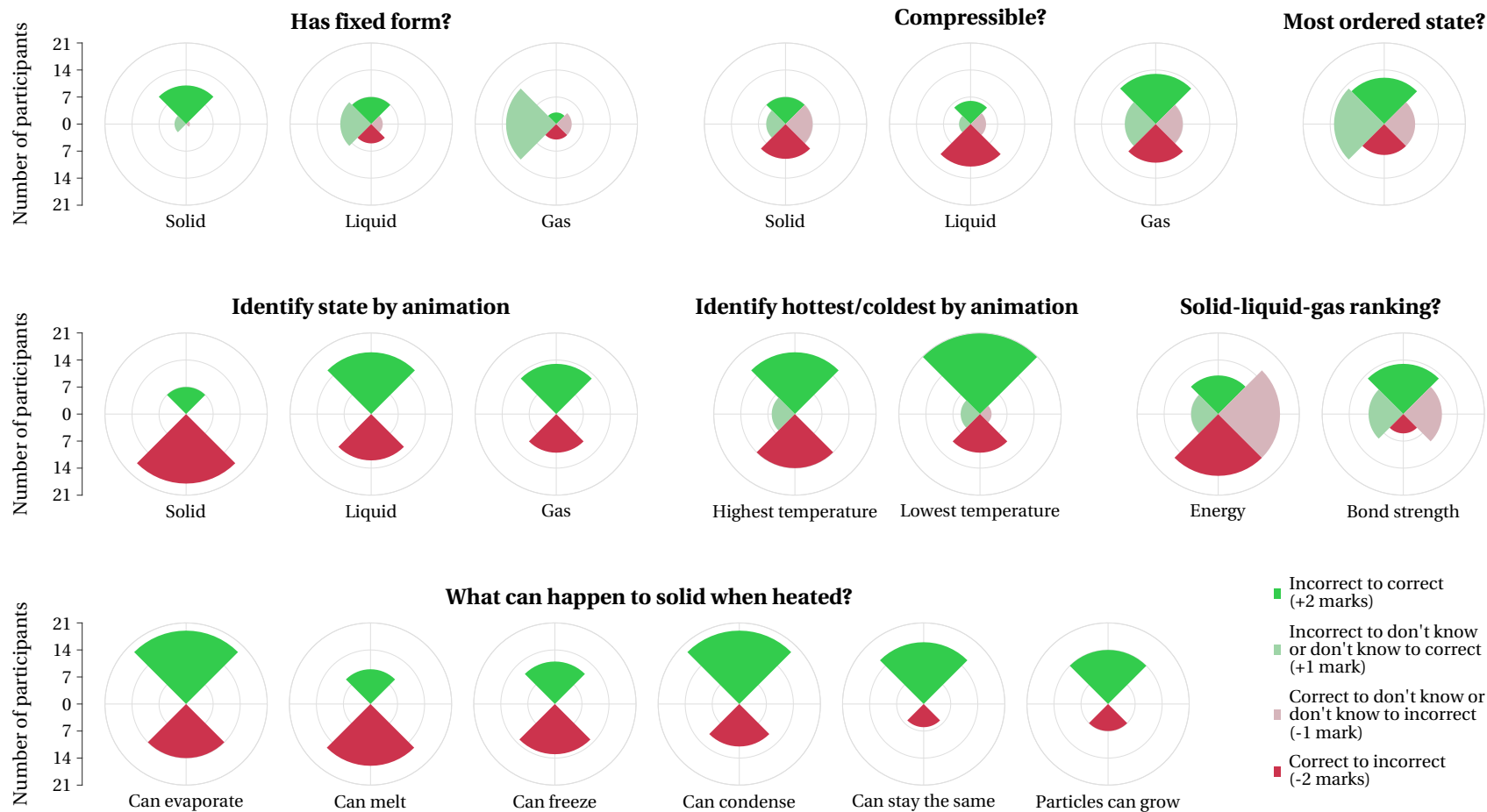


Figure 5.7 – Learning gain/loss from pre-test to post-test in the quantitative Particles in Matter study. Each circle denotes one aspect of the subject that can be learned, see Table 5.1 for the questions probing these. The radii of the red wedges denote the number of participants who lost correct knowledge or gained incorrect knowledge, whereas the radii of the green wedges denote the number of participants who gained correct knowledge or cleared an incorrect knowledge. Participants who did not gain or lose knowledge are omitted in each unit of knowledge.

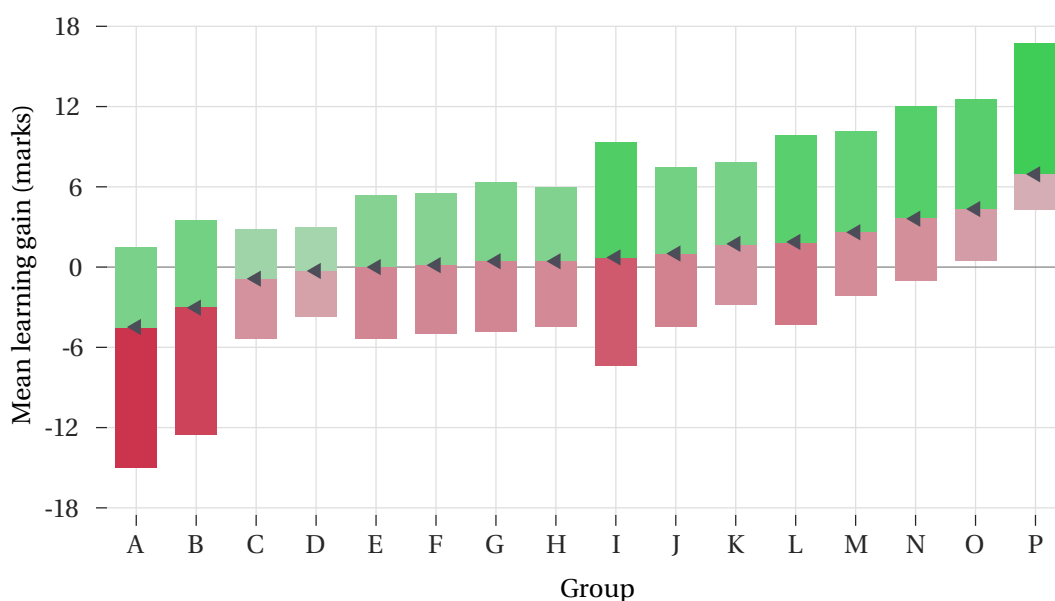


Figure 5.8 – Mean positive learning gains (*i.e.* improvements, given in green), mean negative learning gains (*i.e.* built misconceptions, given in red) and mean net learning gain (*i.e.* sum of mean improvements and mean misconceptions, given with triangular markers) across all groups in the quantitative Particles in Matter study.

Finally, a striking number of participants were observed to build misconceptions in the energy ranking of states. For this question, the answers from most of the participants who misconceived were “Solid > Liquid > Gas” which is the exact opposite of the correct answer. This implies that in the learners’ cognition, the label “energy” may have been linked to a notion of the “*needing energy* to break its bonds apart” variety, instead of the correct notion of “having stored energy”. While the exact nature of this misconception needs more exploration, it is certain that extra care must be taken in this and the other aforementioned aspects of this subject when using a swarm-enhanced activity such as ours.

Overall Performance

Next, we examine the per-learner and per-group learning, in order to evaluate the overall success of our activity in producing learning gain and also to gain an impression of the amount of negative learning produced. In Figure 5.8, the positive, negative and net learning obtained by each group (normalized by the number of learners in groups) is given. It is evident that there is no group where only positive or only negative learning was present; all groups learn and misunderstand some amount of knowledge. However, the 4 groups that show negative net learning (groups A, B, C and D) seem to belong to two categories: Either they have low positive and low negative learning (groups C and D, net learning close to zero), or they have moderate positive learning and an excessive amount of negative learning (groups A and B). These may imply that the groups belonging to the first category interact less with the activity

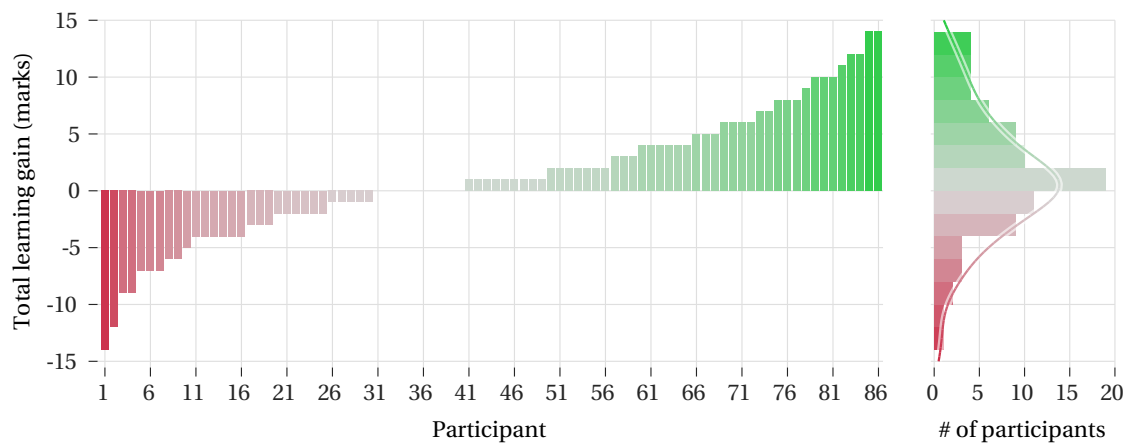


Figure 5.9 – Net learning across all participants in the quantitative Particles in Matter study, on the left, where positive and negative learning are denoted with green and red respectively. The histogram and estimated distribution of learning across all participants is given on the right, showing a slight but clear skew towards the positive end. The mean learning across all participants is measured to be significantly larger than zero (one-sample $t(85) = 2.00$, $p = 0.0489$, $CI_{95\%} = [0.00607, 2.39]$).

or that they are uninterested so that they gain neither positive nor negative input, and that the groups belonging to the second category simply need more teacher intervention to clear the possible buildup of misconceptions during the activity. Naturally, the verification of these claims requires further research.

When we abandon groups and examine the learning across all individual learners (given in Figure 5.9), we observe the distribution of net learning where a skew towards the positive end is present. However, more importantly, the distribution clearly resembles a bell-shaped distribution where most participants are close to the mean, which is itself close to zero. Ideally, even if the distribution is bell-shaped, it would be desirable to have the mean larger than zero, so that there is little overall negative learning. The current performance implies too short activity duration, too little guidance, the lack of a necessary teaching tool or simply unideal testing conditions. More discussion on this issue is provided at the end of this section.

Effect of Swarm Interaction on Learning

Lastly, we examine the effect of swarm interaction on learning with the aforementioned metrics where we examined the effect on negative, positive and net learning. No significant relationship was found between learning and *number of state changes*, *number of grabs* and *total grab time*, further research may conclude whether these metrics are irrelevant to the learning of our subject or not; it may be revealed that inexact measures such as the number of grasps, or observation-oriented measures such as the number of state changes, do not imply useful interaction with the meaningful phenomena available in the activity.

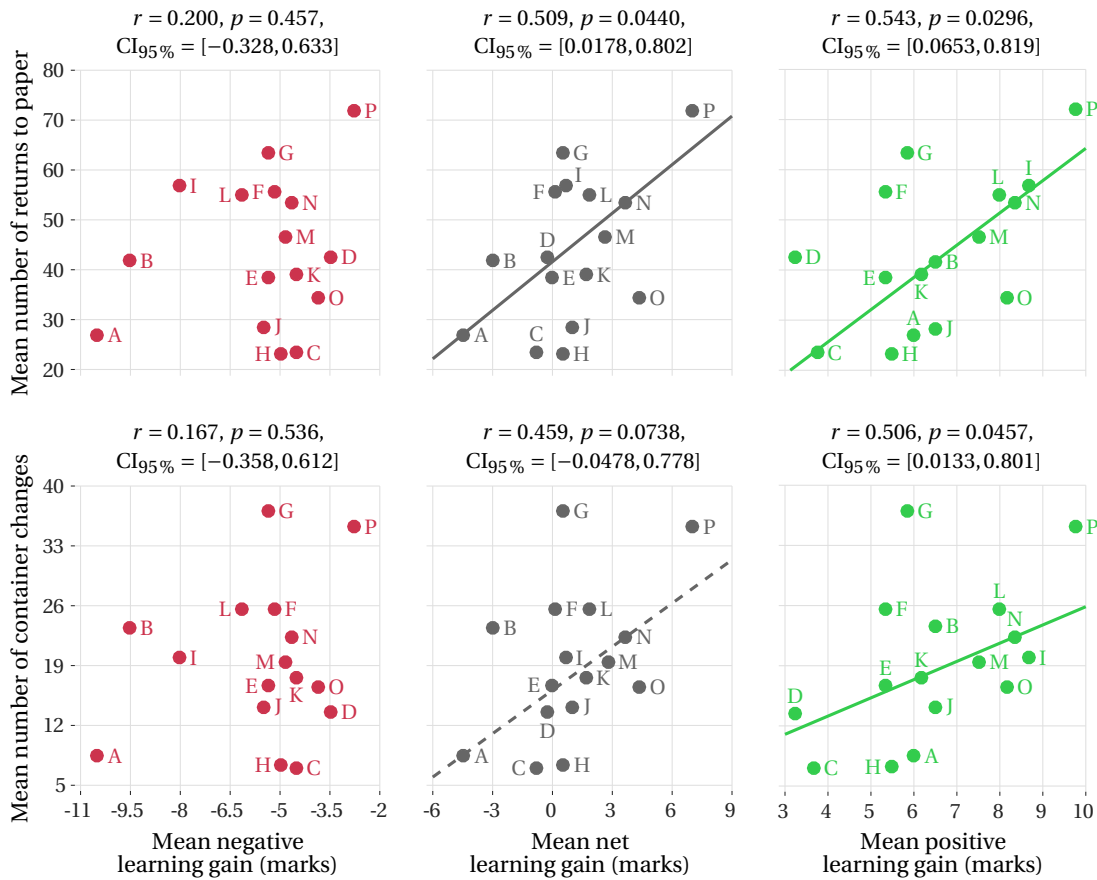


Figure 5.10 – Relationship between learning and swarm interaction measures in the quantitative Particles in Matter study. Each data point represents the mean learning and mean swarm interaction measure within a group (normalized by the number of participants in the group), whose label is given next to the data point. Left (in red), middle (in gray) and right (in green) columns depict the relationships concerning *negative learning gain* (i.e. only built misconceptions), *net learning gain* (i.e. sum of negative and positive learning gains) and *positive learning gain* (i.e. only improvements) respectively. Top and bottom rows depict the relationships concerning the mean number of times when some robot is *returned to paper* and the mean number of times when some robot is *placed in the other container*, respectively. For all pairings, Pearson's correlation test results are given on top, all of which have $n = 14$. When negative learning is considered, no significant increasing relationship between either measure was found; however, the confidence intervals suggest that decreasing relationships likely do not exist, meaning that more interaction with the swarm presumably does not lead to more misconceptions being built in this scenario. Considering positive learning, significant increasing relationships with both measures were found. A final significant increasing relationship was found between net learning gain and returning to paper whereas an almost significant increasing relationship between net learning and container changing was also found. For the increasing relationships, linear least absolute residuals (minimizing the L_1 norm) fits are given. These relationships suggest that more interaction with the swarm may lead to more learning gain in this scenario.

However, significant relationships concerning the *number of container changes* and the *number of returns to paper* were found, which are summarized in Figure 5.10. These relationships imply that groups that tangibly moved the particles around more tended to gain more positive learning, and have likely not gained more negative learning (whereas comparatively little can be said about gaining *less* negative learning). These findings may further imply that said elementary interactions, and possibly more complex ones allowed by these interactions such as the division and merging of particle collections that have different energies, are linked more to the core understanding of the activity, and should be encouraged. On the other hand, it may also be revealed that more interested learners simply interact more with the activity and observe more carefully, which leads to better learning performance; here, interest would be the third factor causing increase in both interaction and learning.

5.3.6 Conclusion

In this study, we performed the first step towards validating our swarm-enhanced learning activity in the form of an “in-the-wild” experiment where the interaction allowed for each participant was very brief. In addition to correct knowledge, a considerable amount of misconceptions were built, for which this brevity may be the culprit. However, it is also likely that the testing conditions were unideal, since the experiment context was essentially a collective field trip for classrooms from local schools where the learners were eager to “play with the next robotic demonstration” after finishing with our activity, of which there were many. Instead, we were obliged to make them undergo a test for the purposes of our own research, which may have affected the results.

However, in any case, we showed that significant positive learning can be generated with our activity, which we find promising. To amplify this gain, as well as to reduce the buildup of misconceptions, we propose in the following section to complement our activity with a classical practical activity commonly used in classrooms. By combining both activities within a planned lesson, we will aim to demonstrate the integration and added value of our swarm-enhanced learning activities to realistic classroom ecosystems. Furthermore, we will compare and contrast the nature of the learning gain provided by our activity and the classical activity, clearly showing the role and advantage of each within our planned lesson.

5.4 Qualitative Validation

5.4.1 Overview

The next step in validating our swarm-enhanced learning activity, which is simultaneously the final step in validating the robotic learning platform proposed in this thesis, is to integrate it into a lesson where the teacher actively uses the robots as a teaching tool, unlike the previously built lesson (in Section 4.4) where the lesson plan tolerates the absence of the teacher. Furthermore, in this validation step, the lesson plan and the didactic sequence is

Chapter 5. Phase IV - Building Tangible Swarms

	Phase	Goals	Time (min)
PRE.	Pre-Test	Assessment of pre-knowledge	20
INT.	Introduction	Introduction to platform and lesson	5
ACT1.	Robotic Activity	Discovery of micro-behaviors of matter	15
	or Practical Activity	Investigation of macro-behaviors of matter	
MID.	Mid-Test	Measurement of learning gain from ACT1	10
ACT2.	Practical Activity	Investigation of macro-behaviors of matter	15
	or Robotic Activity	Discovery of micro-behaviors of matter	
POST.	Post-Test & Closing	Measurement of learning gain from ACT2 Farewell & opinions	10
			Total: 55

Table 5.2 – Particles in Matter lesson plan and didactic sequence used in both experiments. Pre-Test is conducted the day before the lesson. Participants are divided into two groups where one goes through the robotic activity first and the practical activity second, while the other goes through them in the reverse order.

built in collaboration with the teacher who will use our platform in their lesson, through discussions involving the design. After designing this lesson, we will test it with two different classrooms and teachers in two different schools, resulting in two different experiments. The second experiment will feature a teacher initially unfamiliar to our platform and activity, which will provide a second “layer” of usability validation, implying easy integration into existing classrooms. Compared to the quantitative validation phase, we will give more freedom to the learners during testing in both experiments in order to capture learning resulting from “out-of-the-box” and creative thinking, as well as resulting from pre-knowledge that may not be possible to capture through fixed-answer questions. Not only will we attempt to discover the learning gain we are able to produce with this improved lesson through learner-testing, we will also interview the teacher to discover opinions, perceived performance and future prospects from the perspective of another essential stakeholder of our endeavor.

5.4.2 Lesson Design

Using the same swarm-enhanced robotic activity (see Section 5.2.4), we designed a lesson that takes around 55 minutes. The key characteristic of this lesson is that it features both robotic and classical activities: The role of the robotic activity is to open a tangible perspective towards the microscopic behaviors of matter whereas the role of the classical activity (of the practical “laboratory experiments” type that is already commonly used in classrooms for this subject) is to demonstrate the macroscopic behaviors of matter. The conventional, real-world behaviors

are challenging to demonstrate using particle simulations while the microscopic behaviors of particles are difficult to demonstrate using practical activities; our aim in using both activities is to compensate these shortcomings and obtain a lesson that provides a complete and global view of the subject. We believe that this approach will also address the shortcomings of the quantitative validation (through real-world grounding of commonly misunderstood concepts such as energy), as well as demonstrate our platform's readiness of integrability into common classroom practices.

In this composite lesson structure, it is not clear how these microscopic and macroscopic views should be combined effectively; the microscopic view can follow the macroscopic view in order to provide a “zoom-in” methodology of understanding while the reverse can also be done to provide a “zoom-out” methodology. Furthermore, strategies interleaving the two views may also be conceived where exercises composed of microscopic and macroscopic views of the same phenomena (*e.g.* melting of a liquid into a solid) are sequenced. For the purposes of our experiments, we chose to sequence the entire activities (robots after practical or practical after robots) instead of sequencing sub-parts in order to increase the utilization of our robots for the entire classroom; in this way, the classroom can be divided into two groups that use the robots in turns. Naturally, this approach will require an assistant to the teacher who will conduct one of the two activities in parallel; the experimenter undertakes this task in our experiments. However, with enough robots, the classroom could prospectively be divided into teams, each with a dedicated set of robots and laboratory equipment used to perform exercises simultaneously, where the teacher assists teams in sequence.

This approach narrows the lesson plans down to two movements, namely “zoom-in” and “zoom-out”, both of which we seek to evaluate. Furthermore, in addition to performing a pre-test to assess pre-knowledge and a post-test to assess the learning gain from the lesson, we choose to perform a mid-test in between the two activities to clearly determine the nature of the learning gains provided by each type of activity. These tests are mostly of an open writing nature, with short questions and blank space provided for the learner answer texts (and possibly drawings), in order to push the learners in the right subject direction (to discover whether they gained the target knowledge that we are interested in) but otherwise not limit them. The lesson plan that results from these considerations is given in Table 5.2 and the details of each phase is given below.

PRE - Pre-Test

Learners did a pre-test one day before the actual lesson in order to not consume time and to not cause fatigue before the lesson, as well as to reduce the priming effect caused by questions. The test consists solely of open writing questions that ask the properties and the essential characteristics of solids, liquids and gases in an undetailed fashion. Since this phase is not bounded by the lesson time, an ample 20 minutes are allowed where any and all knowledge that fits the question is promoted (*i.e.* “There is no wrong answer to these questions.” is explicitly stated to the learners).

INT - Introduction

Before the start of the lesson, the learners are greeted and briefly introduced to the experimenters, the research project conducted by the experimenters and the subject of the lesson they are about to experience. They are then divided into two separate groups where one is guided towards the robotic activity (to be conducted by the experimenter according to the script designed in collaboration with the teacher) and the other is guided towards the practical activity (to be conducted by the teacher) to begin the lesson.

ACT1/ACT2 - Robotic Activity

Similar to the previously designed activity during quantitative validation, the robotic activity used here is in the form of a semi-guided self-discovery sequence where the team of learners are encouraged to discover the system laws and particle behaviors through their own interactions with the swarm. The assistant (*i.e.* the experimenter in this case) conducting the activity only introduces the kinds of interactions that the learners should test (such as the shake interaction that provides input energy and later the cooler area that freely depletes energy) and asks questions that they should preferably answer (such as which color coded behavior corresponds to which state of matter, not readily answered by the assistant). The first group interacts with the swarm in this way for up to 15 minutes while the second group attends the practical activity, which is described below.

MID - Mid-Test

At the end of the first activity (robotic for the first group and practical for the second group), learners are assembled and are subjected to the same mid-test that lasts up to 10 minutes. It is composed mainly of open writing questions with some multiple choice questions that target ranking among the properties of different states, similar to the related questions in the previously conducted quantitative validation tests. The expected answer content is naturally less than the pre-test due to more limited time, but the learners are reminded that they are not required to re-write content that they have written before in the pre-test, as we are only interested in the learning gain difference compared to the knowledge state before the lesson. It was stressed that “This is not a test to grade you and we are only interested in what *you* think.”. Afterwards, the groups are swapped and directed to the activities they did not experience yet.

ACT2/ACT1 - Practical Activity

The practical activity is designed in the form of a set of “laboratory experiments” that are normally commonly used as part of states of matter lessons. These conventional materials and processes are intended to provide real-world, macroscopic grounding to the microscopic phenomena observed with the swarm of robots, which are explained to be programmed by us to behave as particles in these materials do. The set of experiments made available are:

- Three syringes with air (gas), water (liquid) and pen cap (solid) inside where the ends of syringes are blocked with glue tack. The learners are encouraged to try to compress each state of matter and see if they are indeed successful.
- A candle is lit, then put out after a while. The learners are encouraged to tangibly verify that the partly melted candle (now about 60 °C) is warmer. Then, they are encouraged to see that they can indeed pass their hand over a flame (about 600 °C) very quickly without burning. They are introduced the concept of “temperature” (and indirectly its transfer through the transfer of energy/heat) and encouraged to discuss what it is, corrected by the teacher if they focus on wrong statements.
- A volumetric flask with very thin neck, filled with air, is introduced and the learners are asked how they can bring colored liquid into the thin neck. Then, it is put into boiling water to warm up, removed after sufficiently long and the thin neck is plunged into a colored liquid. The cooling air inside the flask contracts and pulls the colored liquid visibly inside the thin neck. The learners are encouraged to discuss why this happens, where does the cooling effect comes from, and repeat the experiment if they wish.
- A volumetric flask with very thin neck, filled with colored liquid, is put into ice water. After cooling down, it is put into boiling hot water where the colored liquid inside visibly rises within the neck due to expansion. The learners are encouraged to discuss why this happens, repeat the experiment or cool the heated flask again in ice water to see the contraction if they wish.
- A bolt is heated on a flame until glowing hot, then tightly fastened with a metal clamp and immediately put in water. The rapidly cooling bolt contracts and releases itself from the clamp, and the learners are encouraged to discuss why this happens and repeat the experiment if they wish.
- A volumetric flask with thin neck is filled a small amount of water, then heated directly on top of a hot plate. When the water boils and turns into steam, it visibly exits the thin neck. The learners are encouraged to discuss on this energetic behavior and expansion of the hotter matter that is steam.

A portion of these experiments were chosen in order to rectify a number of the common misconceptions observed during the quantitative validation; a larger set of experiments can also be imagined depending on the availability of time. During this activity, the learners are again encouraged to discuss as to why the demonstrated processes occur through questions that trigger these discussions. Similar to the robotic activity, they are not readily given answers. Up to 15 minutes are allocated to interact with these experiments with the help of the teacher who facilitates and guides these interactions, as well as ask questions and encourage discussions.

POST - Post-test & Closing

Finally, at the end of the second activity (practical for the first group and robotic for the second group), learners are assembled again and are subjected to the same post-test that lasts up to 10 minutes. Same questions as the mid-test are asked, except for additional two questions in



(a) Robot-assisted discovery activity. Team of 4 learners (one not visible) tangibly preparing the particles for a heat transfer experiment.



(b) Practical activity. Same team of learners experimenting with states of real-world matter using common laboratory equipment. On the left, learner attempting to compress the liquid in a syringe, which is not possible. In the middle, learner heating a bolt on the Bunsen burner, to later tightly clamp it and rapidly cool it (via soaking it in water) in order to observe contraction through changing temperature which will release it from the clamp.

Figure 5.11 – Scenes from both activities in the qualitative Particles in Matter experiments.

one of the experiments, which is detailed below. Again, as we are only interested in the learning gain difference compared to before the second activity, the learners are encouraged to write only what they freshly learned, on top of the previous activity. After the test, the learners are thanked for their participation and asked their opinions and specifically what they appreciated and did not appreciate with our robots.

5.4.3 Participants, Testing & Data Collection

Our lesson was tested with two different classrooms and teachers in two schools, Leysin American School and Ecole Internationale de Genève; an example scene is given in Figure 5.11. The first classroom consisted of the teacher whom we collaborated with to design the lesson and 8 learners (in 8th grade *i.e.* final year of middle school, around 13 years old, exact age information not collected) which were treated in two groups of 4 learners with 7-8 robots each during the robotic activity; none of the learners had any prior experience with our robots. The experiment conducted with this classroom in Leysin American School was labeled \mathbb{E}_1 . Afterwards, an arranged one-to-one interview with the teacher was also conducted for his opinion, ideas and feedback for the future.

The second classroom consisted of a physics teacher initially unfamiliar with our platform and 23 learners (in 6th grade, 10.9 ± 0.458 years old) who were treated in two lesson iterations (approximately two hours) due to high number of learners. Similar to the teacher, none of the learners had any experience with our robots. In each of these iterations, consisting of 11 and 12 learners, two groups were formed that each consist of 6 learners (5 learners in one instance). The groups that interacted with the swarm of robots were further divided into two teams of three learners (only two learners in one instance) with 6-7 robots each in two independent activities. This way, similar to the quantitative experiment, up to 14 robots coexisted at a given time. The experiment conducted with this classroom in Ecole Internationale de Genève was labeled \mathbb{E}_2 . Afterwards, a brief discussion with the teacher was held for his opinion and ideas.

In both experiments, written answers to each test (given fully in Table 5.3) were collected on paper. \mathbb{E}_1 was conducted in English whereas \mathbb{E}_2 was conducted in the local language (French) and the results of its tests were translated to English afterwards for analysis. Due to the older age group among the participants in \mathbb{E}_1 compared to \mathbb{E}_2 , two additional questions were asked in both tests and two more were asked only in the post-test. In the open writing questions, answers of learners were analyzed for the correct descriptions of units of knowledge without the existence of a predetermined set of correct units. This set was built through the answers of learners where any and every unit of correct knowledge related to the subject was awarded to the learner and then added to the set. Below, the results of these tests, as well as the interview and discussions with the teachers are discussed. The quotes from the learner answers given below have their grammar corrected, their underlying sentence structure adapted but their content and meaning otherwise not modified.

Chapter 5. Phase IV - Building Tangible Swarms

Question	Available answers	Pre?	Mid?	Post?
Describe the properties of <i>solids</i> .	Open writing	E ₁ E ₂	E ₁ E ₂	E ₁ E ₂
What makes a <i>solid</i> a <i>solid</i> ?	Open writing	E ₁ E ₂	E ₁ E ₂	E ₁ E ₂
Describe the properties of <i>liquids</i> .	Open writing	E ₁ E ₂	E ₁ E ₂	E ₁ E ₂
What makes a <i>liquid</i> a <i>liquid</i> ?	Open writing	E ₁ E ₂	E ₁ E ₂	E ₁ E ₂
Describe the properties of <i>gases</i> .	Open writing	E ₁ E ₂	E ₁ E ₂	E ₁ E ₂
What makes a <i>gas</i> a <i>gas</i> ?	Open writing	E ₁ E ₂	E ₁ E ₂	E ₁ E ₂
What happens to a <i>solid</i> when heated?	Open writing	E ₁ E ₂	E ₁ E ₂	E ₁ E ₂
What happens to a <i>liquid</i> when heated?	Open writing	E ₁ E ₂	E ₁ E ₂	E ₁ E ₂
Describe the properties of <i>solids, liquids & gases</i> . What are their differences?	Open writing	E ₁ E ₂	E ₁ E ₂	E ₁ E ₂
Describe the motions of particles in <i>solids, liquids & gases</i> .	Open writing	E ₁ E ₂	E ₁ E ₂	E ₁ E ₂
How do particles <i>gain energy</i> ?	Open writing	E ₁ E ₂	E ₁ E ₂	E ₁ E ₂
Which state has the <i>most energy</i> ? The <i>least energy</i> ?	(a) Solid > Liquid > Gas (b) Solid > Gas > Liquid (c) Liquid > Solid > Gas (d) Liquid > Gas > Solid (e) Gas > Liquid > Solid (f) Gas > Solid > Liquid (g) I don't know	E ₁ E ₂	E ₁ E ₂	E ₁ E ₂
Which state has the <i>strongest bonding</i> ? The <i>weakest bonding</i> ?	(a) Solid > Liquid > Gas (b) Solid > Gas > Liquid (c) Liquid > Solid > Gas (d) Liquid > Gas > Solid (e) Gas > Liquid > Solid (f) Gas > Solid > Liquid (g) I don't know	E ₁ E ₂	E ₁ E ₂	E ₁ E ₂
What is the <i>relationship between bond strength, density and volume</i> ?	Open writing	E ₁ E ₂	E ₁ E ₂	E ₁ E ₂
Under same conditions, which state has the <i>biggest volume</i> ? The <i>smallest volume</i> ?	(a) Solid > Liquid > Gas (b) Solid > Gas > Liquid (c) Liquid > Solid > Gas (d) Liquid > Gas > Solid (e) Gas > Liquid > Solid (f) Gas > Solid > Liquid (g) I don't know	E ₁ E ₂	E ₁ E ₂	E ₁ E ₂
Under same conditions, which state is the <i>most dense</i> ? The <i>least dense</i> ?	(a) Solid > Liquid > Gas (b) Solid > Gas > Liquid (c) Liquid > Solid > Gas (d) Liquid > Gas > Solid (e) Gas > Liquid > Solid (f) Gas > Solid > Liquid (g) I don't know	E ₁ E ₂	E ₁ E ₂	E ₁ E ₂
If you put ice cubes in your drink, they eventually disappear. What happens to them?	Open writing	E ₁ E ₂	E ₁ E ₂	E ₁ E ₂
When you take a cold beverage from the fridge, water droplets appear outside the bottle. Why?	Open writing	E ₁ E ₂	E ₁ E ₂	E ₁ E ₂

Table 5.3 – Pre-test, mid-test & post-test questions for the qualitative Particles in Matter experiments. For fixed-answer questions, correct, incorrect and neutral answers are denoted with green, red and gray respectively. E₁ and E₂ denote whether the question is used in the first and the second experiment respectively.

Symbol	Label	Knowledge
B_g	Buoyancy	Gases are lighter, will go up against gravity.
C_s, C_l, C_g	Compressibility	Solid and liquids can't be compressed but gases can.
D	Difference	Particles move differently in different states (no more details on specific states).
E_f	Energy (friction)	Energy (heat) can be gained by friction.
E_h	Energy (heating)	Energy (heat) can be increased by outside sources.
E_k	Energy (kinetic)	Energy (heat) can be gained kinetically.
E_t	Energy (transfer)	Energy (heat) is transferred between particles.
F_s, F_l, F_g	Form	Solids have form, liquids and gases don't. Liquids and gases take shape of container. Liquids flow. Solids are tangible. Can't pass hand through solid but can pass through liquid and gas.
L_s, L_l, L_g	Light	Solids don't usually pass light, liquids and gases usually do.
O_g	Odor	Gases may have odors.
S_s, S_l, S_g	Spacing	Solids have little space between particles, liquids have more space, gases have considerably more space.
T_e	Transition (evaporation)	Evaporation <i>i.e.</i> change between liquid and gas.
T_m	Transition (melting)	Melting, <i>i.e.</i> change between solid and liquid.
T_u	Transition (sublimation)	Sublimation, <i>i.e.</i> occasional change between solid and gas.
V_e	Velocity (energy)	Particles move faster with increased energy (no more details on specific states).
V_s, V_l, V_g	Velocity	Solid moves very little, liquid moves faster (always in motion), gas moves even faster (still always in motion).
X_s, X_l, X_g	Expansion	Volume expands with increasing temperature.

Table 5.4 – Legend for the units of knowledge discovered in Particles in Matter qualitative experiments. The subscripts *s*, *l* and *g* stand for solid, liquid and gas respectively. See Tables 5.5 and 5.6 for the results using these notations. The units marked with gray do not appear in any learner's answer but were added here for the completeness of the full set of states related to the unit.

Pre-knowledge				Learning gain [mid-test]				Learning gain [post-test]			
<i>A</i> ₁	<i>A</i> ₂	<i>A</i> ₃	<i>A</i> ₄	<i>A</i> ₁	<i>A</i> ₂	<i>A</i> ₃	<i>A</i> ₄	<i>A</i> ₁	<i>A</i> ₂	<i>A</i> ₃	<i>A</i> ₄
<i>F_s</i>	<i>F_s</i>	<i>F_s</i>	<i>F_s</i>	∅	∅	∅	<i>S_g</i>	∅	∅	∅	<i>T_u</i>
<i>F_l</i>	<i>F_l</i>	<i>F_l</i>	<i>F_l</i>	<i>D</i>	<i>V_s, V_l, V_g</i>	∅	<i>V_s, V_l, V_g</i>	∅	∅	∅	∅
<i>F_g</i>	<i>F_g</i>	<i>S_s</i>	<i>F_g</i>	<i>E_h, E_k</i>	∅	∅	<i>E_t</i>	∅	<i>E_h</i>	∅	<i>E_h</i>
<i>L_g</i>	<i>S_s</i>	<i>S_l</i>	<i>C_s</i>	+1	∅	+1	+1	∅	+1	-1	∅
<i>T_m</i>	<i>S_g</i>	<i>S_g</i>	<i>C_g</i>	∅	+1	∅	+1	+1	∅	∅	∅
<i>T_e</i>	<i>T_m</i>	<i>L_g</i>	<i>S_s</i>	∅	+1	∅	+1	+1	∅	+1	∅
	<i>T_e</i>	<i>T_m</i>	<i>S_l</i>	∅	+1	+1	+1	+1	∅	∅	∅
		<i>T_e</i>	<i>L_g</i>	∅	+0.5	∅	+1	+1	+1	∅	∅
			<i>T_m</i>	<i>N/A</i>	<i>N/A</i>	<i>N/A</i>	<i>N/A</i>	+0.5	+1	+1	+1
			<i>T_e</i>	<i>N/A</i>	<i>N/A</i>	<i>N/A</i>	<i>N/A</i>	+0.5	∅	∅	+1

<i>B</i> ₁	<i>B</i> ₂	<i>B</i> ₃	<i>B</i> ₄	<i>B</i> ₁	<i>B</i> ₂	<i>B</i> ₃	<i>B</i> ₄	<i>B</i> ₁	<i>B</i> ₂	<i>B</i> ₃	<i>B</i> ₄
<i>S_s</i>	<i>F_s</i>	<i>F_s</i>	<i>S_s</i>	<i>F_s, F_l, F_g, B_g</i>	∅	∅	<i>X_s</i>	∅	∅	∅	∅
<i>S_l</i>	<i>F_l</i>	<i>F_l</i>	<i>S_l</i>	<i>V_g</i>	<i>V_s, V_l</i>	∅	∅	∅	∅	<i>V_s, V_l, V_g, S_s, S_l, S_g</i>	∅
<i>S_g</i>	<i>F_g</i>	<i>F_g</i>	<i>S_g</i>	∅	<i>E_h</i>	<i>E_h</i>	<i>E_k</i>	<i>E_h</i>	<i>E_k</i>	<i>E_t</i>	∅
<i>V_s</i>	<i>S_s</i>	<i>L_g</i>	<i>V_s</i>	+1	+1	∅	+1	-1	∅	+1	∅
<i>V_l</i>	<i>S_l</i>	<i>B_g</i>	<i>V_l</i>	+1	∅	∅	+1	∅	∅	+1	∅
<i>T_m</i>	<i>S_g</i>	<i>T_m</i>	<i>V_g</i>	+1	+1	+1	+1	∅	∅	∅	∅
<i>T_e</i>	<i>T_m</i>	<i>T_e</i>	<i>T_m</i>	+1	+1	+1	+1	∅	∅	-1	∅
	<i>T_e</i>	<i>T_u</i>	<i>T_e</i>	+0.5	∅	∅	∅	+1	+1	∅	∅
				<i>N/A</i>	<i>N/A</i>	<i>N/A</i>	<i>N/A</i>	+0.5	+0.5	∅	+0.5
				<i>N/A</i>	<i>N/A</i>	<i>N/A</i>	<i>N/A</i>	∅	∅	∅	+1

Table 5.5 – Results from the Particles in Matter qualitative experiment 1 (denoted with \mathbb{E}_1). A_i and B_i denote the learners while F_s, V_s etc. denote the units of knowledge, see Table 5.4 for the full legend. Only the additional gains compared to the previous state are noted in the learning gain columns. +1 denotes a correct answer given to a fixed-answer question, -1 denotes an incorrect answer given later in the post-test and +0.5 denotes a partially correct answer. Robot-enhanced and practical activities are marked with blue and orange respectively.

Pre-knowledge						Learning gain [mid-test]											Learning gain [post-test]										
A_1	A_2	A_3	A_4	A_5	A_6	A_1	A_2	A_3	A_4	A_5	A_6	A_7	A_8	A_9	A_{10}	A_{11}	A_1	A_2	A_3	A_4	A_5	A_6	A_7	A_8	A_9	A_{10}	A_{11}
F_s	T_m	F_s	F_s	F_s	F_s																						
B_g	T_e	F_l	F_l	F_l	F_l																						
L_g		L_g	L_g	T_m	T_m																						
T_m		O_g	T_m	T_e	T_e																						
T_e		T_m	T_e																								
A_7	A_8	A_9	A_{10}	A_{11}																							
F_s	F_s	F_s	F_s	F_s																							
F_l	F_l	F_l	F_l	F_l																							
F_g	F_g	L_g	O_g	L_g																							
V_l	L_g	T_m	T_e	T_m																							
B_g	O_g	T_e		T_e																							
T_m	T_m	T_u																									
T_e	T_e																										
B_1	B_2	B_3	B_4	B_5	B_6																						
F_s	F_s	F_s	F_s	F_s	F_s																						
L_s	F_l	F_g	F_l	F_l	T_u																						
T_m	V_l	V_l	F_g	X_g	T_e																						
T_e	L_l	O_g	T_m																								
	L_g	T_e	T_e																								
B_7	B_8	B_9	B_{10}	B_{11}	B_{12}																						
\emptyset	F_s	F_s	F_s	F_s	F_s																						
	F_l	F_l	F_l	L_g	F_l																						
	L_g	F_g	F_g	T_m	T_m																						
	T_m	T_m	L_g	T_e	T_e																						
	T_e	T_e	T_m	T_e																							

Table 5.6 – Results from the Particles in Matter qualitative experiment 2 (denoted with \mathbb{E}_2). A_i and B_i denote the learners while F_s , V_s etc. denote the units of knowledge, see Table 5.4 for the full legend. Only the additional gains compared to the previous state are noted in the learning gain columns. +1 denotes a correct answer given to a fixed-answer question, -1 denotes an incorrect answer given later and +0.5 denotes a partially correct answer. Robot-enhanced and practical activities are marked with blue and orange respectively.

5.4.4 Results & Discussion - Learners' Perspective

The answers given to each test in both \mathbb{E}_1 and \mathbb{E}_2 were qualitatively analyzed for pre-knowledge and learning patterns specific to the robotic and the practical activities. In the open writing questions, the set of all units of knowledge that appear in the answers was manually extracted and is given in Table 5.4. This way, in addition to explicitly taught and expected units of knowledge such as V_* (velocity characteristics of particles in each state), interesting and unexpected units of knowledge were discovered such as O_g (gases may have odors) and L_* (transparency characteristics of particles in each state). In the fixed-answer questions, correct answers, partially correct answers, as well as learning losses revealed in the post-test were marked. The results characterized this way for \mathbb{E}_1 and \mathbb{E}_2 are given in Tables 5.5 and 5.6 respectively. Below, in appropriate categories, we present our findings and commentaries resulting from the analysis of these results.

Nature of the Pre-Knowledge

In both \mathbb{E}_1 and \mathbb{E}_2 , almost all learners show pre-knowledge about the macroscopic, physical forms of matter (indicated by F_*) in most states which constitutes the majority of their writing. This finding is intuitive as conventional real-world interaction with matter will likely build this information in daily life and questioning done internally by the learner will presumably reveal this information. Some common answers in this category are:

Solids: "You can touch/feel/see them. They are usually hard and dense. You cannot pass your hand through them."

Liquids: "You can change their form/they are unshapen. They are usually not hard. You can pass your hand through them. They take the shape of the container they are put in."

Gases: "You can't touch/hold them. You can't usually see them. They move/fly in the air."

Here, common quotidian approaches of "touching with hand, seeing" to characterize the macroscopic behaviors are found. Furthermore, in both experiments, almost all learners are seen to know that solids can melt (T_m) and liquids can evaporate (T_e) when heated, presumably due to a similar way of thinking. When unexpected knowledge is considered, about half of the learners can state that gases tend to pass light more easily (L_g) and a fewer but considerable number of learners can state that gases may have odors (O_g), both of which we again interpret as relating to the same learner approach of remembering commonplace occurrences. Other than these, no unexpected pre-knowledge was encountered.

Aside from quotidian knowledge leading to macroscopic view elements, more than half of the learners in \mathbb{E}_1 showed pre-knowledge on some aspect of the microscopic views, mainly of the S_* type that describe particle spacing within each state and less commonly of the V_* type describing motions of particles; common answers revealing this fact are:

Solids: “They are made up of particles/molecules/atoms tightly packed/very close together.”

Liquids: “Their particles are tightly packed together/a bit more spread out so they can move around.”

Gases: “Their particles/molecules are very dispersed/spread out/not near each other and move around a lot.”

This pre-knowledge is seldom encountered in \mathbb{E}_2 where the only exception is some learners mentioning that “Liquids are always in motion.” (V_1). This evidences that the learners in \mathbb{E}_1 likely received some formal education on the microscopic views of matter before our experiment as opposed to learners in \mathbb{E}_2 , as there is no means of obtaining this information through quotidian interaction with matter. For this reason, the lesson is experienced as a tangible demonstration, experimentation and reinforcement of previously seen subjects by the learners in \mathbb{E}_1 and a truly initial exposure to the subject matter by the learners in \mathbb{E}_2 as intended.

Learning of Macroscopic and Microscopic Views

Answers given in the mid-test and post-test interventions are analyzed to reveal the patterns in the learning of microscopic and macroscopic views of matter. In both \mathbb{E}_1 and \mathbb{E}_2 , there is learning gain observed concerning the motions of the particles (V_*) which is not unforeseen as this question was explicitly asked. In addition, knowledge concerning particle spacing in each state (S_*) stands out, however less than the knowledge concerning particle motion. Common answers related to this body of microscopic knowledge are:

Solids: “Their atoms/particles are close to each other/stay together/are difficult to separate. They don’t move much.”

Liquids: “Their atoms/particles are close to each other a little bit but not all the time. There is space between particles, they can move. ”

Gases: “Their atoms/particles are far away from each other/don’t get close to each other. They have a lot of energy/can move a lot/very fast.”

Naturally, the gain of this body of knowledge is more evident in \mathbb{E}_2 compared to \mathbb{E}_1 where there was pre-knowledge present. What is more interesting is that the answers built with the help of our lesson resemble closely the pre-knowledge answers built in regular lessons (given above) beforehand by the learners in \mathbb{E}_2 . Apart from V_* and S_* , very little learning gain on other microscopic properties were able to be observed, such as particle bonding force. This may imply that even though this knowledge was learned, our specific questions fell short of drawing them out. Moreover, it is clearly observed (more so in \mathbb{E}_2 than in \mathbb{E}_1) that the learning of these microscopic aspects occurs more by virtue of the robotic activity than the practical activity, which is again intuitive as this activity explicitly depicts such behaviors of particles.

When macroscopic behaviors are concerned, no additional significant learning gain (compared to the quotidian knowledge encountered in the pre-test) was observed as an answer to the “Describe the properties of solids, liquids and gases.” question, given as a result of the practical activity in neither E_1 nor E_2 . However, the practical activity is seen to be more effective in helping the learners answer the “Ice cube” and “Moisture” questions, both related to macroscopic phase change behaviors; the learners that follow the practical activity after the robotic activity give significantly better answers compared to the learners who follow the robotic activity last. Unfortunately, as these questions were not asked in E_2 , there is no observation on the knowledge of this macroscopic behavior aspect taken from this group of younger learners. Following these lines, in a situation with more sufficient time spent on testing, properties such as volume, pressure, expansion and compressibility could possibly be questioned explicitly in order to improve the recognition of macroscopic learning gain. Another method could be to explicitly mention “macroscopic” and “microscopic” views and use these terms when asking questions.

Finally, in no learner’s answers were encountered mentions about robots or artificial colors coding the different states of matter; the elements were always referred to as “particles”, “atoms” or “molecules”. This implies that the abstraction of particles in matter using robots was well understood, and justifies our endeavor of building a ubiquitous tool that does not in fact resemble a robot.

Ranking the States of Matter

The results of fixed-answer questions were used to gather insights about how correctly learners are able to rank the stored energies and bond strengths of the different states, in the same way as the quantitative experiment. Additionally in E_1 , volume and density ranking was further investigated. In all questions, learners in E_1 show more success compared to learners in E_2 presumably due to pre-knowledge or simply due to their older age group. However, learners in E_1 show better learning gain from the practical activity compared to the robotic activity; the results suggest that the practical activity is more successful in teaching these rankings from scratch (or have it readily available due to undetected pre-knowledge), as well as in teaching them to learners who could not grasp it after the robotic activity. However, this is not seen to be the case in E_2 ; the practical activity seems to outperform the robotic activity (when misconceptions are also considered) when it comes before, whereas the robotic activity seems to outperform the practical activity when it comes before. Here, a fatigue effect may have played a role, see below for a discussion on this topic. Finally, more than half of the learners in E_1 showed correct understanding of the increasing/decreasing relationship between volume, density and bond strength. No understanding whatsoever (even partial) related to these relationships was seen in E_2 , showing that concepts such as volume and density must be introduced independently, which was not the case in this lesson.

In the previously conducted quantitative study, a considerable amount of misconceptions (more than the correct learning gain) were built around the energy ranking of states where

the reverse of the correct ranking was learned. This was not seen to be the case in \mathbb{E}_1 . In \mathbb{E}_2 , this phenomenon was again observed in the final answers of the learners who experienced the robotic activity last, where half of the learners gave the reverse answer and a quarter of the learners gave the correct answer. However, when the practical activity is done last, only about a third of the final answers are reverse, which may suggest the preventive effect of the practical activity on building this particular misconception.

Sources of Energy

The learners were questioned on which sources provide energy that can be gained by matter. In \mathbb{E}_1 , significantly more learning on energy gain via heating by outside sources (E_h) is encountered as a result of the practical activity compared to the robotic activity; the use of an open flame within the practical activity is likely to have had a considerable effect. Conversely, other sources of energy gain, such as kinetic (E_k) and more interestingly energy transfer between particles (E_t), are almost exclusively encountered as a result of the robotic activity. Learning of this matter is more sparse but present in \mathbb{E}_2 , where E_k is abundant after the robotic activity but others are rare. These findings imply the effectiveness of the tangible interaction methodology (*i.e.* “shake” to give energy) to demonstrate this specific manner of energy gain. Notable answers revealing these learning gains are:

E_t : “Particles gain energy by colliding with other particles that have more energy/when they touch other particles.”

E_k : “Particles gain energy by moving around/by moving them around faster.”

E_h : “Particles gain energy by heating them up/by fire which heats them up.”

Quantity of Learner Output

Finally, the free writing questions let us observe the amount of output the learners are willing or able to produce. When the total number of words written (for E_2 , counted directly in French without translation to English) after the first activity ($\mathbb{E}_1 = 59.8 \pm 20.3$ words, $\mathbb{E}_2 = 38.2 \pm 21.7$ words) and after the second activity ($\mathbb{E}_1 = 28.5 \pm 26.2$ words, $\mathbb{E}_2 = 28.2 \pm 13.8$ words) are compared, a significant decrease is observed for both experiments, regardless of the order of robotic and practical activities:

\mathbb{E}_1 : Paired $t(7) = 3.47$, $p = 0.0104$, $CI_{95\%} = [9.94, 52.56]$

\mathbb{E}_2 : Paired $t(22) = 2.65$, $p = 0.0148$, $CI_{95\%} = [2.15, 17.76]$

These findings hint at a fatigue effect where learners may be more tired and/or less interested towards the end of the lesson. Another cause may be that the post-test is an extra examination in addition to the mid-test and the learners may have been “bothered” by the obligation to undergo a second test in the same lesson.

From another perspective, when the total number of words written after the robotics activity ($\mathbb{E}_1 = 42.9 \pm 34.7$ words, $\mathbb{E}_2 = 38.9 \pm 18.8$ words) and after the practical activity ($\mathbb{E}_1 = 45.4 \pm 21.2$ words, $\mathbb{E}_2 = 27.5 \pm 17.0$ words) are compared, an interesting result is found where the robotic activity results in more output in \mathbb{E}_2 but not in \mathbb{E}_1 :

\mathbb{E}_1 : Paired $t(7) = 0.169$, $p = 0.871$, $CI_{95\%} = [-37.6, 32.6]$

\mathbb{E}_2 : Paired $t(22) = 3.17$, $p = 0.00443$, $CI_{95\%} = [3.92, 18.8]$

These imply that the robotic activity may have inspired more interest in the younger learners when compared to the practical activity, without implying answer correctness or quality.

5.4.5 Results & Discussion - Teacher's Perspective

The teacher of the classroom in \mathbb{E}_1 , who is an elementary and middle school physics teacher, was interviewed for his opinion and ideas about the use of our platform in his lesson, as well as about the platform in general. He drew attention to the brevity of the effort for our activity to be integrated into his lesson and stated this as a source of potential. When asked about the added value of Cellulo, he stated:

“Any tool that provides a practical example is an advantage. [...] Learners become more familiar with demonstrations directly on their computer, but it’s always entirely imaginary. A practical tool used in the classroom, even if it’s just for a few minutes, moves the topic into the physical realm.”

Upon this, he was asked whether, in his opinion, Cellulo would benefit learners who tend to learn better with physical examples more than learners who tend to learn better with abstract examples (*i.e.* “on paper”). He responded:

“I would say that it benefits both. [...] Learners who like to learn on paper very often do so because there is usually not a right or wrong answer immediately in practical experiences; whereas on paper, you can have a correct solution. So for them, it is very important that they engage in a practical activity, just as much as those who engage better with practical tools because they like using their hands.”

When asked what is the most useful features of Cellulo, he responded:

“I think the most useful feature is that you can touch them, and you can receive haptic feedback so you can feel the forces that they are modeling.”

These illustrate that, from this teacher’s perspective, the key value of Cellulo is its tangibility, and through that, the ability to provide physically interactive examples of models that may otherwise be difficult to provide, or too specific or simplistic (in order to ultimately “have an

exact solution”) when provided by conventional means. When asked whether Cellulo could result in more orchestration load (by theoretically disturbing standard practices) despite these benefits and how exactly he would use it in the classroom, he stated:

“I would use it in two different ways: It would be used by me in front of the whole class where I would be controlling the discussion, or it would be used by small groups within the class. It is the same as any classroom activity, you have to control it so that small groups can use it whilst other learners engage in something else, and that’s just standard management practice. I don’t see it as a distraction. In fact, it is probably the opposite because [Cellulo] is the sort of tool that drives people to focus on what they are going to engage in.”

Here, the teacher’s one envisioned use of Cellulo in general is, from a certain perspective, as a “shared service” used by multiple teams of learners in sequence, which aligns with our use of Cellulo up to now. The other envisioned use of Cellulo is as a non-interactive demonstration performed by the teacher, where the tangibility is dropped but the increased engagement provided by simply employing robots instead of conventional tools is still presumably exploited.

Finally, the teacher was asked about more practical aspects of the development and use of activities built for our platform; more specifically, he was asked whether he would like to be able to program Cellulo or otherwise use existing activities:

“I would like to have the ability to have a quick start-up, with a control panel where I could click and go if the class walked in, but I would like the ability to modify the parameters within each model. This would be a control panel that has different types of models set up, and that displays the parameters that I can change with dragging sliders for instance. [...] What I would like most would be the ability to have a simple interface to define what the robots are doing.”

In this final part of the discussion, the trade-off between giving more control of the activity to the teacher while providing more freedom as to what the activity can offer, and the workload of programming the functionalities that offer this freedom, is encountered. Clearly, the teacher does not envision software development or graphics design as a content creation tool, but a simpler, “control panel-like” software, which presents a challenge.

In addition to this interview, a more brief discussion was held with the teacher of the classroom in \mathbb{E}_2 , where he stated his appreciation of using Cellulo as a practical demonstration in his lesson, and noted that the age group of the learners in his classroom is younger than ideal for this particular subject, and this may have affected the results. Indeed, the answers are simpler and show less mastery in general compared to \mathbb{E}_2 . However, since almost no formal pre-knowledge about the subject was present, the overall learning gain was more compared to \mathbb{E}_1 where such knowledge was present before the lesson. In this sense, for learners in \mathbb{E}_2 , it can be said that our lesson acted as a “trailer” for the states of matter subject.

5.4.6 Conclusion

In this section, we presented the design, execution and results of our final validation effort to assess the ecological performance of our platform. The teaching equipment that was developed throughout this thesis, described in detail in the past 4 chapters, was used to its full potential with its complete set of features: Localization module that lets each robot know where they are in the activity without any limitation to tangible interaction, locomotion module that lets robots move themselves and allows learners move them without concern to damage, haptic feedback module that lets learners feel the modeled forces and finally the swarm platform module that lets us synchronize many robots in the same activity and lets them operate in concert meaningfully.

Using the learning activity that opens up a tangible view into the microscopic structure of matter, designed with the collaboration of a teacher and utilizing this full set of features, we designed a lesson that was built to blend seamlessly with standard practices. We tested this lesson with two classrooms of 31 learners in total where the resulting learning gains were qualitatively assessed in order to reveal the strengths, weaknesses and added value of both robots and standard practices in such a lesson. Finally, we interviewed the teacher that we collaborated with, in order to reveal his view of this integration and validation effort in order to obtain insights that will let us communicate and collaborate more effectively with teachers in the future. In the following chapter, we will return to the global perspective of our project in order to review what we applied, learned and contributed. We will discuss more plainly and mention more practical perspectives, in order to assess the real-world applicability of the advances presented previously in the thesis. We will then conclude with future prospects related to these advances and the outlook enabled by our overall vision and effort.

6 Conclusion

6.1 Overview

In this thesis, we presented the design, development and outcomes of the Cellulo project, in the form of a novel robotic platform that was designed and built from scratch, the supervised validations of its subsystems and the user studies that provide insights and results on how this novel platform performs in the real world. When realizing this novel platform we followed an iterative approach where we interleaved design, development and testing throughout four Phases. This approach, which we believe have fit our exploratory effort exceptionally well, allowed us to adapt ourselves to the most fruitful plan of research at each step, leading to both technological and conceptual contributions to areas ranging from positioning systems, robotic mechanism design, haptic interface design, swarm robot systems and finally R4L.

In order to realize our effort, we began with an examination of the history and state-of-the-art of R4L where we determined the main branches of current research, namely buildable and/or programmable tool-like robots and embodied agent robots with social competencies. We then stated our observations of the characteristics of these approaches regarding what they believed is the added value of robotics to learning, philosophy of how learning works, formal curricula, as well as their positioning with respect to informal learning opportunities. We also argued on how they agree, how they contrast and how other approaches may be useful to explore in order to expand R4L with possibly a third branch of research. We then framed our effort in this thesis, namely what we envisioned to contribute to R4L, as part of this novel, unfamiliar branch that we believe holds untapped potential for learning. We summarized the reasoning behind this belief as the likely existence of potential learning situations and disciplines that would benefit from direct, hands-on interaction with readily available, physical models of objects and phenomena within the related curricula where it is not certain whether building robots or socially interacting with robotic entities would result in a clear advantage.

Moreover, we enhanced this approach with other design principles that we believed would boost acceptance of robots by professionals in real-world environments, which we listed as *ubiquity*, *practicality*, *versatility*, *tangibility* and *multiplicity*. In other words, we stated that the

robotic platform we build should blend into the classroom ecosystem, should not incur extra workload during runtime, should be easy to grasp and apply to a wide variety of situations, should be attractive to the touch and promote physical manipulation, and finally, should be inherently flexible in terms of serving individual learners, multi-learner teams, as well as many of these teams in parallel.

Following the determination of our design directions, Phase I saw the building of an initial version of our platform, namely the hardware and the low-level firmware for 20 robots capable of localization (but not yet mobile), the high-level software means to produce the activity applications and the paper supports, and the testing of the produced platform both in the laboratory and through a playful activity with child learners in a realistic setting. Phase II continued to integrate locomotion capabilities to our robots, while ensuring mechanical robustness against user manipulation, through upgrades to the hardware and the firmware, which we tested again both in the laboratory and with child learners in realistic and arguably harsher conditions. We continued to improve our robots in Phase III with haptic feedback capabilities by upgrading the low-level firmware, as well as the high-level API that enables the useful integration of these features into activities, which we tested through studies conducted both in controlled and realistic conditions, with real users of our system. Finally, in Phase IV, we built a software framework with the aim of easily building tangible swarm activities with our existing robots, through which we implemented a learning activity that was further tested both in classrooms and in the wild, with learners and teachers.

The rest of this chapter is dedicated to discussing the outcomes that we achieved at the end of this exploratory journey, as well as discussing the future directions that other researchers may take, both inside and outside the realm of education. Therefore, following the enumeration of our scientific contributions, we will critically assess the work done until now, point out its various shortcomings and state how we believe future work should mitigate these. We will then revisit our initial research goals and discuss how much our developments and findings have addressed them, as well as propose additional future work that may provide more. Finally, we will state what we believe are the new perspectives we exposed for research and beyond.

6.2 Scientific Contributions

The entirety of the contributions presented in this thesis up to the end of Phase III were previously published in five scientific papers ([114, 140, 142, 117, 191] in chronological order), whereas the contributions in Phase IV are published for the first time in this thesis, all of which we compile below. However, given the large scope and variety of disciplines that we contributed to, both technical and non-technical, we find it beneficial to divide our contributions into two when summarizing them: We will first list our technological contributions, namely those that we believe will benefit entirely different lines of research than R4L as well. We will then list our conceptual contributions, namely those that directly impact R4L through validating our conceptual ideas and philosophy of how robots should enter classrooms.

6.2.1 Technological Contributions

For the purpose of localizing many of our robots within our envisioned activities, we introduced a technique used primarily for commercial smart pens (by brands such as Anoto) into the scientific realm of robotic positioning. Given the state-of-the-art methods, this technique allowed unparalleled robustness against occlusions, required for unrestricted tangible interaction, within an exceptionally lightweight, low-cost setup with a thin form factor. We detailed our implementation of this technique and provided an open source, reusable release of the software pipeline and tools to generate printable documents augmented with localization. Even though these development efforts brought little scientific novelty, we conducted a baseline performance analysis study as a novel contribution that clarified the limits of this technique's accuracy and precision that were not previously documented. We believe many other robotics projects would potentially benefit from this technique, such as ones concerned with localizing a large number of swarm robots without additional communication load.

As part of the next step in our development, we contributed the design of a novel omnidirectional ball drive mechanism, as well as its performance analysis with comparison to a common omnidirectional locomotion mechanism with similar cost and manufacturing precision. Our innovation allowed practically unlimited human manipulation with our palm-sized robots with few, low-cost, off-the-shelf components. Not only did we bring a fresh perspective on ball drives, we believe we improved low cost omnidirectional locomotion prospects and facilitated the integration of such systems into small-sized consumer level robots. This will allow larger freedom on the motion capabilities of such devices that otherwise commonly feature two wheeled differential drive systems for their simplicity, robustness and low cost.

Consecutive to the design and implementation of the locomotion system, we enabled haptic feedback capabilities on our robots that utilized the locomotion mechanism and no other hardware as the source of actuation. We then quantitatively characterized our robot's overall usability in terms of haptics through a user study conducted in controlled conditions. With this effort, we did not intend to obtain high fidelity, wide range haptics, but to demonstrate the novel accomplishment of utilizing a large number of low cost, lightweight, consumer-level devices capable of kinesthetic feedback in workspaces of sizes never before seen for such devices. We believe that this emergent property of our robots will be useful for HCI applications concerned with investigating the added value of haptics in active multi-point tabletop interactions, regardless of the particular area they are found in.

Finally, we presented novel contributions that addressed tangibility and allowed declarative programming on a little-known software framework that we believe holds potential in building novel swarm robot applications targeted to end users and raising the popularity of such emerging applications. From another perspective, our platform achieved the status of being one of the first tangible swarm robot platforms, featuring exceptional degree of accurate localization, as well as haptic output capacity at each swarm element. From yet another perspective, we presented one of the few documented instances of a large number of Bluetooth

devices (more than what can be connected to a single adapter) actively used in the same application, which we believe will be useful for research and applications on networked consumer devices, especially within the scope of the new Internet of Things (IoT) trend.

6.2.2 Conceptual Contributions

First and foremost, we presented the conceptual design of a novel approach for R4L where robots are envisioned neither as social agents nor as buildable/programmable machines, but as hands-on representers of phenomena, which is the main contribution of this thesis. To realize this approach, through our design principles, we built a robotic platform that allows many learners to come together in a single workspace and collaboratively discover the goal phenomena through activities that are easy to set up and orchestrate. As an initial experiment to test these aspects that embody our ideas, we explored how effectively teams of child learners interact with our robots within a playful activity. We conducted this experiment intentionally under the conditions of a school excursion featuring 85 learners from actual classrooms, where they (typically more energetic and less concentrated than usual due to them being away from the everyday classroom environment) successfully interacted with our activity, in the presence of other exciting scientific and robotic demonstrations.

Following this initial exploratory study featuring a playful activity, we began focusing on activities that target learning gains. We conducted a second experiment, again with an exploratory and qualitative nature, using an activity built to teach a curricular subject intentionally chosen from a discipline not particularly popular within R4L. In this experiment that took place as part of a large science festival, we observed how child learners interact with our novel robots that can both move and be moved, which was used as the main feature defining the semantics of the learning activity. Our experiment served about 150 learners and was conducted in even more difficult and less well-defined conditions where participants were free to approach our activity and leave as they wished. By this, we looked briefly for the first time into the learner interaction with such robots that combine physical input and output.

We then continued on to designing a complete lesson with this activity, which we further equipped with a gamified exploitative component that complemented the already existing exploratory component. In yet another experiment, designed to test the effectiveness of this lesson, we measured concrete, quantitative learning gains for the first time with our platform from 24 learners. We conducted this experiment in a more controlled scenario that was more similar to realistic classroom conditions to approach the real world circumstances where our platform would be used. Besides showing that the interaction with our robots within our sub-activities was effectively handled by all learners in the appointed time and measuring the learning that was gained during this limited time, we also investigated learners' exploration patterns when approaching the problem we presented to them, through data collected with no additional equipment or processing than provided by our platform's own hardware and software capabilities.

Finally, we designed a learning activity that highlights the swarm capabilities of our robots where again we chose a curricular subject, making our swarm robot-enhanced activity one of the very few such instances that does not aim to teach swarm robotics or distributed systems. We first tested our activity with 86 learners through an in-the-wild experiment where we showed clear, quantitative learning gains for the majority of learners despite the very limited amount of time that they spent with our activity under similar conditions to the first experiment, where considerable “noise” was present due to the school excursion conditions where learners were eager to follow other exciting demonstrations. Moreover, we quantitatively showed how aspects of tangible swarm interaction affects learning for the first time. We then continued on to designing a lesson through collaboration with a teacher (who had no prior experience with our platform) where common classroom practices were blended into the lesson together with our activity as a teaching resource. In our final experiment, in real classrooms and in the presence of the teacher, we qualitatively measured learning gains from 31 learners which revealed aspects about the nature of knowledge gained with our robots compared to knowledge gained from traditional practices.

In total with all our experiments combined, this thesis involves the participation of more than 370 unique child learners who had the opportunity to have hands-on, experiential interaction with our novel technology. Using these experiments, we observed both qualitatively and quantitatively, in both controlled and unconstrained environments, the nature of these interactions and the learning allowed by them, which we believe forms the initial set of lessons learned from this novel R4L avenue.

6.3 Shortcomings & Future Work

Here, we discuss the shortcomings of the various submodules of our platform, as well as more broad shortcomings that concern R4L, which was intentionally omitted from the relevant chapters until now for the purpose of a more uninterrupted read. Moreover, we discuss short term future work that we believe would address these shortcomings, as well as longer term future work that we believe would be beneficial from other perspectives.

6.3.1 Localization

One of the most immediate shortcomings of our optical localization system is the limitations on the graphics that can be printed alongside the dot pattern that must be clearly perceived by the robots’ cameras in order to be decoded. Currently, we rely on high contrast between each black dot and its surroundings so that the dots can be extracted using computationally inexpensive global thresholding. This prevents darker colors near the color of the dots, as well as other colors that appear as black (such as green) to the monochrome image sensor, to be used within the graphics on any paper that is part of our activities, except *e.g.* very thin printed text that may be tolerated by the error correction mechanism within decoding.

A rapid solution that would respect the currently available low cost consumer printing methods would be to color each dot separately with the most contrasting color with its surroundings and implement a form of local thresholding. This method would certainly incur higher computational cost, but the difference may indeed be marginal which would justify its use. Beyond the capabilities of widespread consumer printers, other solutions could be to print the dots with ink that is only visible in a disjoint spectrum with the printed graphics, and to equip the robot cameras with filters that allow only this spectrum. Another similar solution could be to print the dots with a reflective ink so that higher exposure intensity may be used to drown out the visible graphics but not the dots.

Currently, our decoding pipeline works on the assumption that the imaging plane is exactly parallel to the paper plane, which implies that there is no perspective tilt on the perceived imaginary grid that the dots are placed on. If this assumption is removed, and these tilt angles (two exist, one around each of the u and v axes) could be estimated, we could in theory further estimate the extra distance that the robot is lifted from the paper given that the grid distance is fixed. This would allow 6DOF localization in the vicinity of the paper as long as the camera focus is not lost, which would open new interaction possibilities and add extra robustness to both localization and locomotion whose dynamics change when the robot is tilted.

6.3.2 Locomotion

Perhaps the most critical technical shortcoming of our robots is that the low cost bearings in our ball drive implementation are not robust enough against external contaminants such as dust and rubber shards from the ball wheels that accumulate in the bearing and decrease the performance drastically. It is clear that for long term use, high performance bearings that are robust against contamination should be preferred over our solution. These high performance bearings should include, per ball wheel, at least two 1DOF bearings (*e.g.* ball bearings) that contact the ball wheel around its great circle in order to enclose it, as well as a 2DOF bearing (*e.g.* ball transfer units) that contacts the ball wheel on top, carrying the weight of the robot.

Furthermore, it should be noted that the manufacturing of the ball wheel itself is not trivial, and the misalignment of the ferromagnetic core with respect to the center of the entire wheel caused by manufacturing defects significantly affects performance. Given a 1 mm rubber coating thickness, the most extreme state of misalignment implies 0 mm thickness non-ferromagnetic coating on one point on the surface of the wheel and 2 mm on the opposite point, causing magnet-wheel contact force anisotropy as the wheel rotates, leading to the occasional loss of traction. This problem could be mitigated by removing the ball wheel coating in order to make it drastically more isotropic (which would also lead to different dynamics at the magnet-wheel contact that must be investigated) and coating the paper with a high-friction material in order to ensure robot traction on the support surface.

The dynamics analysis of locomotion was made with certain simplifications, such as the assumption that the mass of the robot is negligible, in order to accommodate the asymmetric

force output of the wheels due to the asymmetric nature of the drive and internal frictions. In a better implementation, these frictions would be less pronounced and a better analysis can be made that takes into account the phases where the robot accelerates and decelerates.

6.3.3 Haptics

The haptics module of our robot is not ideal from various perspectives. For one, tactile feedback capabilities are fairly limited with the modules readily implemented on the robot. Besides tactile feedback, arbitrary complex motion and kinesthetic feedback requires running custom controllers in the application on the master side, which directly controls the robot velocities and force outputs. What would be interesting to explore is the ability to computationally and concisely describe haptic outputs, as well as motion outputs, in the form of code that depend on the kinematics of the robot, as well as externally applied forces, and that can be just-in-time compiled and communicated to the robot for execution. While this would allow the execution of such haptics and motion controllers to operate with the maximally available frequency (about 93 Hz at the time of writing, possibly higher with further optimizations), dynamically changing controllers such as those who depend on the collective states of multiple robots would still be fundamentally out of reach.

From another perspective, any amount or type of haptic feedback we are currently able to generate from our robots is controlled in an open loop. Ideally, our robots require a means of measuring the forces and torque that is output to the outside world, most importantly to the user's grasp. For making these measurements, novel and interesting transducers were recently designed that would aid in obtaining a lower cost than traditional strain gauge-based techniques while also adding other benefits such as compliance; see [233] for such a transducer design that relies on low cost barometric sensors encased in flexible rubber-like materials. Regardless of the sensing mechanism, the ability to measure output forces and torque would allow us to close the haptic feedback loop and ensure a considerably higher degree of fidelity.

6.3.4 Swarm

We designed our declarative physicomimetic robot control framework in order to ease tangible swarm robot application development. While this method does not directly support distributed (*i.e.* "true") swarm applications that allow very large number of agents, it is only our intuition and initial observation that the development of the supported type of applications would be facilitated. To quantify this hypothetical improvement, code produced by our framework should be compared to those produced by other methods and baselines where metrics such as the number of lines of code, legibility, modularity and reusability should be compared. Moreover, ideally, a number of professional developers should be recruited to test the development of a range of real world applications where our framework should again be compared to others in terms of code production and verification efficiency.

Furthermore, we did not quantify the limits of connectivity, the most important of which is the limit on the number of robots robustly supported within a single activity, due to the lack of sufficiently many robots in our possession to conduct this experiment. While the theoretical limit for this exists, the practical limit (expected to be much lower) must be measured by incrementally varying the number of continuously communicating robots within the same activity and measuring the maximum useful bandwidth (*i.e.* maximum control frequency on each robot), after which the network saturates.

A related problem is connection establishment to desired robots, which is currently handled by performing a scan of all nearby devices, filtering on the physical addresses that are collected in order to obtain only our robots and no other devices, and attempting to connect to the desired list of robots among the visible ones in the scan. This method does not guarantee the discovery of all robots in the scan in the presence of noise, and does not allow selective connection to groups of robots, for easily setting up more than one activity with a single set of robots in the same environment, simply because all nearby idle robots appear in the scan. A more scalable method would be to rely on the emerging Near-Field Communication (NFC) technology to physically bring the desired robots close to the master device, at which point the connection attempt is automatically started on both devices. Another solution would be to visually encode the physical addresses of the robots (through *e.g.* LED patterns or exclusive fiducial markers on the bottom of the robots), which would then be mass-decoded in camera images of the master device in order to obtain the desired list of robots to connect to.

6.3.5 Robots for Learning

Considering the main contribution of this thesis, the most crucial shortcomings are related to its R4L aspects. For one, we did not conceivably have enough time within the frame of this thesis to conduct longer term studies with our robots. An important prospect for future research is to conduct these studies in order to reveal important acceptability and performance measures free of the novelty effect. Furthermore, longer term studies would also be valuable to probe the effectiveness of our robots on subjects or collections of interconnected subjects that can only practically be taught over many lessons that possibly take weeks to all execute. Such studies would also be useful to test our approach against robotic and non-robotic baselines where applicable, in order to compare and contrast the added value, strengths and weaknesses of other approaches to those associated with our approach.

While we tested our robots with hundreds of learners, we closely collaborated with only a few teachers. While we followed rational design principles to boost our platform's acceptability in real environments by real professionals, it is essential that future work introduces our platform to more teachers in order to gain more insights on its actual perception and its true performance in their hands. A related shortcoming is that with the current state of our development tools, it is impractical for teachers to be any part of activity software development, which we acknowledged and addressed up to now with the inclusion of professional software

developers in this process. However, letting teachers author content is certainly a valuable prospect for the creation of teacher communities around our platform. It is clearly non-trivial how this would be achieved, but we believe an object-oriented visual programming language may be an advantageous start. Related to this, enabling the programmability of our robots by learners is also a valuable asset, as previously mentioned, for applications such as computational thinking.

Finally, we acknowledge the limitations on the applicability of our robot to the spectrum of learner ages. It is certainly intuitive and qualitatively observable that our platform is better suited for younger ages, preferably up to the end of middle school, with which we conducted the majority of our experiments. After this age, our platform and method of tangibly representing phenomena risks performing in too much of a simplistic manner for learning where more complex and realistic models may be required. While the validity of this claim may not be entirely clear for high school ages and curricula, it is certainly reasonable to assume that this would be the case for higher education where our robots would not be applicable in their current state. However, all of these assertions naturally need scientific validation which we did not provide in this thesis.

6.4 Research Goals Revisited

Our contributions to R4L were made with directions that come from a number of research goals that we envisioned would let us explore previously unimagined ways to teach and learn with robots. We conceptualized a number of design principles that we envisioned would let us more concretely implement technology and end user devices that would address these research goals. Here, we discuss how much of our research goals were achieved through our design principles, developments and findings, and how future work may achieve more:

Build and effectively use robots for learning that are perceived as everyday objects rather than robots by both learners and teachers. – As per our ubiquity principle, we built our robots as unimpressive, “white boxes” and merged them with familiar objects both old and new, namely pieces of paper and commonplace mobile computers. We spent significant effort to make our devices as easy and straightforward to use as possible, ever so often sacrificing capacities found typically in robots, to improve the user experience and ensure that our robots are perceived solely as end user devices. As a result of these efforts, we observed that unfamiliar teachers and learners can quickly approach our platform and start using it effectively. While we observed this phenomenon subjectively, user studies may be performed in the future that objectively probe how the components of our platform are exactly perceived by these end users.

Build simple robots for learning, perceived as tools, that promote other uses than building or programming. – Contrary to the current expectation that a small, mobile robot for learning should be programmable or buildable in some way, we designed our robots to serve the completely different role of interaction device and representer. This allowed us to

imagine different ways that robots could be used for learning, as well as applications to various unpopular subjects. We implemented two activities on atmospheric pressure and states of matter, both of which did not previously contain clear added values from robots for learning, as opposed to more popular subjects from *e.g.* mathematics and geometry which did. Naturally, future work should further expand this versatility portfolio through exploring other added values and building more educational content on our R4L approach.

Build robots for learning enriched with previously unpopular affordances and materials. –

Instead of exploiting previously studied affordances and materials, we pursued other less examined affordances in our robots and synergies with a well known material, namely paper, as they emerged. We thus explored tangible interaction, namely the physical placement and manipulation of robots on one or more sheets of paper; haptic interaction, namely conveying information to the learners via mechanical forces; and swarm interaction, namely exploiting the collective behaviors of many robots for better communicating the core ideas. A reasonable direction for future work is to quantify the added value of these affordances against more commonly used baselines.

Build robots that are part of social interactions among learners and teachers without necessarily being social agents. –

Even though we did not build our robots with social competencies, we built them with the prospect of letting learners and teachers easily work together. We designed our platform in a scalable manner, with particular focus on making our activities easy to reproduce and/or grow in capacity. In almost all of our experiments, we exploited these capabilities to run multiple activities in parallel, each of which contained collaboration within the teams of learners. Beyond this multiplicity prospect, our platform enabled accessibility to the teacher, letting them easily intervene and physically manipulate the activity components in order to orchestrate. Future studies may consider varying the number of parallel activities, as well as the number of robots and learners in the activities, to probe their effect on collaboration measured by ground truth methods outside the capabilities of our platform alone.

Build tool-like robots whose added value to curricular learning is easier to imagine by teachers. –

To address this goal which is indeed tightly connected with the goals of making our robots appear non-robot-like and opening up a rich set of affordances, we attempted to apply our robots to learning in an arguably simpler manner than what is available, as the direct representation of objects and phenomena. We collaborated with a teacher to probe how he imagined the integration of our robots into his lesson, which was achieved in a short amount of time. In the future, as mentioned before, more teachers (who are not necessarily technophiles) must be introduced to our platform with the aim of developing the added values to more diverse curricula.

Use existing classroom materials and practices to improve the integration of our robots into formal education. –

In order to facilitate the prospective acceptance of our platform in the

classroom as part of the daily learning routine, we aimed to use paper, which is one of the most pervasive, easily understood and integral parts of formal education as of now, as also an integral part of activity building and execution with our platform. Moreover, we built our platform to be easy to launch and put away, and imagined that it should be used only when necessary, allowing common practices to coexist harmoniously with our robots. A valuable prospect for the future is to deploy our platform in schools and measure its use in the presence of learners and teachers in their natural environment, and particularly in the absence of researchers who are familiar with the platform.

6.5 Impact and New Perspectives

As we conclude this thesis, we wish to revisit our idea that sparked the Cellulo project, bringing on the developments that led to its current state. Namely, we set out to explore new avenues in which robots could be useful for learning in ways never imagined before, with the hopes of contributing new outlook to the emerging research field that is R4L. Importantly, we did not design a new robotic platform as an improvement on the state-of-the-art that would surpass other platforms in term of teaching efficacy, but as a new tool in the arsenal of researchers and educators. We are continuing to expand Cellulo for education within our own group (*e.g.* [234] at the time of writing) but it is our sincere desire that more researchers explore and exploit what was or can be done with our platform after the publication of this thesis.

We have identified and are currently working on other prospects than education with Cellulo. For one, we are exploring tangible interfaces for visually impaired people, including children, that can potentially highlight the motion and haptics capabilities of Cellulo; an example case would augment an interface such as [235] with mobility and improve the simplicity of its setup. Another application is tangible gaming and gamified activities that serve other main purposes than gaming, where we believe Cellulo's capacity to bring together many tangible robots effortlessly in the same activity may lead to new and exciting opportunities. A related application where we see a strong focus for such ideas is gamified upper arm rehabilitation. Here, we would improve current strategies that rely on heavier setups, cost higher, or provide less entertainment than Cellulo, as well as bridge the gap between rehabilitation in therapy centers and at-home rehabilitation by virtue of our platform's minimal setup requirements; see [236] for our latest efforts. Beyond these, we believe other exciting and creative applications can be found as well with the inspiration we believe we provided in this thesis.

A Anoto Number Sequences

Here, for completeness and reproducibility, we provide the actual Anoto number sequences used in our algorithms, given as examples in the original patent ([113]). The main number sequence used is:

```

0 0 0 0 0 0 1 0 0 1 1 1 1 1 0 1 0 0 1 0 0 0 0 1 1 1 0 1 1 1 0 0 1 0 1 0
0  1  2  3  4  5  6  7  8  9 10 11 12 13 14 15 16 17 18 19 20 21 22 23 24 25 26 27 28 29 30 31 32 33 34 35
1 0 0 0 1 0 1 1 0 1 1 0 0 1 1 0 1 0 1 1 1 1 0 0 0 1 1
36 37 38 39 40 41 42 43 44 45 46 47 48 49 50 51 52 53 54 55 56 57 58 59 60 61 62

```

(A.1)

The secondary number sequences used are (note the extra symbol in the fourth sequence, originally missing from the patent):

```

0 0 0 0 0 1 0 0 0 0 2 0 1 0 0 1 0 1 0 0 2 0 0 0 1
0  1  2  3  4  5  6  7  8  9 10 11 12 13 14 15 16 17 18 19 20 21 22 23 24
1 0 0 0 1 2 0 0 1 0 2 0 0 2 0 2 0 1 1 0 1 0 1 1 0
25 26 27 28 29 30 31 32 33 34 35 36 37 38 39 40 41 42 43 44 45 46 47 48 49
2 0 1 2 0 1 0 1 2 0 2 1 0 0 1 1 1 0 1 1 1 1 0 2 1
50 51 52 53 54 55 56 57 58 59 60 61 62 63 64 65 66 67 68 69 70 71 72 73 74
0 1 0 2 1 1 0 0 1 2 1 0 1 1 2 0 0 0 2 1 0 2 0 2 1
75 76 77 78 79 80 81 82 83 84 85 86 87 88 89 90 91 92 93 94 95 96 97 98 99
1 1 0 0 2 1 2 0 1 1 1 2 0 2 0 0 1 1 2 1 0 0 0 2 2
100 101 102 103 104 105 106 107 108 109 110 111 112 113 114 115 116 117 118 119 120 121 122 123 124
0 1 0 2 2 0 0 1 2 2 0 2 0 2 2 1 0 1 2 1 2 1 0 2 1
125 126 127 128 129 130 131 132 133 134 135 136 137 138 139 140 141 142 143 144 145 146 147 148 149
2 1 1 0 2 2 1 2 1 2 0 2 2 0 2 2 2 0 1 1 2 2 1 1 0
150 151 152 153 154 155 156 157 158 159 160 161 162 163 164 165 166 167 168 169 170 171 172 173 174
1 2 2 2 2 1 2 0 0 2 2 1 1 2 1 2 2 1 0 2 2 2 2 2 0
175 176 177 178 179 180 181 182 183 184 185 186 187 188 189 190 191 192 193 194 195 196 197 198 199
2 1 2 2 2 1 1 1 2 1 1 2 0 1 2 2 1 2 2 0 1 2 1 1 1
200 201 202 203 204 205 206 207 208 209 210 211 212 213 214 215 216 217 218 219 220 221 222 223 224
1 2 2 2 0 0 2 1 1 2 2
225 226 227 228 229 230 231 232 233 234 235

```

(A.2)

Appendix A. Anoto Number Sequences

0 0 0 0 0 1 0 0 0 0 2 0 1 0 0 1 0 1 0 1 1 0 0 0 1
 0 1 2 3 4 5 6 7 8 9 10 11 12 13 14 15 16 17 18 19 20 21 22 23 24
 1 1 1 0 0 1 1 0 1 0 0 2 0 0 0 1 2 0 1 0 1 2 1 0 0
 25 26 27 28 29 30 31 32 33 34 35 36 37 38 39 40 41 42 43 44 45 46 47 48 49
 0 2 1 1 1 0 1 1 1 0 2 1 0 0 1 2 1 2 1 0 1 0 2 0 1
 50 51 52 53 54 55 56 57 58 59 60 61 62 63 64 65 66 67 68 69 70 71 72 73 74
 1 0 2 0 0 1 0 2 1 2 0 0 0 2 2 0 0 1 1 2 0 2 0 0 2
 75 76 77 78 79 80 81 82 83 84 85 86 87 88 89 90 91 92 93 94 95 96 97 98 99
 0 2 0 1 2 0 0 2 2 1 1 0 0 2 1 0 1 1 2 1 0 2 0 2 2
 100 101 102 103 104 105 106 107 108 109 110 111 112 113 114 115 116 117 118 119 120 121 122 123 124
 1 0 0 2 2 2 1 0 1 2 2 0 0 2 1 2 2 1 1 1 1 1 2 0 0
 125 126 127 128 129 130 131 132 133 134 135 136 137 138 139 140 141 142 143 144 145 146 147 148 149
 1 2 2 1 2 0 1 1 1 2 1 1 2 0 1 2 1 1 1 2 2 0 2 2 0
 150 151 152 153 154 155 156 157 158 159 160 161 162 163 164 165 166 167 168 169 170 171 172 173 174
 1 1 2 2 2 2 1 2 1 2 2 0 1 2 2 2 0 2 0 2 1 1 2 2 1
 175 176 177 178 179 180 181 182 183 184 185 186 187 188 189 190 191 192 193 194 195 196 197 198 199
 0 2 2 0 2 1 0 2 1 1 0 2 2 2 2 0 1 0 2 2 1 2 2 2 1
 200 201 202 203 204 205 206 207 208 209 210 211 212 213 214 215 216 217 218 219 220 221 222 223 224
 1 2 1 2 0 2 2 2
 225 226 227 228 229 230 231 232

(A.3)

0 0 0 0 0 1 0 0 1 1 0 0 0 1 1 1 1 0 0 1 0 1 0 1 1
 0 1 2 3 4 5 6 7 8 9 10 11 12 13 14 15 16 17 18 19 20 21 22 23 24
 0 1 1 1 0 1
 25 26 27 28 29 30

(A.4)

0 0 0 0 0 1 0 2 0 0 0 0 2 0 0 2 0 1 0 0 0 1 1 2 0
 0 1 2 3 4 5 6 7 8 9 10 11 12 13 14 15 16 17 18 19 20 21 22 23 24
 0 0 1 2 0 0 2 1 0 0 0 2 1 1 2 0 1 0 1 0 0 1 2 1 0
 25 26 27 28 29 30 31 32 33 34 35 36 37 38 39 40 41 42 43 44 45 46 47 48 49
 0 1 0 0 2 2 0 0 0 2 2 1 0 2 0 1 1 0 0 1 1 1 0 1 0
 50 51 52 53 54 55 56 57 58 59 60 61 62 63 64 65 66 67 68 69 70 71 72 73 74
 1 1 0 1 2 0 1 1 1 1 0 0 2 0 2 0 1 2 0 2 2 0 1 0 2
 75 76 77 78 79 80 81 82 83 84 85 86 87 88 89 90 91 92 93 94 95 96 97 98 99
 1 0 1 2 1 1 0 1 1 1 2 2 0 0 1 0 1 2 2 2 0 0 2 2 2
 100 101 102 103 104 105 106 107 108 109 110 111 112 113 114 115 116 117 118 119 120 121 122 123 124
 0 1 2 1 2 0 2 0 0 1 2 2 0 1 1 2 1 0 2 1 1 0 2 0 2
 125 126 127 128 129 130 131 132 133 134 135 136 137 138 139 140 141 142 143 144 145 146 147 148 149
 1 2 0 0 1 1 0 2 1 2 1 0 1 0 2 2 0 2 1 0 2 2 1 1 1
 150 151 152 153 154 155 156 157 158 159 160 161 162 163 164 165 166 167 168 169 170 171 172 173 174
 2 0 2 1 1 1 0 2 2 2 2 0 2 0 2 2 1 2 1 1 1 1 2 1 2
 175 176 177 178 179 180 181 182 183 184 185 186 187 188 189 190 191 192 193 194 195 196 197 198 199
 1 2 2 2 1 0 0 2 1 2 2 1 0 1 1 2 2 1 1 2 1 2 2 2 2
 200 201 202 203 204 205 206 207 208 209 210 211 212 213 214 215 216 217 218 219 220 221 222 223 224
 1 2 0 1 2 2 1 2 2 0 2 2 2 1 1 1*
 225 226 227 228 229 230 231 232 233 234 235 236 237 238 239 240

(A.5)

*This final symbol of the fourth secondary number sequence is missing in the original patent; only the first 240 symbols are given.

B Particles in Matter Source Code

Given in Listing B.1 is the Particles in Matter activity (presented in Section 5.2.4) source code that utilizes the previously proposed declarative tangible swarm control framework (presented in Section 5.2.3) to achieve a microscopically tangible simulation of solid, liquid and gaseous matter. Transitions in between these states, as well as some other behaviors, are achieved by modulating the behaviors through a `weight` property that varies between 0 and 1.

```
1 CelluloRobotPoolClient{ id: client } //Interface to the robot pool daemon in Figure 5.1
2
3 Swarm{ //Implements SWARM UPDATE from Algorithm 5.1
4     id: swarm
5
6     /* Swarm elements and associated individual behaviors */
7     RepeaterList{ //Extends the built-in Repeater, expects count and provides index
8         count: client.robots.length //Number of elements, as many as robots
9
10        SwarmElement{ //Implements NEW ROBOT POSE AVAILABLE(e,Δt) from Algorithm 5.1
11            id: element
12            robot: client.robots[index] //Associated robot to this element
13
14            /* Properties to export */
15            property ZoneEntryCalculator containerCalculator: priv_containerCalculator
16            property ZoneEntryCalculator coolerCalculator: priv_coolerCalculator
17            property ParticleState particleState: ParticleState{} //Simple object
18            ↪ holding the heat state of element, e.g solidToLiquidProgress = 0.5
19            ↪ means halfway between solid-liquid transition while liquidProgress =
20            ↪ 0.5 means halfway between totally melting and starting evaporating
18            property real halfCoverage:
19            ↪ priv_halfCoverageCalculator.halfCoverages.get(element) //This element's
20            ↪ "half-coverage", see halfCoverageCalculator
19            property bool isGrabbed: priv_grabDetector.isGrabbed
20            property bool isOnPaper: !priv_kidnapDetector.isKidnapped
```

Listing B.1 – Particles in Matter source code, part 1 of 5. Irrelevant parts such as GUI components, as well as some implementation details, are removed; the actual source code corresponding to this portion is about 230 lines long. Continued in the following pages.

Appendix B. Particles in Matter Source Code

```
21     /* Robot-element emergency synchronizers */
22     RobotPositionCatchUp{ c: 10.0 } //Smoothly pulls the element to the robot
23         - position if it can't catch up with the strength parameter c
24     RobotPositionHardSync{} //Immediately pulls the element to the robot
25         - position if it couldn't catch up for too long
26
27     /* Color outputs per element state */
28     ConstantColorOutput{
29         activeState: "Out"
30         color: "#000000"
31     }
32     GradientColorOutput{
33         activeState: "Moving"
34         target: particleState.solidProgress +
35                 - particleState.solidToLiquidProgress + particleState.liquidProgress
36                 - + particleState.liquidToGasProgress + particleState.gasProgress
37         targetsToColors: {
38             0.0 : "#000010",     //Coldest solid color
39             1.0 : "#0000A0",     //Warmest solid color
40             2.0 : "#001000",     //Coldest liquid color
41             3.0 : "#00A000",     //Warmest liquid color
42             4.0 : "#100000",     //Coldest gas color
43             5.0 : "#A00000",     //Warmest gas color
44         }
45     }
46     ConstantColorOutput{
47         activeState: "Moved"
48         color: "#A0A0A0"
49         outputEffect: Cellulo.VisualEffectBreathe
50     }
51
52     /* Individual motions and forces */
53     IndependentOscillation{ //Stored energy in solid and lonely liquid particles
54     property real solitudeWeight: Math.max(0.0, 1.0 - 5*halfCoverage)
55     weight: (1.0 - particleState.liquidToGasProgress)*((1.0 -
56             - particleState.solidToLiquidProgress) +
57             - particleState.solidToLiquidProgress*solitudeWeight)
58     amplitude: 5.0 + 10*particleState.solidProgress +
59             - 1*particleState.solidToLiquidProgress +
60             - 4*particleState.liquidProgress //In millimeters
61     period: 3000 - 1500*particleState.solidProgress -
62             - 100*particleState.solidToLiquidProgress -
63             - 400*particleState.liquidProgress //In milliseconds
64     }
65     IndividualViscousDamping{ //Reduce damping for more liquid and gas freedom
66     c: -2.75 //Viscous damping coefficient, i.e strength
67     weight: 0.25*particleState.solidToLiquidProgress +
68             - 0.75*particleState.liquidToGasProgress
69     }
70     EnforceLinearVelocity{ //Force gas particles to fly away
71     c: 1.0 //Force strength coefficient to enforce velocity
72     weight: 1.0*particleState.liquidToGasProgress
73     desiredVelocity: 50 + 130*particleState.gasProgress //In mm/s
74     }
```

Listing B.1 – Particles in Matter source code continued, part 2 of 5.

```

64     /* Zone-specific logic */
65     ZoneEntryCalculator{ //Main container with A0 paper, calculates entry vector
66         id: priv_containerCalculator
67         paper: CelluloZones.loadZone("/:zones/containerPaper.json") //Polybézier
68             ↳ curve describing border of whole paper
69         zone: CelluloZones.loadZone("/:zones/containerZone.json") //Polybézier
70             ↳ curve describing actual usable zone
71     }
72     ZoneEntryCalculator{ //Cooler with A4 paper, calculates entry vector
73         id: priv_coolerCalculator
74         paper: CelluloZones.loadZones("/:zones/coolerPaper.json") //Polybézier
75             ↳ curve describing border of whole paper
76         zone: CelluloZones.loadZones("/:zones/coolerZone.json") //Polybézier
77             ↳ curve describing actual usable zone
78     }
79     IndividualHeatLoss{ //While inside cooler, apply individual heat loss
80         h: 5.0 //Strength of heat loss
81         weight: priv_coolerCalculator.insidePaper ? 1.0 : 0.0
82     }
83     /* User interaction detectors */
84     KidnapDetector{ //Kidnap from/return to paper detector
85         id: priv_kidnapDetector
86         onKidnapped: element.setState("Out")
87         onReturnedToPaper: element.setState(element.isGrabbed ? "Moved" :
88             "Moving")
89     }
90     GrabDetector{ //Grab/release detector
91         id: priv_grabDetector
92         onGrabbed: {
93             if(element.state == "Moving")
94                 element.setState("Moved");
95         }
96         onReleased: {
97             if(element.state == "Moved")
98                 element.setState(element.isOnPaper ? "Moving" : "Out");
99         }
100     }
101     LaunchDetector{ //"Launch motion" (grab, give velocity, release) detector
102         grabDetector: priv_grabDetector
103         historySize: 3 //Window size for averaging measured velocity
104         onLaunched: element.velocity = launchVelocity
105     }
106     IndividualEnergyDetector{ //Shake to give delta heat
107         grabDetector: priv_grabDetector
108         onEnergyAdded: particleState.changeHeat(energy/10000)
109     }
110 }
111 }

```

Listing B.1 – Particles in Matter source code continued, part 3 of 5.

Appendix B. Particles in Matter Source Code

```
108  /*
109  * Collective and global behaviors for the entire Swarm
110  */
111
112  /* Global rules for all particles */
113  MaxLinearVelocity{ maxVelocity: 185 } //Hard limit in mm/s
114  MaxAngularVelocity{ maxVelocity: 7.5 } //Hard limit in rad/s
115  GlobalViscousDamping{ c: 2.75 } //Damping that prevents excessive movement
116
117  /* Container and cooler borders */
118  BouncyContainer{ //Main container borders become bouncy by the exclusion amount
119    zoneEntryCalculator: function(element){ return element.containerCalculator; }
120    calculateExclusion: function(element){
121      return element.isGrabbed ? 0.0 : 10 + 50*element.particleState.gasProgress;
122    }
123    epsilon: 1000 //Bounciness force strength parameter
124  }
125  StrictContainer{ //Zone borders are strictly uncrossable as long as on paper
126    zoneEntryCalculator: function(element){ return element.containerCalculator; }
127  }
128  StrictContainer{ //Zone borders are strictly uncrossable as long as on paper
129    zoneEntryCalculator: function(element){ return element.coolerCalculator; }
130  }
131
132  /* Collective calculators to not repeat same calculations for each object */
133  HeatSeparationCalculator{ //For each pair of elements, calculates the ideal
134    ↪ separation in mm, that depends on average heat of the two
135    id: priv_idealSeparationCalculator
136    baseSeparation: 80 //In millimeters
137    solidExtraSeparation: 30 //In millimeters
138    solidToLiquidExtraSeparation: 10 //In millimeters
139    liquidExtraSeparation: 20 //In millimeters
140    liquidToGasExtraSeparation: 0 //In millimeters
141    gasExtraSeparation: 0 //In millimeters
142  }
143  HalfCoverageCalculator{ //For each element, calculates a value that is close to 1 if
144    ↪ it is half-surrounded by other elements (for maximum sliding force) but close
145    ↪ to 0 if not surrounded or fully surrounded (for no sliding force)
146    id: priv_halfCoverageCalculator
147    idealSeparationCalculator: priv_idealSeparationCalculator
148  }
149
150  /* Heat transfer mechanism between elements */
151  HeatTransfer{
152    h: 0.02 //Heat transfer strength parameter
153    idealSeparationCalculator: priv_idealSeparationCalculator
154  }
```

Listing B.1 – Particles in Matter source code continued, part 4 of 5.

```

152  /* Collective forces that depend on mutual relationships */
153  PotentialWell{ //Attraction that keeps particles together in solid and liquid
154      epsilon: 400 //Force strength parameter
155      weight: function(element){ return 1.0 -
          ↪ 0.5*element.particleState.solidToLiquidProgress -
          ↪ 0.5*element.particleState.liquidToGasProgress; }
156      idealSeparationCalculator: priv_idealSeparationCalculator
157  }
158  Exclusion{ //Repulsion that keeps particles strictly apart
159      epsilon: 500 //Force strength parameter
160      separation: function(element1, element2){
161          return 65 +
162              20*(element1.particleState.liquidToGasProgress +
          ↪ element2.particleState.liquidToGasProgress)/2 +
163              110*(element1.particleState.gasProgress +
          ↪ element2.particleState.gasProgress)/2;
164      }
165  }
166  SlidingForce{ //Force and that creates the signature sliding liquid motion
167      epsilon: 490 //Force strength parameter
168      weight: function(element){
169          return 0.45*element.particleState.solidToLiquidProgress
170              + 0.55*element.particleState.liquidProgress
171              - 1.0*element.particleState.liquidToGasProgress
172      }
173      halfCoverageCalculator: priv_halfCoverageCalculator
174      idealSeparationCalculator: priv_idealSeparationCalculator
175  }
176  }

```

Listing B.1 – Particles in Matter source code continued, part 5 of 5.

Bibliography

- [1] Seymour Papert. *Mindstorms: Children, Computers, and Powerful Ideas*. Basic Books, Inc., 1980. ISBN 0-465-04627-4. (Cited on page 2.)
- [2] Jean Piaget. *The Construction Of Reality In The Child*. Routledge, 1954. ISBN 0415-21000-3. (Cited on page 2.)
- [3] Walter Gander, Antoine Petit, Gérard Berry, Barbara Demo, Jan Vahrenhold, Andrew McGettrick, Roger Boyle, Michèle Drechsler, Avi Mendelson, Chris Stephenson, Carlo Ghezzi, and Bertrand Meyer. “Informatics education: Europe cannot afford to miss the boat, Report of the joint Informatics Europe & ACM Europe Working Group on Informatics Education”, 2013.
URL:<http://europe.acm.org/iereport/ie.html>. (Cited on page 3.)
- [4] Namin Shin and Sangah Kim. “Learning about, from, and with Robots: Students’ Perspectives”. In *IEEE International Symposium on Robot and Human Interactive Communication (RO-MAN)*, 2007.
URL:<https://doi.org/10.1109/ROMAN.2007.4415235>. (Cited on page 3.)
- [5] EunKyoung Lee, YoungJun Lee, Bokyoung Kye, and Beomseog Ko. “Elementary and Middle School Teachers’ Students’ and Parents’ Perception of Robot-Aided Education in Korea”. In *EdMedia: World Conference on Educational Media and Technology*, pages 175–183, 2008.
URL:<https://www.learntechlib.org/p/28391>. (Cited on page 3.)
- [6] Omar Mubin, Catherine J. Stevens, Suleman Shahid, Abdullah Al Mahmud, and Jian-Jie Dong. “A review of the applicability of robots in education”. *Technology for Education and Learning*, 1:1–7, 2013.
URL:<https://doi.org/10.2316/Journal.209.2013.1.209-0015>. (Cited on page 3.)
- [7] Marina Fridin and Mark Belokopytov. “Acceptance of Socially Assistive Humanoid Robot by Preschool and Elementary School Teachers”. *Computers in Human Behavior*, 33:23–31, 2014.
URL:<https://doi.org/10.1016/j.chb.2013.12.016>. (Cited on page 3.)
- [8] Sofia Serholt, Wolmet Barendregt, Iolanda Leite, Helen Hastie, Aidan Jones, Ana Paiva, Asimina Vasalou, and Ginevra Castellano. “Teachers’ Views on the Use of Empathic Robotic Tutors in the Classroom”. In *IEEE International Symposium on Robot and Human Interactive Communication (RO-MAN)*, pages 955–960, 2014.
URL:<https://doi.org/10.1109/ROMAN.2014.6926376>. (Cited on page 3.)
- [9] Natalia Reich-Stiebert and Friederike Eyssel. “Learning with Educational Companion Robots? Toward Attitudes on Education Robots, Predictors of Attitudes, and Application Potentials for Education Robots”. *International Journal of Social Robotics*, 7(5):875–888, 2015.
URL:<https://doi.org/10.1007/s12369-015-0308-9>. (Cited on page 3.)
- [10] James Kennedy, Séverin Lemaignan, and Tony Belpaeme. “The Cautious Attitude of Teachers Towards Social Robots in Schools”. In *21th IEEE International Symposium in Robot and Human Interactive Communication, Workshop on Robots for Learning*, 2016. (Cited on page 3.)

Bibliography

- [11] David P. Miller, Illah R. Nourbakhsh, and Roland Siegwart. “Robots for Education”. In *Springer Handbook of Robotics*, pages 1283–1301. Springer, 2008.
URL:https://doi.org/10.1007/978-3-540-30301-5_56. (Cited on page 6.)
- [12] Chris Rogers and Merredith Portsmore. “Bringing Engineering to Elementary School”. *Journal of STEM Education: Innovations and Research*, 5(3):17–28, 2004.
URL:<https://search.proquest.com/docview/222795467>. (Cited on pages 6 and 10.)
- [13] Jeffrey Johnson. “Children, robotics, and education”. *Artificial Life and Robotics*, 7(1):16–21, 2003.
URL:<https://doi.org/10.1007/BF02480880>. (Cited on page 6.)
- [14] Maja J. Matarić, Nathan P. Koenig, and David Feil-Seifer. “Materials for Enabling Hands-On Robotics and STEM Education”. In *AAAI Spring Symposium: Semantic Scientific Knowledge Integration*, pages 99–102, 2007.
URL:<https://aaai.org/Papers/Symposia/Spring/2007/SS-07-09/SS07-09-022.pdf>. (Cited on page 6.)
- [15] Orazio Miglino, Henrik Hautop Lund, and Maurizio Cardaci. “Robotics as an Educational Tool”. *Journal of Interactive Learning Research*, 10(1):25–47, 1999.
URL:<https://www.learntechlib.org/p/9274/>. (Cited on page 6.)
- [16] Joshua E. Auerbach, Deniz Aydin, Andrea Maesani, Przemyslaw M. Kornatowski, Titus Cieslewski, Grégoire Heitz, Pradeep R. Fernando, Ilya Loshchilov, Ludovic Daler, and Dario Floreano. “RoboGen: Robot Generation through Artificial Evolution”. In *Artificial Life 14: Proceedings of the Fourteenth International Conference on the Synthesis and Simulation of Living Systems*, 2014.
URL:<https://doi.org/10.7551/978-0-262-32621-6-ch022>. (Cited on page 6.)
- [17] Mohammad Ehsanul Karim, Séverin Lemaignan, and Francesco Mondada. “A review: Can robots reshape K-12 STEM education?”. In *IEEE International Workshop on Advanced Robotics and its Social Impacts (ARSO)*, pages 1–8, 2015.
URL:<https://doi.org/10.1109/ARSO.2015.7428217>. (Cited on page 7.)
- [18] Fabiane Barreto Vavassori Benitti. “Exploring the educational potential of robotics in schools: A systematic review”. *Computers & Education*, 58(3):978–988, 2012.
URL:<https://doi.org/10.1016/j.compedu.2011.10.006>. (Cited on page 7.)
- [19] Rhys Jones, Patrick Haufe, Edward Sells, Pejman Iravani, Vik Olliver, Chris Palmer, and Adrian Bowyer. “RepRap – the replicating rapid prototyper”. *Robotica*, 29(1):177–191, 2011.
URL:<https://doi.org/10.1017/S026357471000069X>. (Cited on page 8.)
- [20] Matt Richardson and Shawn Wallace. *Getting Started with Raspberry Pi*. Maker Media, Inc., 3rd edition, 2016. ISBN 978-1-680-45246-4. (Cited on page 8.)
- [21] Mark Rollins. *Beginning LEGO MINDSTORMS EV3*. Apress, 2014. ISBN 978-1-4302-6437-8.
URL:<https://doi.org/10.1007/978-1-4302-6437-8>. (Cited on page 8.)
- [22] Árpád Takács, György Eigner, Levente Kovács, Imre J. Rudas, , and Tamás Haidegger. “Teacher’s Kit: Development, Usability, and Communities of Modular Robotic Kits for Classroom Education”. *IEEE Robotics & Automation Magazine*, 23(2):30–39, 2016.
URL:<https://doi.org/10.1109/MRA.2016.2548754>. (Cited on page 8.)
- [23] Chi N. Thai. *Exploring Robotics with ROBOTIS Systems*. Springer, Cham, 2015. ISBN 978-3-319-20417-8.
URL:<https://doi.org/10.1007/978-3-319-20418-5>. (Cited on page 8.)

- [24] Hayes Solos Raffle, Amanda J. Parkes, and Hiroshi Ishii. "Topobo: A Constructive Assembly System with Kinetic Memory". In *Proceedings of the SIGCHI Conference on Human Factors in Computing Systems (CHI)*, pages 647–654, 2004.
URL:<https://doi.org/10.1145/985692.985774>. (Cited on page 8.)
- [25] Eric Schweikardt and Mark D. Gross. "roBlocks: A Robotic Construction Kit for Mathematics and Science Education". In *8th International Conference on Multimodal Interfaces (ICMI)*, pages 72–75, 2006.
URL:<https://doi.org/10.1145/1180995.1181010>. (Cited on page 8.)
- [26] Francesco Mondada, Michael Bonani, Xavier Raemy, James Pugh, Christopher Cianci, Adam Klapotocz, Stephane Magnenat, Jean-Christophe Zufferey, Dario Floreano, and Alcherio Martinoli. "The e-puck, a Robot Designed for Education in Engineering". In *9th Conference on Autonomous Robot Systems and Competitions*, volume 1, pages 59–65, 2009.
URL:<https://infoscience.epfl.ch/record/135236>. (Cited on pages 8, 9, and 133.)
- [27] Marco Ruzzenente, Moreno Koo, Katherine Nielsen, Lorenzo Grespan, and Paolo Fiorini. "A Review of Robotics Kits for Tertiary Education". In *Proceedings of 3rd International Workshop Teaching Robotics, Teaching with Robotics: Integrating Robotics in School Curriculum*, pages 153–162, 2012.
URL:<http://citeseerx.ist.psu.edu/viewdoc/summary?doi=10.1.1.458.9540>. (Cited on page 8.)
- [28] Francesco Mondada, Michael Bonani, Fanny Riedo, Manon Briod, Léa Pereyre, Philippe Rétornaz, and Stéphane Magnenat. "Bringing Robotics to Formal Education: The Thymio Open-Source Hardware Robot". *IEEE Robotics & Automation Magazine*, 24(1):77–85, 2017.
URL:<https://doi.org/10.1109/MRA.2016.2636372>. (Cited on page 8.)
- [29] Michael Rubenstein, Bo Cimino, Radhika Nagpal, and Justin Werfel. "AERobot: An Affordable One-Robot-Per-Student System for Early Robotics Education". In *IEEE International Conference on Robotics and Automation (ICRA)*, pages 6107–6113, 2015.
URL:<https://doi.org/10.1109/ICRA.2015.7140056>. (Cited on page 8.)
- [30] Marina U. Bers, Iris Ponte, Catherine Juelich, Alison Viera, and Jonathan Schenker. "Teachers as Designers: Integrating Robotics in Early Childhood Education". *Information Technology in Childhood Education Annual*, 2002(1):123–145, 2002.
URL:<https://www.learntechlib.org/p/8850>. (Cited on page 9.)
- [31] Amanda Sullivan, Elizabeth R. Kazakoff, and Marina Umashi Bers. "The Wheels on the Bot Go Round and Round: Robotics Curriculum in Pre-Kindergarten". *Journal of Information Technology Education: Innovations in Practice*, 12, 2013.
URL:<https://eric.ed.gov/?id=EJ1027385>. (Cited on pages 9 and 18.)
- [32] Erin Cejka, Chris Rogers, and Merredith Portsmore. "Kindergarten Robotics: Using Robotics to Motivate Math, Science, and Engineering Literacy in Elementary School". *International Journal of Engineering Education*, 22(4):711, 2006.
URL:https://www.ijee.ie/articles/Vol22-4/03_ijee1804.pdf. (Cited on page 9.)
- [33] Fanny Riedo, Morgane Chevalier, Stéphane Magnenat, and Francesco Mondada. "Thymio II, a robot that grows wiser with children". In *IEEE Workshop on Advanced Robotics and its Social Impacts (ARSO)*, pages 187–193, 2013.
URL:<https://doi.org/10.1109/ARSO.2013.6705527>. (Cited on page 9.)
- [34] Amanda Sullivan and Marina Umaschi Bers. "Gender differences in kindergarteners' robotics and programming achievement". *International Journal of Technology and Design Education*, 23(3):691–702, 2013.
URL:<https://doi.org/10.1007/s10798-012-9210-z>. (Cited on page 9.)

Bibliography

- [35] Martin Kandlhofer, Gerald Steinbauer, Sabine Hirschmugl-Gaisch, and Johann Eck. "Children discover science: robotics, informatics and artificial intelligence in kindergarten and school". In *Workshop position paper at International Conference on Robotics in Education (RiE)*, 2015. (Cited on page 9.)
- [36] Elizabeth Sklar, Amy Eguchi, and Jeffrey Johnson. "RoboCupJunior: Learning with Educational Robotics". In *RoboCup 2002: Robot Soccer World Cup VI*, pages 238–253, 2002.
URL:https://doi.org/10.1007/978-3-540-45135-8_18. (Cited on pages 9 and 18.)
- [37] Bradley S. Barker and John Ansoerge. "Robotics as Means to Increase Achievement Scores in an Informal Learning Environment". *Journal of Research on Technology in Education*, 39(3):229–243, 2007.
URL:<https://doi.org/10.1080/15391523.2007.10782481>. (Cited on page 9.)
- [38] Florence R. Sullivan. "Robotics and science literacy: Thinking skills, science process skills and systems understanding". *Journal of Research in Science Teaching*, 45(3):373–394, 2008.
URL:<https://doi.org/10.1002/tea.20238>. (Cited on page 9.)
- [39] Kathy A. Mills, Vinesh Chandra, and Ji Yong Park. "The architecture of children's use of language and tools when problem solving collaboratively with robotics". *The Australian Educational Researcher*, 40(3):315–337, 2013.
URL:<https://doi.org/10.1007/s13384-013-0094-z>. (Cited on page 9.)
- [40] Timothy T. Yuen, Melanie Boecking, Erin Price Tiger, Alvaro Gomez, Adrienne Guillen, Analisa Arreguin, and Jennifer Stone. "Group Tasks, Activities, Dynamics, and Interactions in Collaborative Robotics Projects with Elementary and Middle School Children". *Journal of STEM Education: Innovations and Research*, 15(1):39, 2014.
URL:<https://search.proquest.com/docview/1528858640>. (Cited on page 9.)
- [41] Michelle E. Jordan and Reuben R. McDaniel Jr. "Managing Uncertainty During Collaborative Problem Solving in Elementary School Teams: The Role of Peer Influence in Robotics Engineering Activity". *Journal of the Learning Sciences*, 23(4):490–536, 2014.
URL:<https://doi.org/10.1080/10508406.2014.896254>. (Cited on page 9.)
- [42] David Scaradozzi, Laura Sorbi, Anna Pedale, Marian Antonietta Valzano, and Cinzia Vergine. "Teaching robotics at the primary school: an innovative approach". *Procedia - Social and Behavioral Sciences*, 174:3838–3846, 2015.
URL:<https://doi.org/10.1016/j.sbspro.2015.01.1122>. (Cited on page 9.)
- [43] Joan M. Chambers, Mike Carbonaro, and Marion Rex. "Scaffolding Knowledge Construction through Robotic Technology: A Middle School Case Study". *Electronic Journal for the Integration of Technology in Education*, 6:55–70, 2007.
URL:<https://citeseerx.ist.psu.edu/viewdoc/summary?doi=10.1.1.89.5944>. (Cited on page 9.)
- [44] Barbara Ericson, Mark Guzdial, and Maureen Biggers. "Improving Secondary CS Education: Progress and Problems". In *Proceedings of the 38th SIGCSE Technical Symposium on Computer Science Education*, volume 39, pages 298–301, 2007.
URL:<https://doi.org/10.1145/1227504.1227416>. (Cited on page 9.)
- [45] Gwen Nugent, Bradley Barker, Neal Grandgenett, and Viacheslav I. Adamchuk. "Impact of Robotics and Geospatial Technology Interventions on Youth STEM Learning and Attitudes". *Journal of Research on Technology in Education*, 42(4):391–408, 2010.
URL:<https://doi.org/10.1080/15391523.2010.10782557>. (Cited on page 9.)
- [46] Renata Burbaite, Vytautas Stuiikys, and Robertas Damasevicius. "Educational Robots as Collaborative Learning Objects for Teaching Computer Science". In *IEEE International Conference on System Science and Engineering (ICSSE)*, pages 211–216, 2013.
URL:<https://doi.org/10.1109/ICSSE.2013.6614661>. (Cited on page 9.)

- [47] David J. Barnes. "Teaching Introductory Java Through LEGO MINDSTORMS Models". In *Proceedings of the 33rd SIGCSE Technical Symposium on Computer Science Education*, pages 147–151, 2002.
URL:<https://doi.org/10.1145/563340.563397>. (Cited on page 9.)
- [48] Pamela B. Lawhead, Michaele E. Duncan, Constance G. Bland, Michael Goldweber, Madeleine Schep, David J. Barnes, and Ralph G. Hollingsworth. "A Road Map for Teaching Introductory Programming Using LEGO® Mindstorms Robots". *Working Group Reports from ITiCSE on Innovation and Technology in Computer Science Education*, 35(2):191–201, 2002.
URL:<https://doi.org/10.1145/782941.783002>. (Cited on page 9.)
- [49] Frank Klassner. "A Case Study of LEGO Mindstorms™ Suitability for Artificial Intelligence and Robotics Courses at the College Level". *ACM SIGCSE Bulletin - Inroads: paving the way towards excellence in computing education*, 34(1):8–12, 2002.
URL:<https://doi.org/10.1145/563517.563345>. (Cited on page 9.)
- [50] Frank Klassner and Scott D. Anderson. "LEGO MindStorms: Not Just for K-12 Anymore". *IEEE Robotics & Automation Magazine*, 10(2):12–18, 2003.
URL:<https://doi.org/10.1109/MRA.2003.1213611>. (Cited on page 9.)
- [51] Tucker Balch, Jay Summet, Doug Blank, Deepak Kumar, Mark Guzdial, Keith O'Hara, Daniel Walker, Monica Sweat, Gaurav Gupta, Stewart Tansley, Jared Jackson, Mansi Gupta, Marwa Nur Muhammad, Shikha Prasad, Natasha Eilbert, and Ashley Gavin. "Designing Personal Robots for Education: Hardware, Software, and Curriculum". *IEEE Pervasive Computing*, 7(2):5–9, 2008.
URL:<https://doi.org/10.1109/MPRV.2008.29>. (Cited on page 9.)
- [52] Seung Han Kim and Jae Wook Jeon. "Introduction for Freshmen to Embedded Systems Using LEGO Mindstorms". *IEEE Transactions on Education*, 52(1):99–108, 2009.
URL:<https://doi.org/10.1109/TE.2008.919809>. (Cited on page 9.)
- [53] Michael W. Lew, Thomas B. Horton, and Mark S. Sherriff. "Using LEGO MINDSTORMS NXT and LEJOS in an Advanced Software Engineering Course". In *23rd IEEE Conference on Software Engineering Education and Training (CSEE&T)*, pages 121–128, 2010.
URL:<https://doi.org/10.1109/CSEET.2010.31>. (Cited on page 9.)
- [54] Alexander Behrens, Linus Atorf, Robert Schwann, Bernd Neumann, Rainer Schnitzler, Johannes Balle, Thomas Herold, Aulis Telle, Tobias G. Noll, Kay Hameyer, and Til Aach. "MATLAB Meets LEGO Mindstorms—A Freshman Introduction Course Into Practical Engineering". *IEEE Transactions on Education*, 53(2):306–317, 2010.
URL:<https://doi.org/10.1109/TE.2009.2017272>. (Cited on page 9.)
- [55] Jesús M. Gomez de Gabriel, Anthony Mandow, Jesús Fernandez-Lozano, and Alfonso J. Garcia-Cerezo. "Using LEGO NXT Mobile Robots With LabVIEW for Undergraduate Courses on Mechatronics". *IEEE Transactions on Education*, 54(1):41–47, 2011.
URL:<https://doi.org/10.1109/TE.2010.2043359>. (Cited on page 9.)
- [56] Ana Cruz-Martín, Juan-Antonio Fernández-Madrigal, Cipriano Galindo, Javier González-Jiménez, Corin Stockmans-Daou, and José-Luis Blanco-Claraco. "A LEGO Mindstorms NXT approach for teaching at Data Acquisition, Control Systems Engineering and Real-Time Systems undergraduate courses". *Computers & Education*, 59(3):974–988, 2012.
URL:<https://doi.org/10.1016/j.compedu.2012.03.026>. (Cited on page 9.)
- [57] Amruth N. Kumar. "Three Years of Using Robots in an Artificial Intelligence Course: Lessons Learned". *Journal on Educational Resources in Computing (JERIC) - Special issue on robotics in undergraduate education*, 4(3), 2004.
URL:<https://doi.org/10.1145/1083310.1083311>. (Cited on page 9.)

Bibliography

- [58] Olivier Michel. "Cyberbotics Ltd. Webots™: Professional Mobile Robot Simulation". *International Journal of Advanced Robotic Systems*, 1(1):39–42, 2004.
URL:<https://doi.org/10.5772/5618>. (Cited on page 9.)
- [59] Stefano Carpin, Mike Lewis, Jijun Wang, Stephen Balakirsky, and Chris Scrapper. "USARSim: a robot simulator for research and education". In *IEEE International Conference on Robotics and Automation (ICRA)*, pages 1400–1405, 2007.
URL:<https://doi.org/10.1109/ROBOT.2007.363180>. (Cited on page 9.)
- [60] Carlos A. Jara, Francisco A. Candelas, Santiago T. Puente, and Fernando Torres. "Hands-on experiences of undergraduate students in Automatics and Robotics using a virtual and remote laboratory". *Computers & Education*, 57(4):2451–2461, 2011.
URL:<https://doi.org/10.1016/j.compedu.2011.07.003>. (Cited on page 9.)
- [61] Eric Rohmer, Surya P. N. Singh, and Marc Freese. "V-REP: a Versatile and Scalable Robot Simulation Framework". In *IEEE/RSJ International Conference on Intelligent Robots and Systems (IROS)*, pages 1321–1326, 2013.
URL:<https://doi.org/10.1109/IROS.2013.6696520>. (Cited on page 9.)
- [62] Shakir Hussain, Jörgen Lindh, and Ghazi Shukur. "The effect of LEGO Training on Pupils' School Performance in Mathematics, Problem Solving Ability and Attitude: Swedish Data". *Journal of Educational Technology & Society*, 9(3):182–194, 2006.
URL:<https://www.jstor.org/stable/jeductechsoci.9.3.182>. (Cited on page 10.)
- [63] Irina Igel, Ronald Leonel Poveda, Vikram Kapila, and Magued G. Iskander. "Enriching K-12 Math Education Using LEGOs". In *American Society for Engineering Education (ASEE) Annual Conference & Exposition*, 2011.
URL:<https://peer.asee.org/17910>. (Cited on page 10.)
- [64] Stephen Norton. "Using Lego Construction to Develop Ratio Understanding". *Mathematics Education for the Third Millennium: Towards 2010*, pages 414–421, 2004.
URL:<https://citeseerx.ist.psu.edu/viewdoc/summary?doi=10.1.1.520.4837>.
(Cited on pages 10 and 18.)
- [65] Marina U. Bers and Merredith Portsmore. "Teaching Partnerships: Early Childhood and Engineering Students Teaching Math and Science Through Robotics". *Journal of Science Education and Technology*, 14(1):59–73, 2005.
URL:<https://doi.org/10.1007/s10956-005-2734-1>. (Cited on page 10.)
- [66] Kate Highfield. "Robotic Toys as a Catalyst for Mathematical Problem Solving". *Australian Primary Mathematics Classroom*, 15(2):22–27, 2010.
URL:<https://www.learntechlib.org/p/65024>. (Cited on page 10.)
- [67] Eli Silk and Christian Schunn. "Using Robotics to Teach Mathematics: Analysis of a Curriculum Designed and Implemented". In *American Society for Engineering Education (ASEE) Annual Conference & Exposition*, 2008.
URL:<https://peer.asee.org/3764>. (Cited on page 10.)
- [68] Douglas C. Williams, Yuxin Ma, Louise Prejean, Mary Jane Ford, and Guolin Lai. "Acquisition of Physics Content Knowledge and Scientific Inquiry Skills in a Robotics Summer Camp". *Journal of Research on Technology in Education*, 40(2):201–216, 2007.
URL:<https://doi.org/10.1080/15391523.2007.10782505>. (Cited on page 10.)
- [69] Dimitris Alimisis. "Robotics in Education & Education in Robotics: Shifting Focus from Technology to Pedagogy". In *Proceedings of the 3rd International Conference on Robotics in Education (RiE)*, pages 7–14, 2012.
(Cited on page 10.)

- [70] Tassos A. Mikropoulos and Ioanna Bellou. "Educational Robotics as Mindtools". *Themes in Science and Technology Education*, 6(1):5–14, 2013.
URL:<https://www.learnstechlib.org/p/148612>. (Cited on page 10.)
- [71] Morgane Chevalier, Fanny Riedo, and Francesco Mondada. "Pedagogical Uses of Thymio II: How Do Teachers Perceive Educational Robots in Formal Education?". *IEEE Robotics & Automation Magazine*, 23(2):16–23, 2016.
URL:<https://doi.org/10.1109/MRA.2016.2535080>. (Cited on page 10.)
- [72] L. Elena Whittier and Michael Robinson. "Teaching Evolution to Non-English Proficient Students by Using Lego Robotics". *American Secondary Education*, 35(3):19–28, 2007.
URL:<https://www.jstor.org/stable/41406087>. (Cited on pages 10 and 18.)
- [73] Dan Cuperman and Igor M. Verner. "Learning through creating robotic models of biological systems". *International Journal of Technology and Design Education*, 23(4):849–866, 2013.
URL:<https://doi.org/10.1007/s10798-013-9235-y>. (Cited on page 10.)
- [74] Audrey Randall, John Klingner, and Nikolaus Correll. "Simulating Chemical Reactions Using a Swarm of Miniature Robots". In *From Animals to Animats 14: 14th International Conference on Simulation of Adaptive Behavior*, pages 305–316, 2016.
URL:https://doi.org/10.1007/978-3-319-43488-9_27. (Cited on pages 10 and 134.)
- [75] Michael A. Goodrich and Alan C. Schultz. "Human-Robot Interaction: A Survey". *Foundations and Trends in Human-Computer Interaction*, 1(3):203–275, 2008.
URL:<https://doi.org/10.1561/1100000005>. (Cited on page 11.)
- [76] Patrícia Alves-Oliveira, Patrícia Arriaga, Ana Paiva, and Guy Hoffman. "YOLO, a Robot for Creativity: A Co-Design Study with Children". In *Conference on Interaction Design and Children (IDC)*, pages 423–429, 2017.
URL:<https://doi.org/10.1145/3078072.3084304>. (Cited on page 11.)
- [77] Patrícia Alves-Oliveira, Patrícia Arriaga, Guy Hoffman, and Ana Paiva. "Representation of Movement for Robots with Personality: A Co-Design study with Small Groups of Children". In *IEEE International Symposium on Robot and Human Interactive Communication (RO-MAN)*, 2017. (Cited on page 11.)
- [78] Kazuyoshi Wada, Takanori Shibata, Tomoko Saito, and Kazuo Tanie. "Effects of Robot-Assisted Activity for Elderly People and Nurses at a Day Service Center". *Proceedings of the IEEE*, 92(11):1780–1788, 2004.
URL:<https://doi.org/10.1109/JPROC.2004.835378>. (Cited on page 11.)
- [79] Iain Werry, Kerstin Dautenhahn, Bernard Ogden, and William Harwin. "Can Social Interaction Skills Be Taught by a Social Agent? The Role of a Robotic Mediator in Autism Therapy". *Cognitive Technology: Instruments of Mind*, pages 57–74, 2001.
URL:https://doi.org/10.1007/3-540-44617-6_6. (Cited on page 11.)
- [80] Ben Robins, Kerstin Dautenhahn, Rene te Boekhorst, and Aude Billard. "Effects of Repeated Exposure to a Humanoid Robot on Children with Autism". *Designing a More Inclusive World*, pages 225–236, 2004.
URL:https://doi.org/10.1007/978-0-85729-372-5_23. (Cited on page 11.)
- [81] Ginevra Castellano, Ana Paiva, Arvid Kappas, Ruth Aylett, Helen Hastie, Wolmet Barendregt, Fernando Nabais, and Susan Bull. "Towards Empathic Virtual and Robotic Tutors". In *International Conference on Artificial Intelligence in Education*, pages 733–736, 2013.
URL:https://doi.org/10.1007/978-3-642-39112-5_100. (Cited on page 11.)
- [82] Fumihide Tanaka, Aaron Cicourel, and Javier R. Movellan. "Socialization between toddlers and robots at an early childhood education center". *Proceedings of the National Academy of Sciences*, 104(46):17954–17958,

Bibliography

2007.
URL:<https://doi.org/10.1073/pnas.0707769104>. (Cited on page 11.)
- [83] Catherine C. Chase, Doris B. Chin, Marily A. Oppezzo, and Daniel L. Schwartz. “Teachable Agents and the Protégé Effect: Increasing the Effort Towards Learning”. *Journal of Science Education and Technology*, 18(4): 334–352, 2009.
URL:<https://doi.org/10.1007/s10956-009-9180-4>. (Cited on page 11.)
- [84] Fumihide Tanaka and Shizuko Matsuzoe. “Children Teach a Care-Receiving Robot to Promote Their Learning: Field Experiments in a Classroom for Vocabulary Learning”. *Journal of Human-Robot Interaction*, 1(1), 2012.
URL:<https://doi.org/10.5898/JHRI.1.1.Tanaka>. (Cited on pages 11 and 12.)
- [85] Fumihide Tanaka, Kyosuke Isshiki, Fumiki Takahashi, Manabu Uekusa, Rumiko Sei, and Kaname Hayashi. “Pepper Learns Together with Children: Development of an Educational Application”. In *15th IEEE-RAS International Conference on Humanoid Robots (Humanoids)*, pages 270–275, 2015.
URL:<https://doi.org/10.1109/HUMANOIDS.2015.7363546>. (Cited on pages 11 and 12.)
- [86] Séverin Lemaignan, Alexis Jacq, Deanna Hood, Fernando Garcia, Ana Paiva, and Pierre Dillenbourg. “Learning by Teaching a Robot: The Case of Handwriting”. *IEEE Robotics Automation Magazine*, 23(2):56–66, 2016.
URL:<https://doi.org/10.1109/MRA.2016.2546700>. (Cited on pages 11 and 12.)
- [87] Tanya N. Beran, Alejandro Ramirez-Serrano, Roman Kuzyk, Meghann Fior, and Sarah Nugent. “Understanding how children understand robots: Perceived animism in child–robot interaction”. *International Journal of Human-Computer Studies*, 69(7):539–550, 2011.
URL:<https://doi.org/10.1016/j.ijhcs.2011.04.003>. (Cited on page 12.)
- [88] Tony Belpaeme, Paul E. Baxter, Robin Read, Rachel Wood, Heriberto Cuayáhuitl, Bernd Kiefer, Stefania Racioppa, Ivana Kruijff-Korbayová, Georgios Athanasopoulos, Valentin Enescu, Rosemarijn Looije, Mark Neerinx, Yiannis Demiris, Raquel Ros-Espinoza, Aryel Beck, Lola Cañamero, Antione Hiolle, Matthew Lewis, Ilaria Baroni, Marco Nalin, Piero Cosi, Giulio Paci, Fabio Tesser, Giacomo Sommovilla, and Remi Humbert. “Multimodal child-robot interaction: Building social bonds”. *Journal of Human-Robot Interaction*, 1(2):33–53, 2012.
URL:<https://doi.org/10.5898/JHRI.1.2.Belpaeme>. (Cited on page 12.)
- [89] Takayuki Kanda, Takayuki Hirano, Daniel Eaton, and Hiroshi Ishiguro. “Interactive Robots as Social Partners and Peer Tutors for Children: A Field Trial”. *Human-Computer Interaction*, 19(1):61–84, 2004.
URL:<https://dl.acm.org/citation.cfm?id=1466551>. (Cited on page 12.)
- [90] Jeonghye Han, Miheon Jo, Sungju Park, and Sungho Kim. “The Educational Use of Home Robots for Children”. In *IEEE International Workshop on Robot and Human Interactive Communication (RO-MAN)*, pages 378–383, 2005.
URL:<https://doi.org/10.1109/ROMAN.2005.1513808>. (Cited on page 12.)
- [91] Jeonghye Han and Dongho Kim. “r-Learning Services for Elementary School Students with a Teaching Assistant Robot”. In *4th ACM/IEEE International Conference on Human-Robot Interaction (HRI)*, pages 255–256, 2009.
URL:<https://doi.org/10.1145/1514095.1514163>. (Cited on page 12.)
- [92] Chih-Wei Chang, Jih-Hsien Lee, Po-Yao Chao, Chin-Yeh Wang, and Gwo-Dong Chen. “Exploring the Possibility of Using Humanoid Robots as Instructional Tools for Teaching a Second Language in Primary School”. *Educational Technology & Society*, 13(2):13–24, 2010.
URL:<https://www.jstor.org/stable/jeductechsoci.13.2.13>. (Cited on page 12.)

- [93] Tony Belpaeme, James Kennedy, Paul Baxter, Paul Vogt, Emiel E.J. Krahmer, Stefan Kopp, Kirsten Bergmann, Paul Leseman, Aylin C. Küntay, Tilbe Gökşun, Amit K. Pandey, Rodolphe Gelin, Petra Koudelkova, and Tommy Deblieck. “L2TOR - Second Language Tutoring using Social Robots”. In *Proceedings of 1st International Workshop on Educational Robots (WONDER)*, 2015. (Cited on page 12.)
- [94] Goren Gordon, Samuel Spaulding, Jacqueline Kory Westlund, Jin Joo Lee, Luke Plummer, Marayna Martinez, Madhurima Das, and Cynthia Breazeal. “Affective Personalization of a Social Robot Tutor for Children’s Second Language Skills”. In *Proceedings of the Thirtieth AAAI Conference on Artificial Intelligence*, pages 3951–3957, 2016.
URL:<https://dl.acm.org/citation.cfm?id=3016387.3016461>. (Cited on page 12.)
- [95] James Kennedy, Paul Baxter, Emmanuel Senft, and Tony Belpaeme. “Social Robot Tutoring for Child Second Language Learning”. In *11th ACM/IEEE International Conference on Human-Robot Interaction (HRI)*, pages 231–238, 2016.
URL:<https://doi.org/10.1109/HRI.2016.7451757>. (Cited on page 12.)
- [96] Hatice Kose, Neziha Akalin, and Pinar Uluer. “Socially Interactive Robotic Platforms as Sign Language Tutors”. *International Journal of Humanoid Robotics*, 11(01):1450003, 2014.
URL:<https://doi.org/10.1142/S0219843614500030>. (Cited on page 12.)
- [97] Joris B. Janssen, Chrissy C. van der Wal, Mark A. Neerinx, and Rosemarijn Looije. “Motivating Children to Learn Arithmetic with an Adaptive Robot Game”. In *International Conference on Social Robotics (ICSR)*, pages 153–162, 2011.
URL:https://doi.org/10.1007/978-3-642-25504-5_16. (Cited on page 12.)
- [98] LaVonda Brown and Ayanna M. Howard. “Engaging Children in Math Education using a Socially Interactive Humanoid Robot”. In *13th IEEE-RAS International Conference on Humanoid Robots (Humanoids)*, pages 183–188, 2013.
URL:<https://doi.org/10.1109/HUMANOIDS.2013.7029974>. (Cited on page 12.)
- [99] James Kennedy, Paul Baxter, and Tony Belpaeme. “The Robot Who Tried Too Hard: Social Behaviour of a Robot Tutor Can Negatively Affect Child Learning”. In *Proceedings of the Tenth Annual ACM/IEEE International Conference on Human-Robot Interaction (HRI)*, pages 67–74, 2015.
URL:<https://doi.org/10.1145/2696454.2696457>. (Cited on page 12.)
- [100] Olivier A. Blanson Henkemans, Bert P.B. Bierman, Joris Janssen, Mark A. Neerinx, Rosemarijn Looije, Hanneke van der Bosch, and Jeanine A.M. van der Giessen. “Using a robot to personalise health education for children with diabetes type 1: A pilot study”. *Patient Education and Counseling*, 92(2):174–181, 2013.
URL:<https://doi.org/10.1016/j.pec.2013.04.012>. (Cited on page 12.)
- [101] Elaine Short, Katelyn Swift-Spong, Jillian Greczek, Aditi Ramachandran, Alexandru Litoiu, Elena Corina Grigore, David Feil-Seifer, Samuel Shuster, Jin Joo Lee, Shaobo Huang, Svetlana Levonisova, Sarah Litz, Jamy Li, Gisele Ragusa, Donna Spruijt-Metz, Maja Matarić, and Brian Scassellati. “How to Train Your DragonBot: Socially Assistive Robots for Teaching Children About Nutrition Through Play”. In *IEEE International Symposium on Robot and Human Interactive Communication (RO-MAN)*, pages 924–929, 2014.
URL:<https://doi.org/10.1109/ROMAN.2014.6926371>. (Cited on page 12.)
- [102] Iolanda Leite, Marissa McCoy, Monika Lohani, Daniel Ullman, Nicole Salomons, Charlene Stokes, Susan Rivers, and Brian Scassellati. “Emotional Storytelling in the Classroom: Individual versus Group Interaction between Children and Robots”. In *ACM/IEEE International Conference on Human-Robot Interaction (HRI)*, pages 75–82, 2015.
URL:<https://doi.org/10.1145/2696454.2696481>. (Cited on page 12.)
- [103] Raquel Ros, Ilaria Baroni, and Yiannis Demiris. “Adaptive human–robot interaction in sensorimotor task instruction: From human to robot dance tutors”. *Robotics and Autonomous Systems*, 62(6):707–720, 2014.
URL:<https://doi.org/10.1016/j.robot.2014.03.005>. (Cited on page 12.)

Bibliography

- [104] Pierre Dillenbourg, Guillaume Zufferey, Hamed Alavi, Patrick Jermann, Son Do-Lenh, Quentin Bonnard, Sébastien Cuendet, and Frédéric Kaplan. “Classroom Orchestration: The Third Circle of Usability”. In *Connecting Computer-Supported Collaborative Learning to Policy and Practice: CSCL2011 Conference Proceedings*, volume 1, pages 510–517, 2011.
URL:<https://infoscience.epfl.ch/record/168741>. (Cited on page 18.)
- [105] Rainer Mautz. *Indoor Positioning Technologies*. Habilitation thesis, ETH Zürich, 2012.
URL:<https://doi.org/10.3929/ethz-a-007313554>. (Cited on pages 24, 25, and 26.)
- [106] Martin Kaltenbrunner and Ross Bencina. “reacTIVision: A Computer-vision Framework for Table-based Tangible Interaction”. In *1st International Conference on Tangible and Embedded Interaction (TEI)*, pages 69–74, 2007.
URL:<https://doi.org/10.1145/1226969.1226983>. (Cited on page 26.)
- [107] Thomas Lochmatter, Pierre Roduit, Chris Cianci, Nikolaus Correll, Jacques Jacot, and Alcherio Martinoli. “SwisTrack - A Flexible Open Source Tracking Software for Multi-Agent Systems”. In *IEEE/RSJ International Conference on Intelligent Robots and Systems (IROS)*, pages 4004–4010, 2008.
URL:<https://doi.org/10.1109/IROS.2008.4650937>. (Cited on page 26.)
- [108] Tomáš Krajník, Matías Nitsche, Jan Faigl, Petr Vaněk, Martin Saska, Libor Přebušil, Tom Duckett, and Marta Mejail. “A Practical Multirobot Localization System”. *Journal of Intelligent & Robotic Systems*, 76(3):539–562, 2014.
URL:<https://doi.org/10.1007/s10846-014-0041-x>. (Cited on page 26.)
- [109] Markus Windolf, Nils Götzen, and Michael Morlock. “Systematic accuracy and precision analysis of video motion capturing systems - exemplified on the Vicon-460 system”. *Journal of Biomechanics*, 41(12):2776–2780, 2008.
URL:<https://doi.org/10.1016/j.jbiomech.2008.06.024>. (Cited on page 25.)
- [110] Kei Nakatsuma and Hiroyuki Shinoda. “High Accuracy Position and Orientation Detection in Two-Dimensional Communication Network”. In *SIGCHI Conference on Human Factors in Computing Systems (CHI)*, pages 2297–2306, 2010.
URL:<https://doi.org/10.1145/1753326.1753673>. (Cited on page 25.)
- [111] Shigeru Saito, Atsushi Hiyama, Tomohiro Tanikawa, and Michitaka Hirose. “Indoor Marker-based Localization Using Coded Seamless Pattern for Interior Decoration”. In *IEEE Virtual Reality Conference*, pages 67–74, 2007.
URL:<https://doi.org/10.1109/VR.2007.352465>. (Cited on pages 25 and 26.)
- [112] Lode Jorissen, Steven Maesen, Ashish Doshi, and Philippe Bekaert. “Robust Global Tracking Using a Seamless Structured Pattern of Dots”. In *International Conference on Augmented and Virtual Reality*, pages 210–231. Springer, 2014.
URL:https://doi.org/10.1007/978-3-319-13969-2_17. (Cited on pages 25 and 26.)
- [113] Mats Petter Pettersson. “Method and Device for Decoding a Position-Coding Pattern”, December 5 2006. US Patent 7,145,556.
URL:<http://patft1.uspto.gov/netacgi/nph-Parser?patentnumber=7145556>. (Cited on pages 25, 26, and 189.)
- [114] Lukas O. Hostettler, Ayberk Özgür, Séverin Lemaignan, Pierre Dillenbourg, and Francesco Mondada. “Real-Time High-Accuracy 2D Localization with Structured Patterns”. In *IEEE International Conference on Robotics and Automation (ICRA)*, pages 4536–4543, 2016.
URL:<https://doi.org/10.1109/ICRA.2016.7487653>. (Cited on pages 27 and 178.)
- [115] Lukas Hostettler. “High Precision Localization for Tangible Robots based on Structured Patterns”. Master’s thesis, EPFL, Lausanne, Switzerland, 2015. (Cited on page 27.)

- [116] Edward Aboufadel, Timothy Armstrong, and Elizabeth Smietana. “Position Coding”. *arXiv preprint arXiv:0706.0869*, 2007.
URL:<https://arxiv.org/abs/0706.0869>. (Cited on page 28.)
- [117] Ayberk Özgür, Séverin Lemaignan, Wafa Johal, Maria Beltran, Manon Briod, Léa Pereyre, Francesco Mondada, and Pierre Dillenbourg. “Cellulo: Versatile Handheld Robots for Education”. In *ACM/IEEE International Conference on Human-Robot Interaction (HRI)*, 2017.
URL:<https://doi.org/10.1145/2909824.3020247>. (Cited on pages 51, 82, and 178.)
- [118] Roland Siegwart, Illah R. Nourbakhsh, and Davide Scaramuzza. *Introduction to Autonomous Mobile Robots*. MIT Press, 2nd edition, 2011. ISBN 0-262-01535-8.
URL:<http://www.mobilerobots.ethz.ch/>. (Cited on pages 61 and 62.)
- [119] Gilles Mourioux, Cyril Novales, Gérard Poisson, and Pierre Vieyres. “Omni-directional robot with spherical orthogonal wheels: concepts and analyses”. In *IEEE International Conference on Robotics and Automation (ICRA)*, pages 3374–3379, 2006.
URL:<https://doi.org/10.1109/ROBOT.2006.1642217>. (Cited on page 61.)
- [120] Kenjiro Tadakuma and Riichiro Tadakuma. “Mechanical Design of “Omni-Ball”: Spherical Wheel for Holonomic Omnidirectional Motion”. In *IEEE International Conference on Automation Science and Engineering (CASE)*, pages 788–794, 2007.
URL:<https://doi.org/10.1109/COASE.2007.4341852>. (Cited on page 61.)
- [121] Suyang Yu, Changlong Ye, Hongjun Liu, and Jun Chen. “Development of an omnidirectional Automated Guided Vehicle with MY3 wheels”. *Perspectives in Science*, 7, 2015.
URL:<https://doi.org/10.1016/j.pisc.2015.11.056>. (Cited on page 61.)
- [122] Mark West and Haruhiko Asada. “Design of a Holonomic Omnidirectional Vehicle”. In *IEEE International Conference on Robotics and Automation (ICRA)*, volume 1, pages 97–103, 1992.
URL:<https://doi.org/10.1109/ROBOT.1992.220328>. (Cited on page 61.)
- [123] Kenjiro Tadakuma, Riichiro Tadakuma, Keiji Nagatani, Kazuya Yoshida, Steve Peters, Martin Udengaard, and Karl Iagnemma. “Crawler Vehicle with Circular Cross-Section Unit to Realize Sideways Motion”. In *IEEE/RSJ International Conference on Intelligent Robots and Systems (IROS)*, pages 2422–2428, 2008.
URL:<https://doi.org/10.1109/IROS.2008.4651223>. (Cited on page 61.)
- [124] Sunguk Ok, Atsushi Kodama, Yuma Matsumura, and Yoshihiko Nakamura. “SO(2) and SO(3), Omni-Directional Personal Mobility with Link-Driven Spherical Wheels”. In *IEEE/RSJ International Conference on Intelligent Robots and Systems (IROS)*, pages 268–273, 2011.
URL:<https://doi.org/10.1109/IROS.2011.6095179>. (Cited on page 61.)
- [125] Donghwa Jeong and Kiju Lee. “InchBot: A novel swarm microrobotic platform”. In *IEEE/RSJ International Conference on Intelligent Robots and Systems (IROS)*, pages 5565–5570, 2013.
URL:<https://doi.org/10.1109/IROS.2013.6697163>. (Cited on page 61.)
- [126] Mark West and Haruhiko Asada. “Design of Ball Wheel Mechanisms for Omnidirectional Vehicles with Full Mobility and Invariant Kinematics”. *Journal of Mechanical Design*, 119(2):153–161, 1997.
URL:<https://doi.org/10.1115/1.2826230>. (Cited on page 62.)
- [127] Laurent Ferrière and Benoit Raucent. “ROLLMOBS, a new universal wheel concept”. In *IEEE International Conference on Robotics and Automation (ICRA)*, volume 3, pages 1877–1882, 1998.
URL:<https://doi.org/10.1109/ROBOT.1998.680516>. (Cited on pages 62 and 71.)
- [128] Hashem Ghariblu, Ali Moharrami, and Behnam Ghalamchi. “Design and Prototyping of Autonomous Ball Wheel Mobile Robots”. In *Mobile Robots - Current Trends*. InTech Open Access Publisher, 2011.
URL:<https://doi.org/10.5772/25936>. (Cited on pages 62 and 71.)

Bibliography

- [129] Biruk A. Gebre, Zachary Ryter, Sean R. Humphreys, Scott M. Ginsberg, Sean P. Farrell, Anthony Kauffman, William Capon, William Robbins, and Kishore Pochiraju. “A Multi-Ball Drive for Omni-Directional Mobility”. In *IEEE International Conference on Technologies for Practical Robot Applications (TePRA)*, pages 1–6, 2014. URL:<https://doi.org/10.1109/TePRA.2014.6869140>. (Cited on page 62.)
- [130] David M. Ball, Chris F. Lehnert, and Gordon F. Wyeth. “A Practical Implementation of a Continuous Isotropic Spherical Omnidirectional Drive”. In *IEEE International Conference on Robotics and Automation (ICRA)*, pages 3775–3780, 2010. URL:<https://doi.org/10.1109/ROBOT.2010.5509645>. (Cited on pages 62 and 71.)
- [131] Young-Chul Lee, Danny V. Lee, Jae H. Chung, and Steven A. Velinsky. “Control of a redundant, reconfigurable ball wheel drive mechanism for an omnidirectional mobile platform”. *Robotica*, 25(4):385–395, 2007. URL:<https://doi.org/10.1017/S0263574706003158>. (Cited on page 62.)
- [132] Gundula Runge, Gunnar Borchert, Patrick Henke, and Annika Raatz. “Design and Testing of a 2-DOF Ball Drive”. *Journal of Intelligent & Robotic Systems*, 81(2):195–213, 2016. URL:<https://doi.org/10.1007/s10846-015-0247-6>. (Cited on page 62.)
- [133] Tatsuro Endo and Yoshihiko Nakamura. “An Omnidirectional Vehicle on a Basketball”. In *12th International Conference on Advanced Robotics (ICAR)*, pages 573–578, 2005. URL:<https://doi.org/10.1109/ICAR.2005.1507466>. (Cited on page 62.)
- [134] Tom B. Lauwers, George A. Kantor, and Ralph L. Hollis. “A Dynamically Stable Single-Wheeled Mobile Robot with Inverse Mouse-Ball Drive”. In *IEEE International Conference on Robotics and Automation (ICRA)*, pages 2884–2889, 2006. URL:<https://doi.org/10.1109/ROBOT.2006.1642139>. (Cited on page 62.)
- [135] Masaaki Kumagai and Takaya Ochiai. “Development of a Robot Balancing on a Ball”. In *International Conference on Control, Automation and Systems (ICCAS)*, pages 433–438, 2008. URL:<https://doi.org/10.1109/ICCAS.2008.4694680>. (Cited on page 62.)
- [136] Wei-Hsi Chen, Ching-Pei Chen, Jia-Shiuan Tsai, Jackie Yang, and Pei-Chun Lin. “Design and implementation of a ball-driven omnidirectional spherical robot”. *Mechanism and Machine Theory*, 68:35–48, 2013. URL:<https://doi.org/10.1016/j.mechmachtheory.2013.04.012>. (Cited on page 62.)
- [137] Masaaki Kumagai and Ralph L. Hollis. “Development and Control of a Three DOF Spherical Induction Motor”. In *IEEE International Conference on Robotics and Automation (ICRA)*, pages 1528–1533, 2013. URL:<https://doi.org/10.1109/ICRA.2013.6630773>. (Cited on pages 62 and 65.)
- [138] Hongseok Jang, Hyunseok Lee, Hongseok Lee, Taegon Park, Seongsu Jung, and Jongkyu Park. “Design and Analysis of Ultrasonic Motor for Driving Sphere Wheel”. *Ferroelectrics*, 459(1):68–75, 2014. URL:<https://doi.org/10.1080/00150193.2013.838081>. (Cited on page 62.)
- [139] Masaaki Kumagai. “Development of a Ball Drive Unit using Partially Sliding Rollers –An alternative mechanism for semi-omnidirectional motion–”. In *IEEE/RSJ International Conference on Intelligent Robots and Systems (IROS)*, pages 3352–3357, 2010. URL:<https://doi.org/10.1109/IROS.2010.5651007>. (Cited on page 62.)
- [140] Ayberk Özgür, Wafa Johal, and Pierre Dillenbourg. “Permanent Magnet-Assisted Omnidirectional Ball Drive”. In *IEEE/RSJ International Conference on Intelligent Robots and Systems (IROS)*, pages 1061–1066, 2016. URL:<https://doi.org/10.1109/IROS.2016.7759180>. (Cited on pages 63 and 178.)
- [141] Christine M. Pooley and David Tabor. “Friction and Molecular Structure: The Behaviour of Some Thermoplastics”. *Royal Society of London A: Mathematical, Physical and Engineering Sciences*, 329(1578):251–274, 1972. URL:<https://doi.org/10.1098/rspa.1972.0112>. (Cited on page 70.)

- [142] Ayberk Özgür, Wafa Johal, Francesco Mondada, and Pierre Dillenbourg. “Haptic-Enabled Handheld Mobile Robots: Design and Analysis”. In *CHI Conference on Human Factors in Computing Systems (CHI)*, 2017.
URL:<https://doi.org/10.1145/3025453.3025994>. (Cited on pages 71, 92, 100, and 178.)
- [143] Tamás Kalmár-Nagy, Raffaello D’Andrea, and Pritam Ganguly. “Near-optimal dynamic trajectory generation and control of an omnidirectional vehicle”. *Robotics and Autonomous Systems*, 46(1):47–64, 2004.
URL:<https://doi.org/10.1016/j.robot.2003.10.003>. (Cited on page 72.)
- [144] Mandayam A. Srinivasan and Robert H. LaMotte. “Tactual Discrimination of Softness”. *Journal of Neurophysiology*, 73(1):88–101, 1995.
URL:<http://jn.physiology.org/content/73/1/88>. (Cited on page 87.)
- [145] Gianni Campion, Qi Wang, and Vincent Hayward. “The Pantograph Mk-II: A Haptic Instrument”. In *IEEE/RSJ International Conference on Intelligent Robots and Systems (IROS)*, pages 45–58, 2005.
URL:<https://doi.org/10.1109/IROS.2005.1545066>. (Cited on pages 89 and 90.)
- [146] Angelika Peer and Martin Buss. “A New Admittance-Type Haptic Interface for Bimanual Manipulations”. *IEEE/ASME Transactions on Mechatronics*, 13(4):416–428, 2008.
URL:<https://doi.org/10.1109/TMECH.2008.2001690>. (Cited on pages 89 and 90.)
- [147] Carlo Alberto Avizzano, Massimo Satler, and Emanuele Ruffaldi. “Portable Haptic Interface with Omnidirectional Movement and Force Capability”. *IEEE Transactions on Haptics*, 7(2):110–120, 2014.
URL:<https://doi.org/10.1109/TOH.2014.2310462>. (Cited on pages 89 and 90.)
- [148] Motoyuki Akamatsu and Sigeru Sato. “A multi-modal mouse with tactile and force feedback”. *International Journal of Human-Computer Studies*, 40(3):443–453, 1994.
URL:<https://doi.org/10.1006/ijhc.1994.1020>. (Cited on page 89.)
- [149] Andrew H. Gosline, Gianni Campion, and Vincent Hayward. “On The Use of Eddy Current Brakes as Tunable, Fast Turn-On Viscous Dampers For Haptic Rendering”. In *Eurohaptics*, pages 229–234, 2006.
URL:<https://www.cim.mcgill.ca/~haptic/devices/pub/AG-ET-AL-EH-06.pdf>. (Cited on page 89.)
- [150] Randy E. Ellis, Ossama M. Ismaeil, and Michael G. Lipsett. “Design and evaluation of a high-performance haptic interface”. *Robotica*, 14(03):321–327, 1996.
URL:<https://doi.org/10.1017/S0263574700019639>. (Cited on page 90.)
- [151] Paolo Gallina, Giulio Rosati, and Aldo Rossi. “3-d.o.f. Wire Driven Planar Haptic Interface”. *Journal of Intelligent and Robotic Systems*, 32(1):23–36, 2001.
URL:<https://doi.org/10.1023/A:1012095609866>. (Cited on page 90.)
- [152] Daniela Constantinescu, Icarus Chau, Simon P. DiMaio, Luca Filipozzi, Septimiu E. Salcudean, and Farhad Ghassemi. “Haptic Rendering of Planar Rigid-Body Motion using a Redundant Parallel Mechanism”. In *IEEE International Conference on Robotics and Automation (ICRA)*, volume 3, pages 2440–2445, 2000.
URL:<https://doi.org/10.1109/ROBOT.2000.846393>. (Cited on page 90.)
- [153] Tae-Ju Kim, Byung-Ju Yi, and Il Hong Suh. “Load Distribution Algorithms and Experimentation For a Redundantly Actuated, Singularity-Free 3-DOF Parallel Haptic Device”. In *IEEE/RSJ International Conference on Intelligent Robots and Systems (IROS)*, volume 3, pages 2899–2904, 2004.
URL:<https://doi.org/10.1109/IROS.2004.1389849>. (Cited on page 90.)
- [154] Norbert Nitzsche, Uwe D. Hanebeck, and Günther Schmidt. “Mobile Haptic Interaction with Extended Real or Virtual Environments”. In *IEEE International Workshop on Robot and Human Interactive Communication (RO-MAN)*, pages 313–318, 2001.
URL:<https://doi.org/10.1109/ROMAN.2001.981921>. (Cited on page 90.)

Bibliography

- [155] Norbert Nitzsche, Uwe D. Hanebeck, and Günther Schmidt. “Design Issues of Mobile Haptic Interfaces”. *Journal of Robotic Systems*, 20(9):549–556, 2003.
URL:<https://doi.org/10.1002/rob.10105>. (Cited on page 90.)
- [156] Federico Barbagli, Alessandro Formaglio, M. Franzini, Antonio Giannitrapani, and Domenico Prattichizzo. “An Experimental Study of the Limitations of Mobile Haptic Interfaces”. In *Experimental Robotics IX: The 9th International Symposium on Experimental Robotics*, pages 533–542, 2006.
URL:https://doi.org/10.1007/11552246_51. (Cited on page 90.)
- [157] Kyung-Lyong Han, Oh Kyu Choi, In Lee, Inwook Hwang, Jin S. Lee, and Seungmoon Choi. “Design and Control of Omni-Directional Mobile Robot for Mobile Haptic Interface”. In *International Conference on Control, Automation and Systems (ICCAS)*, pages 1290–1295, 2008.
URL:<https://doi.org/10.1109/ICCAS.2008.4694349>. (Cited on page 90.)
- [158] Mine Sarac, Mehmet Alper Ergin, Ahmetcan Erdogan, and Volkan Patoglu. “AssistOn-Mobile: A Series Elastic Holonomic Mobile Platform for Upper Extremity Rehabilitation”. *Robotica*, 32(08):1433–1459, 2014.
URL:<https://doi.org/10.1017/S0263574714002367>. (Cited on page 90.)
- [159] Reymond Clavel. *Conception d’un Robot Parallèle Rapide à 4 Degrés de Liberté [Design of a Fast 4 Degrees of Freedom Parallel Robot]*. PhD thesis, Ecole Polytechnique Fédérale de Lausanne (EPFL), 1991.
URL:<https://doi.org/10.5075/epfl-thesis-925>. (Cited on page 90.)
- [160] Steven Martin and Nick Hillier. “Characterisation of the Novint Falcon Haptic Device for Application as a Robot Manipulator”. In *Australasian Conference on Robotics and Automation (ACRA)*, pages 291–292, 2009.
URL:<http://www.araa.asn.au/acra/acra2009/papers/pap127s1.pdf>. (Cited on page 90.)
- [161] Alejandro Jarillo-Silva, Omar A. Domínguez-Ramírez, Vicente Parra-Vega, and J. Patricio Ordaz-Oliver. “PHANToM OMNI Haptic Device: Kinematic and Manipulability”. In *Electronic, Robotics and Automotive Mechanics Conference (CERMA)*, pages 193–198, 2009.
URL:<https://doi.org/10.1109/CERMA.2009.55>. (Cited on page 90.)
- [162] Scott Brave, Hiroshi Ishii, and Andrew Dahley. “Tangible Interfaces for Remote Collaboration and Communication”. In *ACM Conference on Computer Supported Cooperative Work (CSCW)*, pages 169–178, 1998.
URL:<https://doi.org/10.1145/289444.289491>. (Cited on page 90.)
- [163] Gian Pangaro, Dan Maynes-Aminzade, and Hiroshi Ishii. “The Actuated Workbench: Computer-controlled Actuation in Tabletop Tangible Interfaces”. In *15th Annual ACM Symposium on User Interface Software and Technology (UIST)*, pages 181–190, 2002.
URL:<https://doi.org/10.1145/571985.572011>. (Cited on page 90.)
- [164] Malte Weiss, Florian Schwarz, Simon Jakubowski, and Jan Borchers. “Madgets: Actuating Widgets on Interactive Tabletops”. In *23rd Annual ACM Symposium on User Interface Software and Technology (UIST)*, pages 293–302, 2010.
URL:<https://doi.org/10.1145/1866029.1866075>. (Cited on page 91.)
- [165] Dan Rosenfeld, Michael Zawadzki, Jeremi Sudol, and Ken Perlin. “Physical Objects as Bidirectional User Interface Elements”. *IEEE Computer Graphics and Applications*, 24(1):44–49, 2004.
URL:<https://doi.org/10.1109/MCG.2004.1255808>. (Cited on page 91.)
- [166] Aleksander Krzywinski, Haipeng Mi, Weiqin Chen, and Masanori Sugimoto. “RoboTable: A Tabletop Framework for Tangible Interaction with Robots in a Mixed Reality”. In *International Conference on Advances in Computer Entertainment Technology (ACE)*, pages 107–114, 2009.
URL:<https://doi.org/10.1145/1690388.1690407>. (Cited on page 91.)

- [167] Esben Warming Pedersen and Kasper Hornbæk. “Tangible Bots: Interaction with Active Tangibles in Tabletop Interfaces”. In *SIGCHI Conference on Human Factors in Computing Systems (CHI)*, pages 2975–2984, 2011.
URL:<https://doi.org/10.1145/1978942.1979384>. (Cited on page 91.)
- [168] Masanori Sugimoto, Tomoki Fujita, Haipeng Mi, and Aleksander Krzywinski. “RoboTable2: A Novel Programming Environment using Physical Robots on a Tabletop Platform”. In *8th International Conference on Advances in Computer Entertainment Technology (ACE)*, pages 10:1–10:8, 2011.
URL:<https://doi.org/10.1145/2071423.2071436>. (Cited on page 91.)
- [169] Eckard Riedenklau. *Development of Actuated Tangible User Interfaces: New Interaction Concepts and Evaluation Methods*. PhD thesis, Universität Bielefeld, 2016.
URL:<https://pub.uni-bielefeld.de/publication/2900748>. (Cited on page 91.)
- [170] Mark Marshall, Thomas Carter, Jason Alexander, and Sriram Subramanian. “Ultra-tangibles: Creating Movable Tangible Objects on Interactive Tables”. In *SIGCHI Conference on Human Factors in Computing Systems (CHI)*, pages 2185–2188, 2012.
URL:<https://doi.org/10.1145/2207676.2208370>. (Cited on page 91.)
- [171] Michael Rubenstein, Christian Ahler, and Radhika Nagpal. “Kilobot: A Low Cost Scalable Robot System for Collective Behaviors”. In *IEEE International Conference on Robotics and Automation (ICRA)*, pages 3293–3298, 2012.
URL:<https://doi.org/10.1109/ICRA.2012.6224638>. (Cited on pages 91, 133, and 134.)
- [172] Diana Nowacka, Karim Ladha, Nils Y. Hammerla, Daniel Jackson, Cassim Ladha, Enrico Rukzio, and Patrick Olivier. “Touchbugs: Actuated Tangibles on Multi-touch Tables”. In *SIGCHI Conference on Human Factors in Computing Systems (CHI)*, pages 759–762, 2013.
URL:<https://doi.org/10.1145/2470654.2470761>. (Cited on page 91.)
- [173] James Minogue and M. Gail Jones. “Haptics in Education: Exploring an Untapped Sensory Modality”. *Review of Educational Research*, 76(3):317–348, 2006.
URL:<https://doi.org/10.3102/00346543076003317>. (Cited on page 91.)
- [174] Evan F. Wies, M. Sile O’Modhrain, Christopher J. Hasser, John A. Gardner, and Vladimir L. Bulatov. “Web-Based Touch Display for Accessible Science Education”. In *Haptic Human-Computer Interaction*, pages 52–60. Springer, 2001.
URL:https://doi.org/10.1007/3-540-44589-7_6. (Cited on page 91.)
- [175] Adam M. Brandt and Mark B. Colton. “Toys in the Classroom: LEGO MindStorms as an Educational Haptics Platform”. In *Symposium on Haptic Interfaces for Virtual Environment and Teleoperator Systems (Haptics)*, pages 389–395, 2008.
URL:<https://doi.org/10.1109/HAPTICS.2008.4479982>. (Cited on page 91.)
- [176] David I. Grow, Lawton N. Verner, and Allison M. Okamura. “Educational Haptics”. In *AAAI Spring Symposium: Semantic Scientific Knowledge Integration*, pages 53–58, 2007.
URL:<https://www.aaai.org/Papers/Symposia/Spring/2007/SS-07-09/SS07-09-012.pdf>. (Cited on page 91.)
- [177] Roger Gassert, Jean-Claude Metzger, Kaspar Leuenberger, Werner L. Popp, Michael R. Tucker, Bogdan Vigar, Raphael Zimmermann, and Olivier Lambercy. “Physical Student-Robot Interaction With the ETHZ Haptic Paddle”. *IEEE Transactions on Education*, 56(1):9–17, 2013.
URL:<https://doi.org/10.1109/TE.2012.2219310>. (Cited on page 91.)
- [178] James Minogue, M. Gail Jones, Bethany Broadwell, and Tom Oppewall. “The impact of haptic augmentation on middle school students’ conceptions of the animal cell”. *Virtual Reality*, 10(3-4):293–305, 2006.
URL:<https://doi.org/10.1007/s10055-006-0052-4>. (Cited on page 91.)

Bibliography

- [179] M. Gail Jones, James Minogue, Thomas R. Tretter, Atsuko Negishi, and Russell Taylor. "Haptic Augmentation of Science Instruction: Does Touch Matter?". *Science Education*, 90(1):111–123, 2006.
URL:<https://doi.org/10.1002/sce.20086>. (Cited on page 91.)
- [180] Mohamad A. Eid, Mohamed Mansour, Abdulmotaleb H. El Saddik, and Rosa Iglesias. "A Haptic Multimedia Handwriting Learning System". In *International Workshop on Educational Multimedia and Multimedia Education*, pages 103–108, 2007.
URL:<https://doi.org/10.1145/1290144.1290161>. (Cited on page 91.)
- [181] Eric N. Wiebe, James Minogue, M. Gail Jones, Jennifer Cowley, and Denise Krebs. "Haptic feedback and students' learning about levers: Unraveling the effect of simulated touch". *Computers & Education*, 53(3): 667–676, 2009.
URL:<https://doi.org/10.1016/j.compedu.2009.04.004>. (Cited on page 91.)
- [182] Felix G. Hamza-Lup and Ioana A. Stanescu. "The haptic paradigm in education: Challenges and case studies". *Internet and Higher Education*, 13(1-2):78–81, 2010.
URL:<https://doi.org/10.1016/j.iheduc.2009.12.004>. (Cited on page 91.)
- [183] Jenna L. Toennies, Jessica Burgner, Thomas J. Withrow, and Robert J. Webster. "Toward Haptic/Aural Touchscreen Display of Graphical Mathematics for the Education of Blind Students". In *IEEE World Haptics Conference (WHC)*, pages 373–378, 2011.
URL:<https://doi.org/10.1109/WHC.2011.5945515>. (Cited on page 91.)
- [184] Yeongmi Kim, Sunyoung Park, Hyungon Kim, Hyerin Jeong, and Jeha Ryu. "Effects of Different Haptic Modalities on Students' Understanding of Physical Phenomena". In *IEEE World Haptics Conference (WHC)*, pages 379–384, 2011.
URL:<https://doi.org/10.1109/WHC.2011.5945516>. (Cited on page 91.)
- [185] Petter Bivall, Shaaron Ainsworth, and Lena A. E. Tibell. "Do Haptic Representations Help Complex Molecular Learning?". *Science Education*, 95(4):700–719, 2011.
URL:<https://doi.org/10.1002/sce.20439>. (Cited on page 91.)
- [186] James Minogue and David Borland. "Investigating Students' Ideas About Buoyancy and the Influence of Haptic Feedback". *Journal of Science Education and Technology*, 25(2):187–202, 2016.
URL:<https://doi.org/10.1007/s10956-015-9585-1>. (Cited on page 91.)
- [187] Christian Hatzfeld. "Haptics as an Interaction Modality". In Christian Hatzfeld and Thorsten A. Kern, editors, *Engineering Haptic Devices: A Beginner's Guide*, chapter 2, pages 29–100. Springer London, 2nd edition, 2014. ISBN 978-1-4471-6517-0.
URL:<https://doi.org/10.1007/978-1-4471-6518-7>. (Cited on page 94.)
- [188] Mathieu Le Goc, Pierre Dragicevic, Samuel Huron, Jeremy Boy, and Jean-Daniel Fekete. "SmartTokens: Embedding Motion and Grip Sensing in Small Tangible Objects". In *28th Annual ACM Symposium on User Interface Software & Technology (UIST)*, pages 357–362, 2015.
URL:<https://doi.org/10.1145/2807442.2807488>. (Cited on page 97.)
- [189] Steven Gelineck, Dan Overholt, Morten Büchert, and Jesper Andersen. "Towards an Interface for Music Mixing based on Smart Tangibles and Multitouch". In *International Conference on New Interfaces for Musical Expression (NIME)*, pages 180–185, 2013.
URL:http://nime.org/proceedings/2013/nime2013_206.pdf. (Cited on page 97.)
- [190] V. Gregory Payne and Larry D. Isaacs. *Human Motor Development: A Lifespan Approach*. McGraw-Hill, 8th edition, 2012. ISBN 9780078022494.
URL:http://scholarworks.sjsu.edu/faculty_books/1. (Cited on page 106.)

- [191] Ayberk Özgür, Wafa Johal, Francesco Mondada, and Pierre Dillenbourg. “Windfield: Learning Wind Meteorology with Handheld Haptic Robots”. In *ACM/IEEE International Conference on Human-Robot Interaction (HRI)*, 2017.
URL:<https://doi.org/10.1145/2909824.3020231>. (Cited on pages 115 and 178.)
- [192] Grigori Sidorov, Alexander Gelbukh, Helena Gómez-Adorno, and David Pinto. “Soft Similarity and Soft Cosine Measure: Similarity of Features in Vector Space Model”. *Computación y Sistemas*, 18(3):491–504, 2014.
URL:<https://doi.org/10.13053/CyS-18-3-2043>. (Cited on page 121.)
- [193] Daniel C. Richardson and Rick Dale. “Looking To Understand: The Coupling Between Speakers’ and Listeners’ Eye Movements and its Relationship to Discourse Comprehension”. *Cognitive Science*, 29(6):1045–1060, 2005.
URL:https://doi.org/10.1207/s15516709cog0000_29. (Cited on page 122.)
- [194] Lynne E. Parker. “Multiple Mobile Robot Systems”. In *Springer Handbook of Robotics*, pages 921–941. 2008.
URL:https://doi.org/10.1007/978-3-540-30301-5_41. (Cited on page 129.)
- [195] Alessandro Farinelli, Luca Iocchi, and Daniele Nardi. “Multirobot Systems: A Classification Focused on Coordination”. *IEEE Transactions on Systems, Man, and Cybernetics, Part B (Cybernetics)*, 34(5):2015–2028, 2004.
URL:<https://doi.org/10.1109/TSMCB.2004.832155>. (Cited on page 130.)
- [196] Andreas Kolling, Phillip Walker, Nilanjan Chakraborty, Katia Sycara, and Michael Lewis. “Human Interaction with Robot Swarms: A Survey”. *IEEE Transactions on Human-Machine Systems*, 46(1):9–26, 2016.
URL:<https://doi.org/10.1109/THMS.2015.2480801>. (Cited on page 131.)
- [197] Zsolt Kira and Mitchell A. Potter. “Exerting Human Control Over Decentralized Robot Swarms”. In *4th International Conference on Autonomous Robots and Agents (ICARA)*, pages 566–571, 2009.
URL:<https://doi.org/10.1109/ICARA.2000.4803934>. (Cited on page 131.)
- [198] Phillip Walker, Steven Nunnally, Mike Lewis, Andreas Kolling, Nilanjan Chakraborty, and Katia Sycara. “Neglect Benevolence in Human Control of Swarms in the Presence of Latency”. In *IEEE International Conference on Systems, Man, and Cybernetics (SMC)*, pages 3009–3014, 2012.
URL:<https://doi.org/10.1109/ICSMC.2012.6378253>. (Cited on page 131.)
- [199] Andreas Kolling, Katia Sycara, Steven Nunnally, and Michael Lewis. “Human-Swarm Interaction: An Experimental Study of Two Types of Interaction with Foraging Swarms”. *Journal of Human-Robot Interaction*, 2(2):103–128, 2013.
URL:<https://doi.org/10.5898/jhri.2.2.kolling>. (Cited on page 131.)
- [200] Mike Daily, Youngkwan Cho, Kevin Martin, and Dave Payton. “World Embedded Interfaces for Human-Robot Interaction”. In *36th Annual Hawaii International Conference on System Sciences (HICSS’03)*, 2003.
URL:<https://doi.org/10.1109/HICSS.2003.1174285>. (Cited on page 131.)
- [201] James McLurkin, Jennifer Smith, James Frankel, David Sotkowitz, David Blau, and Brian Schmidt. “Speaking Swarmish: Human-Robot Interface Design for Large Swarms of Autonomous Mobile Robots”. In *AAAI Spring Symposium: To Boldly Go Where No Human-Robot Team Has Gone Before*, pages 72–75, 2006.
URL:<https://aaai.org/Library/Symposia/Spring/2006/ss06-07-011.php>. (Cited on page 131.)
- [202] Dan R. Olsen, Jr. and Stephen Bart Wood. “Fan-out: Measuring Human Control of Multiple Robots”. In *SIGCHI Conference on Human Factors in Computing Systems (CHI)*, pages 231–238, 2004.
URL:<https://doi.org/10.1145/985692.985722>. (Cited on page 131.)

Bibliography

- [203] Shishir Bashyal and Ganesh Kumar Venayagamoorthy. “Human Swarm Interaction for Radiation Source Search and Localization”. In *IEEE Swarm Intelligence Symposium (SIS)*, pages 1–8, 2008.
URL:<https://doi.org/10.1109/SIS.2008.4668287>. (Cited on page 131.)
- [204] Amir M. Naghsh, Jeremi Gancet, Andry Tanoto, and Chris Roast. “Analysis and Design of Human-Robot Swarm Interaction in Firefighting”. In *17th IEEE International Symposium on Robot and Human Interactive Communication (RO-MAN)*, pages 255–260, 2008.
URL:<https://doi.org/10.1109/ROMAN.2008.4600675>. (Cited on page 131.)
- [205] Alessandro Giusti, Jawad Nagi, Luca Gambardella, and Gianni A. Di Caro. “Cooperative Sensing and Recognition by a Swarm of Mobile Robots”. In *IEEE/RSJ International Conference on Intelligent Robots and Systems (IROS)*, pages 551–558, 2012.
URL:<https://doi.org/10.1109/IROS.2012.6385982>. (Cited on page 132.)
- [206] Shokoofeh Pourmehr, Valiallah (Mani) Monajjemi, Richard Vaughan, and Greg Mori. ““You two! Take off!”: Creating, Modifying and Commanding Groups of Robots Using Face Engagement and Indirect Speech in Voice Commands”. In *IEEE/RSJ International Conference on Intelligent Robots and Systems (IROS)*, pages 137–142, 2013.
URL:<https://doi.org/10.1109/IROS.2013.6696344>. (Cited on page 132.)
- [207] Gaëtan Podevijn, Rehan O’Grady, Youssef S. G. Nashed, and Marco Dorigo. “Gesturing at Subswarms: Towards Direct Human Control of Robot Swarms”. In *Towards Autonomous Robotic Systems: 14th Annual Conference (TAROS)*, pages 390–403, 2013.
URL:https://doi.org/10.1007/978-3-662-43645-5_41. (Cited on page 132.)
- [208] Valiallah (Mani) Monajjemi, Jens Wawerla, Richard Vaughan, and Greg Mori. “HRI in the Sky: Creating and Commanding Teams of UAVs with a Vision-mediated Gestural Interface”. In *IEEE/RSJ International Conference on Intelligent Robots and Systems (IROS)*, pages 617–623, 2013.
URL:<https://doi.org/10.1109/IROS.2013.6696415>. (Cited on page 132.)
- [209] Javier Alonso-Mora, Stefan Haegeli Lohaus, Philipp Leemann, Roland Siegwart, and Paul Beardsley. “Gesture Based Human - Multi-Robot Swarm Interaction and its Application to an Interactive Display”. In *IEEE International Conference on Robotics and Automation (ICRA)*, pages 5948–5953, 2015.
URL:<https://doi.org/10.1109/ICRA.2015.7140033>. (Cited on page 132.)
- [210] Luca Mondada, Mohammad Ehsanul Karim, and Francesco Mondada. “Electroencephalography as implicit communication channel for proximal interaction between humans and robot swarms”. *Swarm Intelligence*, 10(4):247–265, 2016.
URL:<https://doi.org/10.1007/s11721-016-0127-0>. (Cited on page 132.)
- [211] Hiroshi Ishii and Brygg Ullmer. “Tangible Bits: Towards Seamless Interfaces Between People, Bits and Atoms”. In *ACM SIGCHI Conference on Human Factors in Computing Systems (CHI)*, pages 234–241, 1997.
URL:<https://doi.org/10.1145/258549.258715>. (Cited on page 132.)
- [212] Hiroshi Ishii, Dávid Lakatos, Leonardo Bonanni, and Jean-Baptiste Labrune. “Radical Atoms: Beyond Tangible Bits, Toward Transformable Materials”. *interactions*, 19(1):38–51, 2012.
URL:<https://doi.org/10.1145/2065327.2065337>. (Cited on page 132.)
- [213] Mathieu Le Goc, Lawrence H. Kim, Ali Parsaei, Jean-Daniel Fekete, Pierre Dragicevic, and Sean Follmer. “Zoids: Building Blocks for Swarm User Interfaces”. In *29th Annual Symposium on User Interface Software and Technology (UIST)*, pages 97–109, 2016.
URL:<https://doi.org/10.1145/2984511.2984547>. (Cited on page 133.)
- [214] Antonio Gomes, Calvin Rubens, Sean Braley, and Roel Vertegaal. “BitDrones: Towards Using 3D Nanocopter Displays As Interactive Self-Levitating Programmable Matter”. In *CHI Conference on Human Factors in*

- Computing Systems (CHI)*, pages 770–780, 2016.
URL:<https://doi.org/10.1145/2858036.2858519>. (Cited on page 133.)
- [215] Francesco Mondada, Edo Franzi, and André Guignard. “The Development of Khepera”. In *Experiments with the Mini-Robot Khepera, Proceedings of the First International Khepera Workshop*, pages 7–14, 1999.
URL:<https://infoscience.epfl.ch/record/89709>. (Cited on page 133.)
- [216] Gilles Caprari, Kai Oliver Arras, and Roland Siegwart. “The Autonomous Miniature Robot Alice: from Prototypes to Applications”. In *IEEE/RSJ International Conference on Intelligent Robots and Systems (IROS)*, volume 1, pages 793–798, 2000.
URL:<https://doi.org/10.1109/IROS.2000.894701>. (Cited on page 133.)
- [217] Micael S. Couceiro, Carlos M. Figueiredo, J. Miguel A. Luz, Nuno M. F. Ferreira, and Rui P. Rocha. “A Low-Cost Educational Platform for Swarm Robotics”. *International Journal of Robots, Education and Art*, 2(1):1–15, 2012. (Cited on page 133.)
- [218] James McLurkin, Andrew J. Lynch, Scott Rixner, Thomas W. Barr, Alvin Chou, Kathleen Foster, and Siegfried Bilstein. “A Low-Cost Multi-robot System for Research, Teaching, and Outreach”. In *Distributed Autonomous Robotic Systems*, pages 597–609. Springer, 2013.
URL:https://doi.org/10.1007/978-3-642-32723-0_43. (Cited on page 133.)
- [219] Joseph Betthausen, Daniel Benavides, Jeff Schornick, Neal O’Hara, Jimit Patel, Jeremy Cole, and Edgar Lobaton. “WolfBot: A Distributed Mobile Sensing Platform for Research and Education”. In *American Society for Engineering Education (ASEE Zone 1)*, pages 1–8, 2014.
URL:<https://doi.org/10.1109/ASEEZone1.2014.6820632>. (Cited on page 133.)
- [220] Mojtaba Karimi, Alireza Ahmadi, Parinaz Kavandi, and Saeed Shiry Ghidary. “WeeMiK: A low-cost omnidirectional swarm platform for outreach, research and education”. In *4th International Conference on Robotics and Mechatronics (ICROM)*, pages 26–31, 2016.
URL:<https://doi.org/10.1109/ICRoM.2016.7886789>. (Cited on page 133.)
- [221] Rico Möckel, Alexander Spröwitz, Jérôme Maye, and Auke Jan Ijspeert. “An Easy to Use Bluetooth Scatternet Protocol for fast Data Exchange in Wireless Sensor Networks and Autonomous Robots”. In *IEEE/RSJ International Conference on Intelligent Robots and Systems (IROS)*, pages 2801–2806, 2007.
URL:<https://doi.org/10.1109/IROS.2007.4399458>. (Cited on page 135.)
- [222] Johan Thelin. “Quick User Interfaces with Qt”. *Linux Journal*, 2011(204), 2011.
URL:<http://dl.acm.org/citation.cfm?id=1972968.1972975>. (Cited on page 137.)
- [223] John Peterson, Gregory D. Hager, and Paul Hudak. “A Language for Declarative Robotic Programming”. In *IEEE International Conference on Robotics and Automation (ICRA)*, volume 2, pages 1144–1151, 1999.
URL:<https://doi.org/10.1109/ROBOT.1999.772516>. (Cited on page 138.)
- [224] Michael P. Ashley-Rollman, Seth Copen Goldstein, Peter Lee, Todd C. Mowry, and Padmanabhan Pillai. “Meld: A Declarative Approach to Programming Ensembles”. In *IEEE/RSJ International Conference on Intelligent Robots and Systems (IROS)*, pages 2794–2800, 2007.
URL:<https://doi.org/10.1109/IROS.2007.4399480>. (Cited on page 138.)
- [225] Stéphane Magnenat, Philippe Rétornaz, Michael Bonani, Valentin Longchamp, and Francesco Mondada. “ASEBA: A Modular Architecture for Event-Based Control of Complex Robots”. *IEEE/ASME Transactions on Mechatronics*, 16(2):321–329, 2011.
URL:<https://doi.org/10.1109/TMECH.2010.2042722>. (Cited on page 138.)
- [226] William M. Spears, Diana F. Spears, Rodney Heil, Wesley Kerr, and Suranga Hettiarachchi. “An Overview of Physicomimetics”. In *International Workshop on Swarm Robotics (SAB)*, pages 84–97, 2005.
URL:https://doi.org/10.1007/978-3-540-30552-1_8. (Cited on page 140.)

Bibliography

- [227] William M. Spears and Diana F. Spears, editors. *Physicomimetics: Physics-Based Swarm Intelligence*. Springer, 2012.
URL:<https://doi.org/10.1007/978-3-642-22804-9>. (Cited on page 140.)
- [228] R. Paul Wiegand, Mitchell A. Potter, Donald A. Sofge, and William M. Spears. *A Generalized Graph-Based Method for Engineering Swarm Solutions to Multiagent Problems*, pages 741–750. 2006.
URL:https://doi.org/10.1007/11844297_75. (Cited on page 140.)
- [229] Emily B. Moore, Julia M. Chamberlain, Robert Parson, and Katherine K. Perkins. “PhET Interactive Simulations: Transformative Tools for Teaching Chemistry”. *Journal of Chemical Education*, 91(8):1191–1197, 2014.
URL:<https://doi.org/10.1021/ed4005084>. (Cited on page 147.)
- [230] University of Colorado. “States of Matter - PhET Interactive Simulations”.
URL:<https://phet.colorado.edu/en/simulation/states-of-matter-basics> (accessed on 19 September 2017). (Cited on pages 147 and 151.)
- [231] Caroline E. Harriott, Adriane E. Seiffert, Sean T. Hayes, and Julie A. Adams. “Biologically-Inspired Human-Swarm Interaction Metrics”. In *Human Factors and Ergonomics Society Annual Meeting*, volume 58, pages 1471–1475, 2014.
URL:<https://doi.org/10.1177/1541931214581307>. (Cited on page 153.)
- [232] Michael A. Goodrich, Brian Pendleton, P. B. Sujit, and José Pinto. “Toward Human Interaction with Bio-Inspired Robot Teams”. In *IEEE International Conference on Systems, Man, and Cybernetics (SMC)*, pages 2859–2864, 2011.
URL:<https://doi.org/10.1109/ICSMC.2011.6084115>. (Cited on page 153.)
- [233] Christian Reeks, Marc G. Carmichael, Dikai Liu, and Kenneth J. Waldron. “Angled Sensor Configuration Capable of Measuring Tri-Axial Forces for pHRI”. In *IEEE International Conference on Robotics and Automation (ICRA)*, pages 3089–3094, 2016.
URL:<https://doi.org/10.1109/ICRA.2016.7487475>. (Cited on page 183.)
- [234] Wafa Johal, Sonia Andersen, Morgane Chevalier, Ayberk Özgür, Francesco Mondada, and Pierre Dillenbourg. “Tangible and Haptic Interaction in Learning with Robots: The Case of a Symmetry Learning Activity”. In *ACM/IEEE International Conference on Human-Robot Interaction (HRI)*, 2018. Submitted. (Cited on page 187.)
- [235] Julie Ducasse, Marc Macé, Marcos Serrano, and Christophe Jouffrais. “Tangible Reels: Construction and Exploration of Tangible Maps by Visually Impaired Users”. In *CHI Conference on Human Factors in Computing Systems (CHI)*, pages 2186–2197, 2016.
URL:<https://doi.org/10.1145/2858036.2858058>. (Cited on page 187.)
- [236] Arzu Guneyesu Ozgur, Wafa Johal, Kshitij Sharma, Ayberk Özgür, Maximilian Jonas Wessel, Friedhelm Christoph Hummel, Francesco Mondada, and Pierre Dillenbourg. “Iterative Design of an Upper Limb Rehabilitation Game with Tangible Robots”. In *ACM/IEEE International Conference on Human-Robot Interaction (HRI)*, 2018. Submitted. (Cited on page 187.)

Ayberk Özgür

EPFL-CHILI

RLC D1 740 (Rolex Learning Center), Station 20

CH-1015 Lausanne, Switzerland

+41 21 69 32983

ayberk.ozgur@epfl.ch

Research Interests

My goal is to build robots that can function in the real world among humans rather than structured laboratory/industrial settings. My vision is to bring together methodologies from multiple disciplines such as mobile robotics, manipulators, human-robot interaction, computer vision, tangible interfaces and haptics, among others. I completed my Ph.D. in the Cellulo project where I designed and built paper-assisted swarm robots for learning.

Education

Ecole Polytechnique Fédérale de Lausanne, Switzerland

CHILI Laboratory, Cellulo project

2014 - 2018

Computer, Communication and Information Sciences Ph.D.

2013 - 2018

Boğaziçi University, İstanbul, Turkey

Computer Engineering B.Sc.

2009 - 2013

* GPA: 3.91

* Participated in Robocup SPL with Cerberus in Mexico City

June 2012

* Conducted robotics research in AILAB

2011 - 2013

* Membership in COMPEC (Boğaziçi University IT Club)

2009 - 2010

Lycée de Galatasaray, İstanbul, Turkey

High School Degree

2004 - 2009

Awards and Honors

- Best Human-Robot Interaction Design Paper award in HRI 2017 **March 2017**
- Best Paper award in RO-MAN 2014 **August 2014**
- Completed Bachelor studies with high honors, ranked 1st out of 56 graduates **June 2013**
- B.Sc. thesis "Tabletop Manipulation in Clutter with Affordable 5-DOF Manipulator" received Best Departmental Undergraduate Thesis award **June 2013**

Publications

- A. Özgür, W. Johal, F. Mondada, P. Dillenbourg, “Haptic-Enabled Handheld Mobile Robots: Design and Analysis”, In Conference on Human Factors in Computing Systems (CHI), Denver. **May 2017**
- A. Özgür, S. Lemaignan, W. Johal, M. Beltran, M. Briod, L. Pereyre, F. Mondada and P. Dillenbourg, “Cellulo: Versatile Handheld Robots for Education”, In 2017 ACM/IEEE International Conference on Human-Robot Interaction (HRI), Vienna. *Best Human-Robot Interaction Design Paper award.* **March 2017**
- A. Özgür, W. Johal, F. Mondada and P. Dillenbourg, “Windfield: Learning Wind Meteorology with Handheld Haptic Robots”, In 2017 ACM/IEEE International Conference on Human-Robot Interaction (HRI), Vienna. **March 2017**
- A. Özgür, W. Johal and P. Dillenbourg, “Permanent Magnet-Assisted Omnidirectional Ball Drive”, In 2016 IEEE International Conference on Intelligent Robots and Systems (IROS), Daejeon. **October 2016**
- L. Hostettler, A. Özgür, S. Lemaignan, P. Dillenbourg and F. Mondada, “Real-Time High-Accuracy 2D Localization with Structured Patterns”, In 2016 IEEE International Conference on Robotics and Automation (ICRA), Stockholm. **May 2016**
- A. Özgür, S. Bonardi, M. Vespignani, R. Möckel and A. J. Ijspeert, “Natural User Interface for Roombots”, In RO-MAN 2014, The 23rd IEEE International Symposium on Robot and Human Interactive Communication, Edinburgh. *Best Paper award.* **August 2014**

Additional Skills

- Proficient in English and French
- Proficient in C, C++, QML, Java and LaTeX
- Skilled in ROS
- Skilled in QtQuick application development
- Skilled in Android application development
- Skilled Linux system administrator and web administrator
- Skilled in embedded systems design
- Skilled in Altium Designer
- Skilled in Solidworks
- Moderate in Matlab, Perl, Python, HTML, CSS, Javascript, Verilog, VHDL

Personal Interests

- Electronics design
- Mechanical design
- Robot design
- Software development